SURFACE ACOUSTIC WAVE DEVICES WITH LOW LOSS AND HIGH FREQUENCY OPERATION

TREVOR NORMAN OLIVER

Doctor of Philosophy

THE UNIVERSITY OF ASTON IN BIRMINGHAM

SEPTEMBER 1989

The University of Aston in Birmingham.

Surface Acoustic Wave Devices with Low Loss and High Frequency Operation.

Trevor Norman OLIVER
Degree of Doctor of Philosophy 1989

SUMMARY

This thesis describes an industrial research project carried out in collaboration with STC Components, Harlow, Essex. Technical and market trends in the use of surface acoustic wave (SAW) devices are reviewed. As a result, three areas not previously addressed by STC were identified: lower insertion loss designs, higher operating frequencies and improved temperature dependent stability.

A review of the temperature performance of alternative quartz crystal orientations shows that greater use could be made of the on-site quartz growing plant. Data is presented for quartz cuts in the ST-AT range. This data is used to modify the temperature performance of a SAW filter.

Several recently identified quartz orientations have been tested. These are SST, LST and X33. Problems associated with each cut are described and devices demonstrated. LST quartz, although sensitive to accuracy of cut, is shown to have an improved temperature coefficient over the normal ST orientation. Results show that its use is restricted due to insertion loss variations with temperature. Effects associated with split-finger transducers on LST-quartz are described.

Two low-loss options are studied, coupled resonator filters for very narrow bandwidth applications and single phase unidirectional transducers (SPUDT) for fractional bandwidths up to about 1%. Both designs can be implemented with one quarter wavelength transducer geometries at operating frequencies up to 1GHz.

The SPUDT design utilised an existing impulse response model to provide analysis of ladder or rung transducers. A coupled resonator filter at 400MHz is demonstrated with a matched insertion loss of less than 3.5dB and bandwidth of 0.05%. A SPUDT device is designed as a re-timing filter for timing extraction in a long haul PCM transmission system. Filters operating at 565MHz are demonstrated with insertion losses of less than 6dB. This basic SPUDT design is extended to a maximally distributed version and demonstrated at 450MHz with 9.8dB insertion loss.

Key words: Surface acoustic wave devices;
Unidirectional transducers;
Temperature coefficient;
Leaky surface wave devices.

ACKNOWLEDGEMENTS

Except where indicated, the work reported here is that of the author. The work was carried out in an industrial organisation, STC Components, and advantage was taken of pre-existing information and results when available. These results are indicated where appropriate.

The author wishes to thank the many colleagues at Aston University and STC Components for help and support throughout this project. In particular thanks are due to the supervisory team comprising Dr. R. L. Brewster, Dr. D. J. van Rest and Mr. D. E. Bower. During the project discussions took place with eminent SAW device experts. Dr. M. F. Lewis of RSRE, Malvern, Dr. T. E. Parker of Raytheon, Lexington and Dr. L. Bickers of British Telecom, Martlesham were most helpful. Dr. Lewis kindly made available an SPUDT device for test (Chapter 5).

Practical assistance was provided by Mr. B. T. Duxon who made many of the SAW devices and Mr. M. P. Cracknell who helped manufacture and matching of test fixtures.

A special thanks goes to David Bower of STC who supervised the project on a day to day basis and who provided a substantial technical input to this thesis.

CONTENTS Page

CONTENTS (continued) Page

CONTENTS (continued) Page

List of Figures

List of Figures (continued) Page

List of Figures (continued) Page

List of Figures (continued) Page

List of Tables

List of Tables (continued) Page

1. INTRODUCTION.

1.1 The Interdisciplinary Higher Degrees Scheme.

This research project has been undertaken within the Interdisciplinary Higher Degrees Scheme (IHD) at Aston University. It is an industrially based project, the collaborating organisation being STC Components of Harlow. The IHD approach to higher degrees by research is slightly unusual and is briefly outlined below. A more detailed review of the scheme is provided by Cochrane[1] and van Rest[2].

The scheme originated in 1968 when both Aston University and the Science Research Council were independently considering the development of problem solving PhD training for industrial careers. Aston was selected with funding from the UGC and studentships from the Science Research Council.

In the late seventies the IHD scheme was subdivided into two streams, Interdisciplinary or ID and Total Technology or TT. The TT stream grew out of the original scheme and is aimed at graduates who have a physical science or engineering background. Projects have a technological bias and collaborators are often large engineering organisations. The coursework brings into play multi-disciplinary aspects such as, marketing, systems thinking, and innovation as well as subject related material considered part of a traditional research project.

This thesis reports on work carried out as part of the Total Technology stream in collaboration with STC Components.

1.2 STC Components.

1.2.1 Company Profile.

STC Components is a management company of STC plc (formerly Standard Telephones and Cables plc). In the 1985 Annual Report[3] the directors described the principal activities of the group as:

Telecommunications
Computers and office equipment
International communications and services
Components and distribution
Research and development - both centrally in research laboratories and individually in divisions.

In his annual statement the chairman, Lord Keith of Castleacre, described how in 1984 and 1985 the company was undergoing major restructuring:

> "...a vigorous programme of cost cutting measures has been implemented across the remaining businesses with particular emphasis on stream-lining the management structure, the reduction of overhead costs and the elimination of non-essential capital expenditure."

The restructuring also included the sale or closure of peripheral activities with the result that during 1985 the total workforce numbers fell from 51,600 to 43,200. Other major figures from STC's 1985 financial summary are as follows:

	£m.
Group turnover	1997.2
UK sales	1278.1
Overseas sales	719.1
Loss before taxation	11.4
Loss for financial year	53.1

In his discussion of future prospects, Lord Keith reported that the vast bulk of restructuring had been completed and the group's competitiveness significantly improved. This statement was substantiated with the group returning to profit in 1986 and 1987.

STC's involvement in long distance undersea telecommunications systems impacts on one of the central themes of this project and is one of the major driving forces for the continued development of SAW devices. Young[4] describes how STC grew out of the London office for the Western Electric Company which, when opened in 1883, was staffed by two men and a boy. In 1925 the company was acquired by the International Telephone and Telegraph Company (ITT) and the UK subsidiary was renamed Standard Telephones and Cables Limited. ITT retained a

shareholding in STC until 1987 when it sold its 24% stake to the Canadian group Northern Telecom Limited.

1.2.2 Company Structure.

During the course of this project (Nov 1984 to Nov 1987) the structure of STC plc changed considerably. In particular the group benefitted from the acquisition of International Computers Limited (ICL) and sold International Aeradio Limited. There were also disposures of parts of group divisions and substantial reorganisation. In 1988 the group lists its activities under three main headings:

Information Systems
Communication Systems
Other Businesses.

The largest activity by turnover is ICL which operates within the Information Systems grouping. Other businesses include STC Defence Systems, STC Electronics Distribution and STC Components.

STC Components, the management division in which this project has taken place, currently comprises five business areas:

Power Components
Micro Devices
Hybrids
Tantalum Capacitors
Quartz Crystals.

1.2.3 The Quartz Crystal Unit.

The Quartz Crystal Unit employs approximately 200 people and is claimed by STC[5] to be Europe's largest integrated crystal plant in terms of its quartz production and range of devices fabricated. STC has been producing quartz components for over fifty years and during that time the Quartz Crystal Unit has moved twice, from London to South Wales during the 1939-45 war and later to Harlow as part of centralisation of related activities onto one site.

The unit produces synthetic quartz for its own needs and

also sells quartz in various forms to other device manufacturers. Quartz is available in several grades from standard to high purity swept grade. Grading is essentially a measure of the quality of the quartz in terms of impurities present and inclusions in the crystal lattice. A measure of the grade of a quartz block is its infra-red quality or Q-factor. Brice[6] reviews the relationship between Q-values and material parameters and states that for electronic devices Q-values must exceed two million. At STC, quartz is regularly produced with Q-values in the range 2.5 to 3.0 million.

Quartz is described by Holmyard[7] as one of the three naturally occuring crystalline forms of silicon dioxide, the others being tridymite and cristobalite. It also occurs in amorphous form as flint, opal and kieselguhr. Further, quartz when coloured with traces of manganese and iron forms amethyst, when pure, transparent and colourless is known as rock crystal, and when in a state of more or less fine division is sand. Although 15% of the Earth's crust is silicon dioxide, electronic grade quartz of reasonable size and purity is rare. About 90% of all such quartz is mined in Brazil.

Prior to 1964 all crystal devices manufactured by STC were made with natural quartz. However, as the supply of quartz became inconsistent, most crystal manufacturers, for example ITT[8] and Croven[9], began work on converting to cultured or synthetic quartz. Synthetic quartz is produced by placing thin "seed plates" of quartz into an aqueous alkaline solution in an autoclave. Quartz chippings are added and the autoclave is then heated to typically 400°C at a pressure of 30,000psi with these conditions being maintained for several weeks. The exact time depends upon the quality and size of bar required. Quartz growth takes place preferentially depending upon the cut axis of the original seed plate.

Upon removal of a quartz block from its autoclave it is x-ray aligned and sliced with reference to a defined crystallographic axis. Several systems of axis definition are used throughout the quartz industry with the most common being by reference to X, Y and Z planes. Any crystal cut orientation can be produced, but the industry has adopted a set of standard cuts which suffice for most applications. These cuts are shown diagramatically in Figure 1. Standard cuts have been defined for their electrical performance and accuracy of alignment.

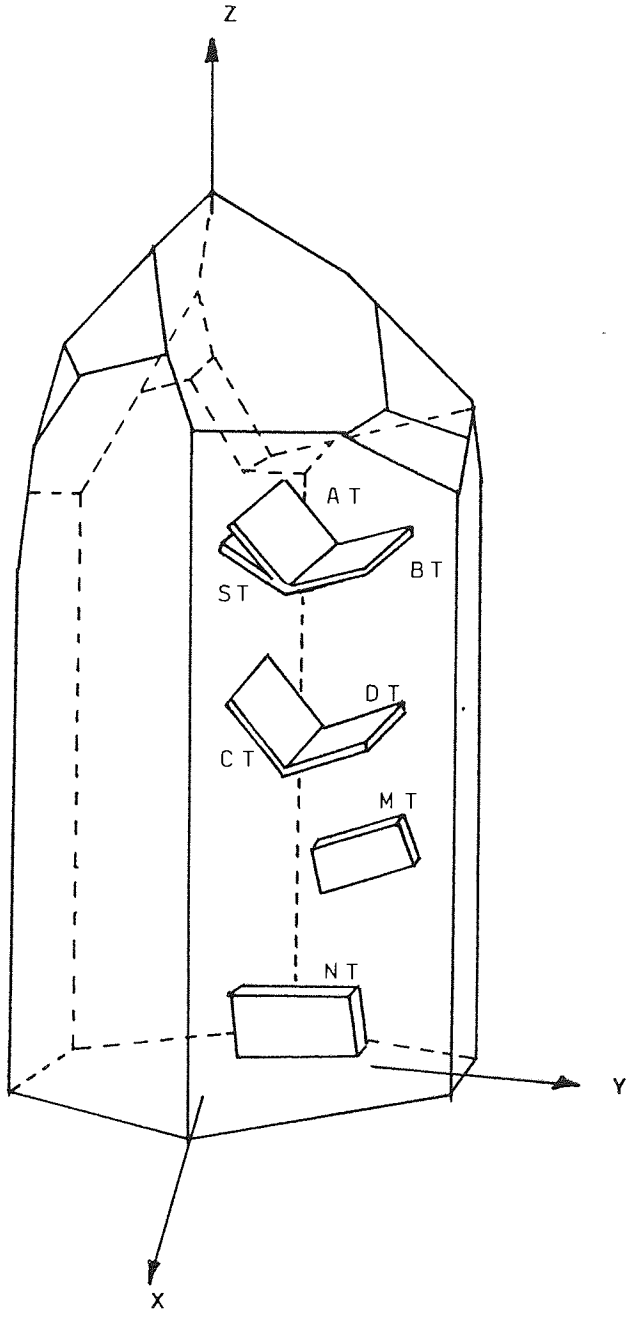

FIGURE 1 Quartz Crystal Block with Standard Angles of Cut

Accuracy usually depends upon the presence of a strong optical reflection from a known crystal plane in the alignment process.

The significance of quartz to the electronics industry lies with its piezoelectric characteristics which were first discovered in about 1880 by the Curie Brothers. They found that in certain crystals mechanical strain produces a proportional electric polarisation and, conversely, an applied electric field produces a proportional mechanical strain. Such crystals are said to be piezoelectric and will produce a mechanical vibration when an alternating electric field is applied. Little practical use was made of this phenomenon until 1917 when X-cut quartz plates were used to generate and detect sound waves in water. Since then the use of quartz crystals as the stable frequency determining element in electronic frequency control circuits and time standards has become widely accepted.

In the electronics field the term "crystal" usually refers to a bulk wave quartz device without additional components or circuitry. STC manufacture and market a range of generic crystals as well as using devices in-house for the production of crystal filters and oscillators. Such devices are available with operating frequencies in the range 200kHz to 80MHz. At the upper frequencies harmonics or overtones are used rather than the fundamental response. For a given quartz orientation and vibrational mode the main limiting factor on device operating frequency is the thickness of the crystal blank. At high frequencies the blanks become too thin to handle or to support reliably. Currently fundamental mode crystals are limited to an upper frequency of about 75MHz.

For crystal devices the important specification parameters are pulling range, that is control voltage induced frequency change, and temperature stability. All piezoelectric structures have vibrations that are temperature dependent. Applications for crystals may require precise frequency control over wide temperature bands. Compensation techniques have been developed which yield devices with frequency shifts of the order of a few parts per million over a full military temperature band of typically -55 C to 125 C. STC manufacture a range of such devices known as temperature compensated crystal oscillators (TCXO). Recently more sophisticated

techniques involving custom designed integrated circuits have resulted in the ICXO or integrated circuit crystal oscillator which is temperature compensated using a third or fifth order polynomial fit to measured overband data. ICXO's are available with stability of better than one part per million.

Crystal devices rely on mechanical vibrations, usually referred to as acoustic waves due to their propagation nature, which travel through the crystal medium. Such techniques are frequency limited to about 100MHz. Higher operating frequencies require a different vibrational mode, namely the use of a surface acoustic wave.

1.3 Surface Acoustic Wave Devices.

1.3.1 History.

As described in Section 1.2, acoustic waves have been utilised in devices for electronic systems for over sixty years, with acoustic propagation through the bulk of the crystal. Surface acoustic wave (SAW) technology in the electronics field has been developed within the last twenty years. However most SAW review articles and texts, for example Morgan[10], credit the discovery of surface waves to Lord Rayleigh. In a paper presented to the London Mathematical Society in 1885, Lord Rayleigh[11] demonstrated theoretically the ability of a semi-infinite isotropic solid substrate to support a mechanical vibration bound to its plane surface.

Surface acoustic waves have been investigated widely as a phenomenon associated with earthquakes. The motion of earthquakes generates both bulk and surface acoustic waves, the surface waves often contributing a major part of the motion because they are guided along the surface in two dimensions. Many important properties of acoustic waves in solids have been developed and demonstrated in the seismology literature. One other important early use of SAW is in ultrasonic flaw detection whereby invisible defects in materials can be detected without damage to the material itself.

In electronics, bulk wave devices have been used in a variety of applications and Morgan[10] describes their two most important attributes as follows:

Acoustic velocities are about 100,000 times lower than those of electromagnetic waves making long delays possible for relatively short device lengths.

Acoustic attenuation can be very low, depending upon the choice of medium, particularly at high frequencies.

In its simplest form, a bulk wave delay line comprises a solid propagation medium with transducers at each end. Delays of several microseconds are possible for each centimetre of device length.

Surface waves for electronic devices were first considered in the early 1960's, the main problem being how to launch and then detect the acoustic waves. Matthews[12] cites John Rowen of Bell Telephone Laboratories with the first basic patent application in 1963. Generally, SAW literature credits White and Voltmer[13] as having first proposed, in 1965, the interdigital transducer (IDT) as a means for SAW launch and detection. As with bulk wave devices, the attractions for using SAW in electronics are low velocity, non-dispersive propagation and low attenuation up to microwave frequencies. There is however one further most important advantage that surface waves have over bulk waves, namely they are accessible. Therefore two design parameters are available rather than one as with bulk wave devices. This accessibility allows greater versatility of design in terms of method of detection and generation and in propagation modification. The interdigital transducer can be so designed as to perform complex signal processing functions.

Such designs require intricate transducer structures and the growth of SAW technology has, according to Morgan[10], been helped by the fact that similar complex topographies were already being produced in the semi-conductor industry using established planar technology. Several integrated circuit fabrication techniques are directly applicable to SAW device manufacture, in particular:

Clean room technology.
Thin metallic film deposition onto polished substrates.
Chemical and plasma etching techniques.

Fine line photolithography.

Since 1965, when the interdigital transducer was first proposed, a wide variety of transducer designs and resultant SAW devices have evolved. In particular, methods have been developed for generating, detecting, focusing, reflecting, guiding and modifying surface acoustic waves. These methods employ a variety of physical principles mostly associated with IDT design. Much work has also been reported on substrates for SAW devices giving a greater variety of materials to meet specific requirements.

1.3.2 The Basic SAW Device.

Much of this section is based upon the review articles of Morgan[10] and Lewis et al[14].

All SAW devices comprise some form of IDT on a piezoelectric substrate (Figure 2). An IDT consists of a series of interleaved metallic fingers on the polished surface of a chosen crystal substrate. The electrodes are of a specified thickness and well-defined pitch. For a piezoelectric substrate a propagating surface wave is accompanied by an electric field localised at the surface. Therefore a surface wave can be produced by applying an alternating voltage to the array of metal strips. By reciprocity a similar transducer will also detect surface waves, converting a mechanical disturbance to an electrical output waveform.

A simple SAW device is outlined in Figure 2. Each IDT of this SAW transversal filter is bi-directional, that is acoustic waves are launched in both directions. It follows that in the direction of interest there is a 50% conversion loss equivalent to a 3dB attenuation at each transducer. Spurious reflections can arise when the reverse direction acoustic waves are scattered or reflected by the edge discontinuity of the SAW chip. These are reduced by the application during fabrication of absorber strips.

Ignoring all other loss mechanisms and assuming a SAW device is measured in a matched system with no return losses, the minimum attenuation of a transversal filter is 6dB. Spurious effects preclude device operation in this mode and typically devices are deliberately

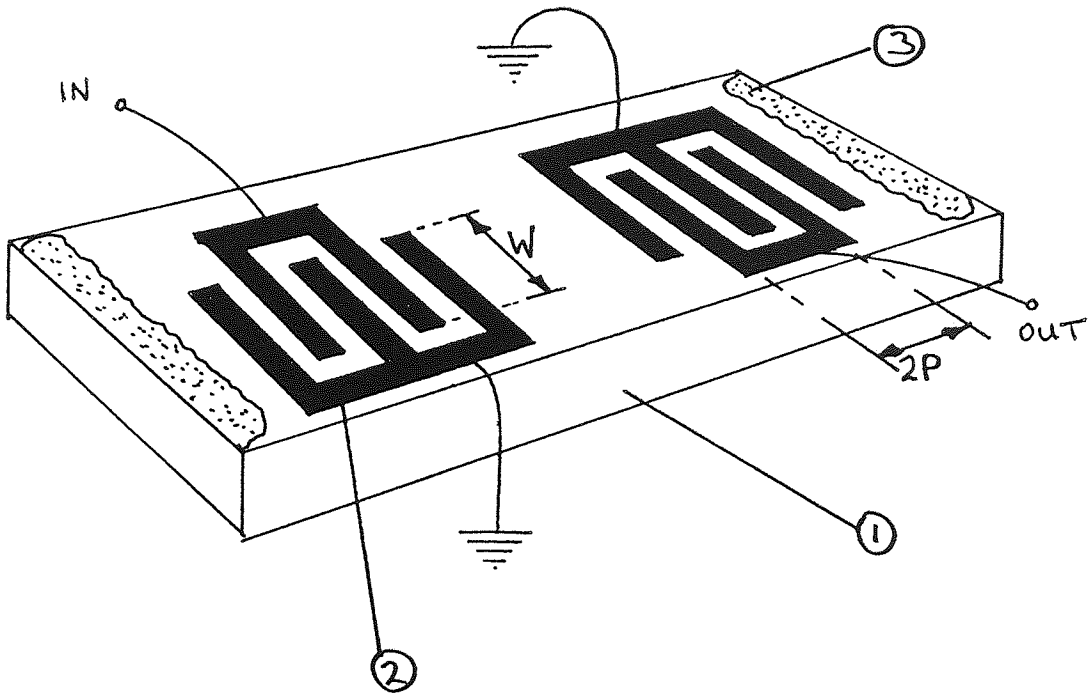

W - Aperture
P - Period

1 Piezoelectric substrate
2 Interdigital transducer
3 End absorber

FIGURE 2 Basic SAW Device

mis-matched with resultant insertion losses in the range 15 to 30dB. The reduction of bi-directional loss through the use of unidirectional IDT's forms one of the central themes of this project.

Many device types are now available based upon the structure of Figure 2. In all cases the design of the IDT finger pattern must ensure efficient coupling between the transducer and the piezoelectric substrate at the desired operating frequency. This is generally achieved by designing the finger-period of the IDT, that is the centre to centre inter-electrode spacing, to be equal to one half of the acoustic wavelength at the synchronous frequency for a given SAW velocity. It follows that for a unity mark-to-space ratio the electrode finger width and inter-electrode gap will be one quarter wavelength. In some instances devices are designed with other finger widths and mark-to-space ratios other than unity. However, applying the usual criterion developed above, a SAW filter designed to operate at 1GHz will have an electrode width given by:

$$\text{Electrode width} = \frac{\lambda_o}{4} \qquad \text{where } \lambda_o = \frac{V}{Fc}$$

and λ_o = acoustic wavelength
V = acoustic velocity
Fc = synchronous frequency

Taking the free surface velocity for ST-X quartz the acoustic wavelength is found from:

$$\lambda_o = \frac{3157 \text{ m/s}}{1 \text{ GHz}}$$

$$= 3.157\text{um}.$$

Therefore a 1GHz SAW device requires an electrode width of 0.786um.

In practice the actual SAW velocity is lower than the free surface value due to the presence of metal fingers on the device surface. Nonetheless the result demonstrates that the submicron geometries required for day to day SAW device manufacture are smaller than all

but the highly specialised requirements of the semiconductor industry.

The frequency limits of SAW device operation are primarily a function of line geometry and device size. At frequencies lower than a few tens of MHz devices become too large such that acoustic diffraction and dispersion effects become significant. At frequencies greater than 1GHz major problems are photolithographic line definition and process repeatability.

Choice of substrate is highly dependent upon application. The most important parameters are overband temperature stability and fractional bandwidth. Table 1 lists the more common materials used in SAW device production. For most applications the choice is between quartz and lithium niobate. Lithium niobate is chosen where wider fractional bandwidths are required. It has a much higher piezoelectric coupling coefficient, k^2, than quartz and allows generation and detection of acoustic waves with relatively few fingers in each IDT. However the temperature performance of lithium niobate is inferior to that of quartz. The temperature characteristic of SAW substrate materials is defined as the temperature coefficient of delay or TCD. From Table 1 it can be seen that the TCD values for common substrates are:

ST-X Quartz	-	0.03ppm/$(^oC)^2$
Y-Z Lithium Niobate	-	91ppm/^oC

where ST-X and Y-Z indicate the crystallographic cut.

A 100°C temperature range, centred on the inversion temperature, will give rise to frequency variations of:

ST-X Quartz	-	75ppm
Y-Z Lithium niobate	-	9100ppm.

Quartz is preferred for applications requiring a very high frequency stability over a wide temperature band. As most applications requiring such high levels of stability are for military and professional use, rather than high volume consumer applications such as TV IF filters, it follows that most of STC's output falls into this category.

This project is concerned only with devices made on quartz and which fall into three main categories:

TABLE 1 Properties of Piezoelectric Materials for SAW Devices

Substrate	Free Surface Velocity (m/s)	Piezoelectric Coupling Coefficient k^2 (%)	Optimum No. of Finger Pairs	Optimum Fractional Bandwidth (%)	Temperature Delay Coefficients 1st order $\times 10^{-6}/^{\circ}C$	2nd order $\times 10^{-9}/^{\circ}C^2$
Quartz						
ST-X	3157	0.14	23	4	0	30
$LiNbO_3$						
Y-Z	3488	5.0	4	25	91	--
128°Y-X	3977	5.6	4	27	72	--
$LiTaO_3$						
Y-Z	3254	0.76	10	10	35	--
X-112°YZ	3288	0.6	11	9	18	--
BGO						
(110)-<001>	1620	0.85	10	10	130	--
$AlPO_4$						
Y-X	2750	0.3	16	6	0	270
$Li_2B_4O_7$						
X-Z	3515	1.0	9	11	0	230

Transversal filters
Delay lines
Resonators.

Additionally, some aspects of device fabrication technology are reviewed, including improvements to processing techniques through optimising the selection of quartz cuts. Reference is also made to early work in the field of SAW sensors and specifically to the SAW accelerometer.

1.3.3 Applications of SAW Devices.

This section provides an overview of the market and applications for SAW devices. Two recent review papers, Lewis et al[14] and Hartmann[15], together describe technical developments and trends, and predict the major areas for future growth. Lewis proposes three important attractions associated with SAW devices:

> SAW devices operate in the frequency range of 10MHz to several 1GHz and so fill a technology gap between lumped component and microwave techniques. Also with bandwidths in the range 10kHz to 500MHz they embrace many of the requirements of both communications and radar systems.
>
> The accessibility of the acoustic wave allows great flexibility and ingenuity of design giving a diverse range of devices and the scope for improvements in performance, size and cost.
>
> SAW devices utilise well established photolithographic techniques and are therefore highly reproducible in mass production, cheap, rugged and suitable for integration into modern microelectronic circuitry.

Lewis identifies six device groups as follows:

Delay lines and multi-strip couplers.
Bandpass filters.
Filter banks.

Dispersive delay lines.
Oscillators and resonators.
Convolvers.

Whilst other writers, for example Morgan[10], may group device types differently, this list generally covers all generic forms. SAW sensors which are described briefly by Lewis usually incorporate a basic device type. Hartmann[15] discusses more fully the field of SAW sensors.

STC have concentrated their effort in four areas:

Bandpass filters.
Resonators and oscillators.
Delay lines.
Sensors (accelerometers).

The reasons for such specialisation are varied and partly historical. A move away from earlier in-house work on frequency synthesisers has precluded any serious work on filter banks. Both dispersive delay lines and convolvers belong to a specialised market which STC has preferred not to approach. Further, convolvers and many dispersive delay line configurations are fabricated on lithium niobate or similar high coupling coefficient materials.

The four areas in which STC operates are reviewed below.

1.3.3.1 Delay Lines and Multi-strip Couplers.

Delay lines and multi-strip couplers were (Lewis et al[14]) the earliest SAW device configurations to receive extensive investigation. In a simple delay line, the time delay is a function of the centre to centre separation of the input and output transducers. Tapped delay lines take advantage of the planar structure of SAW devices and allow fixed incremental delays. A more sophisticated version is the programmable tapped delay line where the amplitude and/or phase of each output is programmed electronically and the outputs summed.

With the SAW delay line relatively large delays of up to about 75us can be achieved without the need to fold the acoustic path. On ST-X quartz a delay of 1us corresponds to an acoustic path length of 3.2mm. Murray and White[16] list the main application areas of delay lines as:

Radar.
Electronic countermeasure systems.
Target simulation.
Discriminator circuits.

At STC delay lines are also used as the frequency selective element in SAW oscillators where a wider pulling range is required than that achievable with the more usual resonator oscillator. As with most SAW devices the main advantage of the SAW delay line is that the delays are highly reproducible.

The multi-strip coupler (MSC) is rarely used in any designs developed by STC. However it is reviewed briefly because of its importance in SAW technology. In its simplest form the MSC is an array of metal strips which couple acoustic waves from one path to another as shown in Figure 3. The basic property of the MSC (Lewis et al[14]) is that it allows complete energy transfer from one track to the other over a bandwidth of up to 100% on any piezoelectric substrate. However, the number of strips required in the MSC varies inversely with the piezoelectric coupling coefficient, k^2, and even on high k^2 materials such as lithium niobate the MSC occupies a substantial fraction of the substrate area. For this reason, the use of the MSC on quartz, which has a low k^2, is generally impractical.

The MSC has two important properties. Firstly, the frequency response of a device is simply the product of the responses of the individual IDT's. This is not always true in the absence of an MSC where, for example, both transducers may be weighted. Secondly, unwanted bulk waves generated at the upper IDT remain in the upper device track and do not contribute any spurious signal to the output. High quality bandpass filters generally incorporate an MSC. MSC's are also used in novel devices to reduce bi-directional IDT loss. These devices will be reviewed in Chapter 3.

1.3.3.2 Bandpass Filters.

Lewis et al[14] describe the bandpass filter as a delay line which is tapped at uniform time intervals with each tap output weighted and then all taps summed on a common bus. This description can be applied directly to the IDT

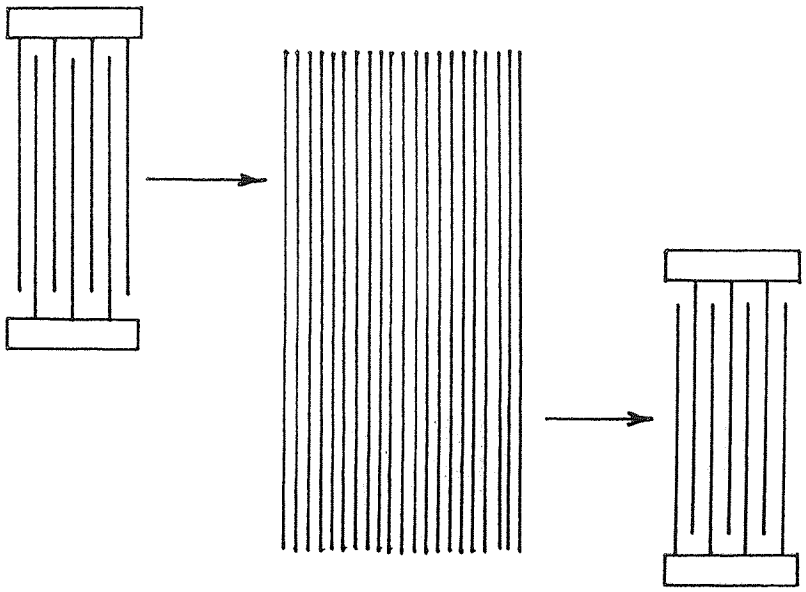

Number of coupler strips $N_T \propto 1/k^2$

$\lesssim 100$ for $LiNbO_3$

FIGURE 3 Multi-Strip Coupler

where transducer fingers are positioned at uniform intervals and are connected electrically with busbars. Each finger can be taken as a weight in the summation with the degree of weighting dependent upon the finger position and overlap as shown in Figure 4a. The overlap between adjacent fingers is called the aperture. One of the most common weighting techniques, apodisation, involves varying the finger overlap (Figure 4b). In order that the overall filter response is simply the product of the two transducer responses it is usual to weight only one IDT. Although the MSC overcomes this problem it is only used on high k^2 materials.

Apodisation may give rise to diffraction effects when the finger overlaps are of the same order as the operating wavelength. These effects, which can substantially affect device performance, are overcome by using alternative weighting techniques. One such alternative is withdrawal weighting which has two forms. In both cases a uniform transducer either has fingers disconnected or removed, finger withdrawal (Figure 4c), or the finger connect sequence is modified, source withdrawal (Figure 4d). The disconnect sequence is evaluated as part of the device design procedure. These relatively coarse weighting techniques are more suited to devices with many fingers, that is to narrow bandwidth filters.

SAW transversal filters are used primarily at intermediate frequency (IF) stages where the high device insertion loss of 15 to 30 dB does not greatly affect the system signal-to-noise ratio. All writers (for example, Lewis et al[14], Murray and White[16] and Hartmann[15]) agree that the largest single application to date for SAW devices is IF filtering in television receivers. In this mass production market, price, which is the prime consideration, equates to chip size. Low bulk wave cuts of lithium niobate, suitable for SAW generation, have been developed to specifically reduce device size and most TV filters are now made on 128° Y-X lithium niobate.

At STC, all filters are custom designed for the military and professional market. Most batches are small in number ranging from a few units to several hundred devices per order. Applications fall within two areas; filters and local oscillators for military communications and airborne radio receivers, and timing extraction filters in high bit-rate transmission systems such as optical fibre based pulse code modulation (PCM). As the STC group

FIGURE 4 Transducer Weighting Techniques

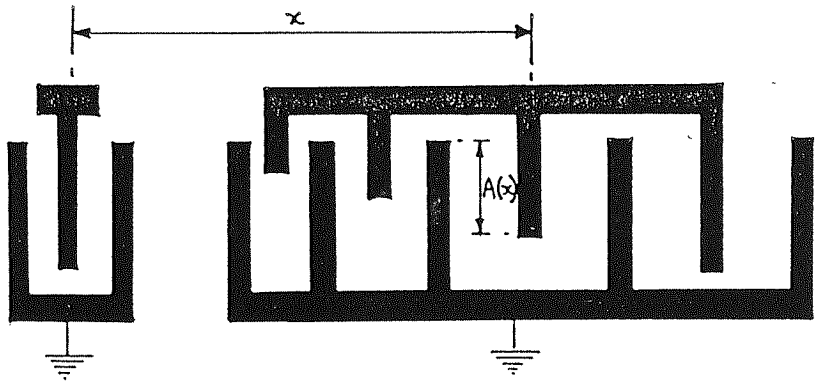

Generalised SAW IDT with
position dependent aperture and period
(a)

Apodised IDT
(b)

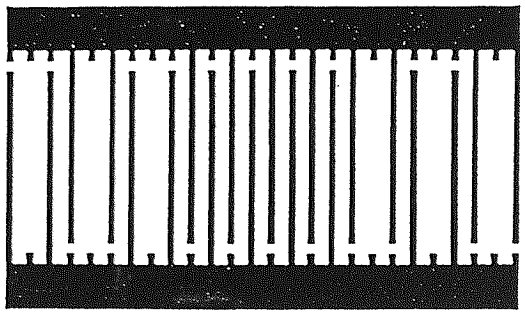

Finger-withdrawal weighted IDT
(c)

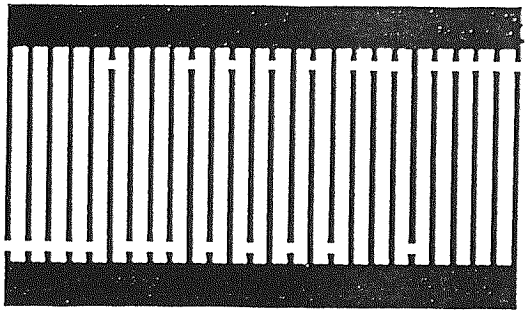

Source-withdrawal weighted IDT
(d)

has a worldwide reputation in telecommunications systems it follows that much work on SAW filters is targetted at meeting the increasing demands of optical fibre PCM systems.

1.3.3.3 Resonators and Oscillators.

The SAW resonator comprises an acoustic resonance cavity formed by two reflector gratings between which is placed a means of launching and detecting acoustic waves. Figure 5 shows the two common forms of SAW resonator where either a single or pair of transducers is used to launch/detect acoustic waves. The grating or mirror is highly reflective, consisting of either grooves or metal strips. Morgan[10] describes how this structure has two different frequency selective elements, the mirror grating and the cavity resonances. Device design ensures that all but the chosen cavity resonance are suppressed by the frequency response of the reflection grating.

Coldren and Rosenberg[18], in a review of SAW resonators, describe how ST-X quartz is chosen for all but the most specialised applications because of its thermal stability and zero power flow angle. That is, the propagation direction remains close to the normal of the wave front.

A useful measure of resonator performance is the device "Q". Unloaded Q is a theoretical measure of the resonant cavity taking into account propagation losses but ignoring any external load. Loaded Q describes how a device performs in a real system where there will be some energy loss at the input and output ports. Generally most high frequency test equipment simulates measurement on a 50ohm line and therefore, except in special circumstances where devices are matched into a 50ohm system, most routine Q measurements are on unmatched devices in a 50ohm test fixture. For all practical purposes Q is defined as:

$$Q = \text{Centre frequency}/3\text{dB bandwidth.}$$

Q values of over 10,000 are achievable, with Q reducing as device frequencies increase. Such high Q values require that devices are stable over a specified temperature band and that any ageing effects are minimised. Therefore great care is required during fabrication and packaging.

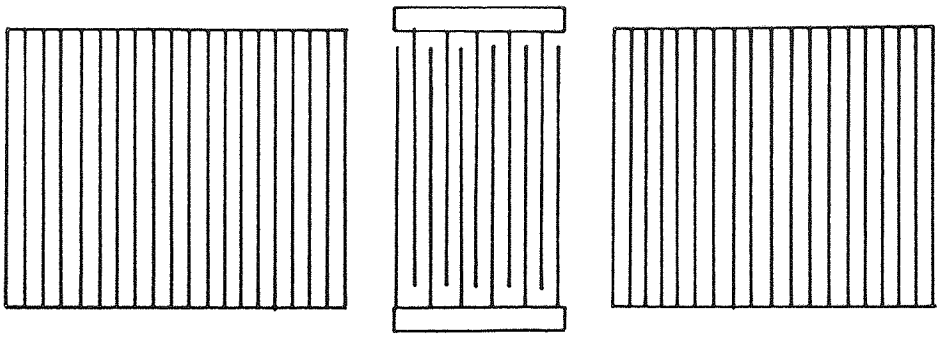

One-port resonator

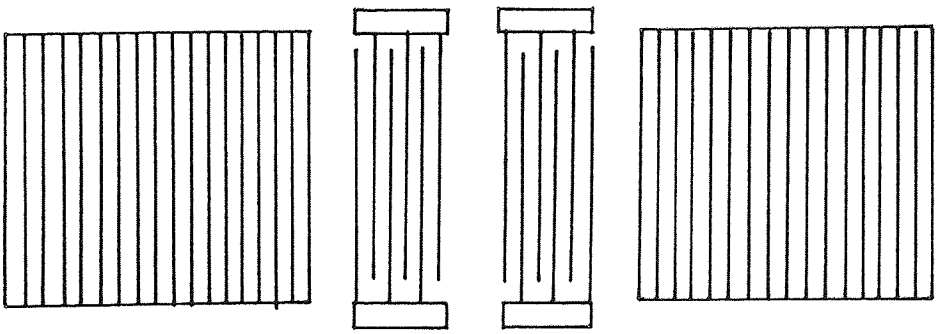

Two-port resonator

FIGURE 5 SAW Resonators

The SAW resonator is a single or two port standing wave device. Typical unmatched losses are in the range 6 to 10dB with matched losses as low as 1 to 2dB. Resonators can be used as very narrow bandwidth front-end filters where very low loss is essential to maintaining the signal-to-noise ratio. In this area Coldren and Rosenberg[18] claim that the SAW resonator has little competition. However, the main application for the SAW resonator is as the frequency determining element of an oscillator feedback loop.

Murray and White[16] give power consumption and size as the advantages of using a SAW oscillator. Lewis et al[14] critically review SAW oscillators in comparison with traditional bulk wave "crystal" oscillators and conclude that the inferior temperature performance of the SAW unit is offset by its higher operating fundamental frequency. Higher fundamental frequencies imply greater separation between the output frequency and closest spurious sidelobes in microwave generation. Lewis lists the main applications of SAW oscillators in the range 50MHz to 1.5GHz as:

Miniature UHF FM transmitters.
Local oscillators.
Microwave generation.

1.3.3.4 SAW Sensors.

Lewis et al[14] claim SAW oscillators will play a significant part in worldwide activity in sensor research and development. Hartmann[15] views sensors as the next major growth area for SAW technology and predicts new high volume applications such as wireless labelling. White[17] reviews the SAW sensor field and identifies several existing and new applications including:

Acceleration	Rotation
Temperature	Mechanical positioning
Pressure	Optical scattering
Force	Vapour sensing
High voltage	Biological sensing.

SAW devices are particularly suitable for sensor applications because they have a direct frequency output which is compatible with most monitoring and control systems. At STC the field of acceleration sensors is

being investigated by groups working on silicon devices and on SAW devices. Main areas of application will be for inertial and sub-inertial guidance systems.

The SAW accelerometer is based upon a resonator pair, one fixed and one hinged. Under an applied acceleration the hinged unit deflects causing a frequency shift which is directly related to the applied acceleration over a given range. Device accuracy is temperature limited and current development work aims to reduce these temperature effects.

1.3.4 Technical and Market Trends.

Hartmann[15] reviews the current market for SAW devices and predicts that future trends will be influenced primarily by a move in electronic system architecture from VHF to UHF frequencies. In the ten years to 1985 the worldwide market has grown by approximately 25% annually to $100 million and, says Hartmann, will reach $1 billion by 1995. Much of this market growth is in the high volume area of IF filters for TV and video cassette recorders. Hartmann cites the main factors influencing the future SAW development and market growth as follows:

The growth of the television market in the Third World.

Greater penetration of cable television into the domestic market with an increase in first IF stage frequencies from around 40MHz up to 1000MHz.

The development of high definition television requiring a precise UHF IF SAW filter.

The development of digital video transmission.

The growth of direct broadcasting by satellite again requiring UHF IF SAW filters.

Cellular radio systems requiring low loss SAW filters at 800 to 900 MHz.

Radiopagers with low loss front-end SAW filters to improve interference rejection.

This growth area also includes garage door control, medical alert systems and wireless security. Also, in cordless telephones, digitising will improve quality and signal security.

Broadband local area networks will require SAW based local oscillators, transmitter filters and receiver filters.

Most of these applications are addressed by the high volume SAW device manufacturers and are not under active investigation at STC. However the technological trends are still applicable in STC's sphere of interest, namely, military communications hardware and professional data and telecommunications systems. These market segments, which require relatively small scale production, comprise four main applications:

Filters for optical fibre PCM applications up to 700MHz at present but extending to 1.2GHz and beyond in the immediate future.

Narrowband filters for military communications systems, both low loss front-end and IF.

Precision oscillators for military and professional systems and telecommunications.

Accelerometers for inertial navigation systems.

Of these four areas STC's major involvement is in retiming filters for repeatered optical fibre systems. Rosenberg et al[19] describe the development of long-haul submerged optical fibre PCM transmission systems and specifically cite the need to improve SAW timing recovery filters. In particular, an improvement in insertion loss would reduce post-filter amplification and power consumption and allow wider margins in integrated circuits.

Hartmann[15] gives six technology challenges for SAW device designers. They are:

Improved low loss filters.
Improved packaging.

Higher operating frequencies (well above 1GHz).
Programmable filters.
More accurate filter design techniques.
Improved materials and processing.

In Chapter 2 the basis for this project will be shown to include three of Hartmann's challenges, namely a reduction in filter insertion loss coupled with improvements in materials and fabrication techniques to allow higher frequency devices to be produced.

1.4 Project Objectives.

The full statement of the project is developed in the next chapter. Here the aim is to briefly outline the project boundaries.

The STC Quartz Crystal Unit began the production of SAW devices in 1978 to complement its range of bulk wave crystal products. Once established in the professional and military market-place STC defined research and development objectives for SAW devices. In the light of the market trends outlined in section 1.3.4, the main area of research was initially to be low loss SAW devices, a field in which the company had no experience.

In the early stages of the project it became apparent that the research boundaries needed to be extended to take into account the move to higher frequencies and to look for means of improving device temperature stability. Further, these objectives of lower loss, higher frequencies and improved temperature drift are bound together in the basic requirement for a well understood and repeatable manufacturing process.

Therefore the objective of this project became the development, within the confines of existing design and production hardware, of the capability to design and manufacture SAW devices with:

Reduced insertion loss.
Improved temperature performance.
Higher operating frequencies.

For the company the objective was to maintain and improve its position in the SAW market-place.

2. PROJECT DEFINITION.

2.1 Original Problem Concept.

The aim of this chapter is to describe how the project was conceived and the conditions prevailing in terms of production and design methods.

Traditionally SAW filters have insertion loss values in the range 15 to 30 dB. Whilst rarely being advantageous, in some applications such losses can be tolerated. For example, the loss of a delay-line in the feedback loop of a SAW oscillator can be compensated by increased amplifier gain. However, in receiver front-end filtering high losses in the RF stage degrade the system signal-to-noise ratio. Timing recovery filters in repeaters for digital transmission systems will operate with high insertion losses but the increased power supply demands of submerged off-shore repeaters will impact on system design. In both front-end filter and low power applications, losses of the order of a few dB are required.

Many techniques for reducing loss are well documented and show a trade-off between insertion loss, ease of fabrication and device complexity. Few of these techniques have been commercially exploited, most being suited to very small scale or laboratory production. STC required a full review of low loss techniques with a view to adopting designs that could be adopted without large scale modification to existing processes. This formed the starting point for this project.

During the first year the objectives were redefined and new boundaries established such that at the first annual review the current title was adopted. A description of the influences on this decision-making process requires a brief review of the SAW facility at STC.

STC began manufacture of SAW devices in 1978 and in the period 1978-84 the annual production grew relatively slowly. This was partly due to concentration on very low volume, high value applications and small pre-production sample orders. STC's commitment to SAW production was reflected in the substantial investment in production, test and design hardware. In 1984-85 the SAW department began to see the results of earlier sample work and received large orders for SAW filters for new optical

fibre PCM systems. This rapid expansion of output committed both CAD hardware and testing equipment to the near full-time needs of production. At the same time the need to develop a low-loss design capability increased with more and more potential customers specifying reduced loss levels.

This apparent conflict of interests was resolved during the early stages of the project by the interaction of three separate factors which altered the project emphasis.

Firstly, the review of literature (Chapter 3) suggested that some low-loss design techniques could be developed relatively simply and to a first order with minimum design complexity.

Secondly, customers began to request improved or specific temperature characteristics from device manufacturers which suggested a review of materials was necessary.

Thirdly, the trend to higher frequencies required a thorough review of processing techniques with the aim of improving transducer finger definition to well below 1 micron on a regular production basis.

The low-loss aspect of the project had already been identified. The second aspect, temperature compensation, raised the advantage of access to in-house quartz. Many writers, for example Minowa et al[20] and Rosenberg et al[19], have shown that system temperature performance can to some extent be compensated by careful choice of SAW substrate. One of the first tasks undertaken in the project was to characterise a range of near-standard quartz substrates to meet the growing customer requirement of specific temperature versus frequency performance. Newly reported quartz orientations were also identified in the literature review.

The trend to achieve higher operating frequencies required a review of the critical aspects of production techniques, namely photolithography, and a search for low-loss techniques that did not require fine line definition.

At the first project review it was possible to establish the project boundaries:

Insertion loss improvements.

To identify techniques available using both filter and resonator designs and implement with both design programmes and fabrication procedures.

Frequency versus Temperature Improvements.

To fully exploit in-house quartz by categorizing a range of cuts close to ST-X. Also to identify new cuts and to test them experimentally.

Upper Frequency Limitations.

To review processing techniques and identify designs suitable for implementation at high frequencies, using existing production hardware.

2.2 The STC SAW Fabrication Facility.

Much is written about the design of SAW devices. In comparison very little is documented on the details of production. SAW manufacturers develop their own methods, some of which are kept as closely guarded secrets (Matthews[12]). Whilst the general fabrication routines are similar to the planar techniques of integrated circuit manufacture, the details and individual processes can vary considerably. Figure 6 shows an actual process path taken from a production manual. The process path shows all operations including inspections from substrate delivery to package inspection. Not included is substrate preparation, that is the growing, orientation, slicing and polishing of the quartz, operations which do not take place in the SAW department.

The many processes can be grouped under the following main headings:

Substrate preparation.
Substrate cleaning.

STC COMPONENTS LTD.	
QUARTZ CRYSTAL UNIT	PP/SAW/7
SA116A MANUFACTURE AND INSPECTION	SHEET 1 OF 2

Optical Preparation
including CPS/SAW/1

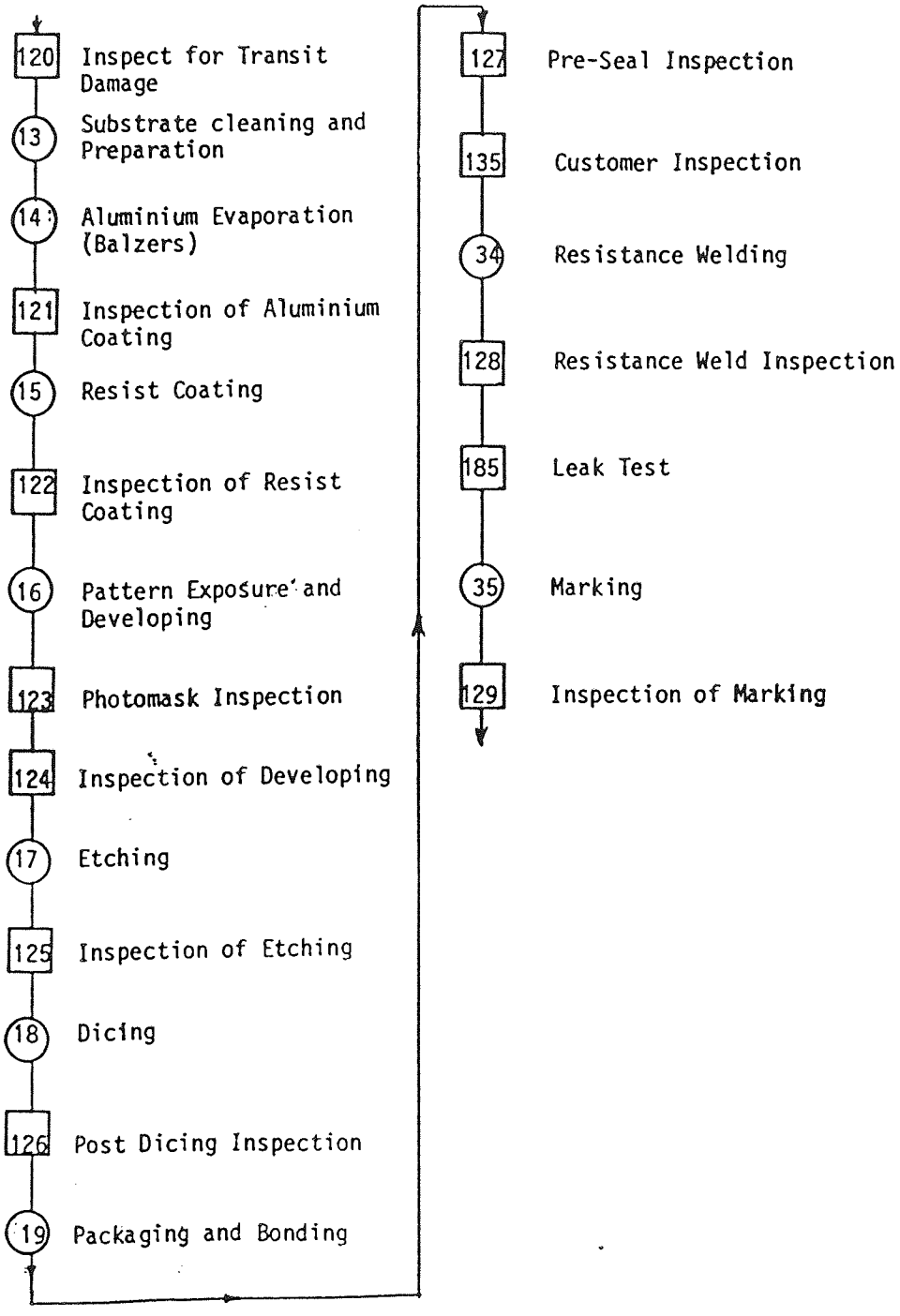

FIGURE 6 Fabrication Flow Chart

Metal film deposition.
Photolithography.
Substrate dicing.
Device packaging.
Testing.

It is implicit from the nature of a SAW device that the propagation surface should be as clean as possible. Whilst this sets standards for the optical polishing of substrates it also requires that all SAW fabrication takes place in a "clean room" dedicated to SAW production. At STC a Class 100 clean room, to defence standard 05-35/1, is available in which temperature, relative humidity and particle counts are maintained within pre-set limits. Lighting is filtered to prevent UV exposure of photo-sensitive chemicals used in photolithography. The STC SAW clean room is of the recirculating, horizontal, laminar flow type (Walton[21]). The clean room specification is:

Temperature	20 +/-1°C
Relative Humidity	50 +/-5%RH
Lighting	1000lux at bench level
Noise level	65dB(A)
Particle count	less than 100 @ 0.5um.

2.3 Fabrication Methods.

2.3.1 Substrate Preparation and Cleaning.

The preparation routines employed at STC are as described by Matthews[12] with embellishments based upon the company's quartz crystal background and user experience. Quartz substrates of a specified orientation and thickness are cut from a high grade block to a tolerance of typically better than +/- 5 minutes of arc. Substrates are then chemically polished on one surface to a required thickness, flatness and degree of polish.

Unlike the circular wafers produced for integrated circuit manufacture, most SAW substrates are rectangular, typically 30mm by 25mm. These dimensions are dictated partly by the size of the single quartz crystal that can be grown in reasonable conditions. Larger substrates would include a section through the original seed. Although the seed area could be ignored or removed when dicing, it is thought that it may cause larger substrates

to bow and hence degrade the transfer of electrode pattern from photomask to substrate. Usual practice is to avoid the seed when cutting the quartz block, which limits substrate dimensions.

Substrate cleaning is a critical part of SAW device manufacture as surface contaminants will influence the adhesion of the metal film and will degrade the performance of the device itself, possibly affecting long term ageing characteristics. Most SAW manufacturers develop their own cleaning routine based loosely upon those published (for example Matthews[12]), and jealously guard the final specification. Cleaning is usually in two stages involving the removal of soluble organic contaminants in solvents such as trichloroethane and propanol followed by the removal of more stubborn contaminants in chromic acid or an ammonium hydroxide/hydrogen peroxide mix. The cleaning specification details soak times, temperatures and deionised water rinses.

Film thicknesses of less than 750Å tend to suffer an effect called "pinholes" due to poor adhesion between the film and the substrate. These pinholes are very small (less than 0.5um in diameter) and, except in severe cases, can be ignored on low frequency devices where finger widths are greater than 1.0um. On higher frequency devices it has been found necessary to deposit a metallic interlayer to aid adhesion (see for example Tanski[22]). STC have developed a process for depositing a monolayer of titanium, although other materials such as chromium are also used. This substantially reduces the problem of pinholes which can cause line/finger breaks on fine line devices.

2.3.2 Metal Film Deposition.

The two most commonly used techniques for transferring the SAW device finger pattern from the photomask to the substrate are lift-off and etching. Both require a metal film to be deposited but in the case of lift-off the pattern is etched in a negative photoresist prior to film deposition. In the alternative process, used at STC, the metal film is deposited and then coated with positive photoresist.

Following cleaning and surface pre-treatment, the

substrates are loaded into a Balzers evaporator. Under a high vacuum (less than 2×10^{-6} Torr) an electron beam is directed into a crucible of very pure aluminium which evaporates and is deposited upon the polished surface of the quartz substrates. During this process the substrates are rotated at high speed in a supporting "planet" to ensure even film coating. The process is closed-loop controlled with a separate monitor crystal. The manufacturers of the system claim an accuracy of +/- 10Å with typical SAW devices having film thickness in the range 500 to 2000Å.

The deposition of a high quality, uniform aluminium film of known thickness is essential to the successful manufacture of devices within given production yield limits.

2.3.3 Photolithography.

Matthews[12] reviews the various methods of transferring the electrode pattern from a photomask onto the metal film on a SAW substrate. The process is a set of separate routines, each with their own specification. A basic outline of the photolithographic process is shown in Figure 7. SAW device production has several unique problems that must be addressed. These are mainly due to the need to resolve an array of sub-micron lines with unity mark-to-space ratio on a highly reflective substrate. At these dimensions conditions for interference are ideal as the incident Ultra Violet light wavelength and the photoresist film thickness are of similar values. Therefore great care is needed to produce devices using conventional UV mask-aligners.

The mask-aligner is one of the most important tools in SAW device manufacture. In the mask-aligner the coated SAW substrate, with its photoresist film, is brought into hard contact with the photomask and exposed to UV light for a pre-determined time. It is essential that the mask is clean and that the UV light is correctly collimated. The UV light source is a mercury vapour lamp with a wavelength of approximately 400nm (0.4um). The aligner manufacturers claim that this system will allow line resolution down to approximately 1.0um. At STC, devices have been produced on a small scale with linewidths of 0.5 to 0.6um. To consistently produce devices with finer lines requires lower wavelength light sources such as

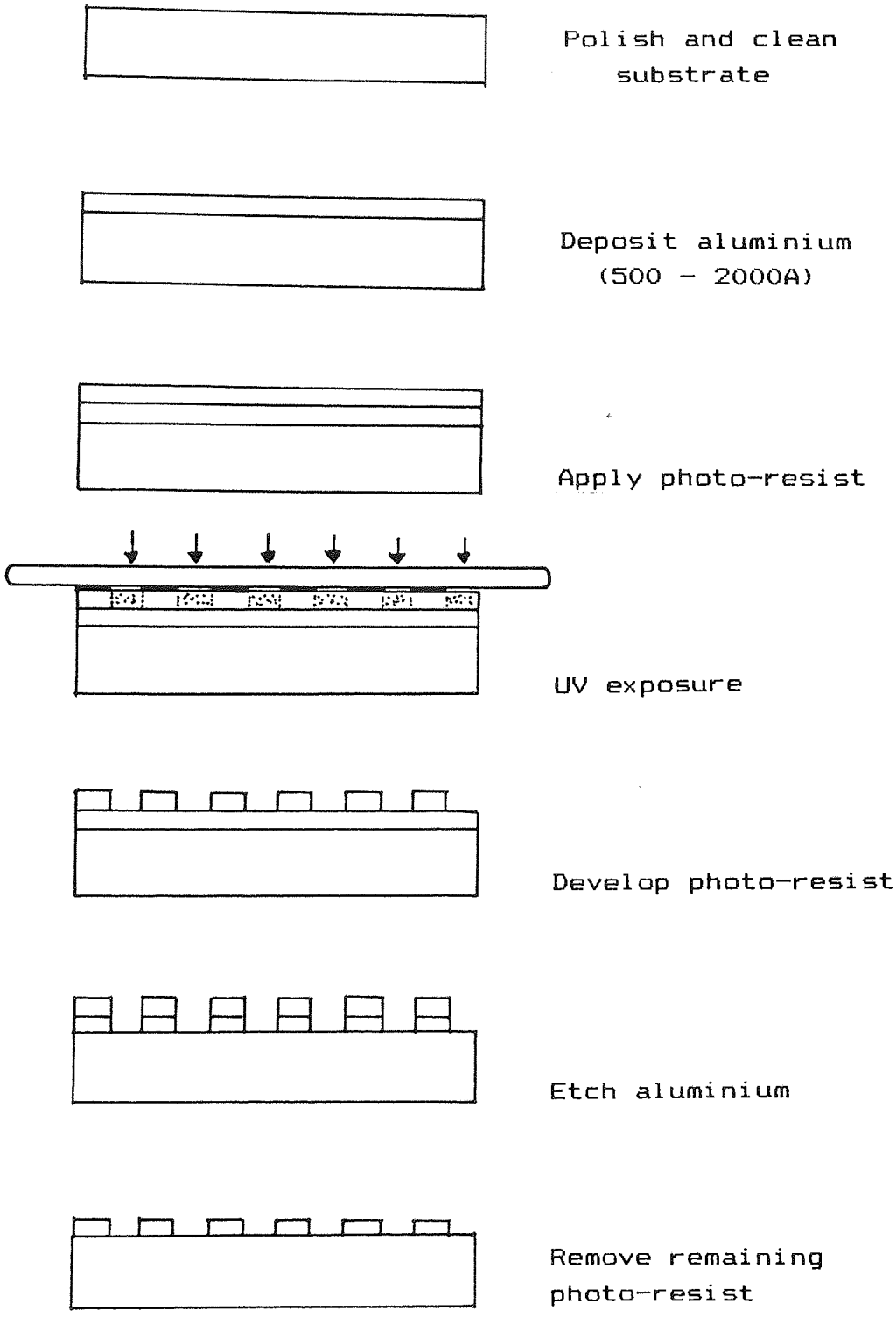

FIGURE 7 Photolithography

deep-UV or Excimer laser. However, a change in light source would require a complete review of the manufacturing process.

The problem of a highly reflective surface coupled with fine line geometries manifests itself as a rounding of the resist profile after the exposed resist is developed and washed away. Ideally the resist profiles should be vertical to ensure well controlled etch rates. Therefore to clean out the valleys between the resist peaks prior to etching the substrates are given a brief exposure to an oxygen plasma, referred to as a plasma de-scum. The objective of this process is to compensate for the non-unity mark-to-space ratio in the photo-resist, such that subsequent etching of the aluminium film will produce a corrected mark-to-space ratio at dimensions down to 0.5um.

The plasma de-scum is used to correct a processing control problem. Other techniques are available to improve resist profile. These include special resists to reduce reflections and dark chrome plated photomasks.

At STC, two etching routines are available, chemical etch and plasma etch. Chemical or wet etching of aluminium films is based upon a solution containing orthophosphoric, nitric and acetic acid. One of the problems with chemical etching is local variations, whereby line edges exhibit small scale roughness and occasionally aluminium remains between fingers creating shorts. On most devices small shorts can be "blown" and edge roughness is less significant at larger linewidths.

Where edge roughness is significant, plasma etching is used to produce a significantly improved profile. This is usually necessary on finger widths below 1.0um. STC have developed an improved plasma etching technique specifically for fine line SAW devices. In comparison with chemical techniques, plasma etching offers the potential for increased device yield and improved performance.

2.3.4 Substrate Dicing.

Successful photolithography yields a substrate containing a few tens to several hundred individual SAW devices, the number being greater the higher the frequency of

operation.

The dicing process itself requires the solution of several handling problems. Firstly the SAW substrate surface must be protected with a coating of photoresist. Secondly the substrate must be held rigidly during dicing. A special flexible plastic tape is available which is stretched across a support ring with an adhesive layer uppermost. The substrate is carefully attached to the centre of the plastic film and the complete supporting frame is held by a vacuum chuck.

The final handling problems are associated with the removal of the protective layer of photoresist from the die surfaces and the removal of the individual die from the support film. Several techniques are used depending to some extent upon the size of the die. These techniques take one of two possible routes. Either the whole substrate is cleaned prior to die removal or the die are first removed and then cleaned. In either case, once removed, a final inspection and oxygen plasma clean takes place.

2.3.5 Device Packaging.

This is an area of considerable research and development and a discussion on packing design considerations is included in Matthews [12]. The integrity of the device package will influence the electrical performance characteristics, survivability and long term ageing. The main objective of the packaging exercise is to interface the SAW device with the outside world. Here interface must include physical protection. The process basically involves fixing the SAW die onto a base (or header), attaching wires between the SAW transducers and header pins, and then encapsulating the device in an inert gas with a lid or cover.

The work reported in this thesis adopts the standard packaging practice and techniques in use at STC. It is worth noting that STC have undertaken a considerable amount of unreported development work on the improvement of ageing rates in SAW filters for submerged repeater retiming applications. Ageing rates have been reduced to such low levels that special test equipment has had to be designed to allow accurate determination of these rates (Dawson[23]). This work has helped to identify:

The most suitable adhesive for fixing the die to the header.

The necessary curing cycle in terms of temperature and time to ensure complete curing and outgassing of the adhesive.

Improved methods of die orientation relative to the header to reduce ageing and also reduce electrical breakthrough.

New package designs to improve the electrical performance of high frequency (above 1GHz) devices.

Whilst there are some device applications where the saw die is mounted directly onto a circuit board with the entire board being encapsulated, all STC SAW die are mounted and sealed as individual, stand-alone devices.

In a typical packaging process gold-plated headers and nickel or nickel-plated caps are cleaned and baked to remove contaminants. The SAW die is then attached to the header with an epoxy or polyimide paste and an acoustic absorber is applied to the ends of the SAW die to reduce spurious end reflections. Once the adhesive has been cured, devices are given a final extended bake (typically 60 hours) in a vacuum oven and are then sealed in a dry nitrogen atmosphere. Lids are attached to the header by either resistance or seam weld and as the weld takes place a trace of helium gas is added to aid the detection of leaks. At all stages of the process extensive quality control checks are necessary on parameters such as dew point, temperature and vacuum level.

2.3.6 Testing

The electrical performance specifications derived by customers are often exacting and to very close tolerence. These factors require that devices are tested at several stages of manufacture to improve final yield, to reduce added value and also to identify any systematic errors in production. Testing during production is used as a means of coarse filtering and usually only gross failures are rejected.

STC have facilities for fully automatic testing using a Hewlett Packard HP8753A network analyser. This test equipment can make measurements in the frequency or time domain, and also allows the unwanted effects of test jigs and fixtures to be gated out of the measured response. Jigs must be constructed such that undue force is not required to insert or remove devices. Damage to pins or to the gold plated header can result in device rejection. At the same time, firm contact is needed between the jig and device to reduce spurious effects. To ensure repeatability of results it is sometimes necessary to supply near-exact copies of jigs with devices. Even in such cases it is extremely difficult to achieve identical electrical responses from jigs that are physically near-identical. In such cases it is necessary to "tune" jigs to a standard device.

On some devices long term ageing at elevated temperatures is necessary before approved devices can be despatched. This is now essential on retiming filters for long-haul submerged repeaters, where a lifetime of 25 years is expected (Dawson[23]).

2.4 Design Procedures.

The SAW design process converts a customer specification into a working device by providing the process engineers with a photomask, quartz substrates and instructions. The process is iterative as the SAW device design includes building of prototypes and, if necessary, modification to mask design and/or to processing detail. Where possible, design iterations involve changes to the fabrication specification rather than the purchase of expensive new photomasks. These changes are usually related to the thickness of the aluminium film deposited. More recently, and partly as a result of information produced during this project, performance modifications to a given photomask have been achieved by selecting a different quartz cut and compensating with rotation of the device structure during the mask alignment process. However, only minor performance modifications can be made in processing using these techniques and therefore it is essential that the photomask design process meets as closely as possible the customer specification at the first attempt.

Design and specification of the photomask can be broken

down into several stages, target specification, transducer design, materials selection and photomask layout. Given a target electrical performance each of the interdigital transducer layouts are generated. The transducer design is then converted into a geometrical layout that can be given to a mask-maker. Finally a chromium-coated glass mask is manufactured, in STC's case by a contract mask-making house. The mask-maker will examine the final mask for faults such as line breaks, shorts and other discontinuities, but the very fine line dimensions mean that only when the mask is used for device manufacture can it be fully evaluated.

Within the SAW department at STC the major design task is the generation of an interdigital transducer pattern. All design takes place on a Hewlett-Packard 9845B desk top computer using a suite of programs which run independently, but import and export data in a standard format. The following sections describe the design process used by STC with some reference to general concepts (see also Matthews [12] and Morgan [10]).

2.4.1 Filter Design.

Surface wave filters belong to the class of filters known as tranerval filters or finite impulse-response filters. Generally electronic filtering using, for example, lumped element LC circuits is viewed in the frequency domain and the passbands and stopbands result from resonances in the LC networks. A desired frequency response, low pass, high pass or band pass, is achieved by adjusting the reactive components of the lumped elements.

Frequency filtering can also be viewed in the time domain. The incoming signal in the form of a propagating wave is passed through a number of delay paths and the delayed signals are summed to give an output (see Figure 8). Some of the delayed signals will add constructively to form the passband and others destructively to form the stopband, and therefore the incoming signal is filtered. The development of the interdigital transducer allowed practical realisation of transversal filters due to the lower acoustic velocity and smaller wavelengths. The individual electrodes of the interdigital transducer can be thought of as the taps of a transversal filter with summation on the electrode busbars. In Figure 8 the taps of a tranversal filter are shown to have individual

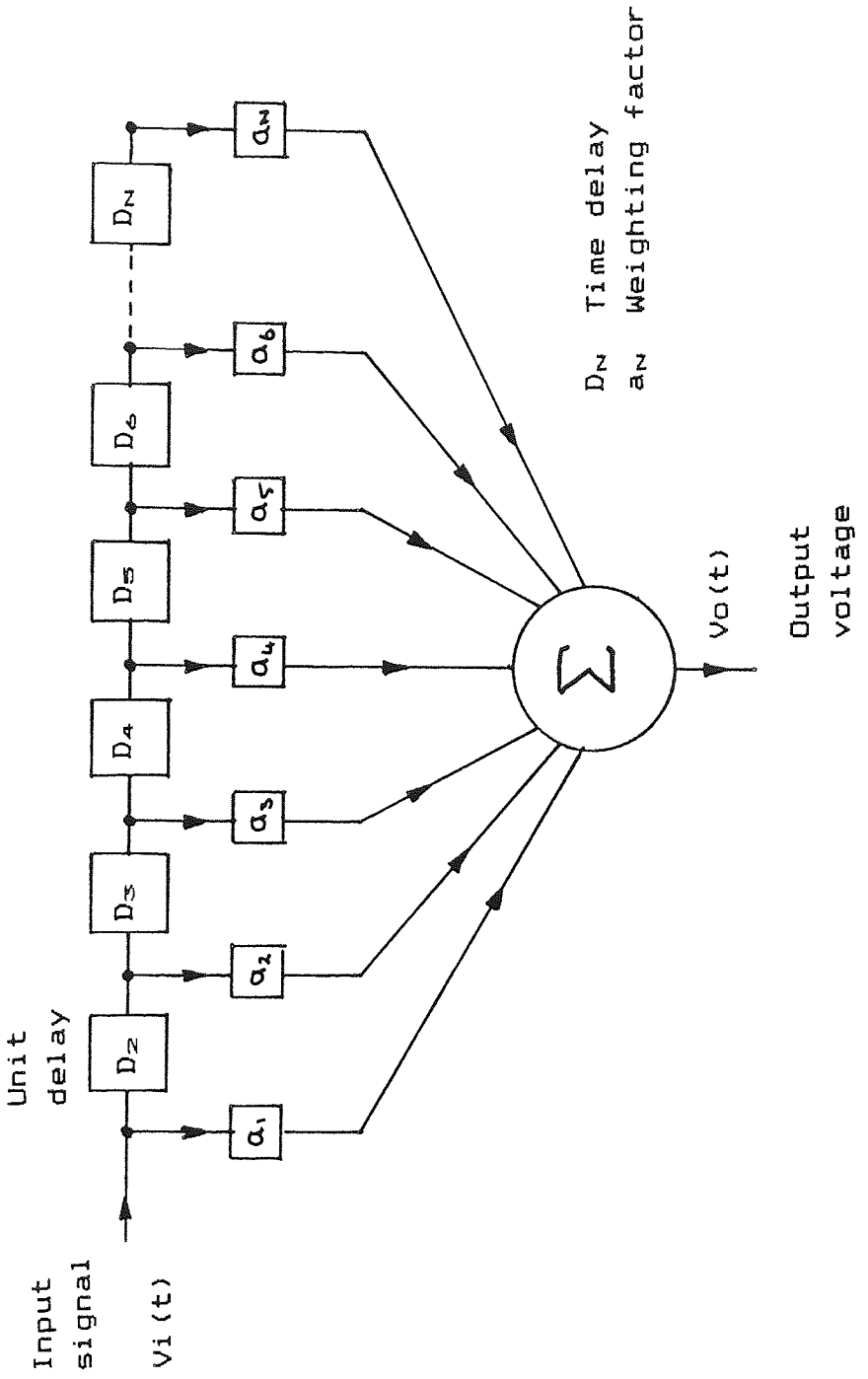

FIGURE 8 Transversal Filter

weights. The most common means of weighting the output from each "tap" of a SAW filter is to vary the overlap between adjacent electrodes (apodisation).

Several models are available and well documented for the design of SAW transducers and complete filters. One of the most common is the impulse-response model, and a modified version of this model has been developed by STC for SAW filter design. Whilst this is a simplified model and ignores many second-order effects, it is generally considered adequate for low coupling coefficient substrates such as quartz. The basis of this model is that an electrical impulse when applied to the input transducer electrodes will produce a surface distortion. This distortion propagates away from the input transducer and induces an output voltage as each delta function distortion passes under one of the electrodes of the output transducer. For a filter of two transducers, the total impulse-response is the convolution of the individual impulse-responses and the frequency response is the Fourier transform of the impulse-response.

When undertaking the design of a SAW filter, the first task of the designer is to decide how to split the total response between the two transducers. Several approaches are possible and much depends upon the experience of the designer. For example, the required response could be split equally between the two transducers or almost entirely based upon one transducer with the other being of a wide bandwidth. Generally transducers are designed to meet specific requirements of stopband rejection, passband shape, roll-off, bandwidth, insertion loss, nulls etc.

The STC design capability consists of over forty separate analysis and synthesis programs, some of which are design aids such as editing tools and others are modified programs to include weighting and window techniques. They allow a flexible route to a final working device and to be most effective require considerable knowledge input. The design procedure begins with the creation of a target specification file for each of the two transducers. This specification allows critical aspects of the required response such as roll-off or passband shape to be given a design weighting.

Synthesis programs are available which convert the output of the target specification into a connect sequence for

a transducer. The designer must choose the general transducer format as separate programs are used for uniform or weighted transducers. The response of the resulting transducers can be analysed either singly or as a complete filter. If necessary, modifications can be made to the transducers to more closely achieve the desired response.

Once the transducers have been designed the next step is to "construct" the SAW device by defining the exact cut of quartz substrate and metal film thickness. These decisions are dependent upon application details such as temperature performance and transducer impedances. The relationship between transducer period and operating frequency has been described in Chapter 1. The centre to centre transducer spacing determines the group delay of the SAW filter.

The final task converts the design into a repeat pattern which is used by the mask-maker to produce a photomask. To assist the mask-maker, it is necessary to specify the SAW device transducers in terms of "address units". An address unit is the fixed linewidth generated by the E-beam when writing the SAW transducer pattern onto the photomask. When dimensioning a SAW device the designer ensures that the specified finger widths can be built up from an integer number of defined address units. In general address units are specified in the range of 0.2 to 0.5um to an accuracy of 0.001um. This places a known limitation on the accuracy of photomasks and in most cases slight process modification is required to achieve the correct centre frequency.

The low-loss investigation takes into account the design procedures available as well as the ability to input data on new quartz cuts. The technical review of Chapter 3 identifies devices that can be analysed with the minimum of modification to existing procedures. As a result, work reported concentrates on the single phase unidirectional transducer, a structure which also satisfies production constraints.

2.4.2 Resonator Design

The basic structure and application of SAW resonators is described in Chapter 1, Section 1.3.3.3. The SAW resonator is one example of a surface wave reflection

grating device, others being pulse compression filters and reflective array compressors (see for example Matthews[12]). In the SAW resonator, a periodic array of grooves or metal electrodes form a reflection grating which reflects the propagating acoustic wave. Two such gratings create an acoustic resonant cavity in which there are two frequency selective mechanisms (Morgan[10]), the frequency variation of the reflection coefficient and the cavity resonances. All but one of the cavity resonances can be suppressed because the reflection coefficient value approaches unity over only a small frequency band.

The magnitude of the reflection coefficient for a single grating element is very small, typically less than 0.01, and therefore a practical grating consists of several hundred stripes or grooves. A practical resonator must include some means of launching and detecting acoustic waves. There are two common arrangements both of which require an IDT to be placed in the resonant cavity (Figure 9). A one-port device uses a single IDT placed between the reflectors, represented as an equivalent circuit with a series resonant arm in parallel with the transducer capacitance (Figure 9(a)). This circuit is identical to that of conventional bulk-wave resonators. The two-port resonator has two IDT's placed between the reflector gratings with an equivalent circuit as shown in Figure 9(b). This is the more usual configuration of a SAW resonator as would be used as the frequency selective element in a SAW oscillator.

Matthews[12] describes one of the most attractive features of reflection grating devices as being their defect tolerance. In reflection gratings, common defects such as line breaks or unwanted joins cause only very small effects. In transversal filters such defects in the interdigital transducer can cause electrical shorts or open circuits. This is particularly useful at high frequencies and with high 'Q' resonators where it becomes difficult to manufacture defect-free devices.

The design procedure for SAW resonators is more compact than that for filters. A single program based upon the scatter matrix model of Rosenberg and Coldren[24] analyses a two-port resonator structure on ST-X Quartz with a 1:1 mark-space ratio. The program is not a synthesis procedure in that the designer must input all necessary information to physically describe the

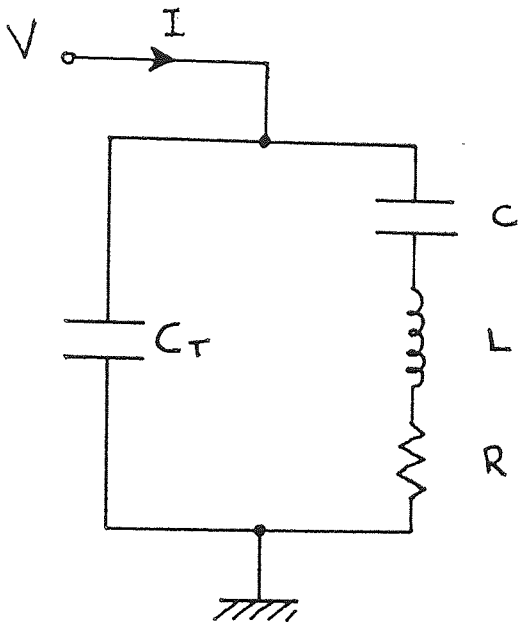

One-port resonator

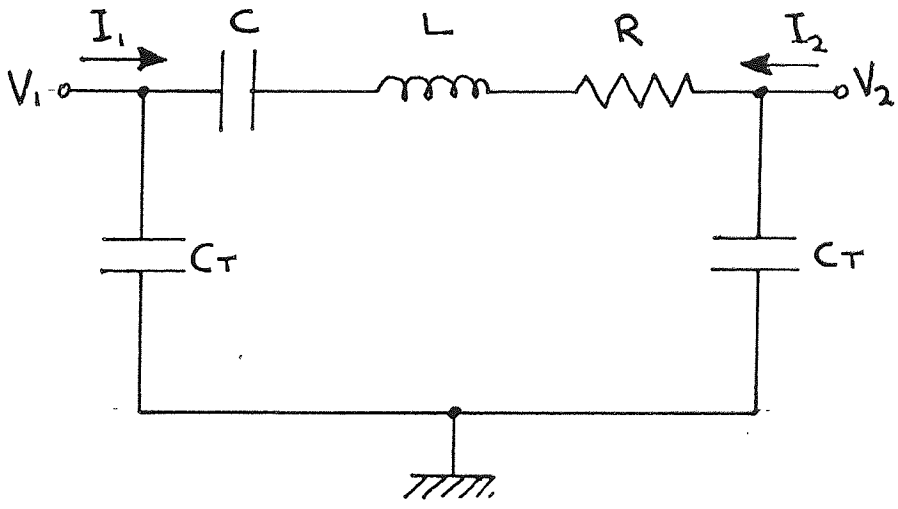

Two-port resonator

FIGURE 9 Equivalent Circuit for a Resonator

resonator. This information includes:

Number of transducer fingers
Number of reflector stripes/grooves
Transducer-transducer gap
Grating transducer gap
Film thickness.

The program assists the designer in prompting for answers within specific ranges of values. However the design relies upon the considerable knowledge of the designer to adjust the device details in a non-automatic iterative manner.

Datta[25], in reviewing SAW resonator design, describes the importance of the apparent penetration depth of the reflection grating. Around the synchronous frequency of the mirror array the stripes will be separated by one half wavelength and reflected acoustic waves will add in phase. Although the reflectivity of each stripe is small, an array of many stripes will have a total reflectivity approaching 100%. The array will appear as a single reflector located some distance into the grating. This penetration depth is important in determining the cavity length when two reflectors are used as a resonator. This information is also used to locate the transducers such that they are positioned at acoustic potential maxima. STC have a program which searches for near ideal penetration depths and hence reflector lengths for a given device specification.

Once a design has been optimised, the geometrical layout for photomask specification is identical to the method used for SAW filters. STC design a limited range of SAW resonators, all based upon shorted aluminium striped reflectors and mostly with uniform transducers comprising single finger or split finger electrodes. A few structures have been made using apodised transducers but with generally inferior results.

The paired or coupled resonator is a specific type of narrow band low-loss filter and is reviewed in Chapter 3. Work reported demonstrates the potential for coupled resonator filters with very low insertion loss. The effect of device layout and interconnect method is also demonstrated with practical results.

2.5 Summary.

This chapter has described the influences on the scope of this research project. The need for development in three distinct but related areas has been outlined. These are, reduced insertion loss, improved temperature performance and higher operating frequencies. Successful achievement of these goals also requires a review of manufacturing processes. The salient points from the review in Chapters 1 and 2 are:

STC operate in the professional, low volume, high value market, specifically telecommunications and military radio.

The existing fabrication procedures allow production of high frequency devices, albeit with variable yield.

STC do not appear to fully exploit the availability of in-house grown quartz.

STC have not responded to the need for low insertion loss devices.

Two devices, central to STC's marketplace, were chosen for detailed development and form the vehicles for this research project. They are:

A PCM retiming filter at frequencies upto 700MHz and suitable for eventual manufacture at 1.2GHz.

A narrowband filter suitable for front-end RF application at frequencies in the range 400-500MHz.

3. TECHNICAL REVIEW.

3.1 Insertion Loss.

3.1.1 Loss Mechanisms.

Datta[25] reviews, in a study of SAW bandpass filters, first and second-order loss mechanisms. Insertion loss, for the transmitting IDT, is defined as the power delivered to the forward travelling surface wave as a fraction of the available power. Based upon the equivalent circuit of Figure 9, the insertion loss, in dB, is

$$IL = -10\log_{10}\frac{0.5Vt^2Ga}{V^2/4Rg} \qquad (1)$$

The factor of 0.5 is due to the bidirectionality of the IDT. This equation can be rewritten as

$$-10\log_{10}\frac{2GaRg}{(1 + GaRg)^2 + [Rg(2\pi fC_T + Ba)]^2} \qquad (2)$$

where:

V	Source voltage
Vt	Voltage across the IDT
Ga	Radiation conductance
Rg	Source impedance
C_T	Transducer capacitance
Ba	Radiation susceptance

Datta comments that the overall frequency response of an IDT comes from two sources; the design of the IDT itself, with transmitter response function u(f), and external circuit conditions which give a contribution Hm(f). Ga and Ba are usually strongly frequency dependent compared to $2\pi fC_T$. If Ga is much smaller than $2\pi fC_T$, the frequency dependence of Hm over the passband can be ignored. However, if Ga is comparable to $2\pi fC_T$, Hm can contribute significantly, thus distorting the passband shape. The ratio of $2\pi fC_T$ to Ga is termed the acoustic quality factor, Qa, that is

$$Qa = \frac{2\pi fC_T}{Ga} \qquad (3)$$

at centre frequency.

A high Qa signifies a weak coupling; a low Qa indicates strong coupling.

Lewis et al[14] give a peak value for Ga, that is a value at centre frequency, fo, of:

$$Ga = 8foCsN^2k^2 \qquad (4)$$

where: Cs Capacitance per finger pair
N Number of finger pairs
k^2 Piezoelectrical coupling coefficient.

From this is developed the concept of optimum (maximum) fractional bandwidth for a given substrate material. This optimum condition holds for the case of acoustic quality factor, Qa, being equal to the electrical quality factor, Qe. From equations (3) and (4) it follows that;

$$Qe = \frac{\pi}{4Nk^2} \qquad (5)$$

and the optimum number of finger pairs, N(opt), is given by;

$$N(opt) = \left(\frac{\pi}{4k^2}\right)^{1/2} \qquad (6)$$

Values for N(opt) and for the corresponding fractional bandwidth for substrates are given in Table 1 (page25). Lewis[14] explains, that this argument does not mean that wide bandwidth devices cannot be made on low k^2 substrates. It does, however, signify that larger than optimum fractional bandwidths will incur an insertion loss penalty such that, even when tuned, an IDT will have an insertion loss greater than the 3dB minimum.

Datta[25] gives design examples for typical IDT configurations and shows that, for an ideal lossless structure, mis-match losses far exceed the bidirectional loss. Typical results for an apodised IDT on lithium niobate, with a 10% fractional bandwidth at 100MHz, are

Bidirectional loss - 3dB
Mis-match loss - 12dB
Apodisation loss - 1dB

The mis-match loss can be removed completely by conjugate or magnitude matching (Datta[25]). As most IDT's require interfacing with 50ohm source/load, conjugate matching requires an LC network to transform the IDT impedance to equal the load/source impedance at centre frequency. This result follows from equation (2) by leaving out the susceptive part, i.e.;

$$IL = 10 \log_{10} \frac{2GaRg}{(1 + GaRg)^2} \qquad (7)$$

When matched, the condition Rg = 1/Ga is satisfied, and in equation (7) the value of IL reduces to $10\log_{10}(0.5)$, or 3dB. Datta[25] comments on this result, which signifies that any IDT can be conjugate matched to a minimum loss of 3dB. To avoid the filter response being that of the LC circuit and not the IDT, it is important to select substrates according to fractional bandwidth. Alternatively, if larger than optimum bandwidths are required, they cannot be ideally matched and a larger insertion loss must be tolerated.

Associated with the problem of minimum loss and matching is the second-order condition of triple-transit echo. This problem is described in most SAW device texts, for example, Matthews[12], Lewis et al[14] and Datta[25]. Triple-transit echo (TTE) arises because of the nature of the IDT. Having two acoustic ports and one electrical port, it is impossible to simultaneously match all ports. The TTE is that portion of the main acoustic signal that is reflected from the output transducer back to the input transducer and returned again, by reflection, to the output transducer. TTE lags the main acoustic signal by twice the time delay between transducers, and vectorially adds with the main signal to create distortion. This distortion manifests itself, in the frequency domain, as a periodic ripple in the passband.

The level of triple-transit suppresion (TTS), is directly linked to the degree of matching of the IDT to its generator or load. Snow, writing in Matthews[12], illustrates the trade-off between insertion loss and TTS, as shown in Figure 10. This shows that when the transmission loss for an IDT is at a minimum, 3dB for conjugate matching, the reflection loss is 6dB per transducer. Therefore with perfect matching, and ignoring

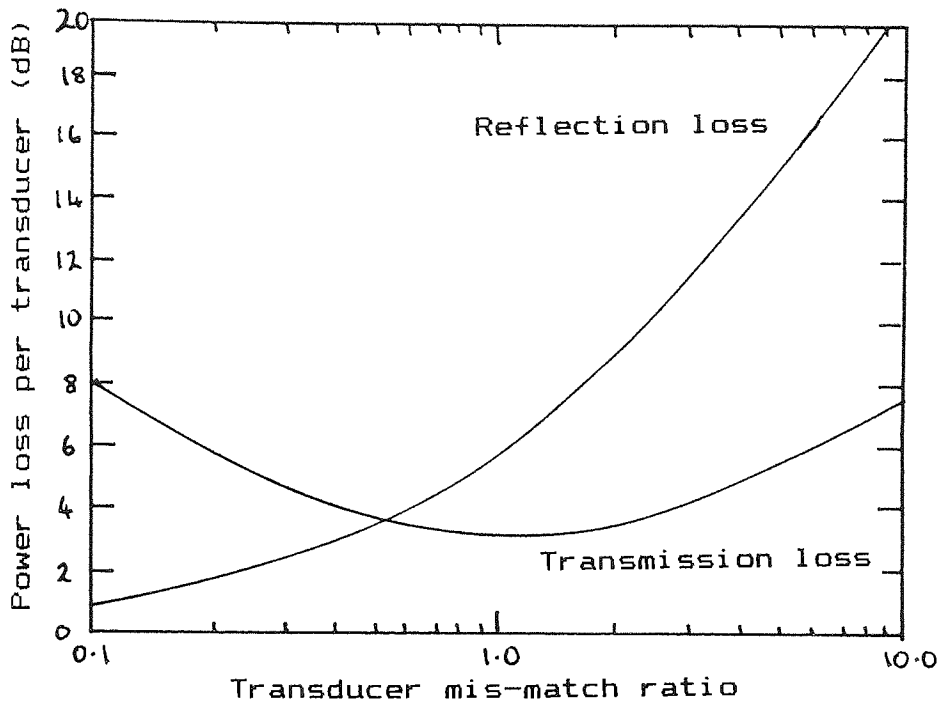

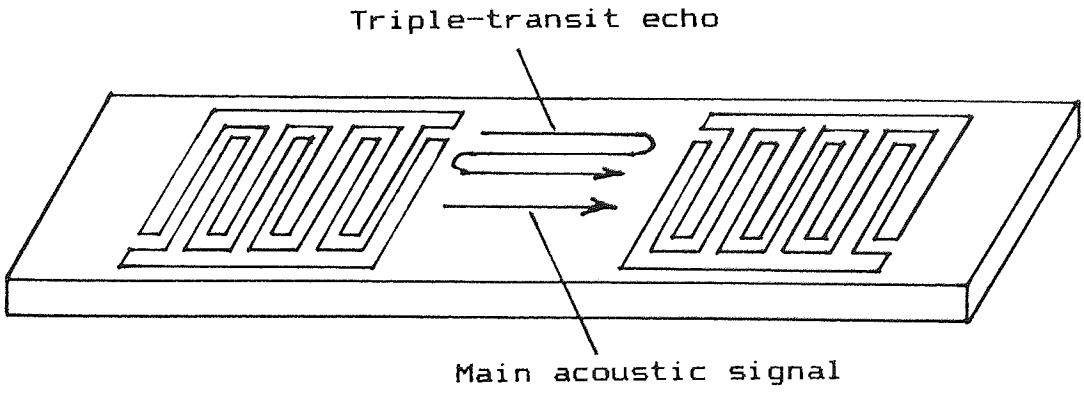

Figure 10 Triple Transit Signal

all other loss mechanisms, the minimum TTS is 12dB. Associated with this is a passband ripple of 4dB peak to peak (Matthews[12]). This situation is unacceptable (Lewis et al[14]), and most devices are deliberately operated in a mis-matched condition with resultant insertion losses much greater than the 6dB minimum. In practice filters and delay lines are often used without matching.

Various schemes have been put forward to reduce the TTE and hence allow conjugate matching and therefore low insertion loss. Most ideas have sought to achieve unidirectionl transmission of the acoustic wave. Before discussing these methods, which form the basis for much of the project work reported later, there are several other loss mechanisms that need to be mentioned.

TTE is one of several internal reflections arising because of regenerative effects. Mechanical electrical loading (MEL) also gives rise to internal reflections (Datta[25]). MEL reflections are caused by the edge discontinuities of the electrodes. IDT's with single-finger or solid electrodes have electrode spacings of half an acoustic wavelength, and therefore MEL reflections add constructively giving passband distortion. This problem can be overcome by using split-finger electrodes such that the spacing between fingers becomes one quarter of a wavelength and MEL reflections cancel. This solution creates the additional problem of fine-line resolution on high frequency devices.

There are several other sources of loss. These include (Lewis et al[14]), acoustic diffraction and propagation losses, beam steering effects, the excitation of unwanted bulk waves, end effects due to fringing of the electrostatic field and ohmic losses due to current flow in the electrodes. The level of some of these problem effects can be reduced at the design stage. For example, choice of substrate reduces beam steering and hence diffraction effects. Unwanted bulk waves can be attenuated by ensuring that the back surface of the SAW substrate is roughened or simply not polished.

3.1.2 Unidirectional Transducers.

The objective of this review is to identify techniques

that will allow the realisation of a high frequency (greater than 500MHz), low-loss SAW filter for PCM timing extraction.

Lewis et al[14], writing in 1984, list the major solutions which have been proposed to reduce the three-port IDT to a two-port by completely decoupling one acoustic port. These are:

Multi-strip-coupler designs (Marshall et al[26])
Three-phase unidirectional IDT (Rosenfield et al[27])
Group-type unidirectional IDT (Yamanouchi et al[28])
Single-phase unidirectional IDT (Hartmann et al[29])
Interdigitated IDT (Lewis[30])

More recently other techniques have been reported including:

Floating electrode single-phase structures (Yamanouchi and Furoyashiki[31])
Natural single-phase unidirectional IDT (Wright[32])

In addition many papers report specific improvements to these general methods.

The multi-strip coupler (MSC) mirror (Marshall et al[26]) utilises the track changing properties of the MSC. The concept is shown in Figure 11. To give complete power transfer between tracks an MSC must be of a defined transfer length, L_T. At a distance $L_T/2$ only half the power is transferred, but with a 90° phase lead (Figure 11a). Further, if an MSC of length $L_T/2$ is fed with a signal in track A and the outputs from tracks A and B are switched round (Figure 11b), all the power emerges from the input port in track A. Marshall et al[26] demonstrate this with a U-shaped MSC as shown in Figure 11c. With a tuned and matched bidirectional IDT placed within the U, but off-set from the centre by one-eighth wavelength in the forward direction, the phase difference of the waves incident upon the arms of the "U" will be 90°, and all the acoustic energy will appear in one direction (Figure 11d).

Marshall et al[26] demonstrate the U-shaped MSC device on lithium niobate, producing a filter with 4.5dB insertion loss and a 22MHz bandwidth at a centre frequency of 122MHz. Marshall argues that this technique has advantages of:

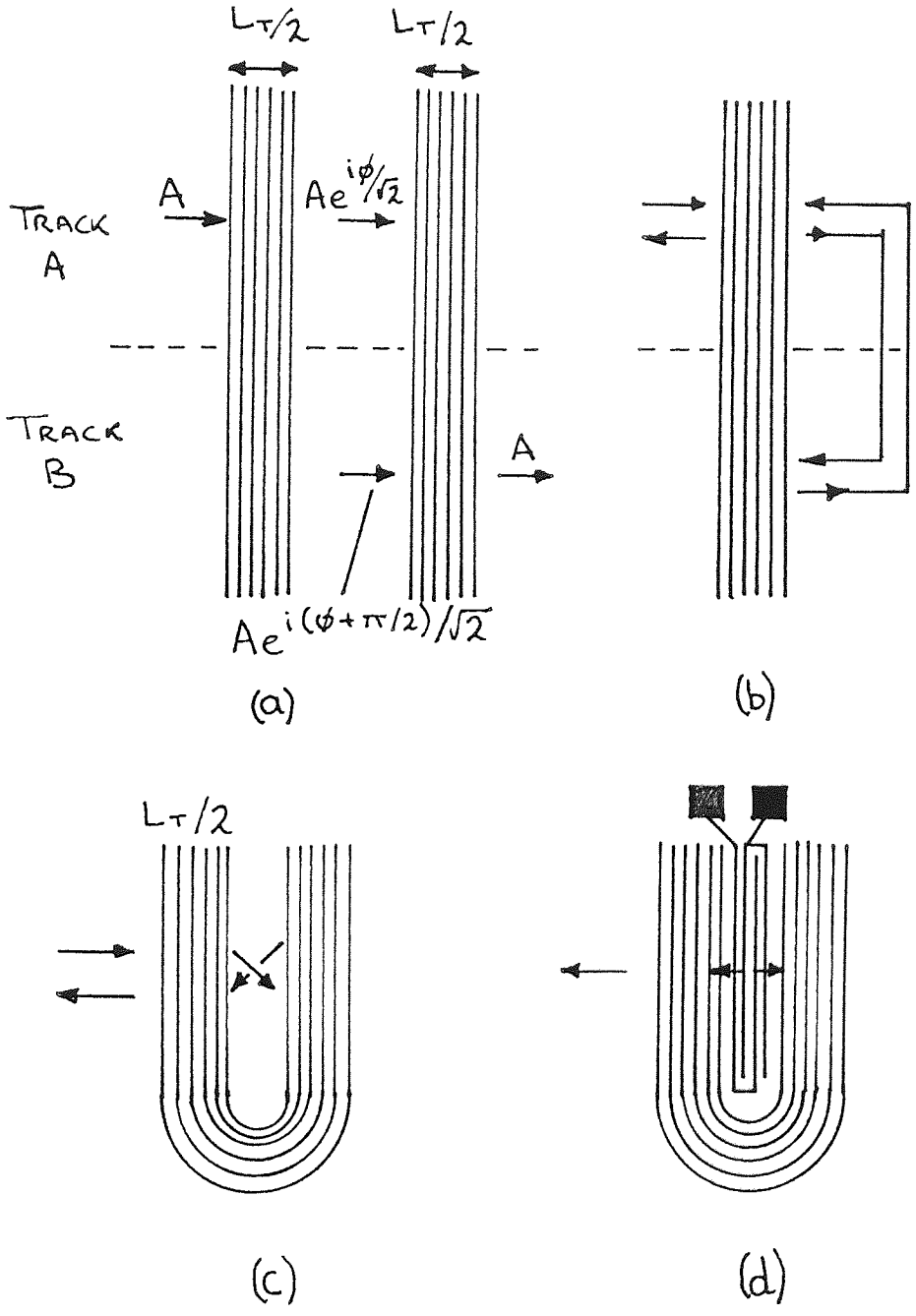

FIGURE 11 MSC Unidirectional Transducer

Ease of manufacture (single metallisation)
Suitable for wide bandwidths
No additional electronics components.

Disadvantages are associated with the U-shape, which requires extra substrate area and introduces parasitic losses. Marshall et al[26] propose that to reduce the 20% energy loss in the reflector, a piezoelectrically inactive layer should be introduced between the curved part of the MSC and the substrate. This would increase fabrication complexity. The technique will also only work effectively on high k^2 substrates and not on quartz.

The three-phase unidirectional transducer (TPUDT) first described by Rosenfield et al[27], reduces bidirectional loss by exciting the surface wave with three sets of IDT's driven 120° out of phase. The layout of a TPUDT device is shown in Figure 12. Each IDT has three electrodes per acoustic wavelength, each being driven via a phase shifting network, such that waves add constructively in the forward direction only. Rosenfield et al [27] argue that the MSC structure described above has problems of increased parasitic losses with long IDT's, and is not suitable for narrowband devices, unlike the TPUDT.

Rosenfield et al demonstrate both narrowband and wideband devices, the former with 3dB loss at 90MHz centre frequency, and the latter with 2dB loss at 33MHz. In the narrowband version the triple-transit suppression was 54dB. Lewis et al[14] describe the disadvantages of the TPUDT. These are fabrication complexity, arising from the need for two metallisation processes and air-gap cross-overs, and the matching complexity to give three-phase drive. The matching circuit of Rosenfield et al[27] has a total of 14 separate components.

Yamanouchi et al[28] first proposed the group-type unidirectional transducer (GUDT) as a means of overcoming the fabrication complexities of the TPUDT. The structure of the GUDT is shown in Figure 13. It comprises groups of electrodes, each group containing relatively few electrodes. These are arranged collinearly and are excited via a 90° phase shift. The in-phase and quadrature ports are spacially separated by 1/4 wavelength and have identical filter responses. The surface waves add constructively in the forward direction, and cancel out in the reverse, thus producing

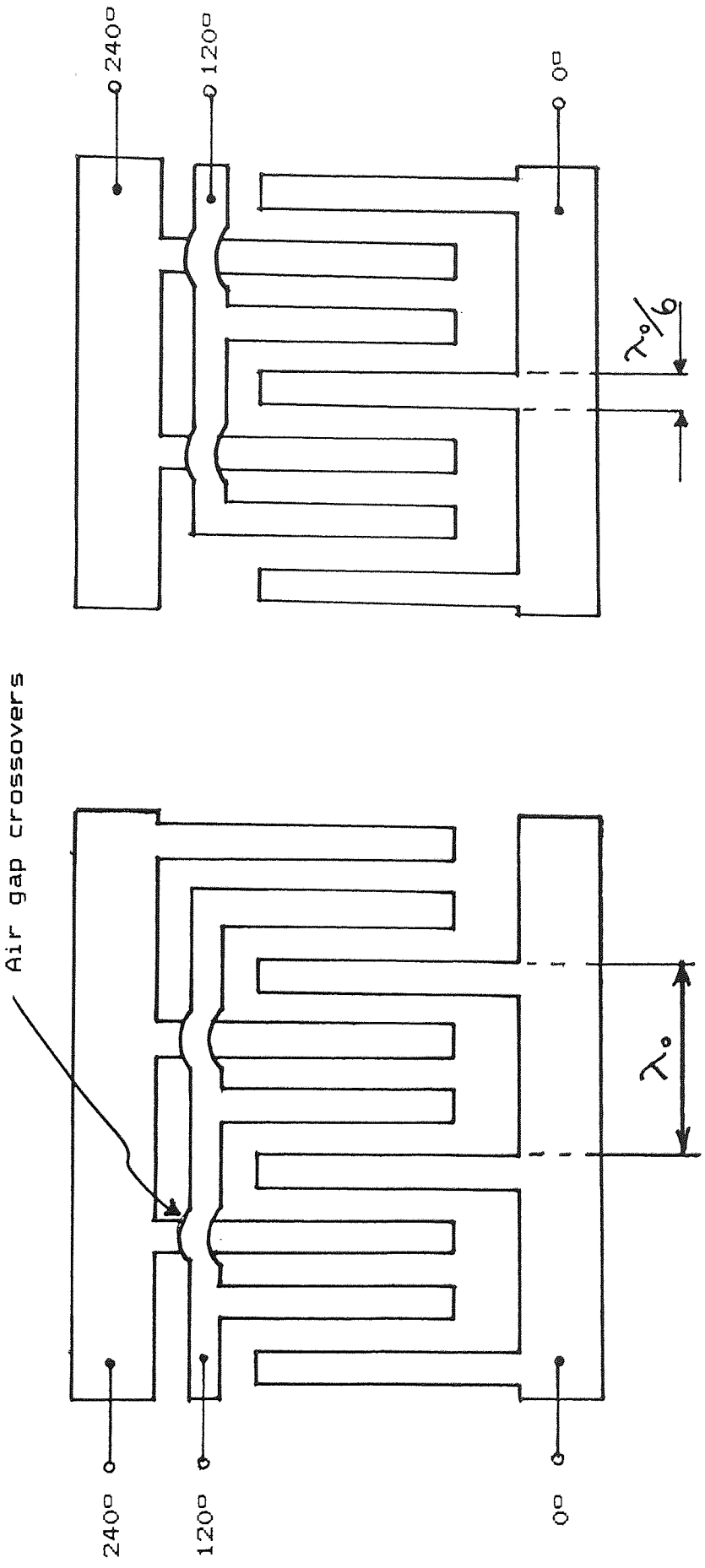

FIGURE 12 Three-Phase Unidirectional Transducer

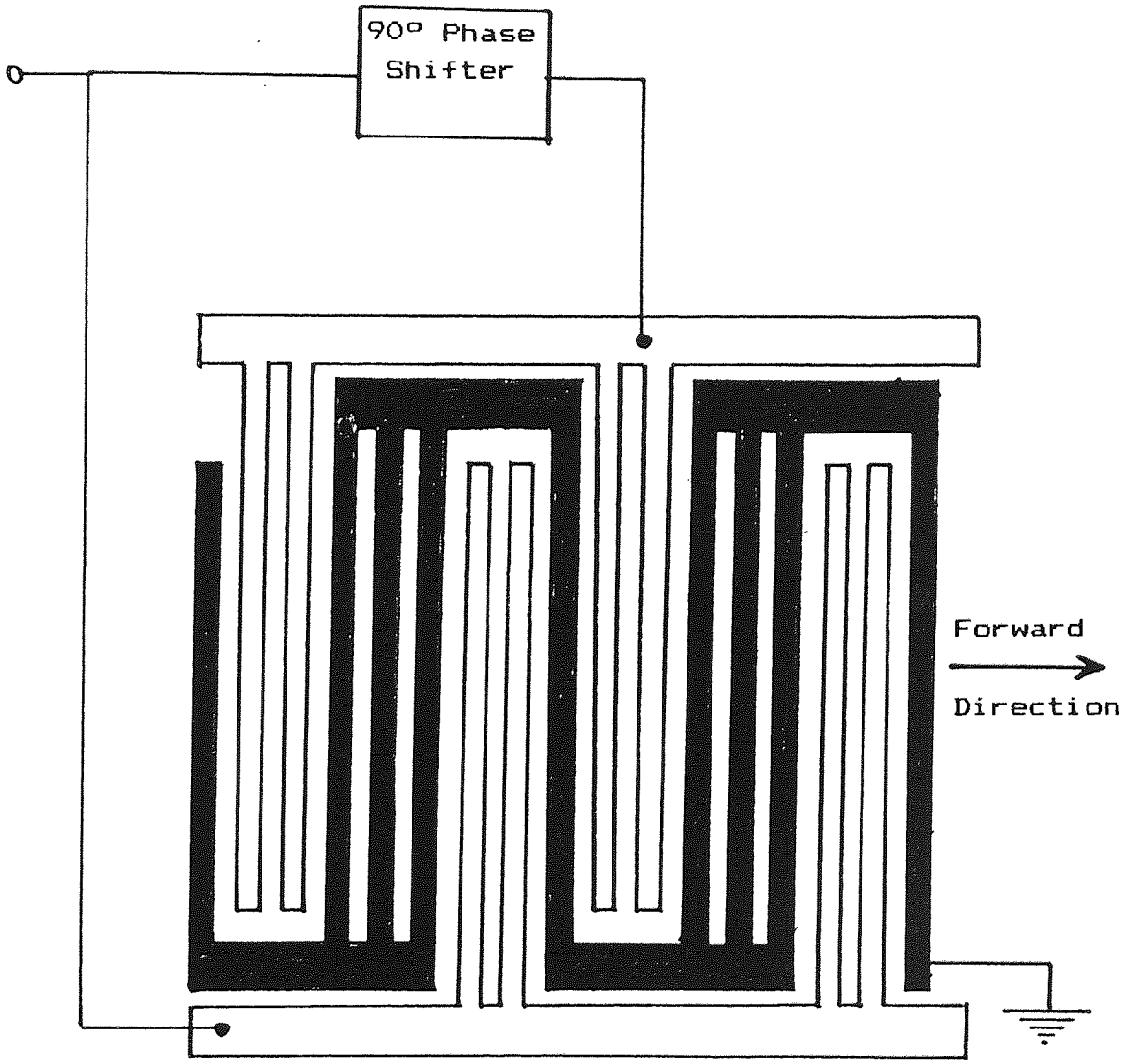

FIGURE 13 Group-Type Unidirectional Transducer

unidirectionality. Narrow bandwidth devices are made by increasing the number of groups. However, to ensure sidelobe suppression, Yamanouchi et al[28] show that the number of electrodes per group for the sender IDT should not equal that of the receiver IDT.

A GUDT device is demonstrated on lithium niobate with an insertion loss of 1.0dB and passband ripple of 0.2dB at a centre frequency of 99.2MHz. The 90° phase shift was achieved with a length of coaxial cable and there were no other matching components. The GUDT has the advantage of requiring only one processing step and does not require complex air-gap cross-overs.

Yamanouchi et al[28] accept that the coaxial cable phase shifter is unacceptable and propose an LC network. Lewis et al[14] argue that this is essentially a need for matching components, albeit not as complex as the TPUDT. Malocha et al[33] describe a tuning network using only two elements per transducer. Gautam et al[34] propose the incorporation of the tuning components onto the SAW chip itself in the form of thin film capacitors and integrated micro-inductors. This structure lends itself to large-scale manufacture and could be applied to the high volume SAW filter market.

It has long been recognised that half the minimum insertion loss of a single bidirectional device can be recovered by the addition of a third transducer. The interdigitated interdigital transducer(IIDT), proposed by Lewis[30], extends this idea to include four or more IDT's. The minimum theoretical insertion loss reduces according to:

$$IL = 10 \log_{10} ((N+1)/N) \text{ dB}$$

where N+1 is the number of input transducers and N is the number of output transducers. Lewis demonstrates a device on lithium niobate at 150MHz, with a 2dB insertion loss and >20dB stopband. This device has the advantage of requiring only a single metallisation step. However Lewis argues that it requires high k^2 materials and is therefore not a suitable structure for quartz.

Much recent work has been based on the single-phase unidirectional transducer (SPUDT) first proposed by Hartmann et al[29]. The SPUDT utilizes internal reflections within the IDT to achieve unidirectional

behaviour. The structure requires a centre of reflection one-eighth of a wavelength transposed from the centre of transduction. This is achieved, see Figure 14, by adding extra metalisation to one finger only of each split-finger in the IDT. The split-fingers reduce internal reflections in transduction. The extra metal overlays act as a separate reflector giving constructive interference in the forward direction only.

Hartmann et al[29] compare experimentally two devices, fabricated on ST-X quartz, which are identical except for the additional metal overlay. The SPUDT has a minimum insertion loss, when tuned, of 6.5dB compared to 12.5 dB for the bidirectional device. In addition, the SPUDT increased TTS from 20 to 25dB. Hartmann et al argue that these figures, whilst encouraging, are not as good as expected due to surface contamination problems.

The basic result, that unidirectionality requires a functional shift of one-eighth wavelength between IDT's and floating fingers, has been utilised in two important SPUDT designs. Yamanouchi and Furuyashiki[31] have proposed the floating electrode unidirectional transducer (FEUDT). In this device, see Figure 15, a combination of open and shorted metal strips are introduced based upon a normal split-finger electrode structure. The FEUDT utilises the principle that the acoustic impedance of a floating finger is greater than that of the free surface. Conversely, the acoustic impedance of shorted fingers is less than that of the free surface. Therefore by correct placement of the floating electrodes it is possible to ensure constructive addition of acoustic waves in the forward direction.

A device has been demonstrated on lithium niobate at 100MHz with an insertion loss of 2.3dB. Although this structure requires only a single fabrication step, it is based upon split-finger geometry. Further, to achieve the desired offsets requires the photolithographic resolution of dimensions as small as $\lambda_o/20$, with obvious implications on production difficulties at high frequencies.

The second device type to be based upon the results of Hartmann et al[29] is that of Lewis[35]. This device, Figure 16, is based upon a "ladder" transducer arrangement which has a sampling effect on the transducer frequency response. The basic arrangement comprises a transducer with offset reflector banks in the spaces

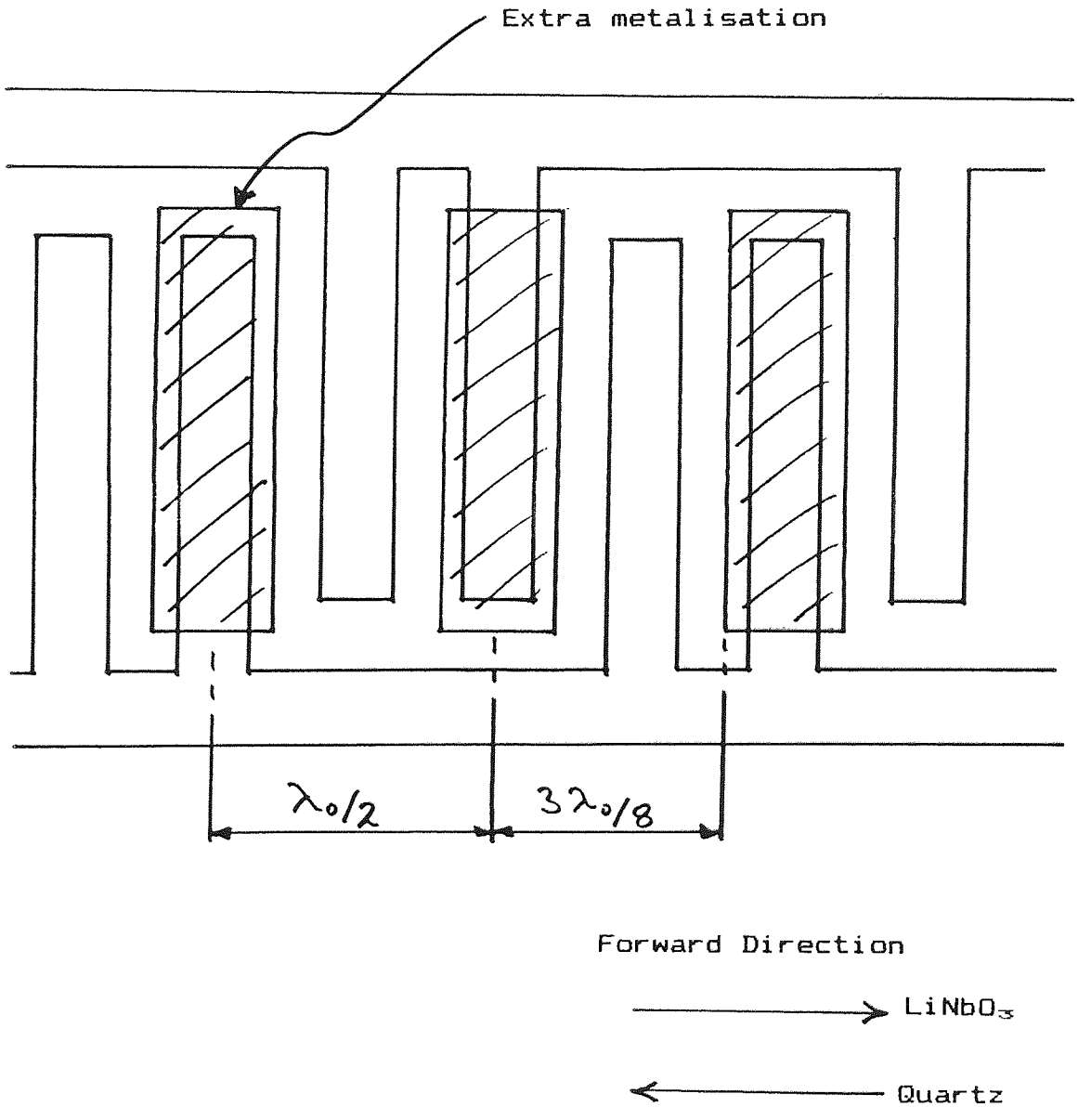

FIGURE 14 Single-Phase Unidirectional Transducer

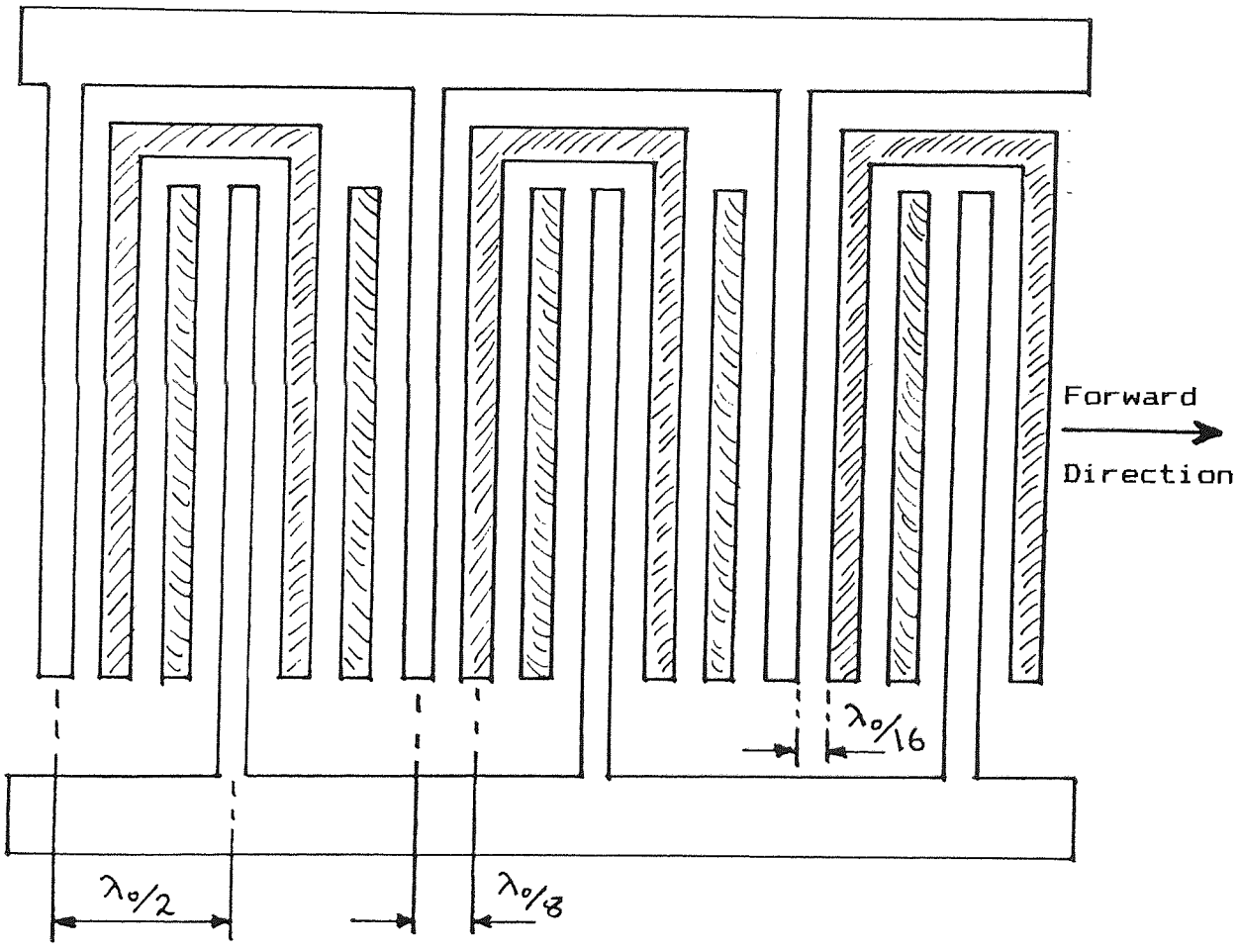

FIGURE 15 Floating Electrode Unidirectional Transducer

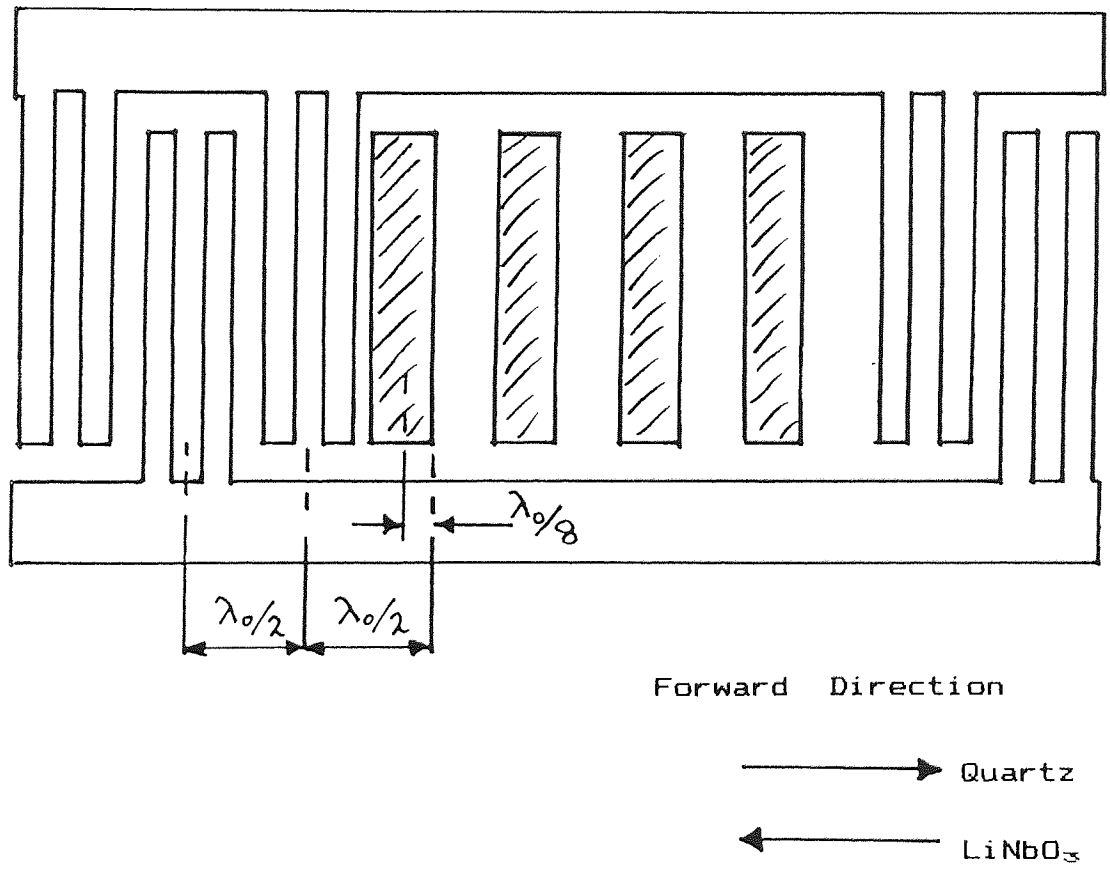

FIGURE 16 SPUDT with Offset Reflectors

between the active rungs of the "ladder". Lewis argues that although the device will occupy marginally more space than the equivalent unidirectional structure, it has the great advantage of single stage fabrication.

Lewis demonstrates this structure on lithium niobate, showing a matched 2.7dB insertion loss at 100MHz centre frequency. In each transducer the reflectors are offset one-eighth wavelength (the Hartmann result) towards the other transducer. Lewis also comments that the effect of sampling in a ladder structure is to introduce spurious sidelobes at intervals equal to the inverse of the sampling period. For a device of two transducers this problem can be reduced by interleaving the frequency reponses of each transducer such that only the main reponses combine. In the Lewis[35] device the rung to rung spacings are different for each transducer, thus creating different sampling periods. To reduce the problem of spurious reflections this device utilises split-finger electrodes in the active rungs.

This device requires single-stage fabrication with an upper frequency limitation imposed by split-finger electrodes. This problem has been overcome (Lewis[36]) with the use of "blooming" reflectors. These are placed either side each active transducer rung and are offset one-quarter wavelength towards the rung (Figure 17]). The purpose of these additional reflectors is to cancel the reflections that arise from the quarter wavelength active fingers. Lewis shows that on devices operating at 400MHz on ST-quartz the effect of the blooming reflectors is to substantially reduce the strong distortion in the passband.

Lewis[36] demonstrates devices, on quartz, utilising this rung, or ladder, structure at 400MHz. Each transducer contains both blooming and unidirectional transducers. With a bandwidth of approximately 300kHz and matched loss of 6dB the resultant passband plots show minimal ripple and very little deviation from linear phase. In addition to the advantage of simple fabrication, Lewis claims that this structure can employ various reflection mechanisms as well as reflectors of arbitrary dimensions. The main disadvantage is given as the limited out-of-band rejection due to sampling effects.

A very recent addition to SPUDT techniques is the natural SPUDT proposed by Wright[32]. As with other SPUDT

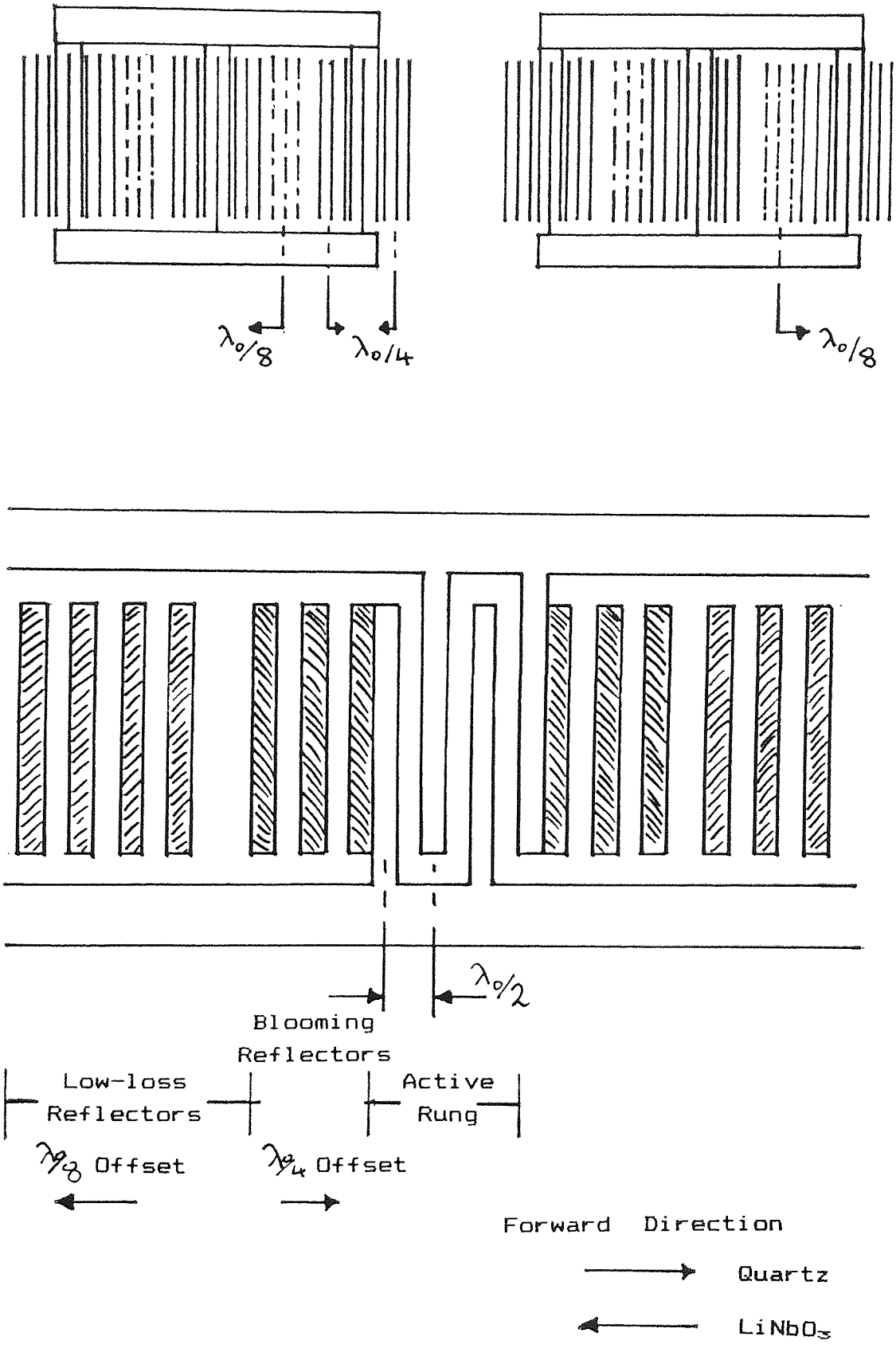

FIGURE 17 SPUDT with Offset and Blooming Reflectors

methods, the objective of this structure is to separate the centres of transduction and reflection in an IDT by one-eighth wavelength. The NSPUDT approach utilises special unconventional asymmetric crystal orientations. Wright shows that these orientations exist for most common SAW substrates. The main advantage of the NSPUDT is that the transducers are symmetrical with two electrodes per wavelength. The structure is therefore simple to fabricate from the photolithography viewpoint and is suitable for high frequency operation.

The major disadvantage of the NSPUDT (Wright[32]), is that for a given orientation and metalisation thickness the sense of directionality is fixed. A filter comprising two NSPUDT's would therefore be difficult to manufacture. A compromise device could contain a NSPUDT and a conventional IDT. Wright demonstrates test NSPUDT patterns on quartz and lithium niobate at approximately 100MHz. Typical results show directivity figures in the range 15-20dB. The results suggest fabrication difficulties associated with the need to locate the NSPUDT structure in terms of phase angle, magnitude of reflectivity and crystal orientation.

3.1.3 SAW Resonator Filters.

The previous section has reviewed the reported approaches to unidirectional transduction and low insertion loss. All were based upon transversal filter designs. It has long been recognised that where very narrow bandwidths are required the SAW resonator becomes an excellent low loss filter. This technique is now reviewed.

The SAW resonator is most often used as the frequency determining element in the feedback loop of a SAW oscillator, as described in Section 1.3.3.3. Many writers, for example Coldren and Rosenberg[18], Staples and Smythe[37] and Shreve[38], describe the SAW resonator as a very narrow bandwidth filter. A typical STC resonator may have the following characteristics in a 50ohm system:

Centre frequency	500MHz
Insertion loss	10dB
Loaded Q	10,000
Bandwidth (3dB)	50kHz
Bandwidth (%)	0.01%

Impedance matching of a SAW resonator using a simple LC arrangement reduces the insertion loss and lowers the device Q value, resulting in a larger fractional bandwidth. Insertion loss values as low as 1dB are achievable. Applications are limited, partly due to the problem of temperature stability (Lewis et al[14]). Even when manufactured on ST-X quartz, the potential frequency shift over a typical temperature band of -55°C to +125°C is 240ppm. In the 500MHz example this equates to a frequency variation with temperature of 120kHz, or +/-60kHz, whereas the matched bandwidth will be of the order of 100kHz. Lewis et al[14] highlight the search for improved temperature performance through the identification of new quartz cuts and alternative acoustic waves.

Multi-pole resonator filters have been developed to utilise the low insertion loss capability of SAW resonators. The work reported here will concentrate on two-pole, or coupled devices. Cross and Schmidt[40] review three configurations of two-pole resonator filters, collinear acoustic coupling, multi-strip coupling and transducer coupling (Figure 18). Much work has been reported on developments of these techniques, for example Coldren et al[39], Coldren and Rosenberg[41,18], Shreve [38] and Debois [42], and on other coupling techniques such as folded acoustic and waveguide.

Cross and Schmidt[40] review the basic coupling techniques. In the collinear structure the central grating, which is common to both cavities, is the coupling element. The strength of the central grating determines how much power is transferred from one cavity to the other.

In both multi-strip and transducer coupling each cavity has a distinct set of gratings. The resonators are conveniently arranged in parallel with the acoustic power in two separate tracks. In the multi-strip device coupling is effected by simply extending the electrodes of the coupler into both cavities. The degree of coupling is determined by the length and/or by the number of electrodes in the coupler.

In the transducer coupled structure a second transducer is placed in each cavity. The cavities are then coupled

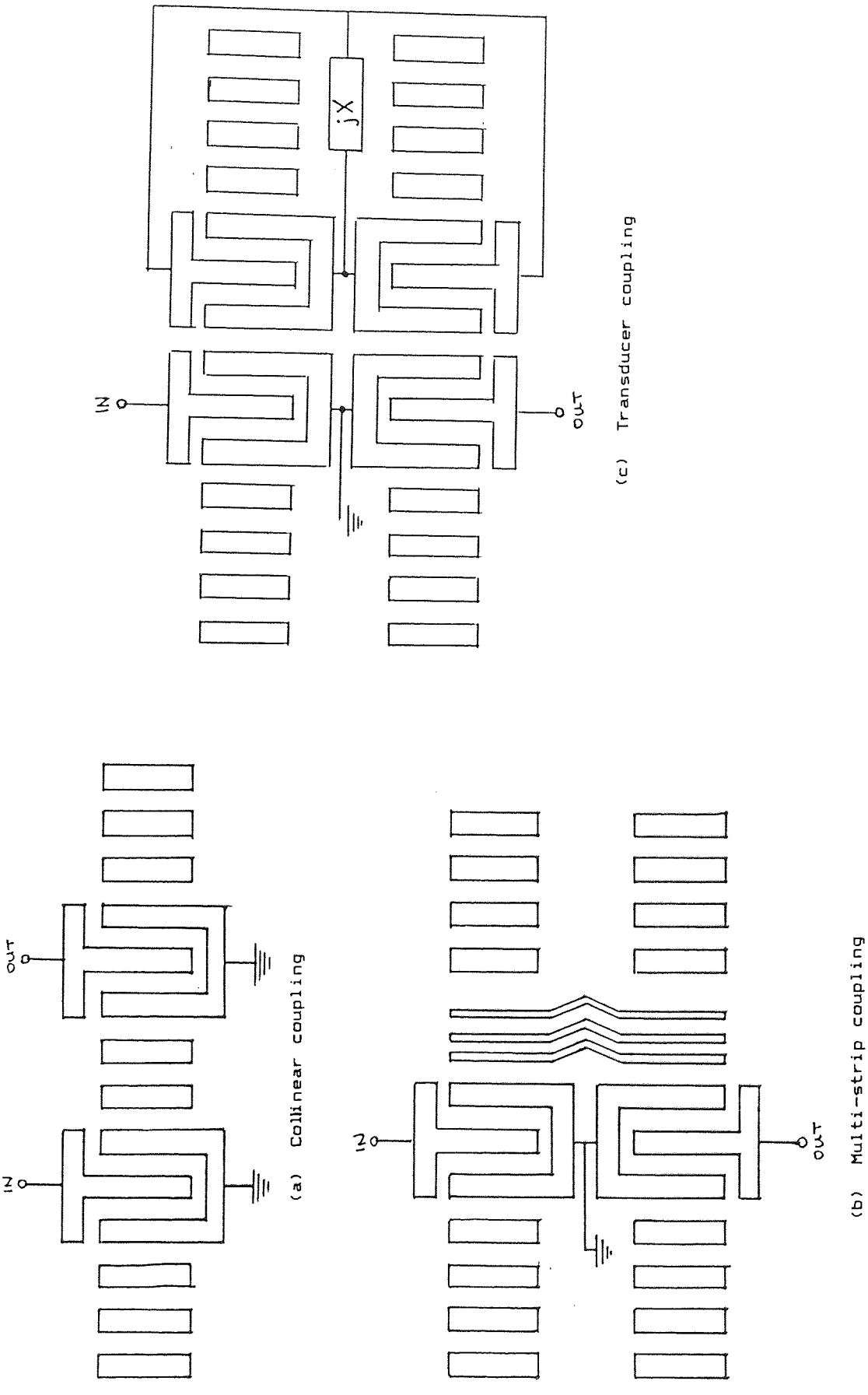

FIGURE 18 Coupled Resonator Filters

by connecting the transducers together, either directly or through an external electrical network. The external network provides a means for adjusting both the strength and phase of the cavity coupling. In its basic form this structure simply comprises a pair of two-port resonators with an external matching/connection circuit.

Cross and Schmidt[40] comment on the relative advantages of these three approaches. Collinear coupling is easy to design because coupling between cavities can be accomplished without disturbing the intrinsic cavity properties. As less energy is lost through end-gratings, collinear coupling also gives lower insertion loss. Multi-strip coupling offers the lowest sidelobes without the need for critical alignment of the coupler within the cavity. However the technique can be applied only on high coupling substrates. Transducer coupling offers flexibility through the use of external matching components. This external circuit can be used to contribute to passband shaping and as a convenient means for post-fabrication trimming of device performance.

Many practical examples of coupled resonator filters have been reported. Staples and Smythe[37] demonstrate a transverse coupled device on quartz at 75MHz with an insertion loss of 1dB and bandwidth of 70kHz. Shreve[38] describes a two-pole, transducer coupled device at 148MHz with a 42kHz bandwidth and 3.4dB insertion loss. Shreve also decribes some of the fabrication difficulties and trade-offs. In particular, frequency variation due to fabrication can be greater than device bandwidth. Also, wider bandwidths require greater matching complexity resulting in reduced side-lobe suppression.

Shreve[38], Debois[42] and Meyer and Gunes[43] address some of the fabrication problems of SAW resonator filters. Debois argues that random errors in manufacture preclude all but transducer coupling for close tolerance devices. With this technique, the reactive load on coupling transducers allows independent trimming and frequency adjustment. Debois also describes practical devices with split-finger electrodes and cosine weighting of transducers. Meyer and Gunes illustrate the problem of matching and packaging a six-pole 217MHz filter comprising three two-pole sections. Each two-pole filter has two reflection minima which are matched independently to the 50ohm line. When connected the three sections require matching into each individual header. The

resultant device has a bandwidth of 40kHz and loss of 10dB.

Coldren and Rosenberg[18] highlight the problem of temperature stability. It is argued that ST-X quartz is required for most coupled resonator applications, and that in some situations an improved temperature coefficient is desirable. A reduced temperature shift would result in easier manufacture due to narrower bandwidths being required.

3.1.4 Insertion Loss - Summary

Section 3.1 has reviewed the loss mechanisms in SAW filters and has described reported approaches to achieving low-loss through unidirectional transducers and coupled resonator filters. These two techniques satisfy separate and distinct requirements, based on fractional bandwidth.

Unidirectional transducer devices are low-loss transversal filters and have been reported with salient parameters as follows:

Centre frequency	100 - 400MHz
Fractional bandwidth	upto 25%
Insertion loss	as low as 1dB

This project requires the identification of a technique that will allow reliable fabrication of transversal filters for PCM transmission system retiming applications. Filters must be made on quartz with the following target specification:

Centre frequency	500 - 700MHz
Q	400 - 800
Bandwidth	1.0 MHz nominal
Insertion loss	5 - 10dB
Side-lobe rejection	>15dB

In addition, a requirement for a high degree of repeatability implies a minimum level of matching and fabrication complexity. Also, the need to manufacture on quartz immediately precludes techniques involving multi-strip couplers.

When ease of manufacture and matching are considered, the

most obvious choices are the group-type and single-phase unidirectional transducers. Lewis et al[14] argue that the SPUDT lends itself to simple matching, typically one inductor per transducer, whereas the GUDT requires at least two matching components per transducer.

The SPUDT structure proposed by Lewis[36] is the basis for the unidirectional transducer work in this project. Previous work suggests that this structure lends itself to simple manufacture within the specifications listed above.

Coupled resonator filters are applicable only at narrow bandwidths. Whilst a single resonator can be used as a very narrow bandwidth filter at frequencies upto 1.0GHz, coupled resonator devices have been reported as follows:

Centre frequency	75 - 250MHz
Fractional bandwidth	0.03%
Insertion loss	as low as 3dB

This project requires the development of a fabrication capability in narrow bandwidth, front-end RF filters with the following target specification:

Centre frequency	400 - 500MHz
Bandwidth	200kHz (0.05%)
Insertion loss	3.5dB maximum
Temperature band	-40 to +85°C

All writers agree that transducer coupled resonators offer the best approach in terms of flexibility and device trimming. Coldren and Rosenberg[18] argue that in some cases the temperature coefficient of ST-X quartz compromises device performance. In this project, work on transducer coupled resonators also includes a search for improved temperature performance. This is reported in the next section.

3.2 Temperature Performance.

3.2.1 Background.

This project is concerned only with SAW devices on quartz. In Sections 2.1 and 2.5 the reasons behind STC's involvement in quartz and possible areas for exploitation of in-house material are described. Traditionally ST-X

quartz has been used mainly because of its high thermal stability and zero power flow angle (Coldren and Rosenberg[18]). Although quartz has a zero first order temperature coefficient of delay, see Table 1, in some applications the second order coefficient must be compensated.

Lewis[44] reviews temperature compensation techniques applicable to SAW devices. Nine distinct approaches are given:

New orientations of existing materials
New piezoelectric crystals
Composite materials
New acoustic propagation modes
Temperature compensation through mechanical strain
Temperature compensation through external electrical components
Compensation through two SAW components
The use of multiple SAW paths connected electrically in parallel
Ovening of SAW devices

Lewis argues that although two materials are in general use as SAW substrates, quartz and lithium niobate, neither is ideal when all relevant parameters are considered for a particular application. For example, at bandwidths above 4% ST-X quartz devices suffer additional insertion loss and the alternative, lithium niobate, has a poor temperature stability. Also, SAW resonators for wide temperature band application are liable to a frequency drift greater than the 3dB bandwidth.

Lewis comments that whilst in theory full and detailed searches have been made for new improved orientations on quartz, this search has been hampered by the lack of a satisfactory set of elastic constant data. Lewis concludes that, for simple SAW components and narrow-band filters and resonators, the most likely temperature compensation techniques will be new propagation modes, new materials and to a lesser extent new cuts of existing materials. New materials are outside the scope of this project. The next section reviews new cuts, some of which utilise new propagation modes.

3.2.2 Temperature Compensation - New Cuts.

ST-X quartz is a singly rotated cut, requiring only one alignment and rotation of the crystal block in manufacture. It is also described as a +42.75° rotated Y-cut with acoustic propagation in the X-direction. The X, Y and Z terms refer to the crystal axes. This teminology is used at STC and therefore is adopted for this report. Another common crystallographic reference system (Brice[6]) is based upon Euler angles (θ, ϕ, ψ). Under this system ST-X quartz is described as having Euler angles

$$\theta = 132.75^\circ$$
$$\phi = 0$$
$$\psi = 0$$

Singly rotated cuts are simpler to manufacture, especially where a high rotational accuracy is required.

Several writers have reported complete searches for zero temperature coefficient of delay (TCD), examples being Newton[45] and Williams et al[46]. Newton reports several singly rotated cuts showing improvements over ST-X quartz with at best a TCD of -0.015ppm/°C². Williams et al concentrate on doubly rotated cuts and demonstrate several cuts with a TCD of approximately 0.01ppm/°C². Lewis et al[14] comment that such cuts have not generally been adopted due to increased fabrication difficulty.

This review has identified three recently reported cuts that may be applicable to SAW resonators and filters. These are:

SST	Lukaszek and Ballato[47]
X33	Webster[48]
LST	Shimizu and Tanaka[49]

The SST-cut combines a Y-axis rotation of -49.2° with a propagation direction of approximately 22° to the X-axis. Substrate preparation requires two rotations. Advantages claimed for the SST-cut are:

Improved TCD, 40% better than ST-quartz.
Higher coupling constant, 23% better than ST.
Lower acoustic attenuation.
Higher acoustic wave velocity.

Lukaszek and Ballato[47] show that small changes in acoustic propagation direction create large performance changes. Webster[48] argues that this sensitivity is a major disadvantage of the SST-cut.

X33-quartz is a singly rotated X-cut substrate with acoustic propagation in the Y-Z plane, rotated 33.44° from the Y-axis. Webster[48] claims that this cut offers relatively simple orientation. The main advantage of the X33-cut is a TCD of -0.0209 compared to -0.037ppm/°C² for ST-quartz. Additionally Webster argues that the X33-cut allows easy turnover-temperature manipulation by simple rotation of the SAW pattern at the photolithography stage. A similar modification on ST-quartz requires a new substrate at a different Y-axis rotation (Minowa et al[20]).

Both SST and X33 orientations utilise a true surface wave. Lewis[44] claims that other modes are needed for substantial temperature compensation improvements. These alternative waves generally travel just below the surface and are named surface-skimming bulk waves. Such waves have the added advantage of higher acoustic velocity.

Shimizu and Tanaka[49] describe the wave propagating in the LST-cut as a leaky surface wave. The LST-cut is a singly rotated Y-cut with acoustic propagation in the X-direction. It is therefore similar in orientation to the ST-cut but has Y-axis rotation of approximately -75° compared with +42.75° for ST-quartz (Figure 19). Selection of this particular cut, by Shimizu and Tanaka, is based upon an analysis of the electro-mechanical coupling constant, TCD and attenuation constant over the full range of rotated Y-cuts. It is reported that over a small range of rotation angle only the leaky surface wave will be generated. Further, at certain angles the attenuation constant will be small, coupled with a very low TCD. These parameters are shown in Figure 20.

Shimizu and Tanaka[49] present experimental results for a range of LST-cuts with Y-rotations of -74.3° to -75.3°. Several advantages are claimed based upon trials with a simple interdigital transducer:

Improved TCD, approximately 5 times better than ST.
Higher acoustic velocity, 25% better than ST.
Low attenuation constant, compared with other non-SAW, such as surface skimming bulk waves.

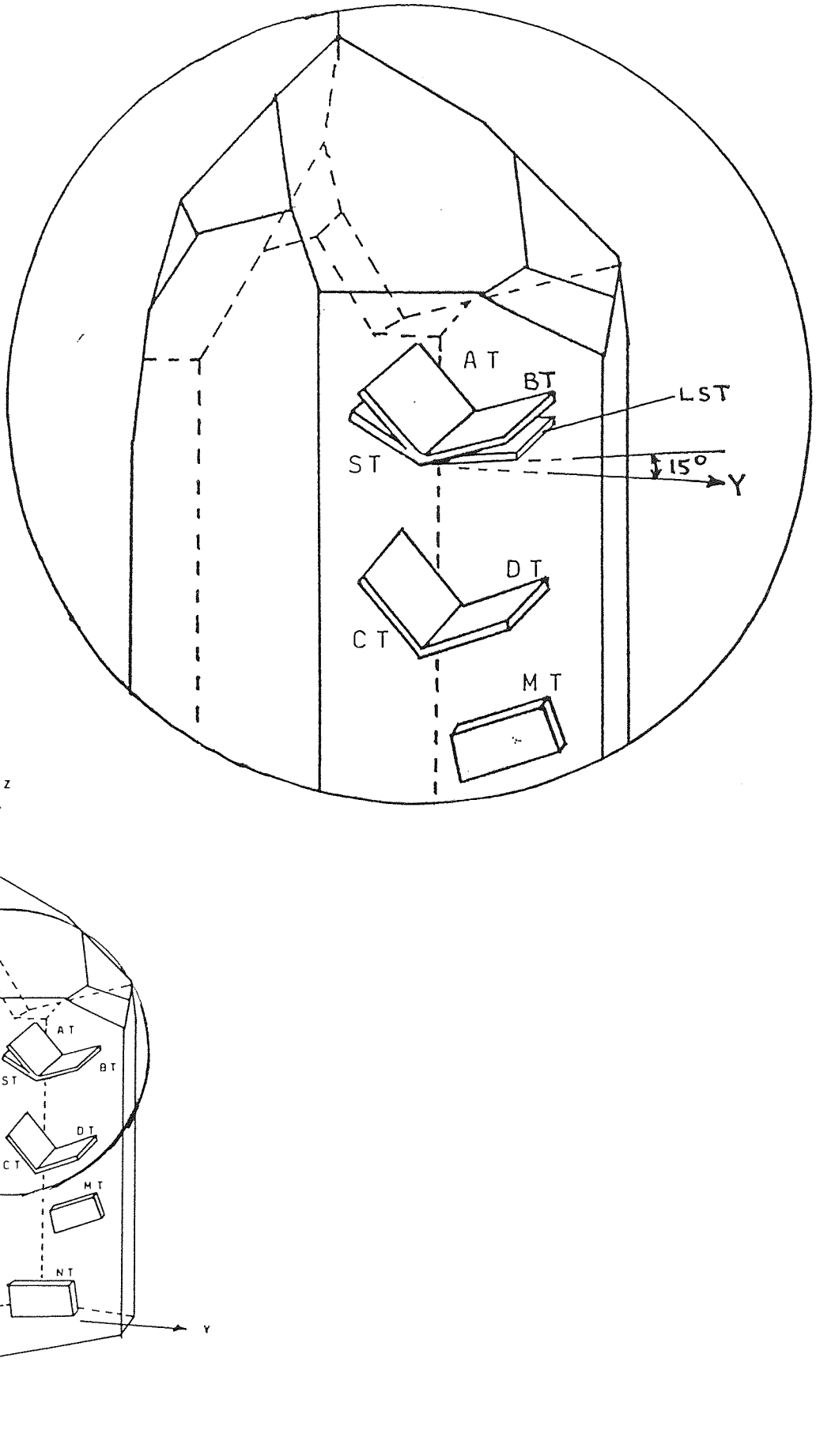

FIGURE 19 The LST Orientation

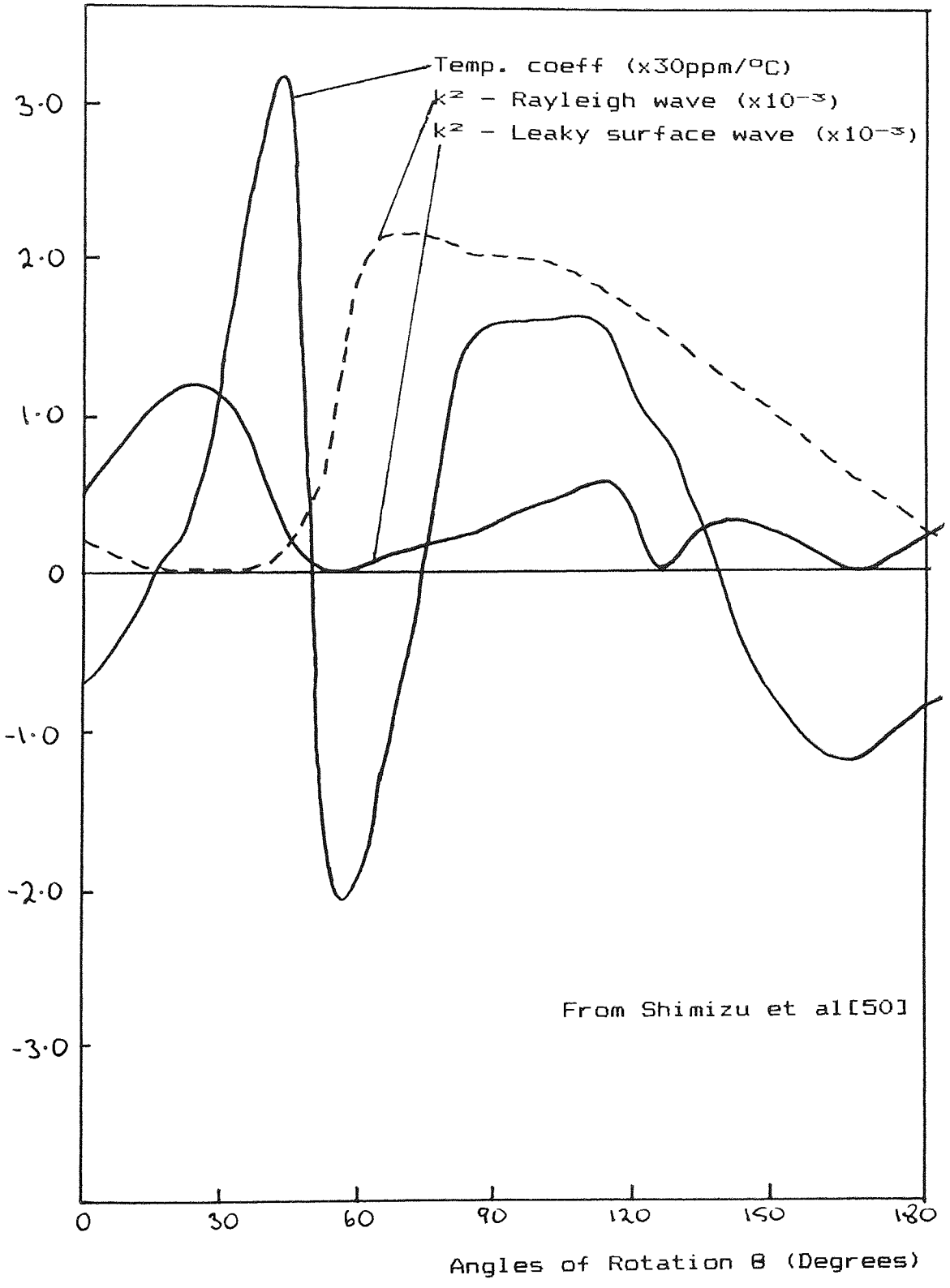

FIGURE 20 Leaky Surface Wave v Rayleigh and Shear Waves

The reported results also indicate large variations in TCD for relatively small changes in orientation. For example, based upon a temperature range of -20°C to +80°C, LST75.3 yields a parabolic frequency shift of +/-10ppm, whereas LST74.3 gives a linear shift of +/-30ppm.

3.2.3 Temperature Compensation - Existing Cuts.

Section 2.1 described briefly an area of SAW device technology not addressed at STC, namely device performance adjustment through choice of substrate. Traditionally SAW devices are fabricated on ST-X quartz due to its temperature performance and zero power flow angle. Generally SAW device designers aim to place the TCD parabola turning point at the centre of the device temperature band. Again, for most applications ST-X quartz proves most suitable.

System designers are now specifying both a TCD and a particular turning point. An example is the optical fibre repeatered transmission system. Rosenberg et al[19] describe how the temperature performance of the SAW retiming filter can be chosen to compensate other circuit effects. In general filter performance must be as close as possible to that achievable on ST-X quartz.

Minowa et al[20] describe methods for tuning SAW devices. These are based upon adjustments to crystal cut angle and propagation direction. Results published cover a range of rotated Y-axis angles between ST(42.75°) and AT(35.3°). Figure 21 depicts the three main results in graphical form. The plots show:

As the Y-rotation increases the turnover temperature decreases, for a given normalised metal film thickness.

The phase velocity increases as the Y-rotation increases.

For a given Y-rotation, the phase velocity increases as the angle of propagation from the X-axis increases.

The phase velocity decreases as the metal film thickness increases.

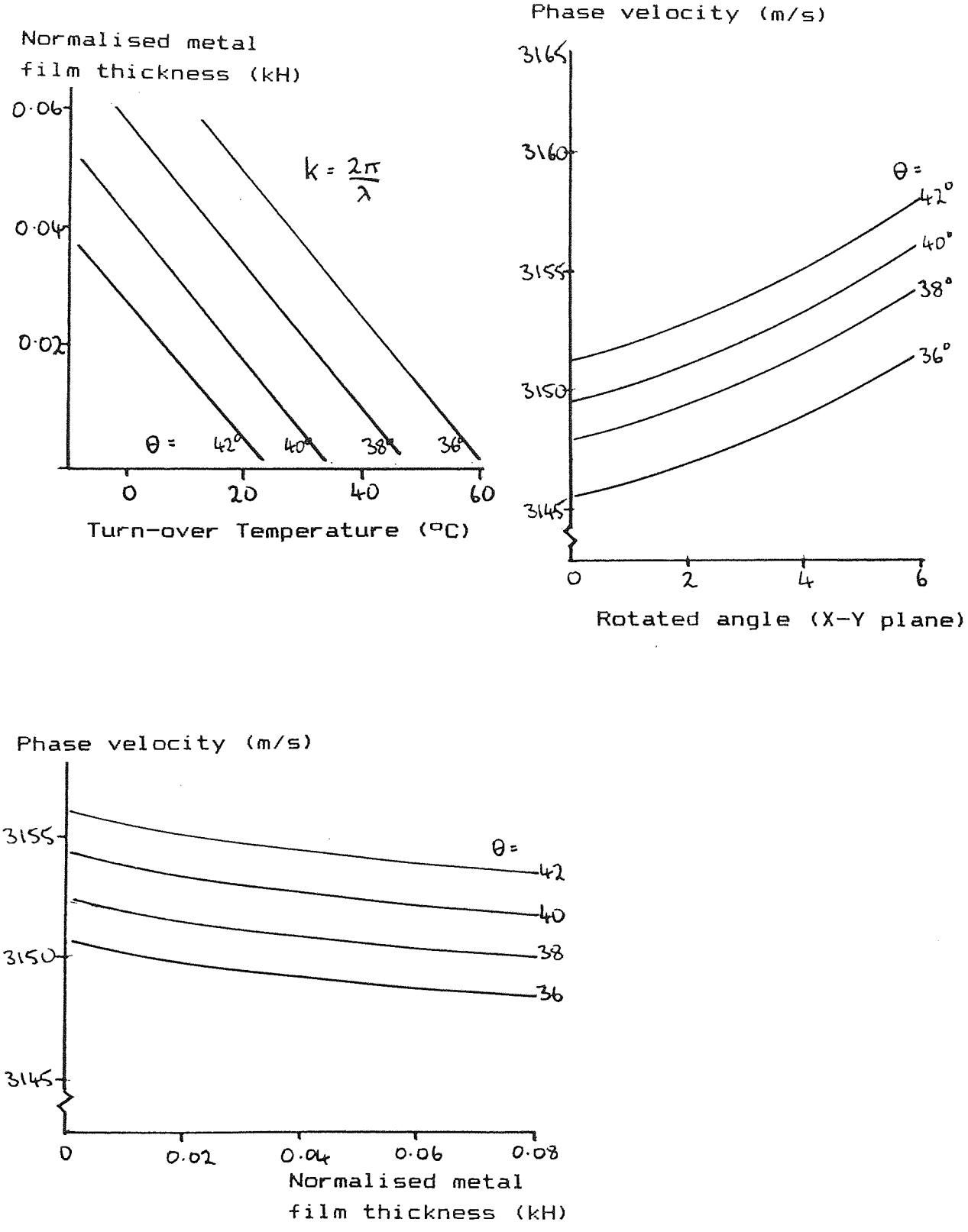

From Minowa et al[20]

FIGURE 21 Performance of Y-rotated Cuts Near ST

Minowa et al argue that these relationships allow a simplified approach to the design or tuning of SAW devices.

3.2.4 Temperature Performance - Summary.

Section 3.2 has reviewed the problem of temperature induced frequency drift and the approaches to reducing the problem. Of the various techniques available, as described by Lewis[44], only two, new cuts and new propagation modes, have been identified as being within the scope of this project. These are newly reported cuts of SST and X33, with Rayleigh wave acoustic propagation, and LST-quartz with leaky surface wave propagation. Published results show substantial TCD improvement over ST-X quartz with the LST-cut offering greatest improvement. Also, both SST and LST-cuts have a higher acoustic velocity than ST-X quartz and give the potential for higher operating frequencies and easier fabrication at existing frequencies.

The use of substrate selection as a means of modifying device performance has been described. A range of cuts between the AT and ST orientations have been analysed by Minowa et al[20]. These have the benefit of single rotation and are relatively easy to align. The results also provide a method for performance modification, within certain limits, without the need for expensive photomask redesign. These limits are imposed by the finite accuracy and range of photomask alignment in the photolithographic process.

3.3 Summary.

The purpose of Chapter 3 has been to review the current technology of SAW devices in order to identify techniques for meeting the objectives of Chapter 2. These objectives are basically the development and extension of company capabilities to meet the growing requirement for:

Higher operating frequencies
Reduced insertion loss
Improved temperature performance.

As STC operates in a well-defined market niche, two device types fundamental to future company growth have been selected for development. These are a high bit-rate PCM retiming filter and a low-loss narrowband filter.

The technical review has considered device complexity, both in manufacturing and design, with the aim of adopting an approach within existing processing capabilities. On the basis of the literature search, research has been concentrated in the following areas:

The development of the single-phase unidirectional transducer (SPUDT) as a low-loss PCM retiming filter. Advantages are ease of manufacture and use compared to other techniques, even though other methods may offer performance advantages. Single-finger transducers should ease fabrication of high frequency devices.

The development of transducer-coupled resonator filters for narrow-bandwidth front-end filtering applications. Transducer coupling provides for greater flexibility.

Experimental analysis of new quartz cuts with, reportedly, improved temperature performance. These also offer the potential for higher operating frequency.

Experimental analysis of a range of quartz orientations close to the ST-cut. This should lead to greater design and manufacturing flexibility.

4. TEMPERATURE PERFORMANCE.

4.1 Scope.

Within the scope of improved temperature performance, this project has two main objectives.

To measure the temperature characteristics of quartz cuts in the AT-ST range, thus enabling greater flexibility in design (as required by users such as Rosenberg et al[19]) and the potential to correct for minor mask errors.

To demonstrate usable SAW devices on newly identified quartz cuts. Generally, only experimental or diagnostic designs have been reported to date.

4.2 AT-ST Characteristics.

4.2.1 Methodology.

Chapter 3 has identified the work of Minowa et al[20] with regard to quartz performance. Exploitation of these results in a production environment requires the generation of empirical data based upon the actual manufacturing process and hardware.

This project identified a specific need for such data in the design of PCM retiming filters. By coincidence, a substantial amount of data had previously been produced as part of an ageing exercise on 295.6MHz filters. This device was therefore selected as the vehicle for this work. Three inter-dependent factors are examined:

The effect of crystal cut on turnover temperature.

The effect of crystal cut on centre frequency.

The effect of pattern mask rotation on centre frequency.

Although the trend of these results is known, the data generated includes machine and process constants that cannot be predicted accurately from the theory. Data on

the three effects listed above allows the designer to modify a device performance, within definable limits, without requiring a new photomask, thus saving both time and cost.

The 295.6MHz filter chosen for this work had been in production for some time. It had originally been designed for implementation as the timing extraction filter in the repeaters on TAT-8, the first trans-atlantic optical fibre link. The system, including the filter, is now in operation. Therefore reliable photomasks and a considerable database of results for this device on ST-X quartz were available. The filter comprises two uniform split-finger transducers with one transducer operating at the fundamental frequency and the other at the third harmonic. An outline specification for the filter is as follows:

Centre frequency	-	295.6MHz
3dB bandwidth	-	370kHz
Insertion loss	-	14dB
Side-lobe attenuation	-	>25dB
Temperature range	-	0 to 40°C
Group delay	-	1600ns
Phase linearity	-	+/-10°

Performance plots for a typical TAT-8 device are shown in Figure 22. In practice the manufacturing specification includes maximum and minimum performance limits. In view of the quoted temperature range of 0 to 40°C an ideal device requires a turn-over temperature of 20°C to minimise frequency drift. From the large amount of production test data available, the actual turnover temperature for TAT-8 filters on ST-X quartz was in the range -3 to +20°C with an average of 13°C.

In view of the advantages associated with the ST-X cut, only cuts in the AT-ST range were to be investigated. This is equivalent to a Y-rotation range of 35.3°(AT) to 42.75°(ST). A range of quartz substrates was obtained covering 36° to 41°. Limited quantities at some orientations restricted the total number of experiments.

Using the standard TAT-8 photomask and process specification, filters were made and tested at each cut angle. Results would allow the effect of crystal cut angle on both centre frequency and turnover temperature to be evaluated. Minowa et al[20] show that moving the

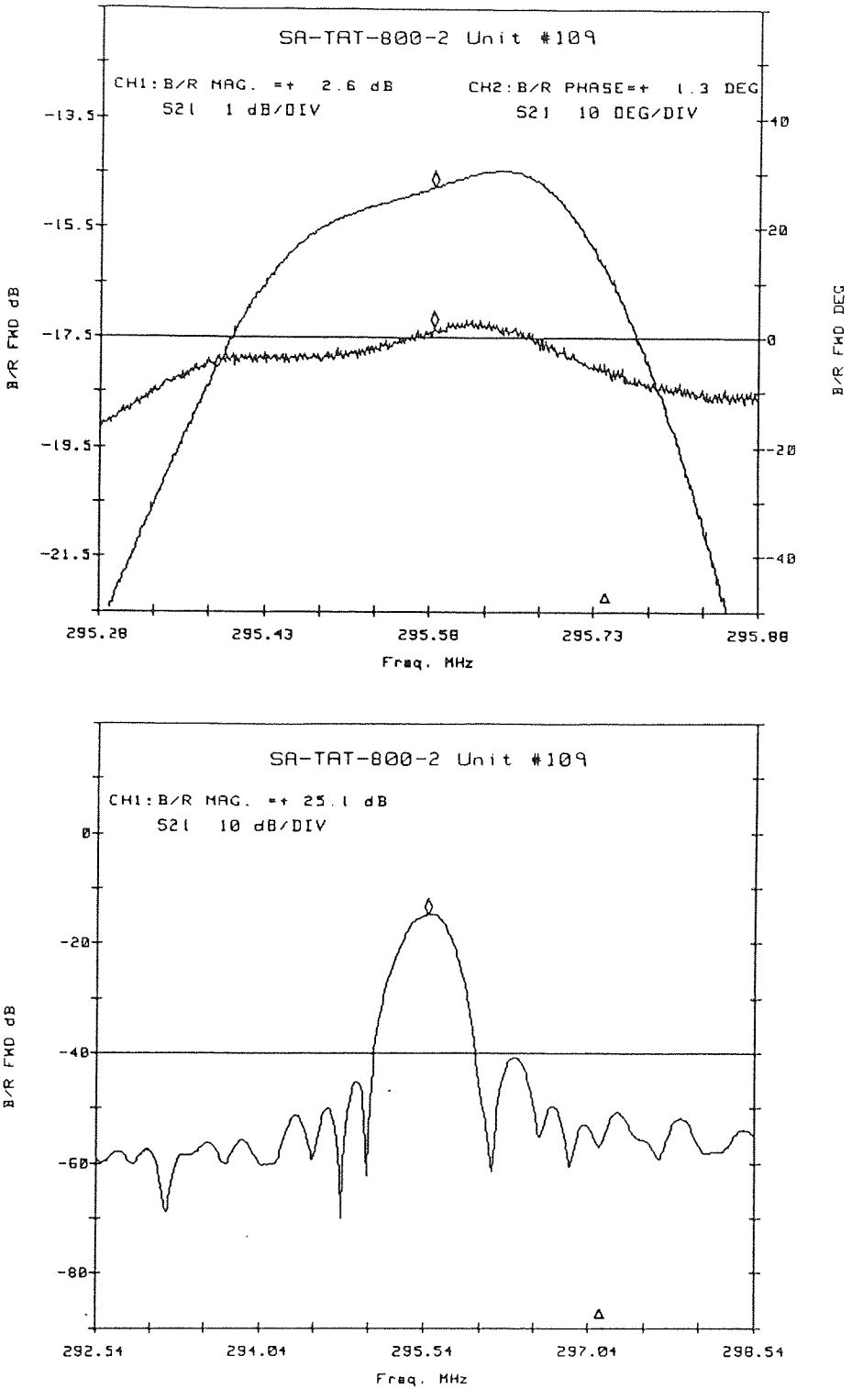

Note: The jaggedness in HP8505A plots is an artefact of the measurement system and not the SAW device

Passband plot shows linearised phase

FIGURE 22 Performance of Standard TAT-8 PCM Filter

Y-rotation from ST towards AT reduces the phase velocity and, consequently, the centre frequency. At the same time the turnover temperature increases.

Therefore, moving to another near-ST cut has the desired result of increasing the turnover temperature, coupled with the unwanted result of reducing the centre frequency. Although minor frequency adjustment is possible by altering the metal film thickness, this is not desirable as it may require modifications to an existing circuit and is not appropriate for large adjustments.

Minowa et al indicate that, on a given Y-orientation, rotating the angle of propagation away from the X-axis increases the centre frequency. This is achieved at the mask alignment stage of the photolithographic process. Normally the quartz substrate has its X-axis visually aligned to the photomask and hard contact is made. The mask aligner table incorporates a vernier operated rotation facility. Following X-axis alignment it is possible to rotate the substrate with respect to the mask. In practice the required X-axis shift is specified as a number of vernier rotations.

To complete the characterisation of the AT-ST range it is necessary to measure the effect of X-axis rotation. To a first order this effect is independent of the Y-axis cut. Therefore data on X-axis rotations from different cuts is used, thus utilising substrate material more efficiently.

4.2.2 Results.

Experimental devices were made from quartz substrates measuring 30mm x 25mm x 0.5mm thick. The accuracy of crystal cut was specified by the STC optical department as better than 5 minutes of arc. Standard processing techniques were employed and devices were mounted and sealed in 14-pin dual-in-line packages. Normal inspection techniques were used at all stages of production such that devices submitted for test were of standard quality. Production 50ohm test fixtures were used for electrical testing using a calibrated Anritsu Spectrum Analyser and Tracking Generator. Overband temperature testing took place in a Gallenkamp environmental chamber with a resistance thermometer probe fixed to the test jig.

For each device that passed all quality checks the following electrical performance data was recorded at room temperature (23 +/-2°C):

Minimum insertion loss(IL)
Centre frequency(fo)
Bandwidth at 3dB points(BW)
Level of first sidelobe(SL)

Also, for each device, overband temperature measurements were based on the measured centre frequency at five temperatures:

-10, 5, 20, 35 and 50°C.

An example of a complete set of data for one device is shown in Table 2 and in Figures 23 and 24. The device is on the YX1(40°) cut. Figure 23 shows the close-in passband performance of both attenuation and phase. Also shown is the level of close-in sidelobes. Figure 24 illustrates the overband performance. The solid curve is a computed parabolic fit to the test data. The computer also shows the error between the fitted curve and the experimental points and gives an indication of the "quality" of the data.

A summary of the data obtained for characterisation of the AT-ST range is given in Tables 3 and 4. Table 3 gives the results for all cuts investigated without X-axis rotation. Table 4 gives the frequency offsets generated at several levels of X-axis rotation, measured as turns of the vernier screw. Some of these results were carried forward from earlier work on the same device. These are indicated in the table.

From these results it is possible to construct three plots which together describe the performance of TAT-8 filters in the ST-AT quartz range. These are shown in Figures 25, 26 and 27. In each case a simple linear fit programme has been used to generate the line of best fit to the experimental data. The three main relationships for the TAT-8 filter were found to be as follows:

Turnover temperature v Y-axis rotation
$T(t/o) = 383.84 - 8.81\ \theta$ (°C)

Centre frequency v Y-axis rotation
$fo = 291.956 + 0.082\ \theta$ (MHz)

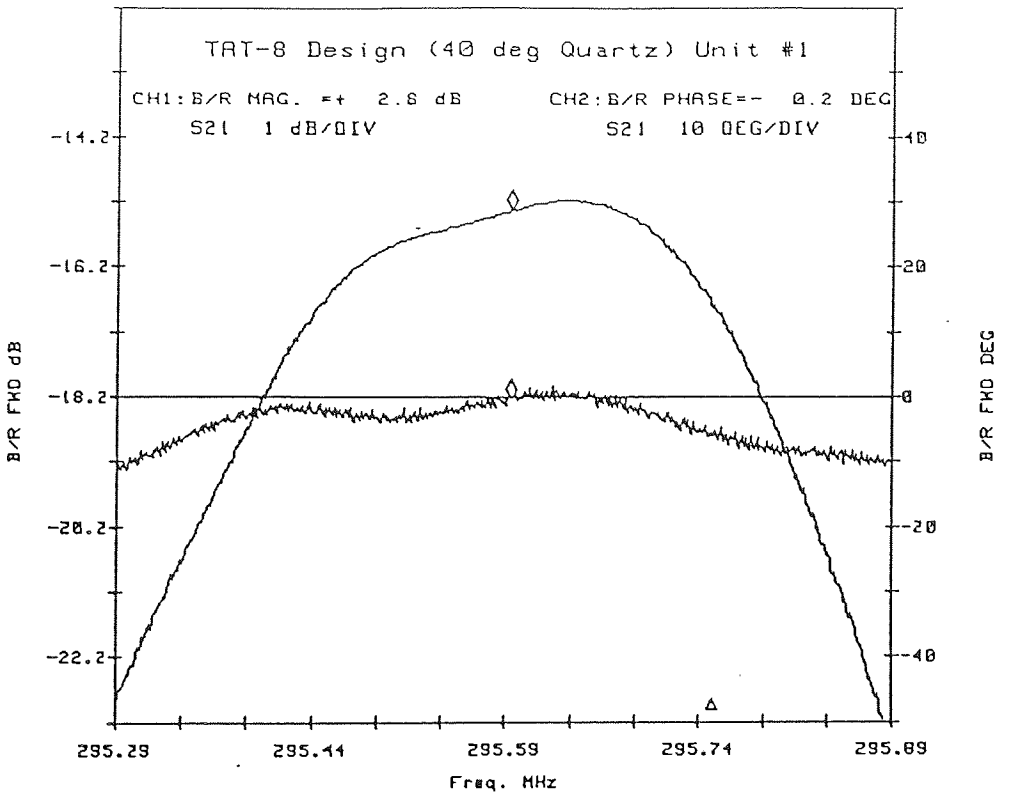

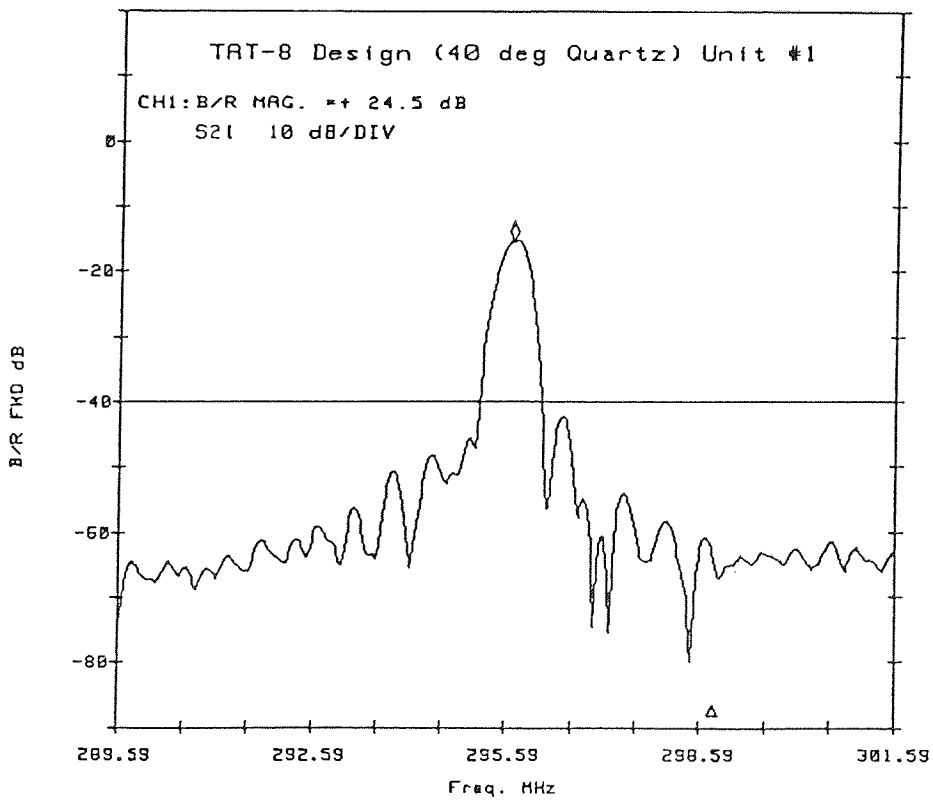

FIGURE 23 PCM Filter on YX1(40°) Quartz - Attenuation

Program PARTEM - Version 1 (Parabolic Fit)

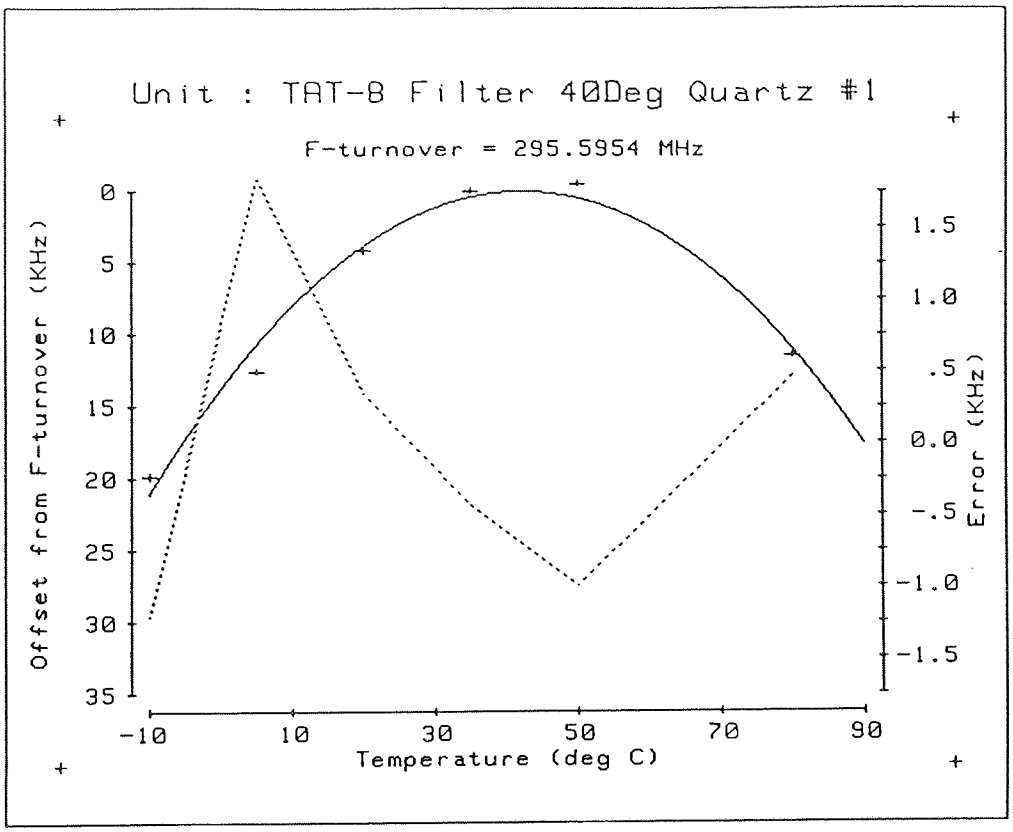

Program PARTEM - Version 1

Polynomial Fit to SAW Data
Unit I.D. : TAT-8 Filter 40Deg Quartz #1

J	Coeff(J)
0	+2.955816E+02
1	+6.523706E-04
2	-7.719579E-06

Pt	X(Pt) deg C	Y(Pt) (MHz)	Poly MHz	Err MHz
1	-10.00	295.575500	295.574285	-1.2145E-03
2	5.00	295.582800	295.584650	+1.8500E-03
3	20.00	295.591200	295.591541	+3.4071E-04
4	35.00	295.595400	295.594958	-4.4238E-04
5	50.00	295.595900	295.594901	-9.9929E-04
6	80.00	295.583900	295.584365	+4.6547E-04

Max-error = .001850
RMS-error = .001035

Turnover = 42.254 deg C
Freq-turn = 295.595 MHz
Para term = -2.61154E-08

FIGURE 24 PCM Filter on YX1(40°) Quartz - Temperature

Effect of Crystal Cut Angle Θ
on Turn-over Temperature

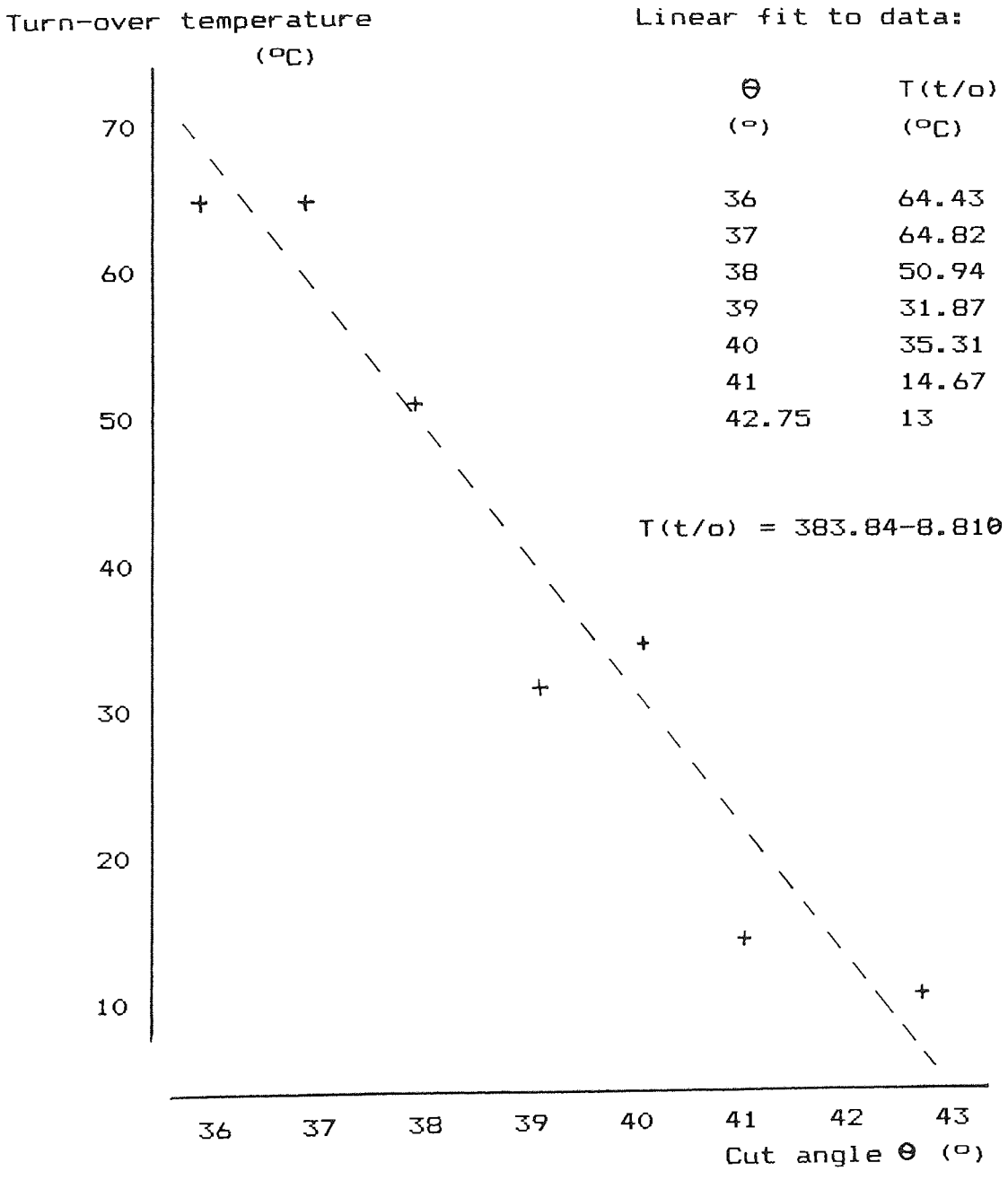

Linear fit to data:

Θ (°)	T(t/o) (°C)
36	64.43
37	64.82
38	50.94
39	31.87
40	35.31
41	14.67
42.75	13

T(t/o) = 383.84-8.810

FIGURE 25 Turnover Temperature v Cut Angle

Effect of Crystal Cut Angle θ
on Centre Frequency for 295MHz PCM Filter

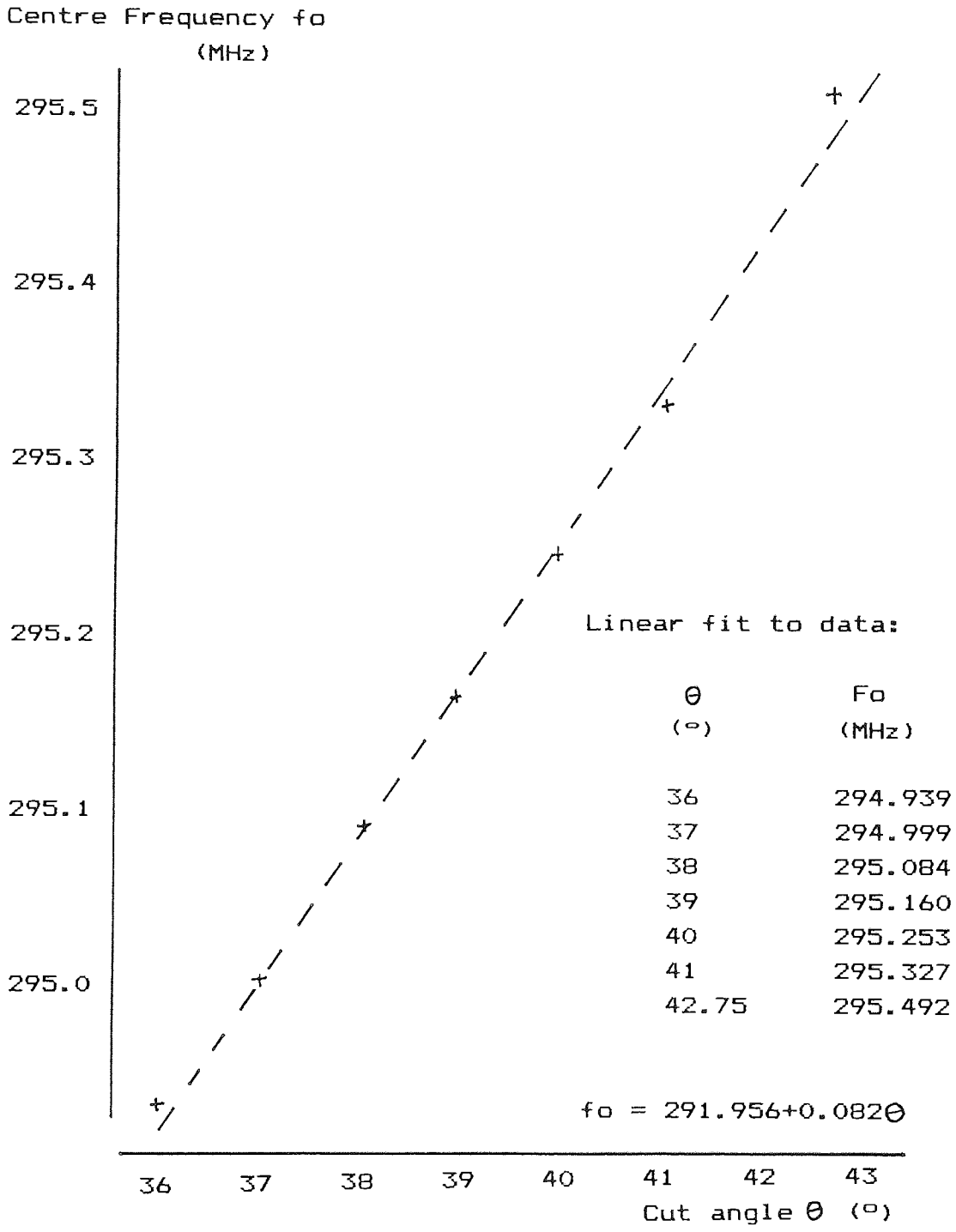

FIGURE 26 Centre Frequency v Cut Angle

Effect of Pattern Mask Rotation
on Centre Frequency (295MHz PCM Filter)

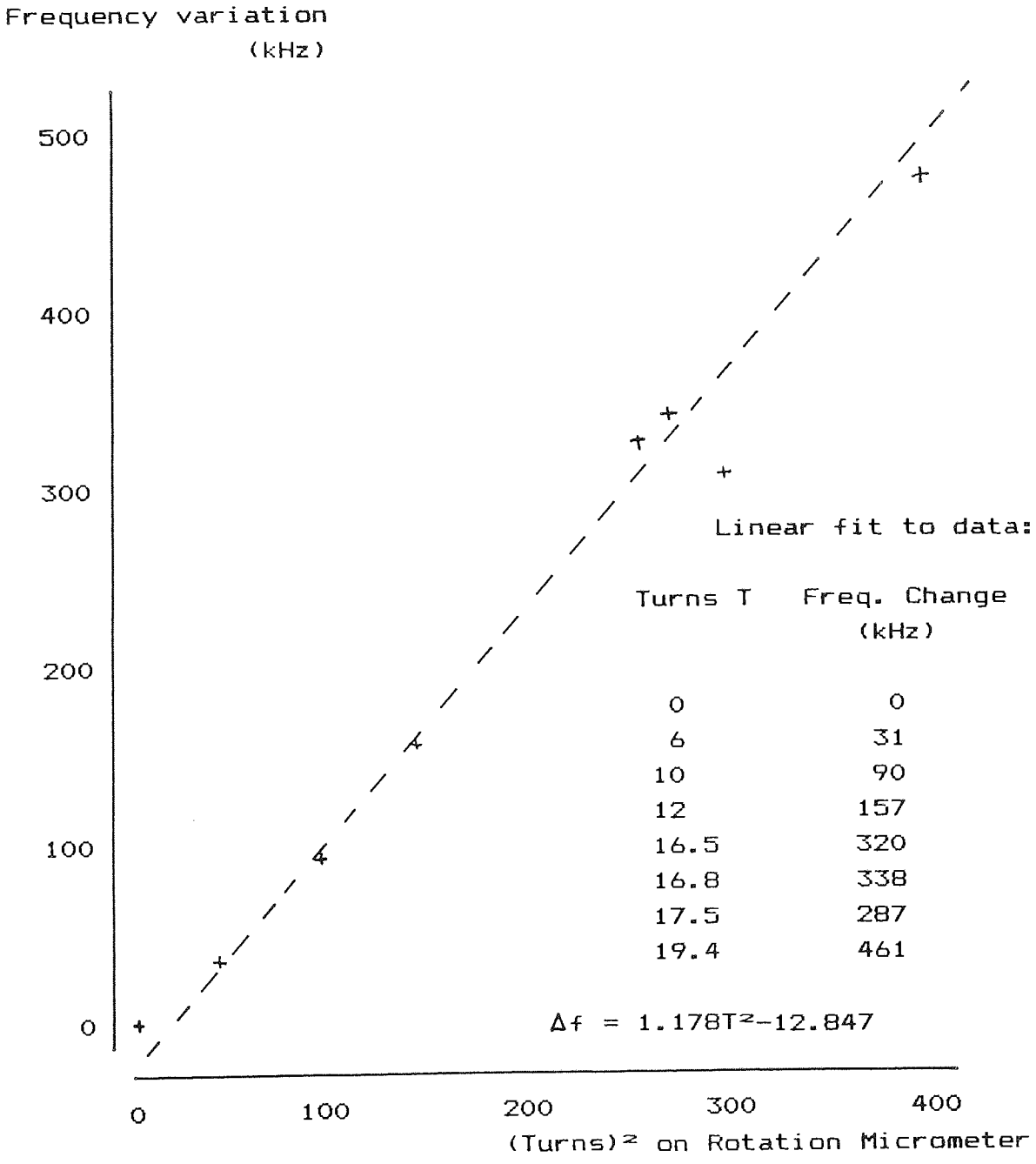

FIGURE 27 Centre Frequency v Mask Rotation

Insertion loss	(IL)	dB	-	14.6
-3dB frequency	(FL)	MHz	-	295.3942
-3dB frequency	(FH)	MHz	-	295.7875
Centre frequency	(Fo)	MHz	-	295.5909
Sidelobe atten.	(SL)	dB	-	26.6
3dB Bandwidth	(BW)	kHz	-	393.3

(a) Electrical performance data

Temp (°C)	FL (MHz)	FH (MHz)	Fo (MHz)
-10	295.3849	295.7660	295.5755
5	295.3879	295.7776	295.5828
20	295.3946	295.7878	295.5912
35	295.3955	295.7952	295.5954
50	295.3974	295.7944	295.5959
80	295.3802	295.7875	295.5839

Computed turnover temperature - 42.3°C
(see Figure 24)

(b) Overband temperature data

Note:

Results for TAT-8 device on YX1(40°), 16.8 turns X-axis rotation, device No.1. (30 April 1985)

TABLE 2 AT-ST Results Example.

Y-axis Rotation (°)	No in Sample	Centre Frequency (MHz)	Turnover Temperature (°C)
36	6	294.939	65
37	6	294.999	65
38	5	295.084	51
39	5	295.160	32
40	2	295.253	35
41	6	295.327	15
*42.75(ST)	19	295.492	13

TABLE 3 AT-ST Results, Y-axis Rotation and Turnover Temperature.

X-axis Rotation (Vernier Turns)		Frequency Offset	
T	T^2	(kHz)	(ppm)
0	0	0	0
*6.0	36.0	31	105
*10.0	100.0	90	305
*12.0	144.0	157	531
16.5	272.3	320	1083
16.8	282.8	338	1144
*17.5	306.3	287	971
19.4	376.4	461	1560

Note:

* indicates results from previous work (unpublished)

TABLE 4 AT-ST Results, X-axis Rotation

Centre frequency change v X-axis rotation

$\Delta f = 1.178T^2 - 12.847$ (kHz)

where T(t/o) = turnover temperature
θ = Y-axis rotation (or cut angle)
fo = centre frequency
Δf = frequency change
T = turns on the alignment vernier (X-axis rotation)

These relationships have also been used to satisfy a real production requirement of relocating the turnover temperature from 13 to 30°C on TAT-8 devices. This test of the accuracy of data produced required a second iteration to meet the required specification. Results are shown in Table 5.

4.2.3 Discussion.

These results have demonstrated the advantage of in-house availability of quartz material. Using normal production acceptance criteria, TAT-8 devices have been realised on a range of Y-axis cuts. Moving away from the ST-X cut, accepted as the best for SAW devices in view of its temperature performance and zero power-flow angle, has not degraded the resulting frequency, phase or temperature performance.

Specifically, the results show that by selection of quartz, the SAW designer can choose a turnover temperature within a 60°C range. Also the ST-AT range gives potential for frequency shift of 2000ppm (600kHz for the TAT-8 devices). Finally, X-axis rotation of up to 20 turns on the photomask aligner gives a frequency shift of 1500ppm (450kHz on the TAT-8 device).

These frequency variations are much larger than those associated with design changes to the metal film thickness where values of a few hundred parts-per-million are usual. Therefore such relationships are useful where a device performance needs to be changed without the need for an expensive new photomask and the associated delivery lead-time.

The test of the data, reported in the results section, required a second iteration to precisely locate frequency

Specification	Existing Device	First Process Iteration (A)	(B)	Second Process Iteration
Centre Freq(MHz)	295.60	295.71	295.65	295.59
Film thickness(A)	650	650	650	650
Quartz cut(°)	42.75	40	41	40
X-axis rot(Turns)	10	19.4	16.5	16.8
Turnover Temp(°C)	13	32	26	32
No. in sample	*	5	6	11

Notes:

* - results based on large number of production devices

The first process iteration assumed a second would be required. Therefore two quartz cuts were processed in the same run.

TABLE 5 AT-ST Results - Production Test.

and turnover temperature. This is often necessary in production due to process variations in photolithography. However, in this case it may have been partly due to the limited raw data available, limits imposed by quartz availability. The plots of Figures 25, 26 and 27 show inconsistencies that may be due to these factors. Confidence in the results requires a considerable amount of further data at both different metallisation thicknesses and at other centre frequencies. However the accuracy and predictability of the test demonstrates the viability of this design approach.

4.2.4 Recommendations for further work.

As discussed above, additional experimental work is needed to generate raw data for the TAT-8 plots. This needs to be supplemented with devices at different frequencies and metallisation thicknesses.

The work reported has utilised a PCM filter design where the device is required to operate over a narrow temperature band. Further, any SAW propagation off-axis due to beam-steering is not as critical as in high-Q resonators. Therefore, additional work should include SAW resonators which are required to operate over military temperature bands such as -55°C to +125°C. An advantage of test work on high-Q resonators is that the centre frequency can be accurately measured, thus giving high quality temperature drift data.

4.3 New Quartz Cuts.

4.3.1 Methodology.

In Chapter 3 several new quartz orientations have been identified from the literature review. These are claimed to offer combinations of improved temperature performance and higher acoustic wave velocities when compared with the ST-X cut. The objective of the work reported here is to examine the performance of these cuts on real devices and therefore to assess suitability for production. The three cuts investigated are X33, SST and LST.

Ideally any new cut is most useful if applicable to both filters and resonators. Existing ST-X and AT device designs were selected as the basis for the investigation.

The resonator work was based on a high-Q device with a nominal 263MHz centre frequency on AT quartz. Filters were processed using a PCM filter design, the device operating at approximately 440MHz on ST quartz. Both devices had been in production for some time and therefore comparative data was available.

The 263MHz resonator mask includes several transducer options, amongst which are single-finger and split-finger designs, with the same mirror characteristics in each case. Single and split-finger transducers gave unexpectedly different results as will be discussed below.

One of the objectives of this work is to identify cuts that perform in a similar manner to ST but with improved TCD and higher acoustic velocity. Further, orientations that allow the use of existing design routines are preferred. The reported work on new cuts tends to identify the major advantages with only passing reference to disadvantages. For processing reasons limitations need to be fully understood.

Lukaszek and Ballato[47] demonstrate the SST-cut in the form of a 192MHz delay line claiming reduced acoustic attenuation, higher phase velocity and improved TCD when compared with ST-cut. No results are presented for resonators on SST. The turn-over temperature is also shown to be more dependent on X-axis propagation direction than ST. Although of advantage where a turn-over shift is required, this feature may increase processing errors. Therefore, results from resonator devices allow accurate determination of TCD and indicate other effects, such as beam steering, which may degrade performance. Based upon the reported work the SST-cut with propagation at 23° to the X-axis was selected.

Webster[48] presents theoretical results for the X33-cut. A substantial improvement of TCD is claimed in comparison with ST-cut. The X33-cut allows the turn-over temperature to be adjusted by simple transducer rotation with a resultant shift of approximately 100°C per one degree of rotation. With optical alignment accuracy of +/-5' there exists a potential processing error of +/-8°C. Webster also describes a large power flow angle for the X33-cut, 2.7° compared with zero for the ST-cut, which will seriously degrade resonator performance and require compensated transducers in SAW filter designs. The

precise cut chosen for the work reported here is X33.44°, that is, an X-cut substrate with SAW propagation at 33.44° to the Y-axis.

The LST-cut, as reported by Shimizu and Tanaka[49] and Shimizu et al[50], appears to offer both substantially improved TCD and higher acoustic velocity. Results show that a small change in the Y-axis rotation alters both the turn-over temperature and parabola constant. Shimizu et al use diagnostic devices to demonstrate the leaky surface wave and a 1.82GHz filter to illustrate the higher acoustic velocity. Shimizu et al also show that the electro-mechanical coupling coefficient and attenuation constant for the LST-cut are similar to values for the ST-cut. In view of the effect of Y-axis rotation on device performance three cuts are reported here with rotations of -75.33°, -75.0° and -74.33°.

Although the quartz cuts reported are at orientations new to STC, standard SAW grade quartz blanks measuring 30mm x 20mm x 0.5mm were used for all experimental work. The blanks were processed such that the required propagation direction is parallel to the longer edge. Full details on all cuts investigated are listed in Table 6. To ease reference to the LST-cuts the following names are adopted, LST7420, LST75 and LST7520.

A full set of resonator tests were performed. Devices were mounted in TO8 packages and electrically tested in a calibrated test jig in a 50ohm unmatched condition. Tests comprised both attenuation characteristics and overband temperature measurements. For each quartz cut, both split-finger and single-finger devices were tested. On ST and AT-cuts the split-finger devices are known to give a less distorted response due to cancellation of internal reflections. The centre frequency on both split and single-finger device types is approximately the same, within mask error limitations.

Due to material shortages the PCM filter tests on new quartz did not include the X33-cut. Also as the performance on ST and AT is similar, only AT devices were fabricated. The main purpose of the filter trials was to demonstrate devices with acceptable insertion loss, bandwidth, passband shape and phase linearity. In practice a target centre frequency is achieved through mask design. The filters were mounted in 14-pin DIL packages and tested in a calibrated 50ohm test jig.

Quartz Cut	Designation-STC Processing	Euler Angles(°)		
		0	0	
ST	YX1(+42.75)	0	132.75	0
AT	YX1(+35.3)	0	125.3	0
X33	XY1(0)[33.44]	90	33.44	90
SST	YX1(-42.9)[23.0]	0	40.8	23
LST7420	YX1(-74.2)	0	15.8	0
LST75	YX1(-75.0)	0	15.0	0
LST7520	YX1(-75.2)	0	14.8	0

Notes:

YX1(A)[B] - (A) describes rotation with respect to first named axis (Y-axis), [B] describes rotation with respect to second (X) axis. Where no [] is indicated the rotation is zero.

Euler angles are on a 0 to 90 to 180 basis, not (-90) to 0 to +90.

The angles quoted are those given in the relevant technical articles. Accuracy of optical alignment is described in the text.

TABLE 6 Details on Quartz Orientations

4.3.2 Results - SAW Resonators

Figure 28 describes the 263MHz resonator used for these tests. The device was designed to operate on AT-quartz with a 12um acoustic wavelength. This was chosen simply to aid the mask-maker. Finger widths are 3um and 1.5um for the single-finger and split-finger transducers respectively. Main features of the device are the use of shorted strips in the reflectors and the position of the transducers in the cavity which locate the transducer fingers on the standing-wave anti-nodes to provide optimal electro-mechanical coupling. All devices were fabricated with an aluminium film thickness of 1500Å.

All frequency measurements were made using a Hewlett-Packard 8505A Network Analyser with output to an H-P plotter. Overband temperature measurements were made with the SAW device mounted in a calibrated Gallenkemp environmental chamber. Considerable soak times were allowed between readings to allow temperature stabilisation. Initially, an Anritsu Spectrum Analyser and Tracking Generator were used for frequency measurement. However, during the experimental period a Hewlett-Packard 8753A Network Analyser was coupled to the environmental chamber and this was used for more rapid data gathering in later trials.

Approximately 20 quartz slices were made available at each orientation. In supplying the quartz material the STC Optical Department commented upon the difficulty of aligning the LST-cuts. Alignment relies upon X-ray reflection from known crystallographic planes. Only very weak reflections were available for LST-cut alignment. Therefore the accuracy of the LST material provided was specified as +/-10', compared with +/-5' for all other cuts.

Preliminary experiments suggested that a substantial centre frequency difference between split-finger and single-finger devices was being observed. As each quartz slice, when processed, included both device types it was decided to retain and differentiate these devices during testing. Following preliminary processing trials, a full experimental processing operation was completed with two slices at each orientation. All slices were plasma etched to give improved line edge definition. Following

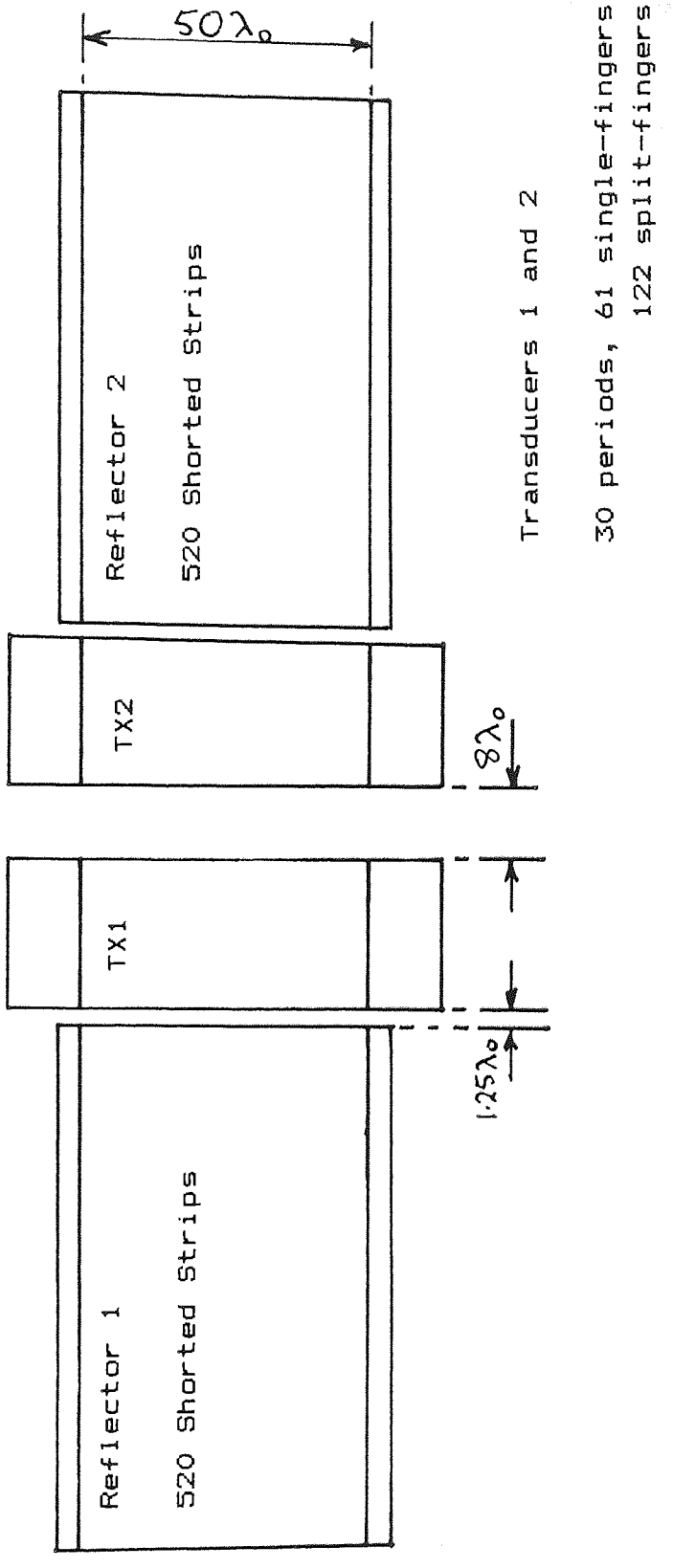

FIGURE 28 263MHz Resonator Layout

substrate dicing, individual die were inspected to normal quality levels and samples were passed for mounting and sealing into TO8 packages.

Detailed results on frequency measurements are listed in Tables 7 to 15. In each case the device type is indicated together with insertion loss, centre frequency, 3dB bandwidth and Q. For the LST7420 and LST7520 cuts a second slice was processed to gain additional split-finger devices. A results summary, which gives the overall average values for each slice, is shown in Table 16.

Frequency versus attenuation plots were also obtained for sample devices from each cut. Samples were chosen to show performance differences between split-finger and single-finger transducer operation, with the exception of the LST7520 cut where only a single-finger sample was available. For each device plots for passband and close-in stopband were obtained. Measurements were made at room temperature. The resultant plots are shown in Figures 29 to 41.

The same sample devices were also used for overband temperature testing. Centre frequency readings were taken for each device at five temperature levels, -20, 0, 20, 40, and 60°C. A curve fitting programme was then used to generate a frequency versus temperature plot as shown previously in Figure 24. Full frequency/temperature data is not given here although the temperature performance plots for each quartz cut are shown in Figures 42 to 48. These plots also indicate the offset error required to fit a second order polynomial to the test data. Table 17 lists the salient features for each device, namely turn-over(-under) temperature and parabola constant.

4.3.3 Discussion - SAW Resonators.

The frequency versus attenuation plots of Figures 29 to 41 and the corresponding Tables 7 to 15 illustrate several important features.

The ST and AT-cut results are typical of high-Q resonators and, as expected, the AT devices operate at a lower frequency than those on ST. This result is comparable with that for the 295.6MHz filter of Table 3. Also, the choice of single or split-finger transducer

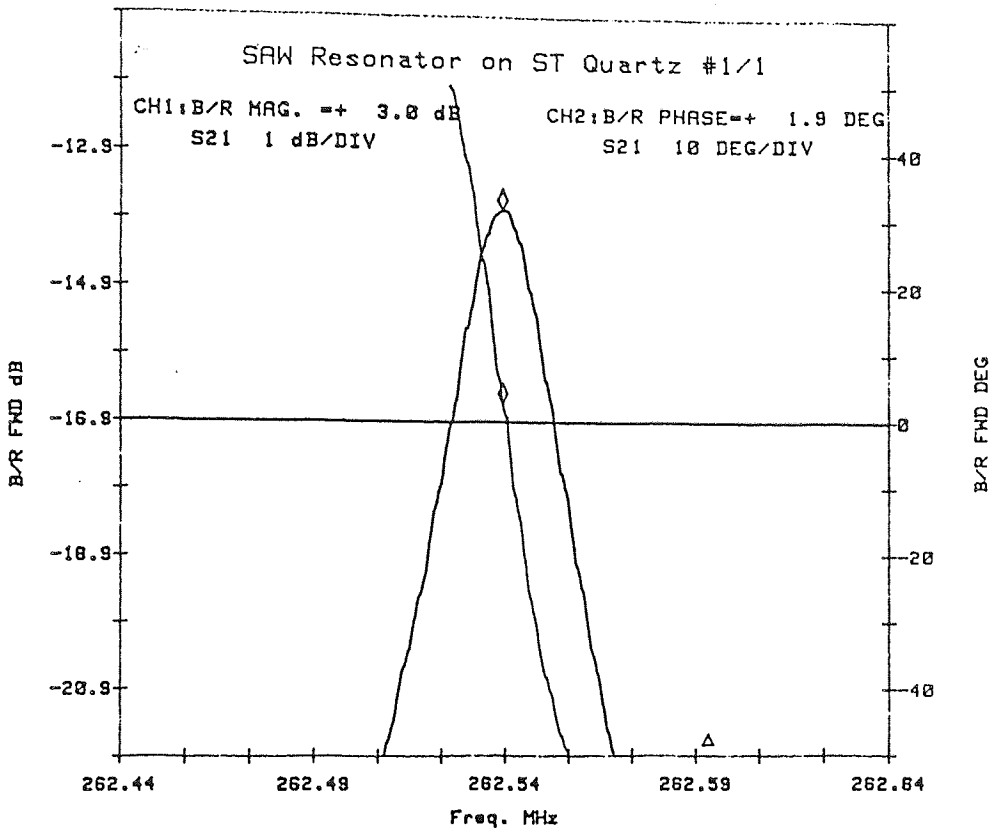

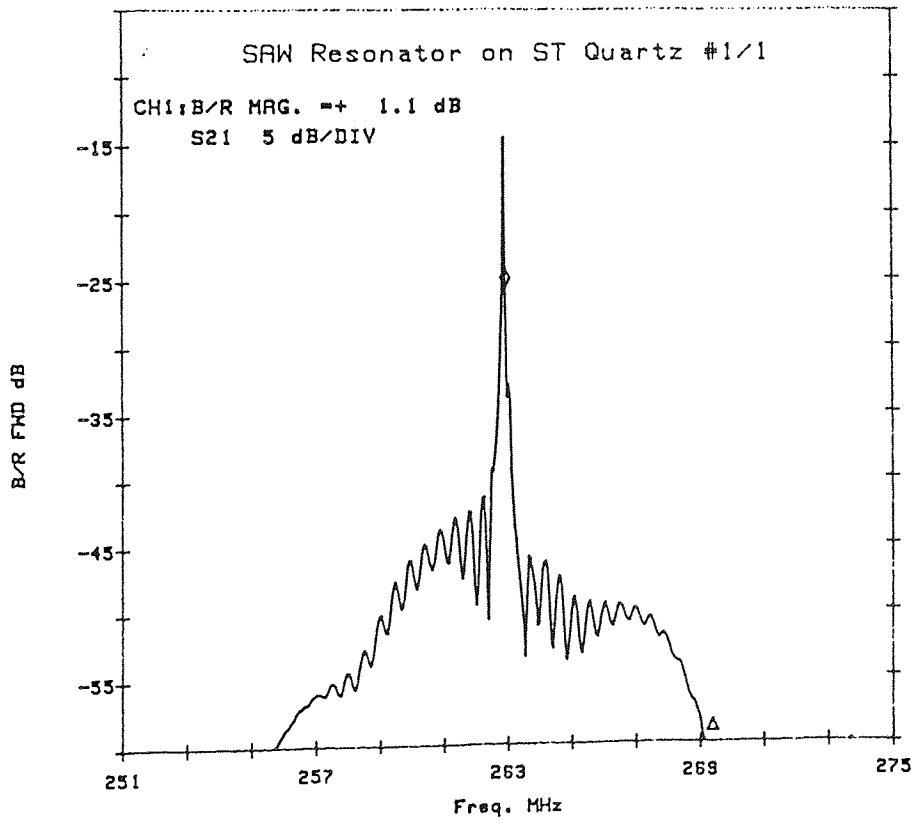

FIGURE 29 SAW Resonator on ST-Quartz unit 1/1
(Single-Finger Transducers)

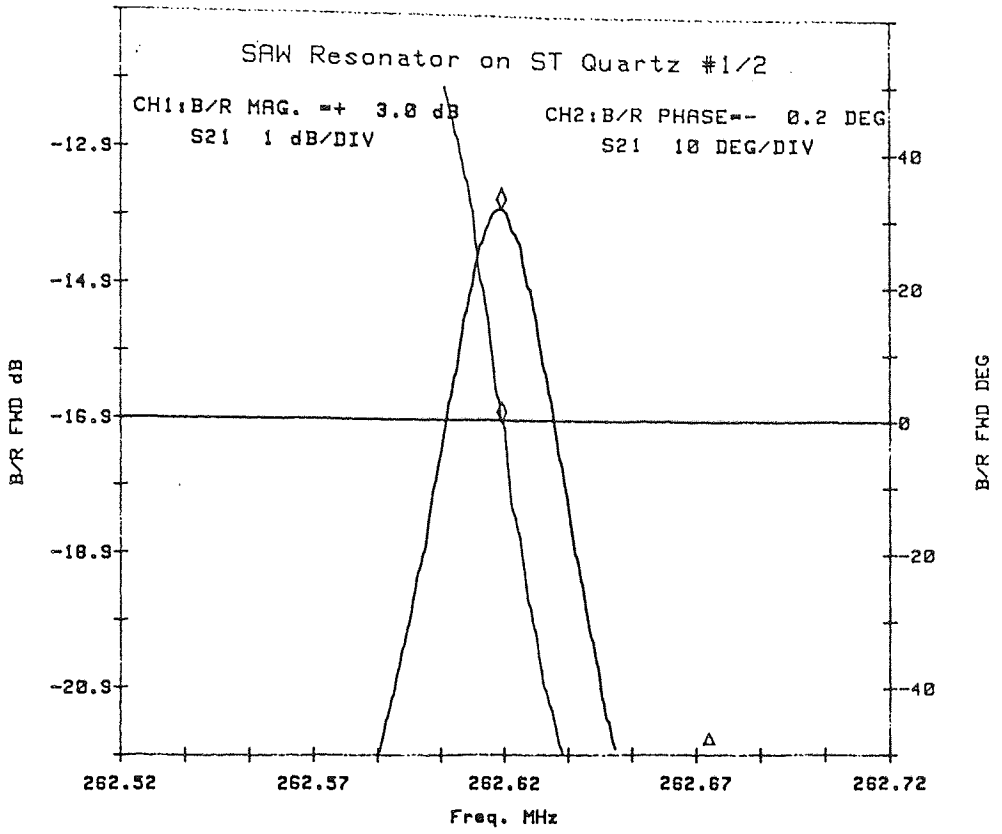

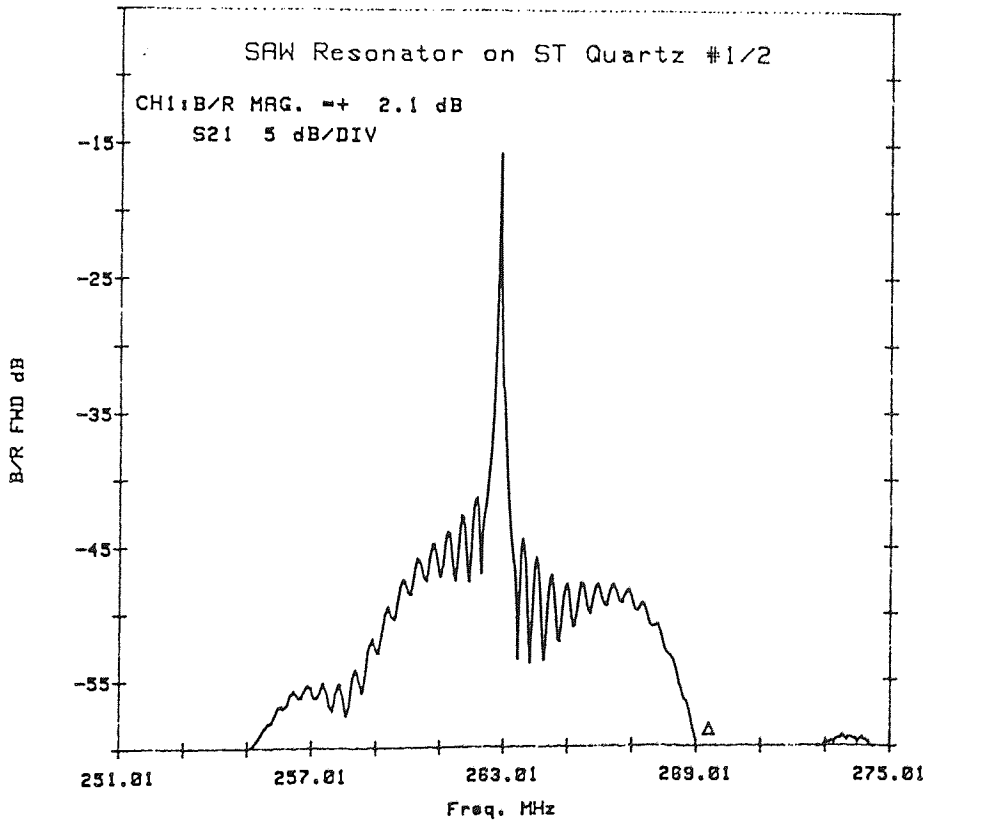

FIGURE 30 SAW Resonator on ST-Quartz unit 1/2
(Split-Finger Transducers)

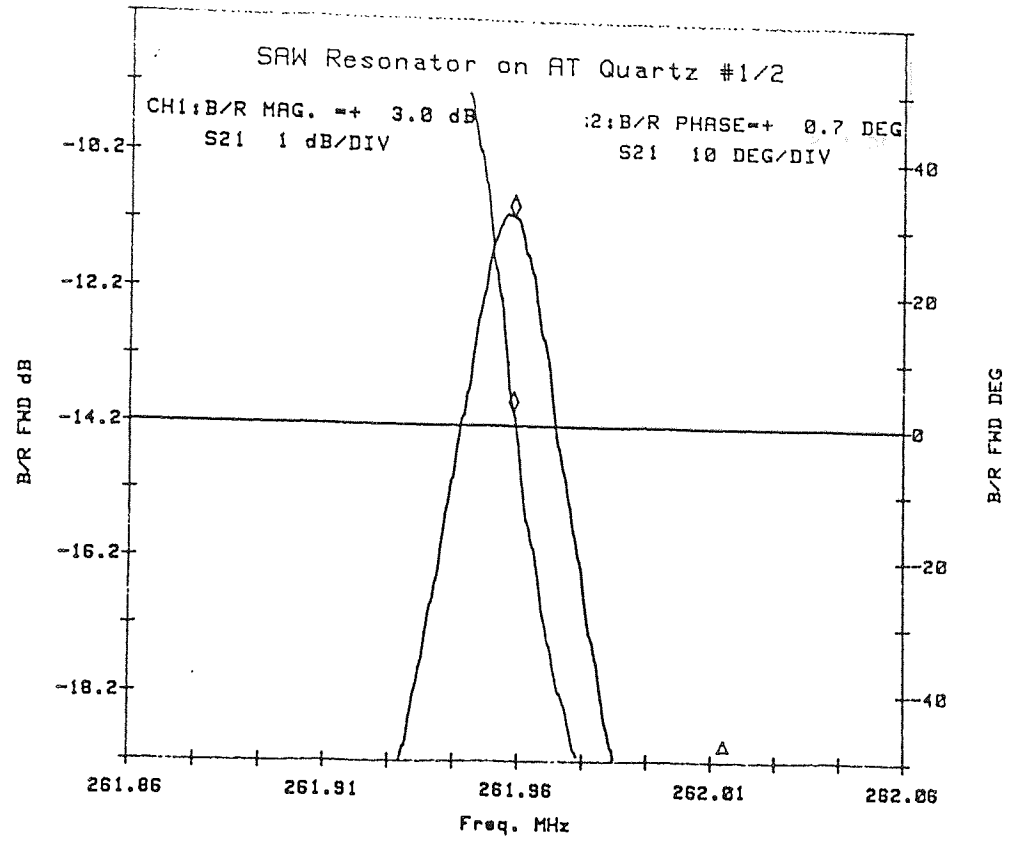

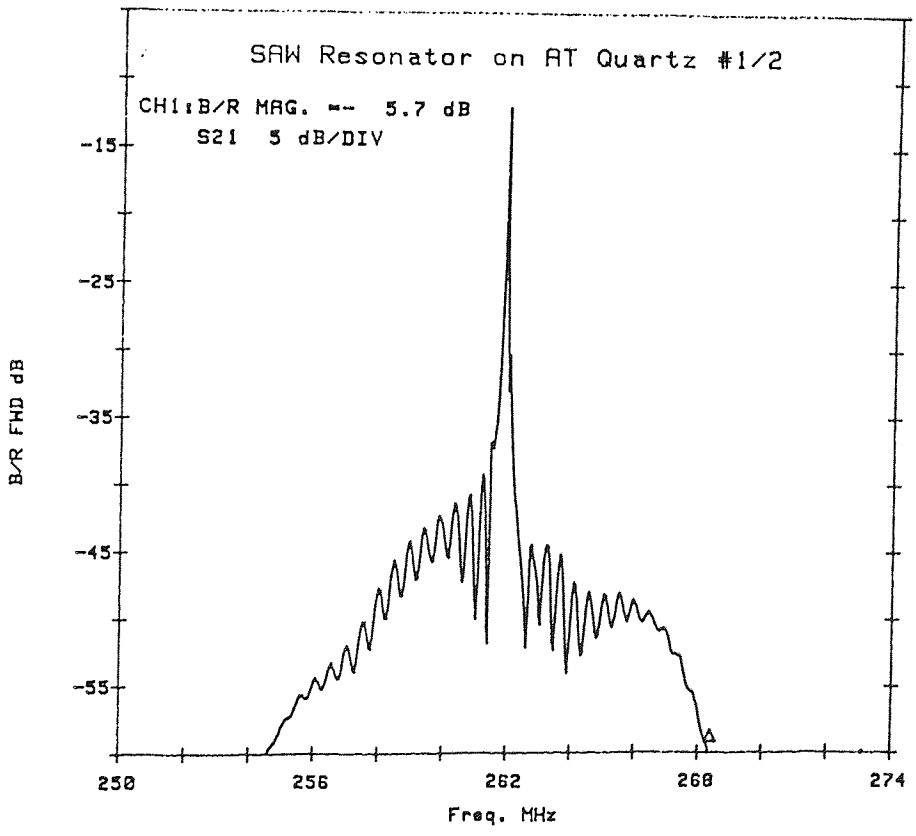

FIGURE 31 SAW Resonator on AT-Quartz unit 1/2
(Single-Finger Transducers)

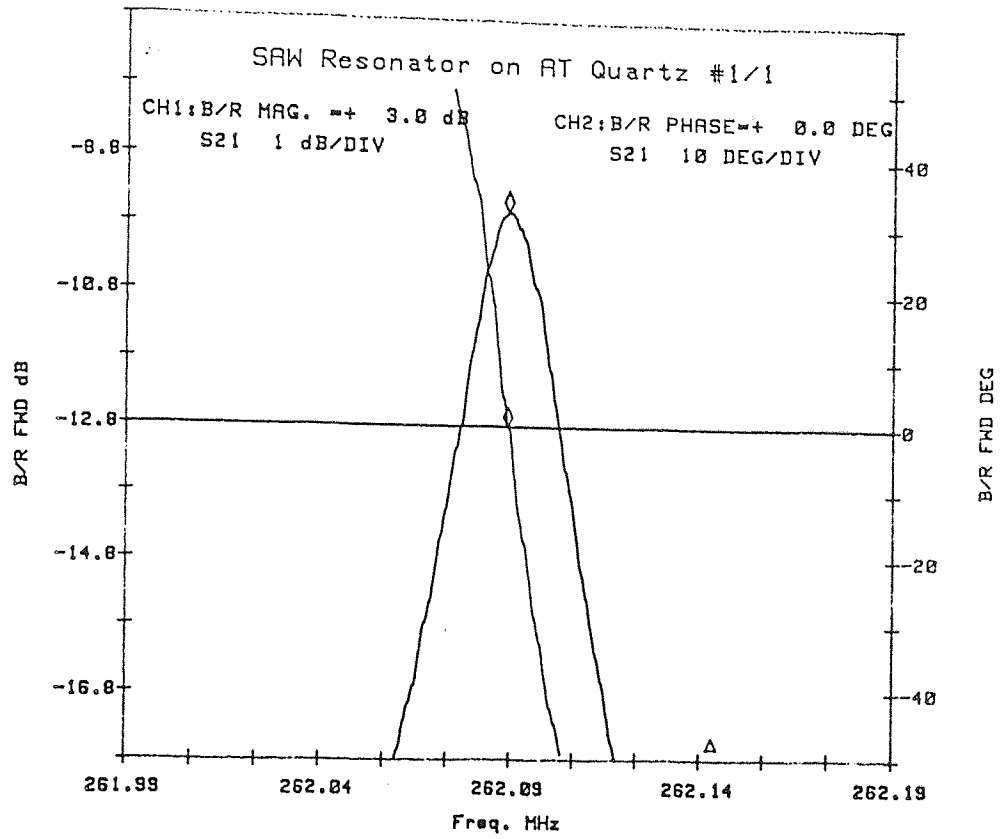

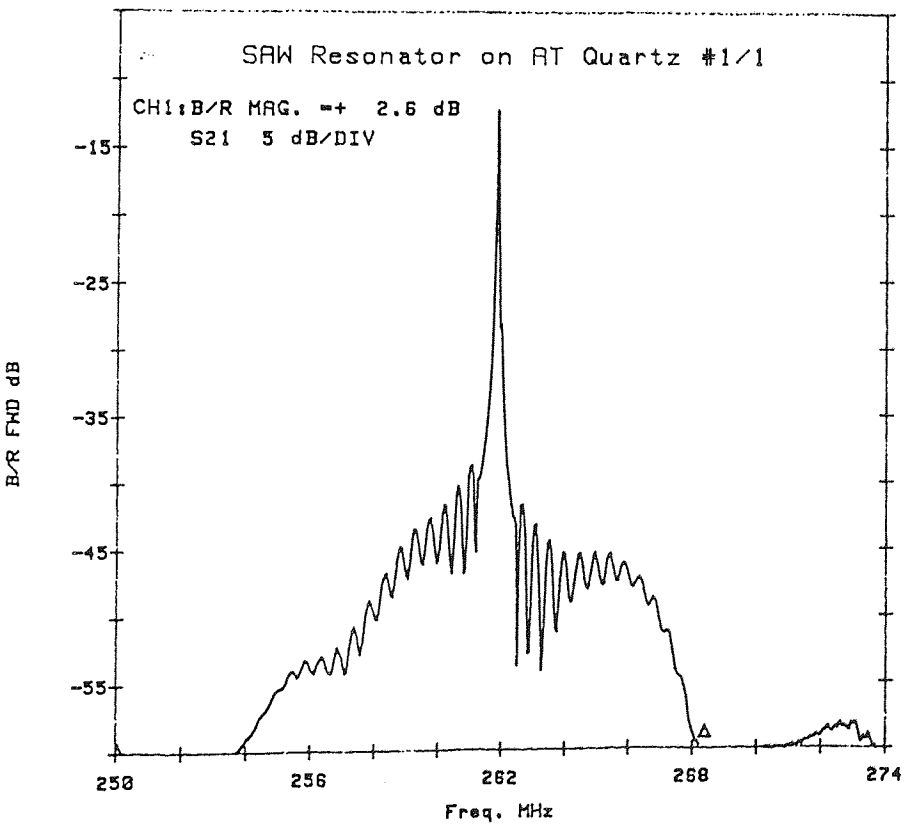

FIGURE 32 SAW Resonator on AT-Quartz unit 1/1
(Split-Finger Transducers)

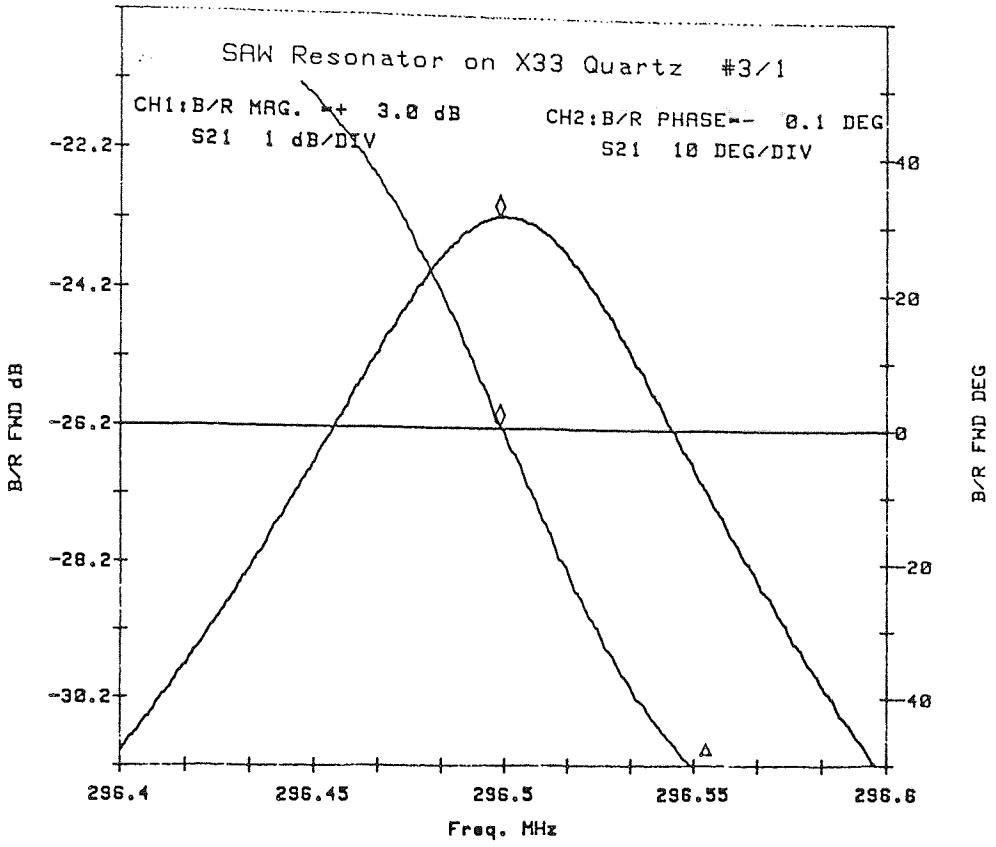

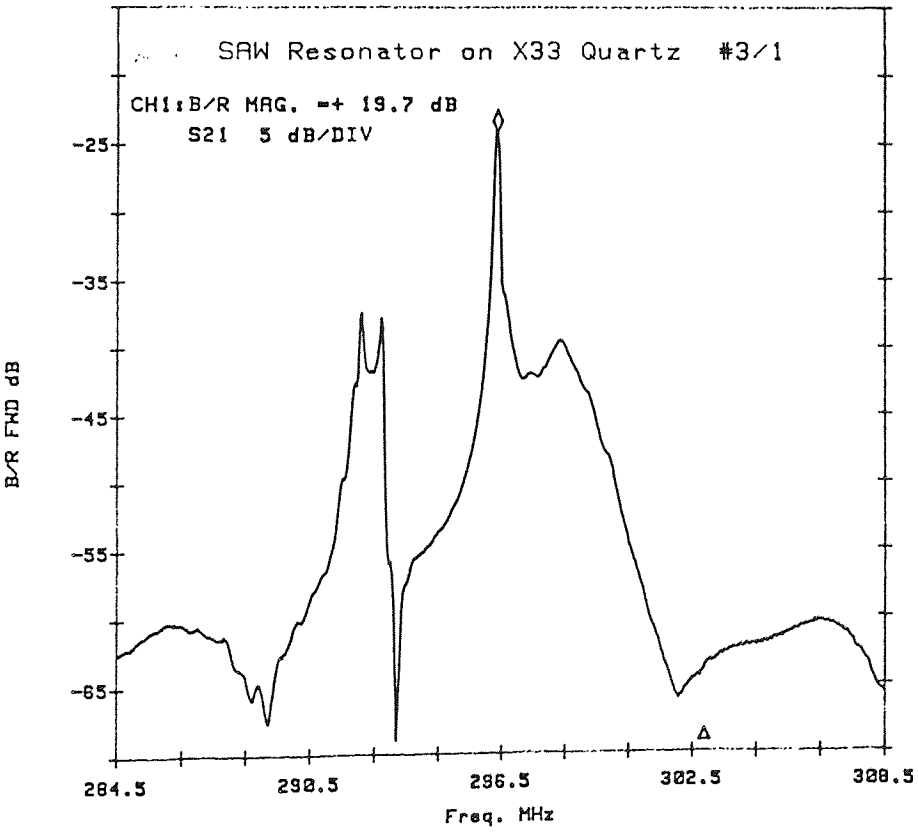

FIGURE 33 SAW Resonator on X33-Quartz unit 3/1
(Single-Finger Transducers)

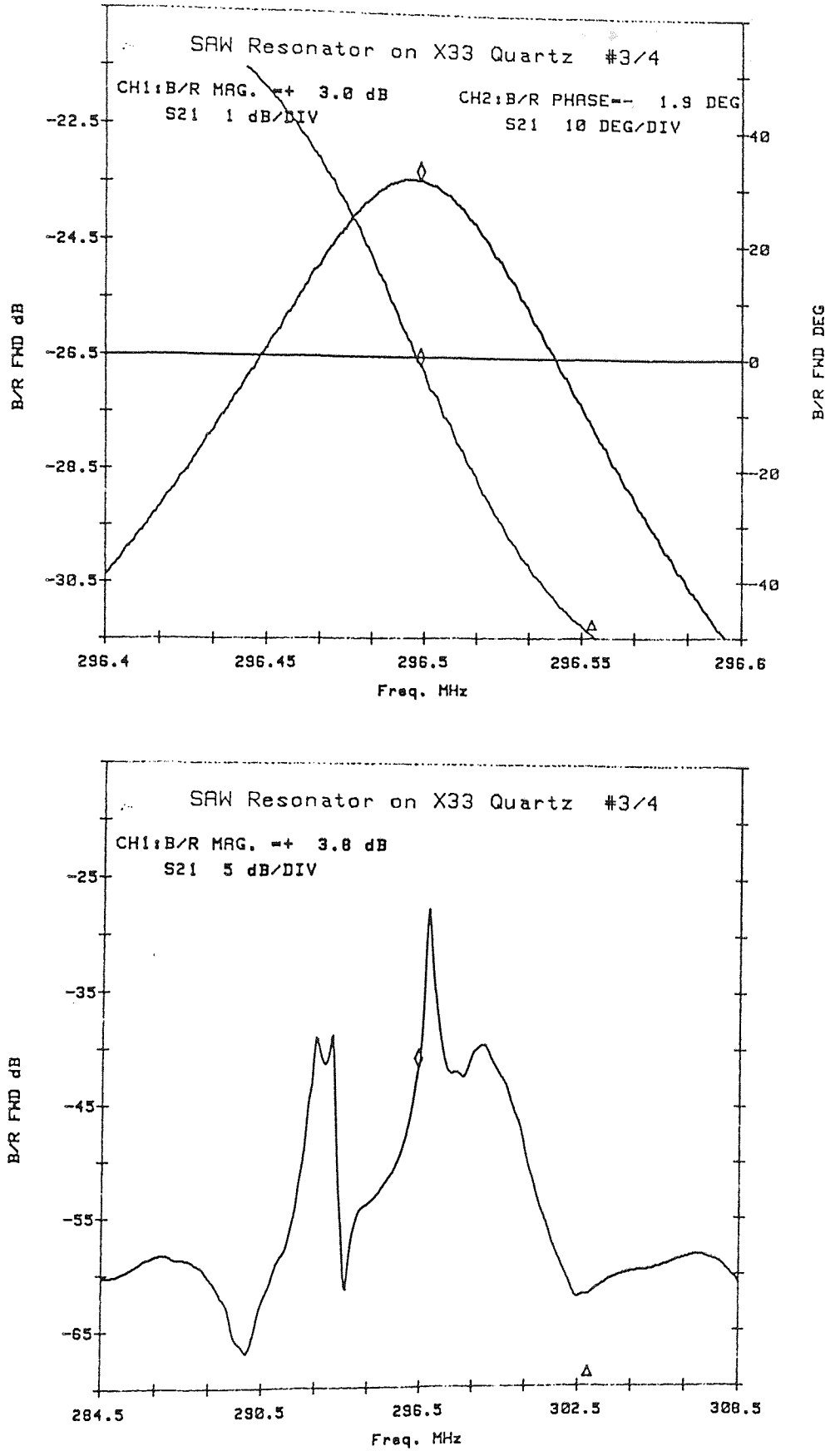

FIGURE 34 SAW Resonator on X33-Quartz unit 3/4
(Single-Finger Transducers)

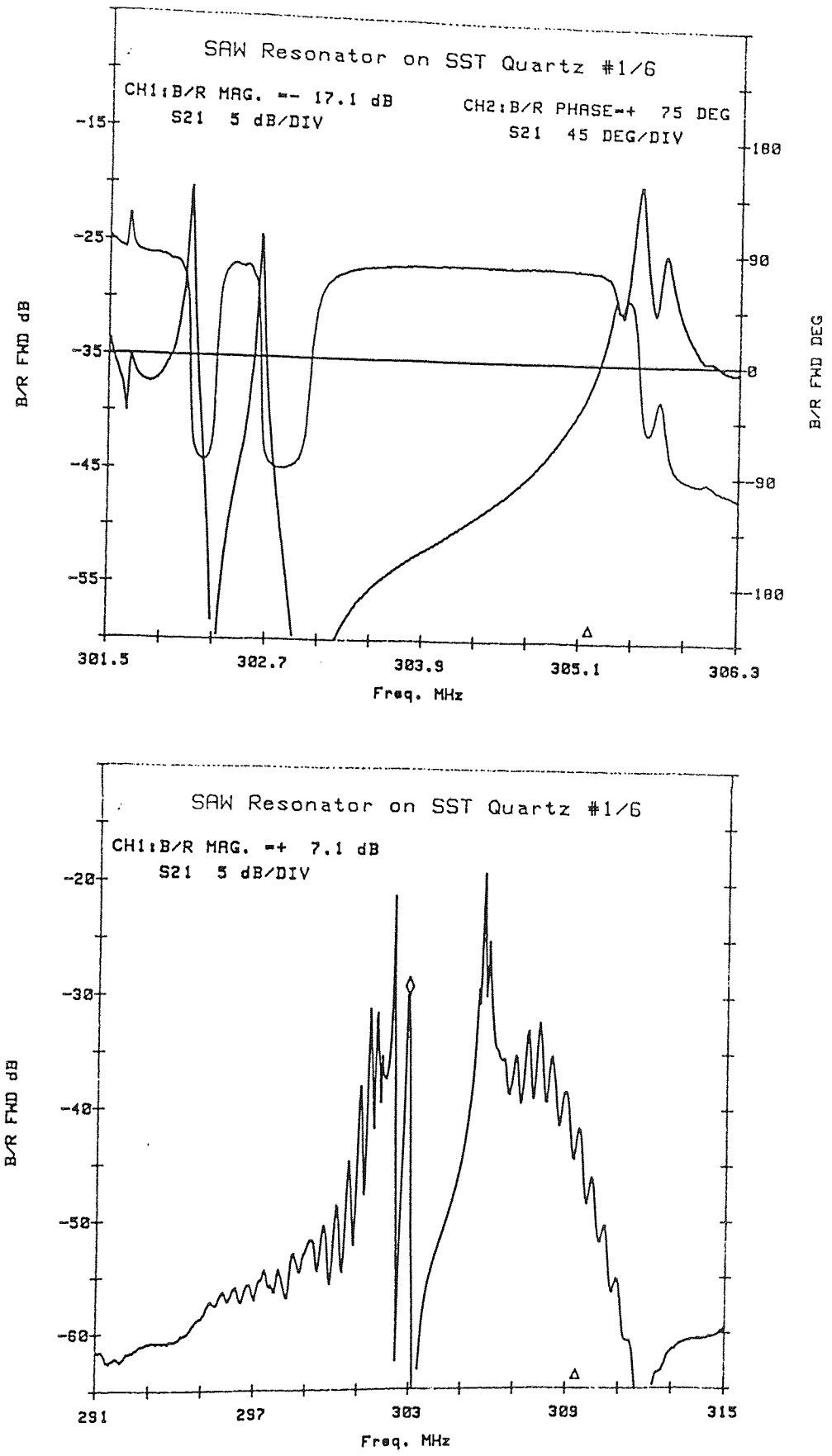

FIGURE 35 SAW Resonator on SST-Quartz unit 1/6
(Single-Finger Transducers)

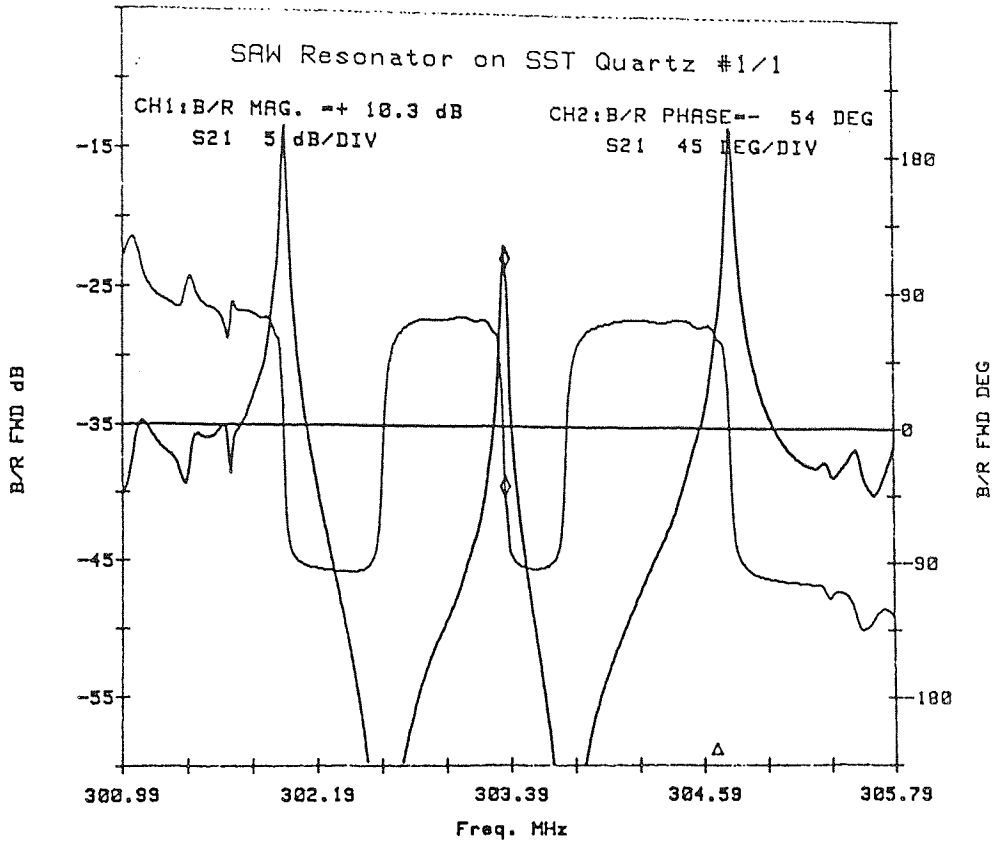

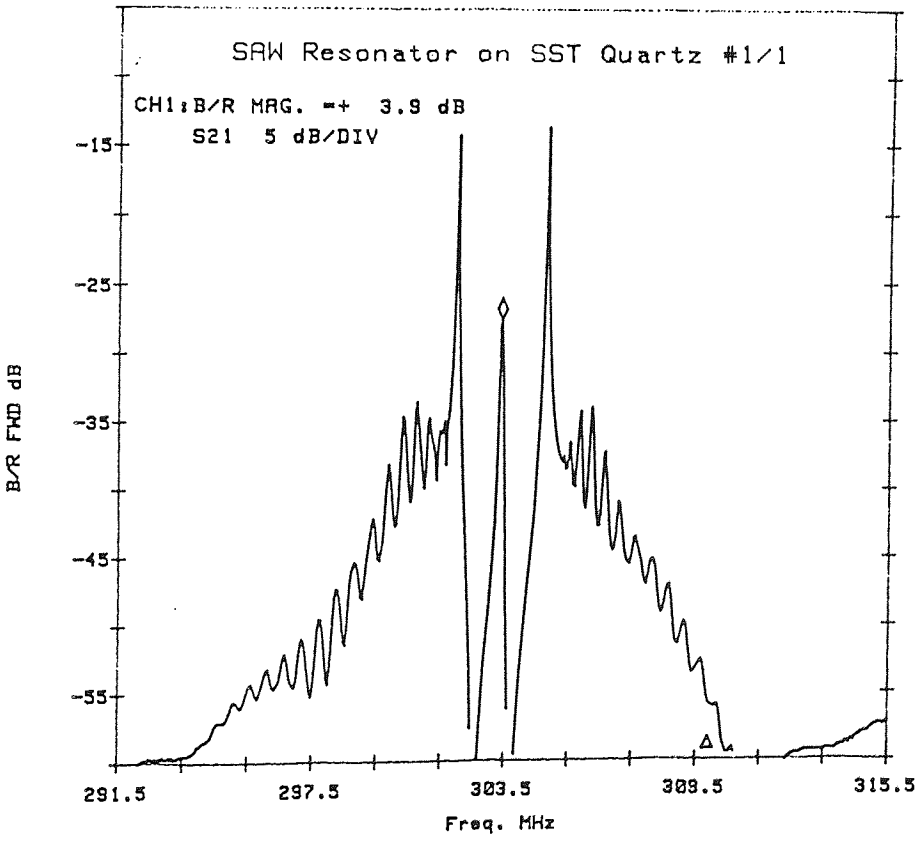

FIGURE 36 SAW Resonator on SST-Quartz unit 1/1
(Split-Finger Transducers)

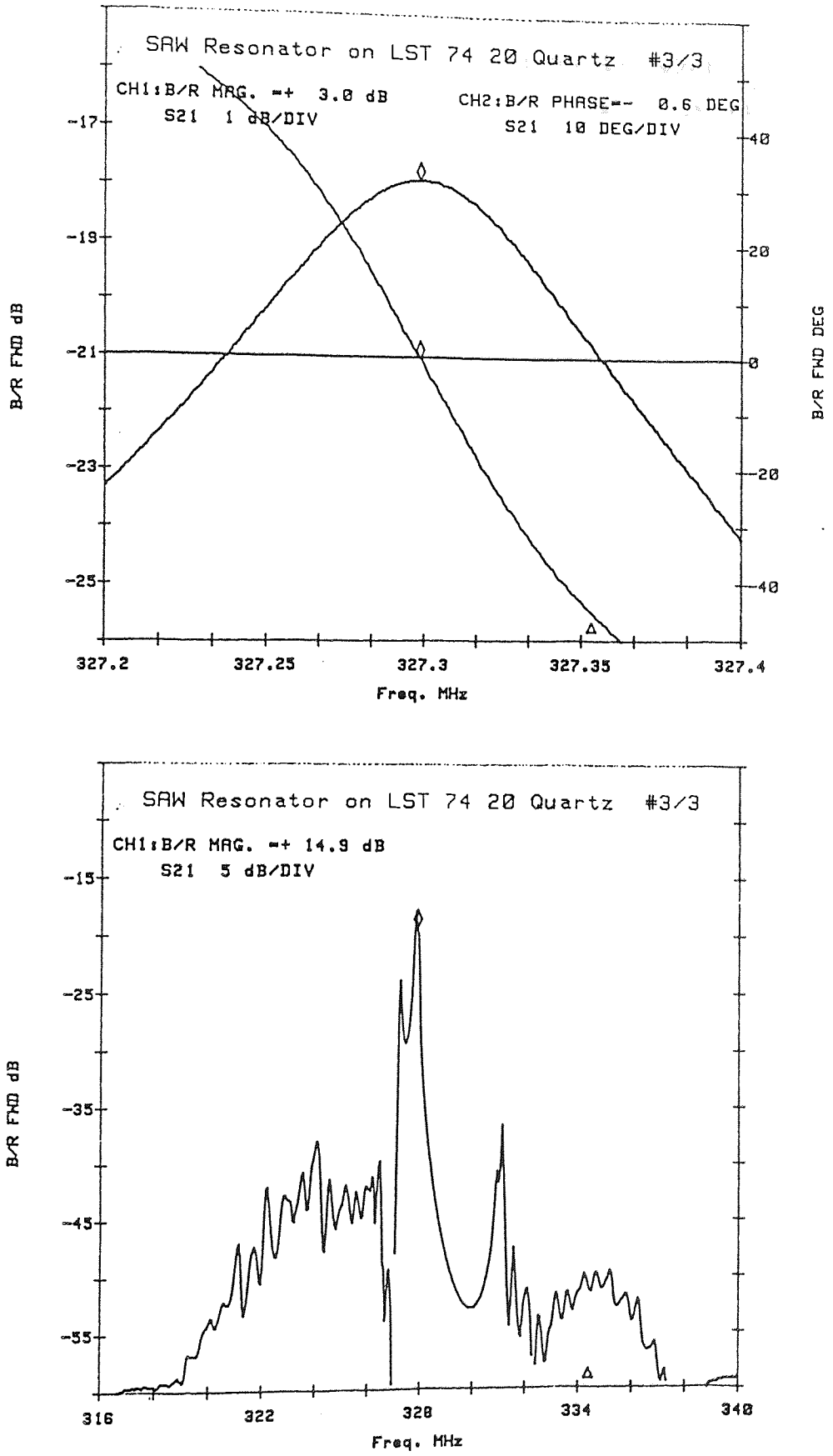

FIGURE 37 SAW Resonator on LST7420-Quartz unit 3/3
(Single-Finger Transducers)

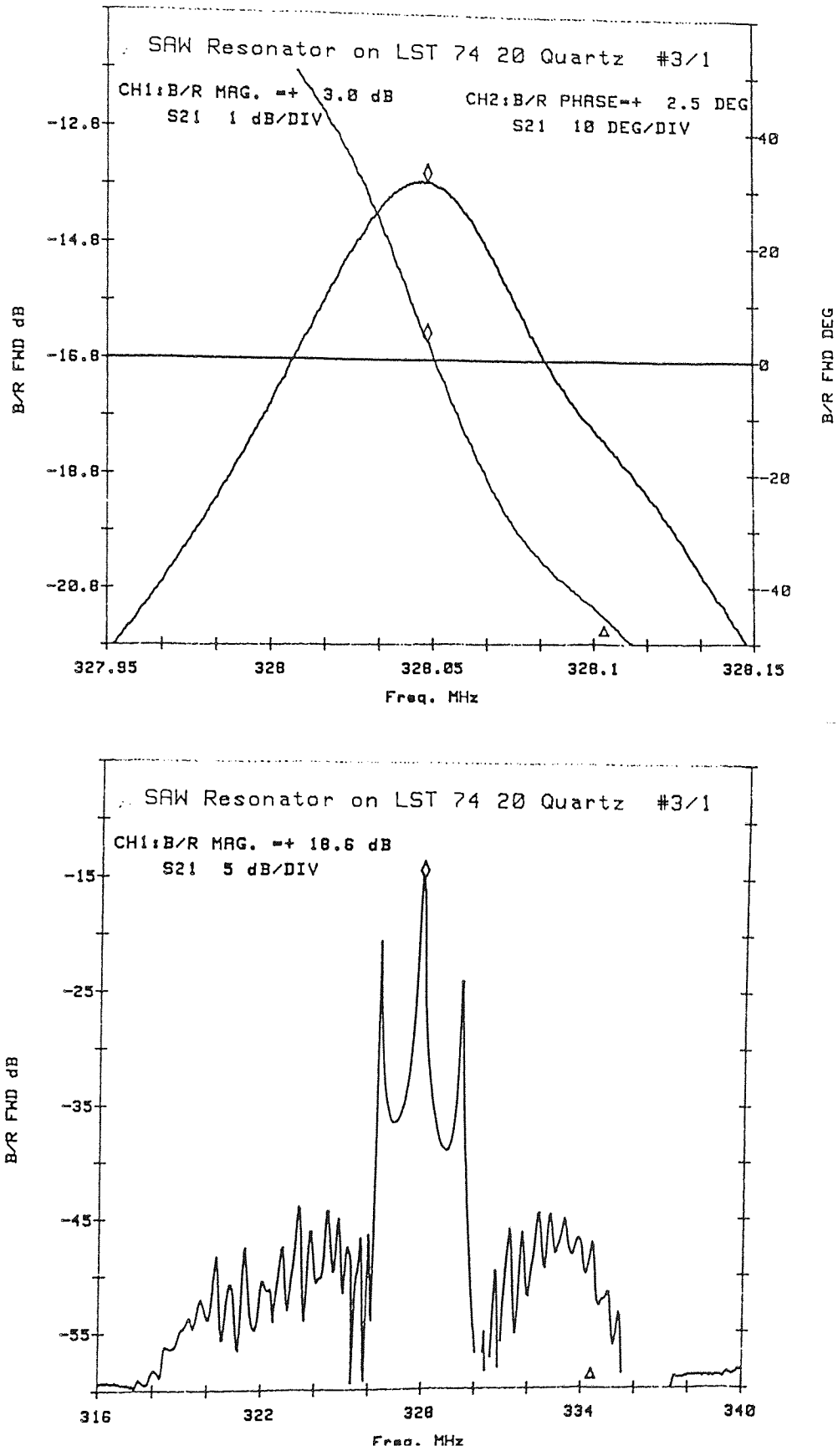

FIGURE 38 SAW Resonator on LST7420-Quartz unit 3/1
(Split-Finger Transducers)

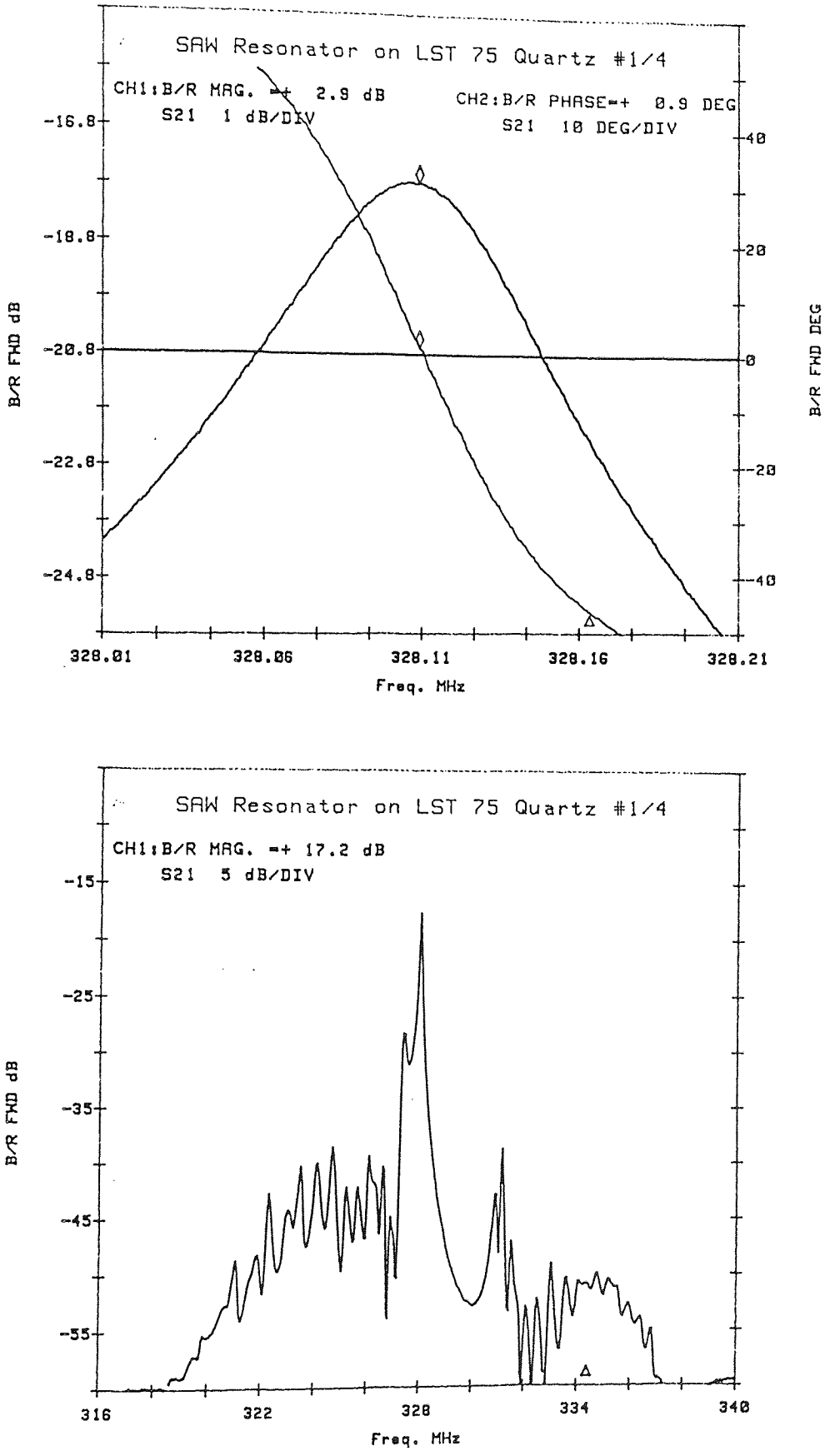

FIGURE 39 SAW Resonator on LST75-Quartz unit 1/4
(Single-Finger Transducers)

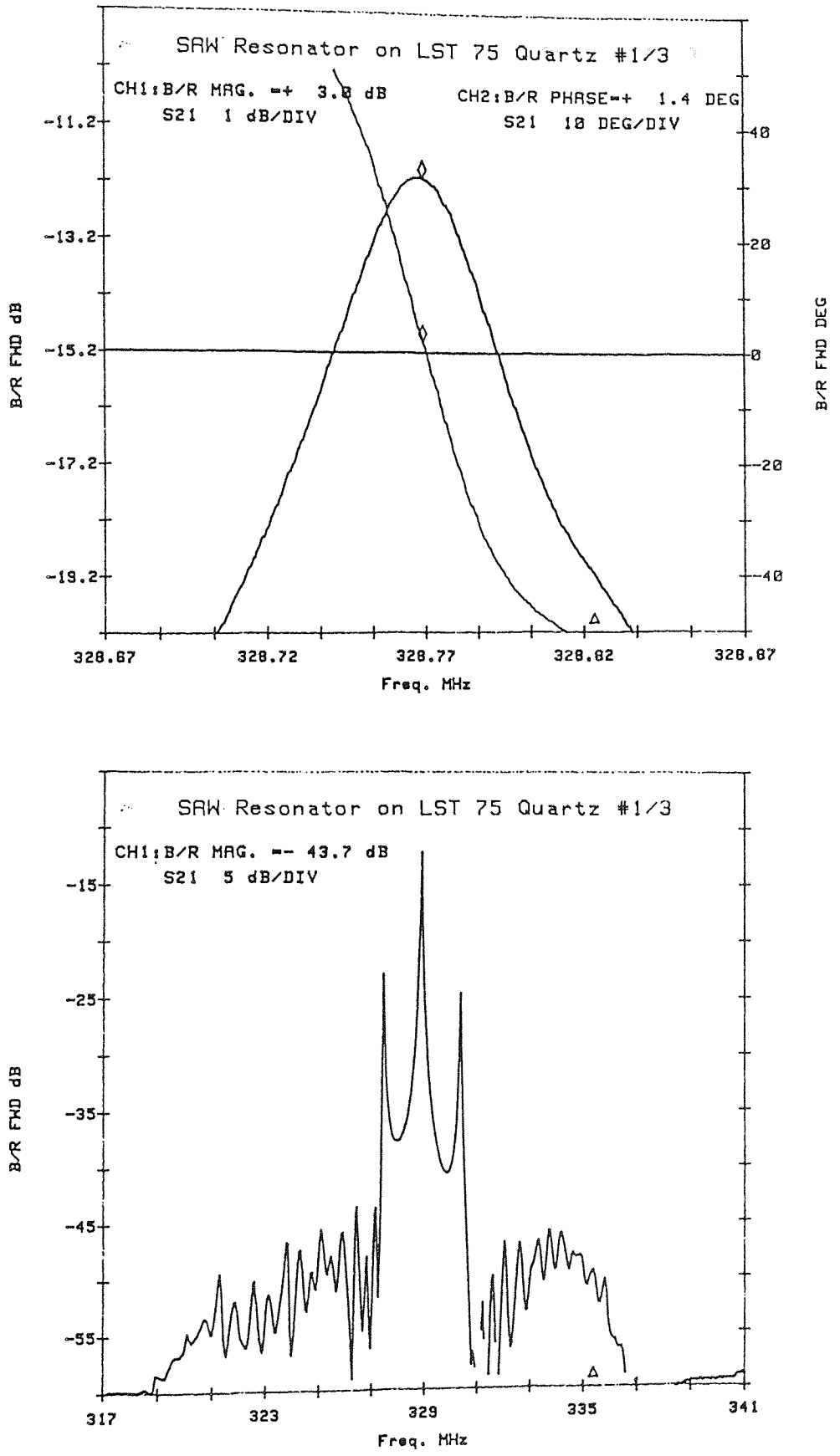

FIGURE 40 SAW Resonator on LST75-Quartz unit 1/3
(Split-Finger Transducers)

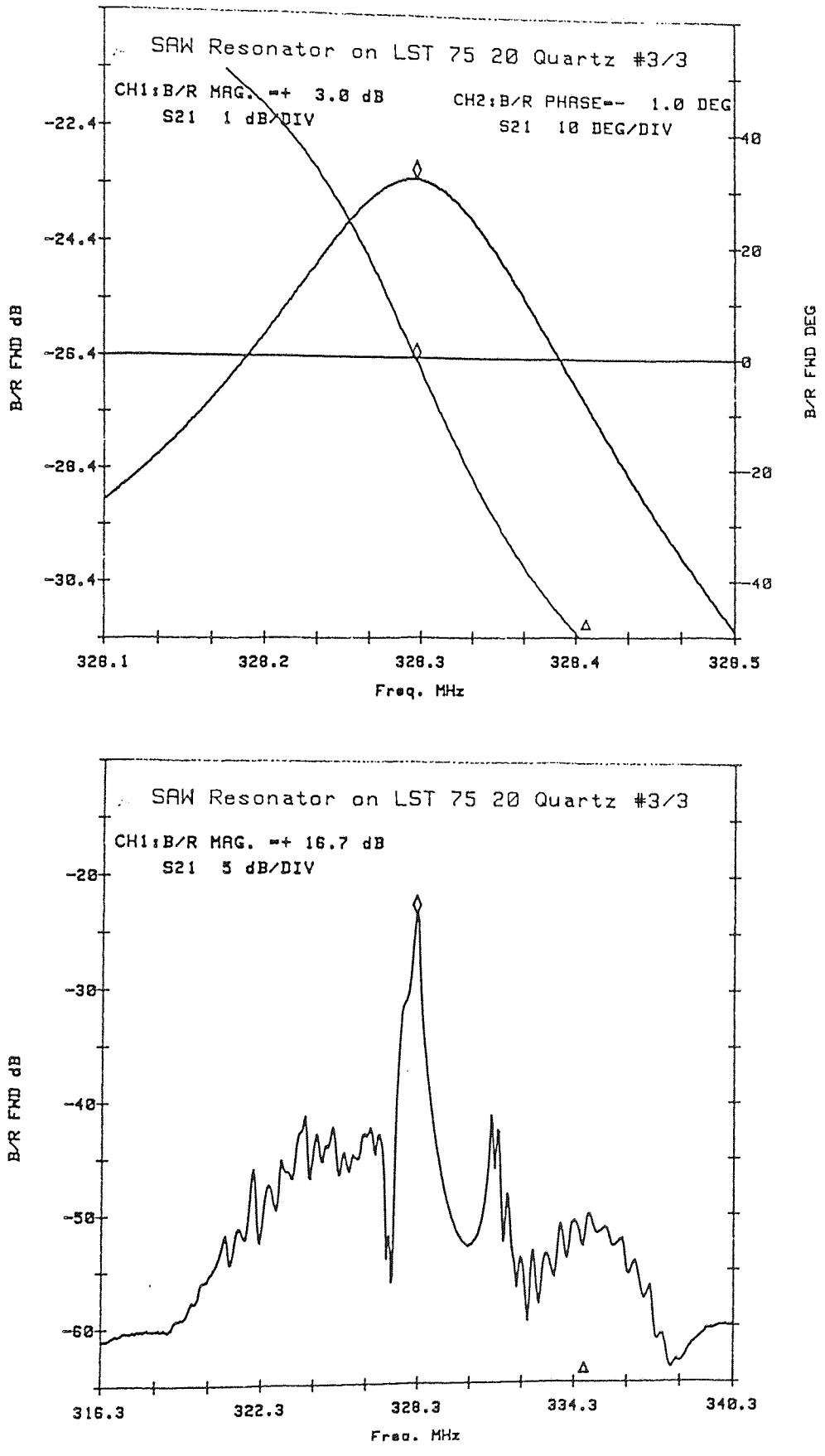

FIGURE 41 SAW Resonator on LST7520-Quartz unit 3/3
(Single-Finger Transducers)

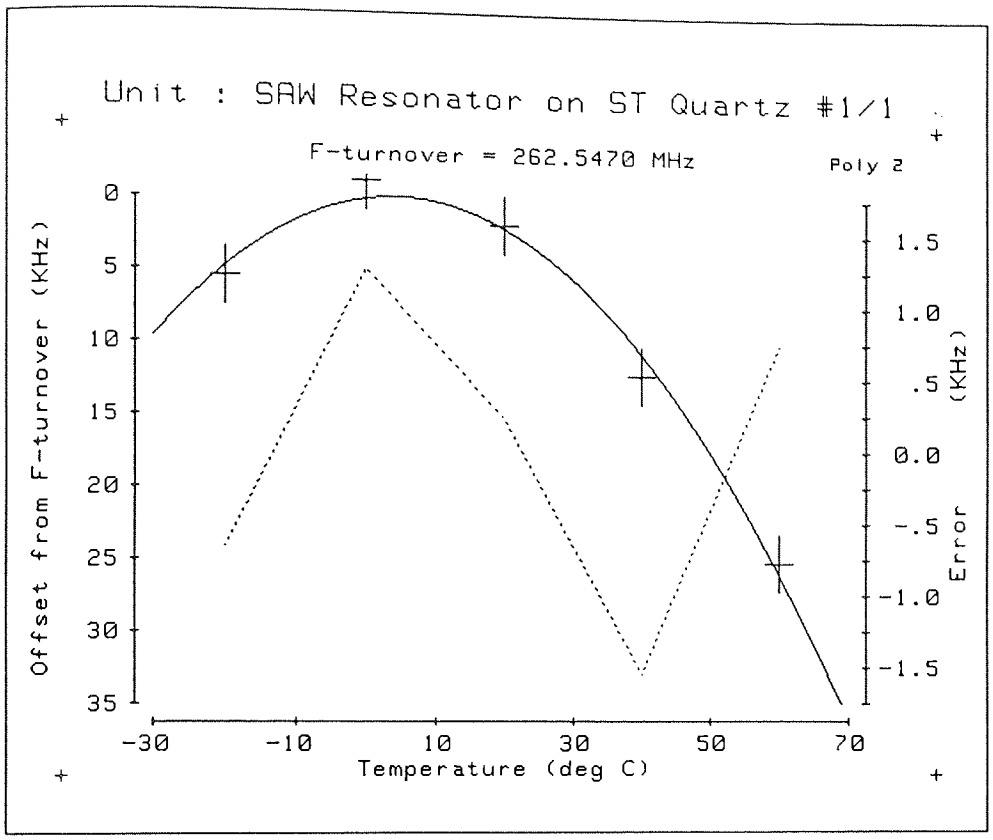

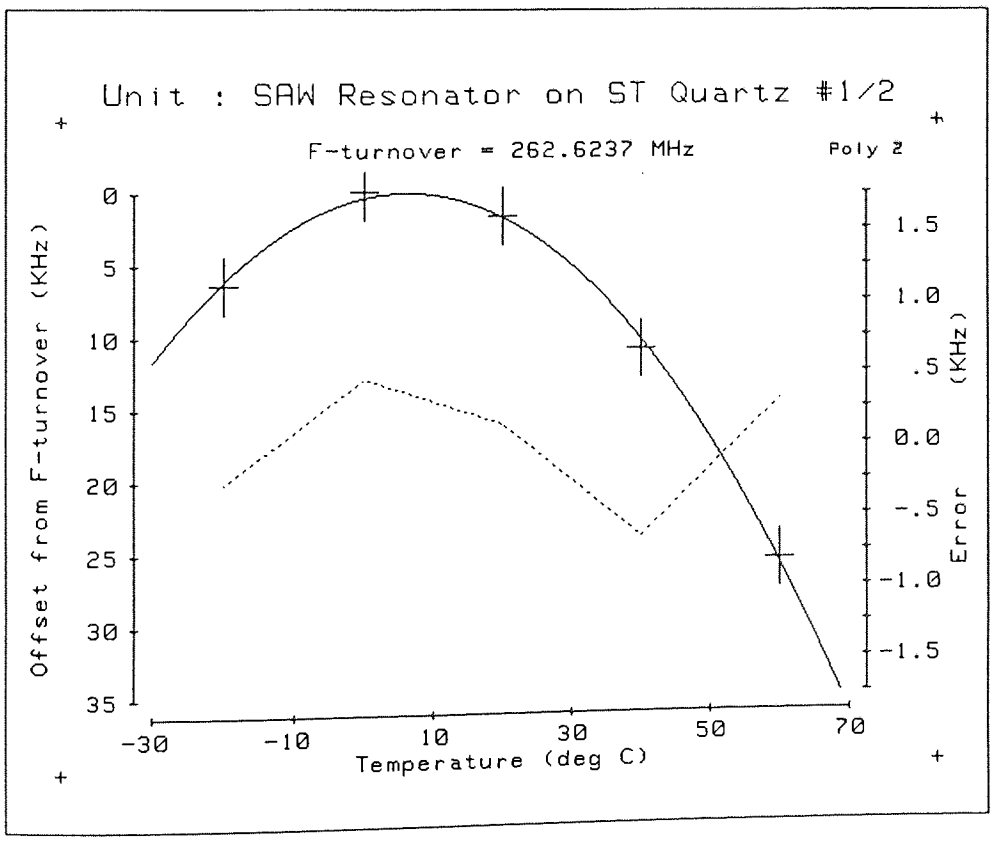

FIGURE 42 ST-Quartz Temperature Performance

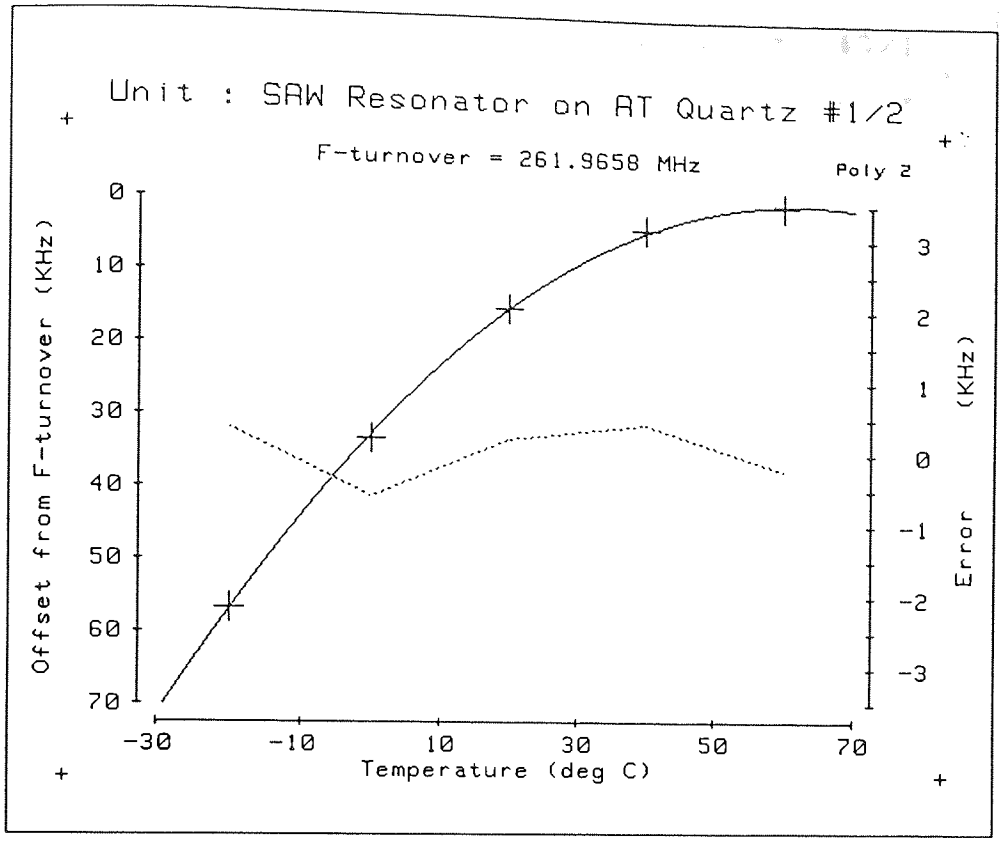

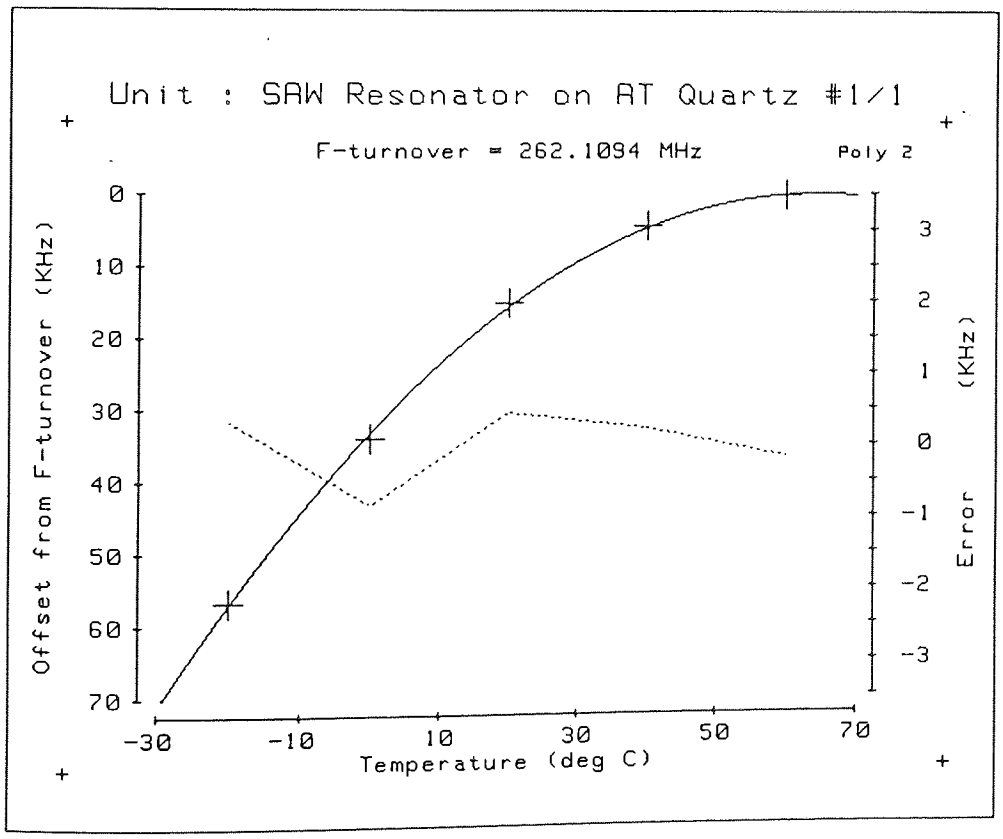

FIGURE 43 AT-Quartz Temperature Performance

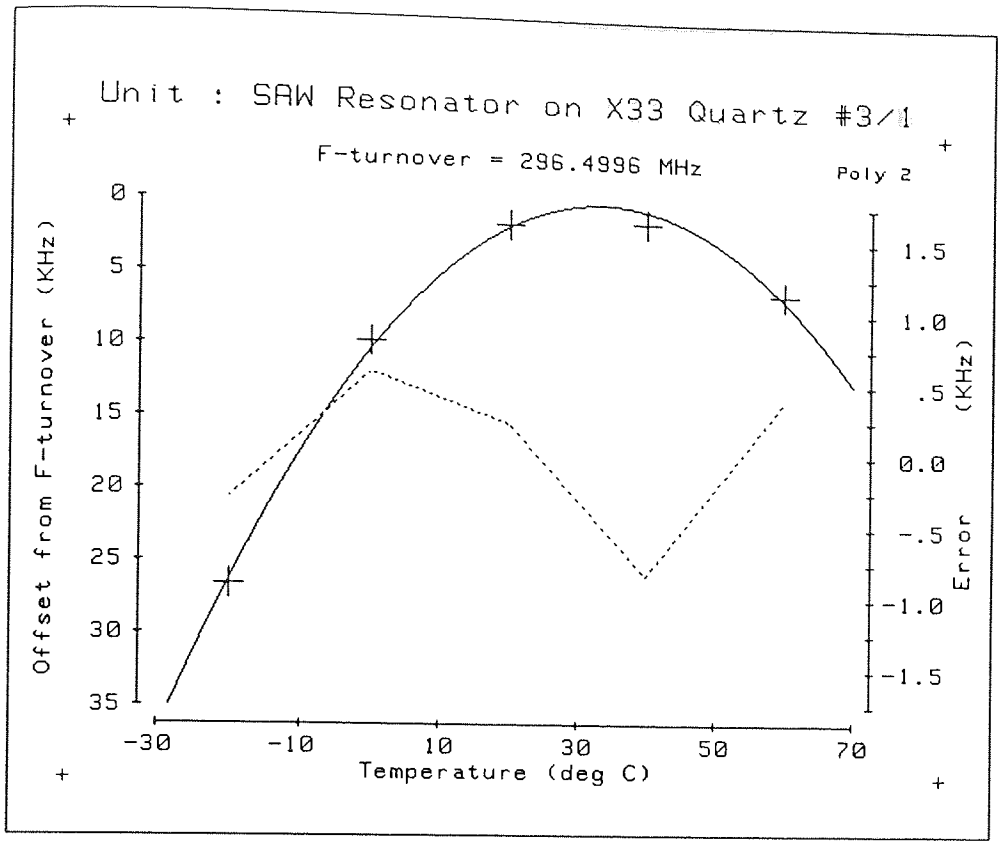

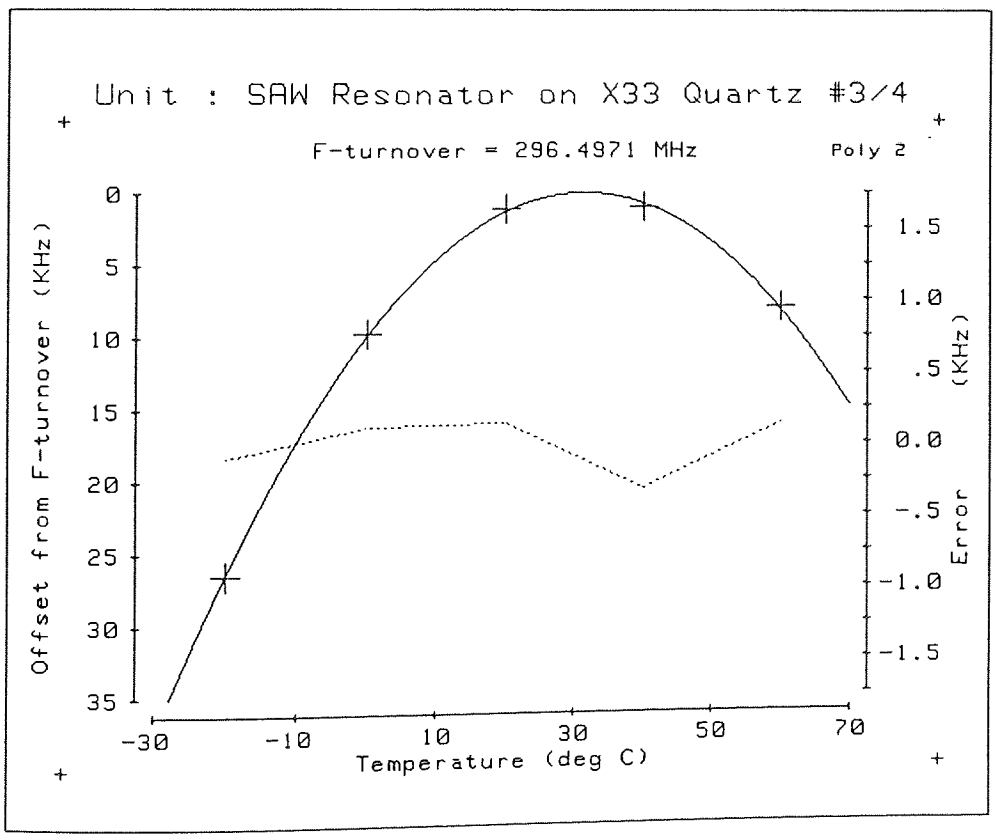

FIGURE 44 X33-Quartz Temperature Performance

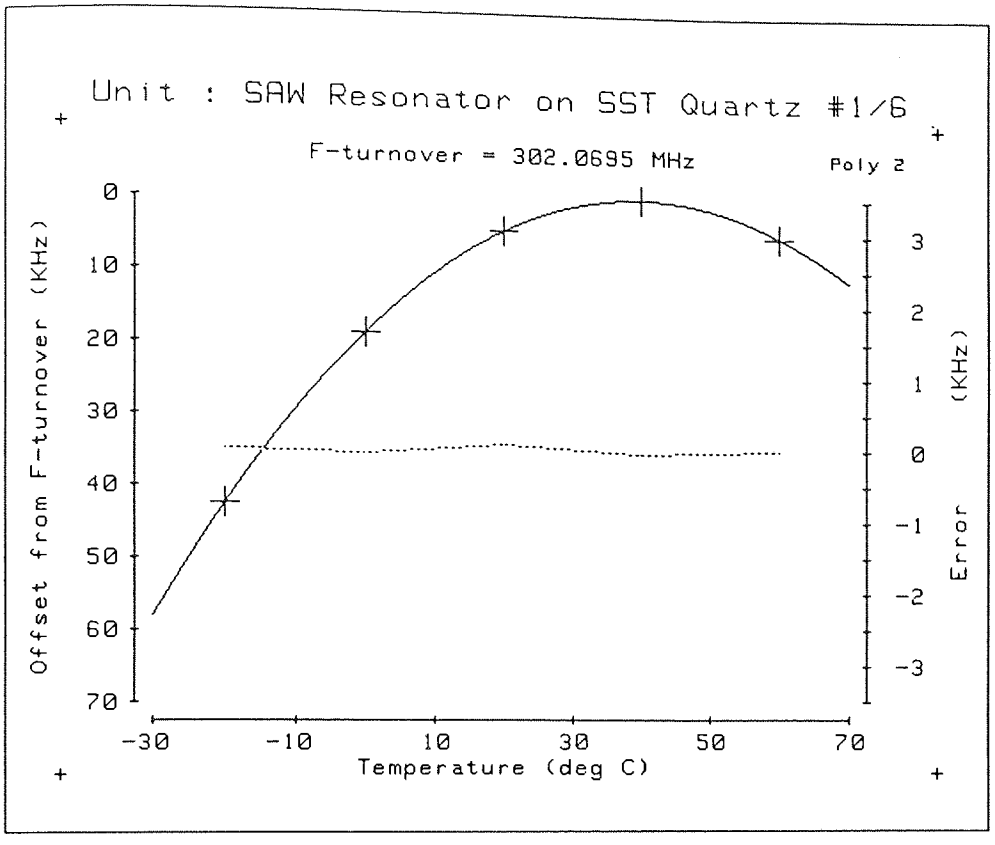

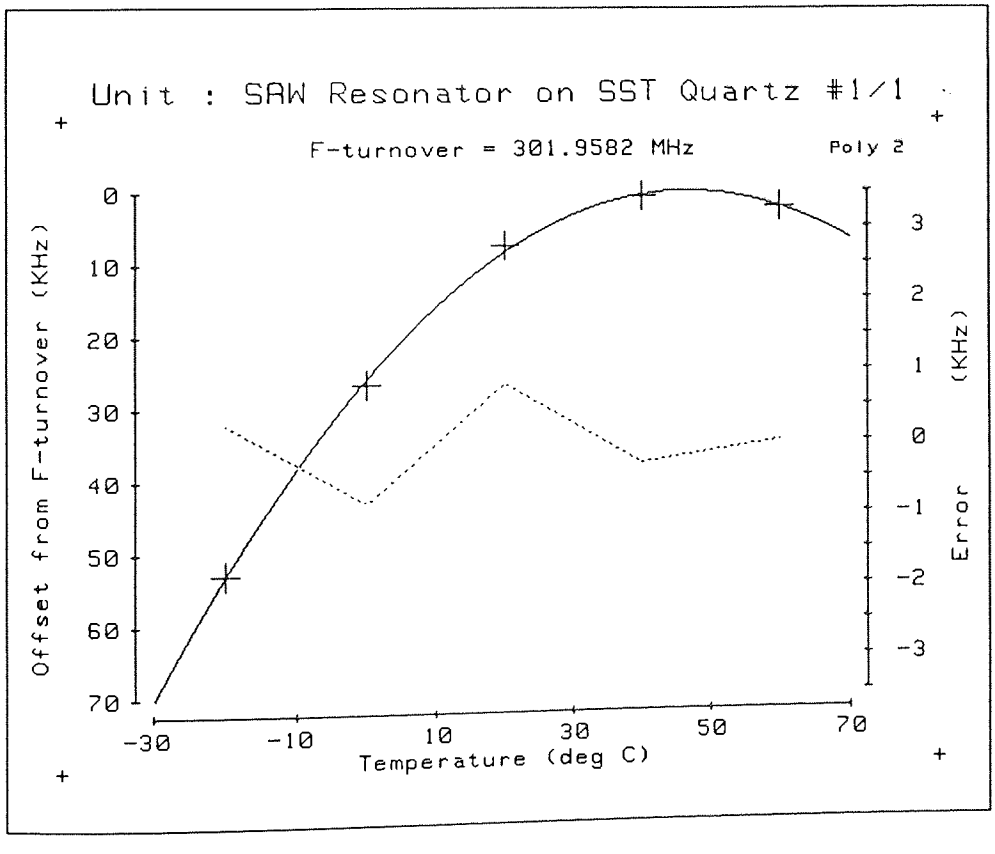

FIGURE 45 SST-Quartz Temperature Performance

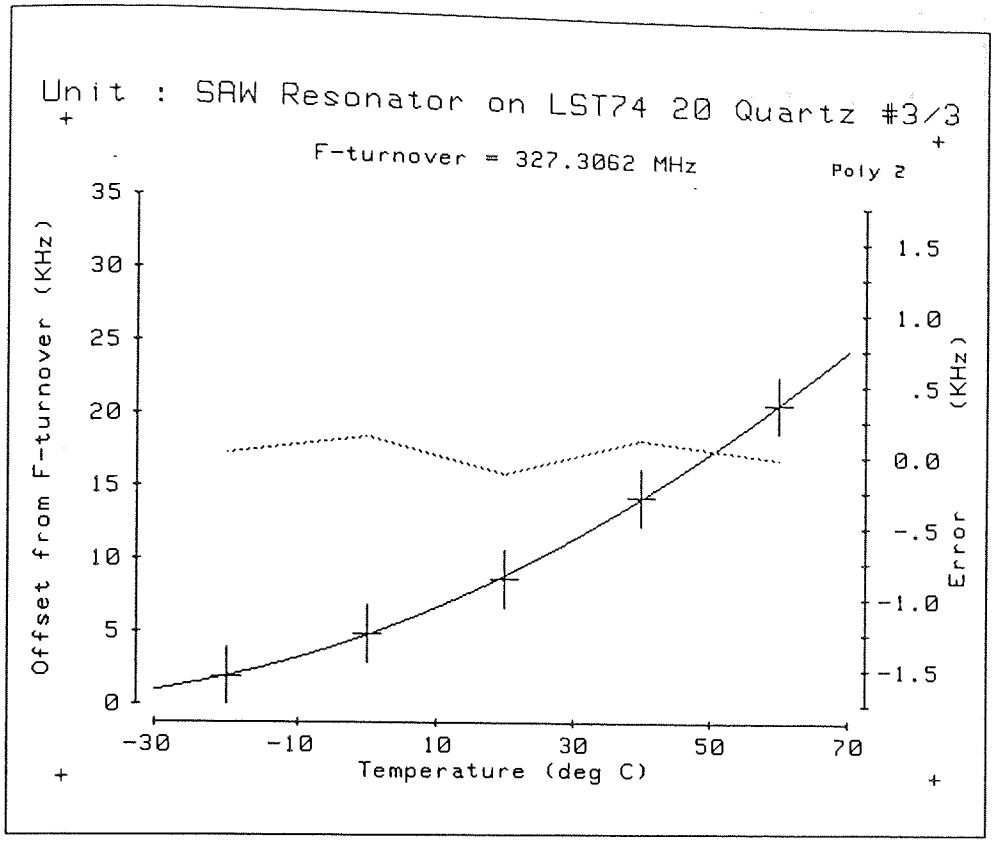

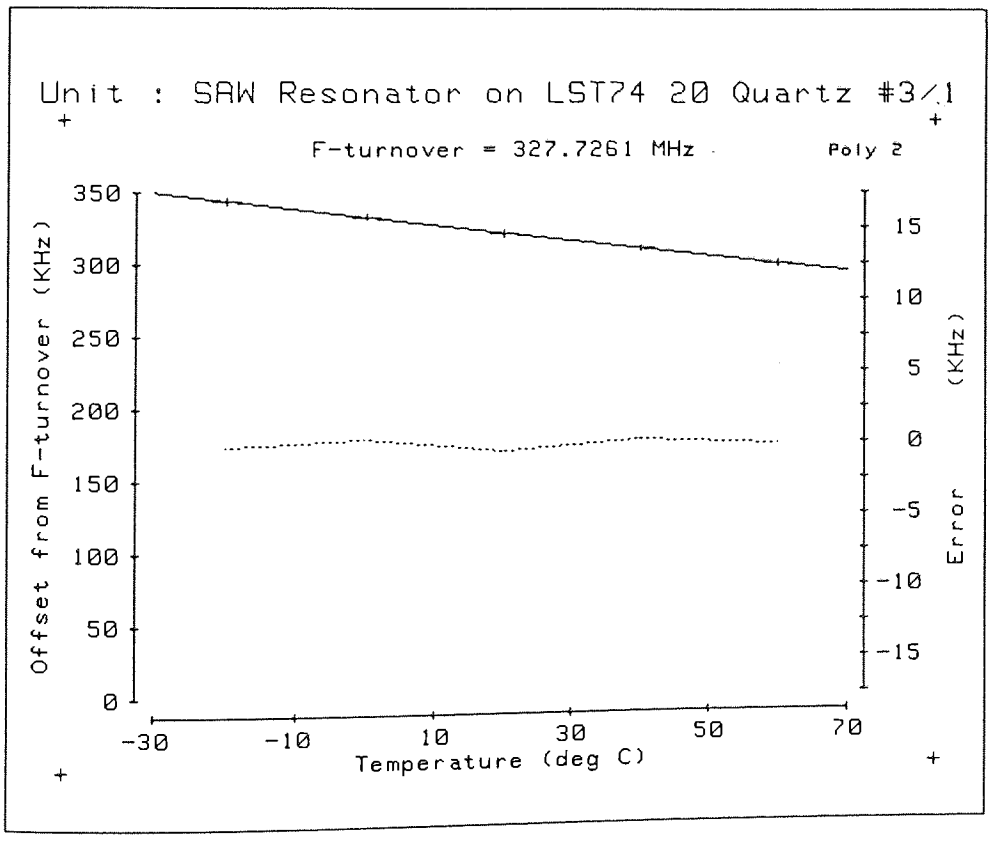

FIGURE 46 LST7420-Quartz Temperature Performance

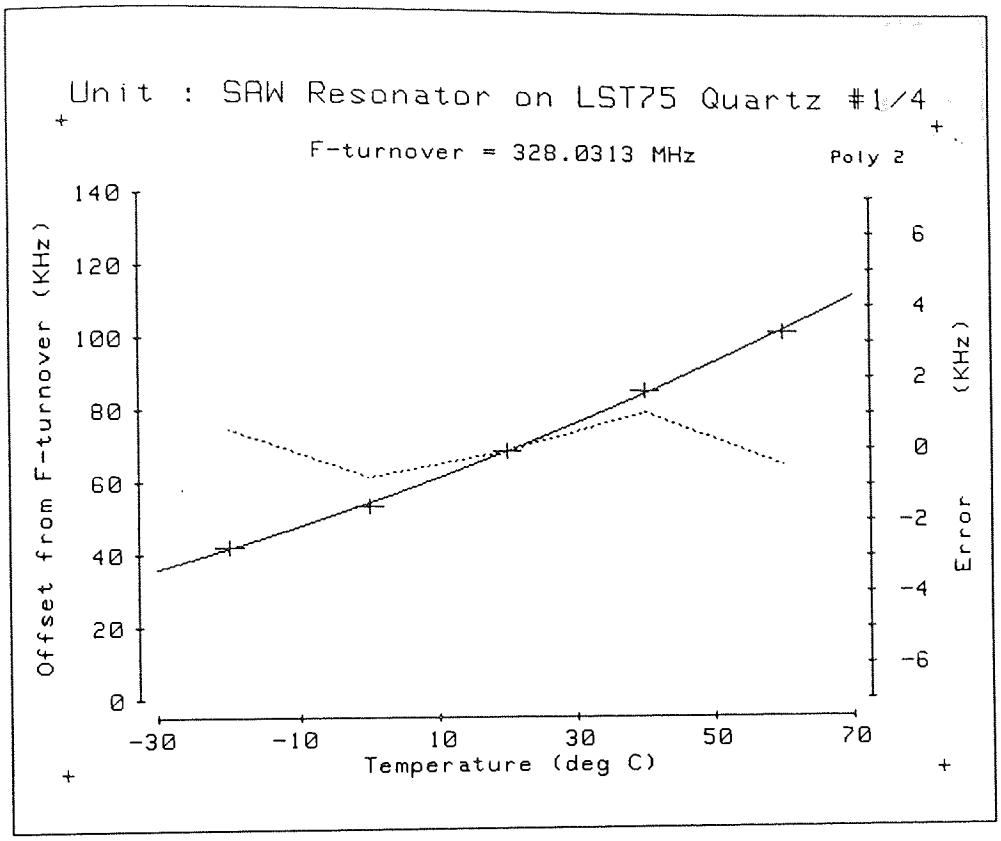

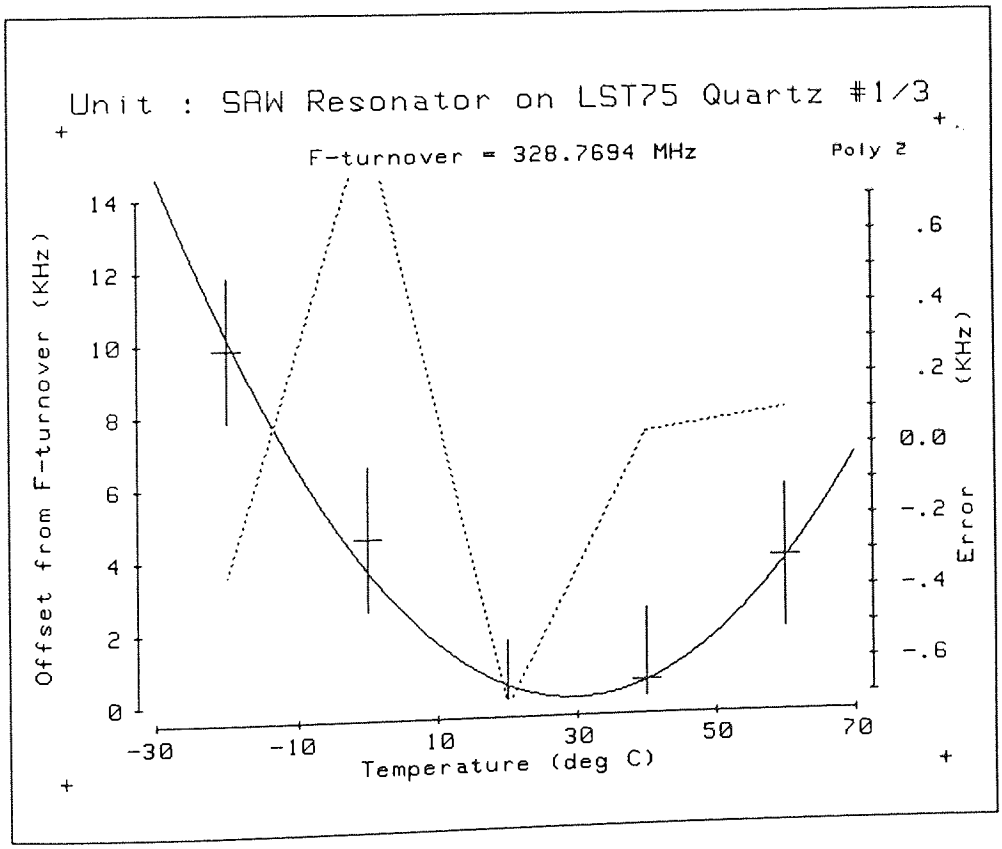

FIGURE 47 LST75-Quartz Temperature Performance

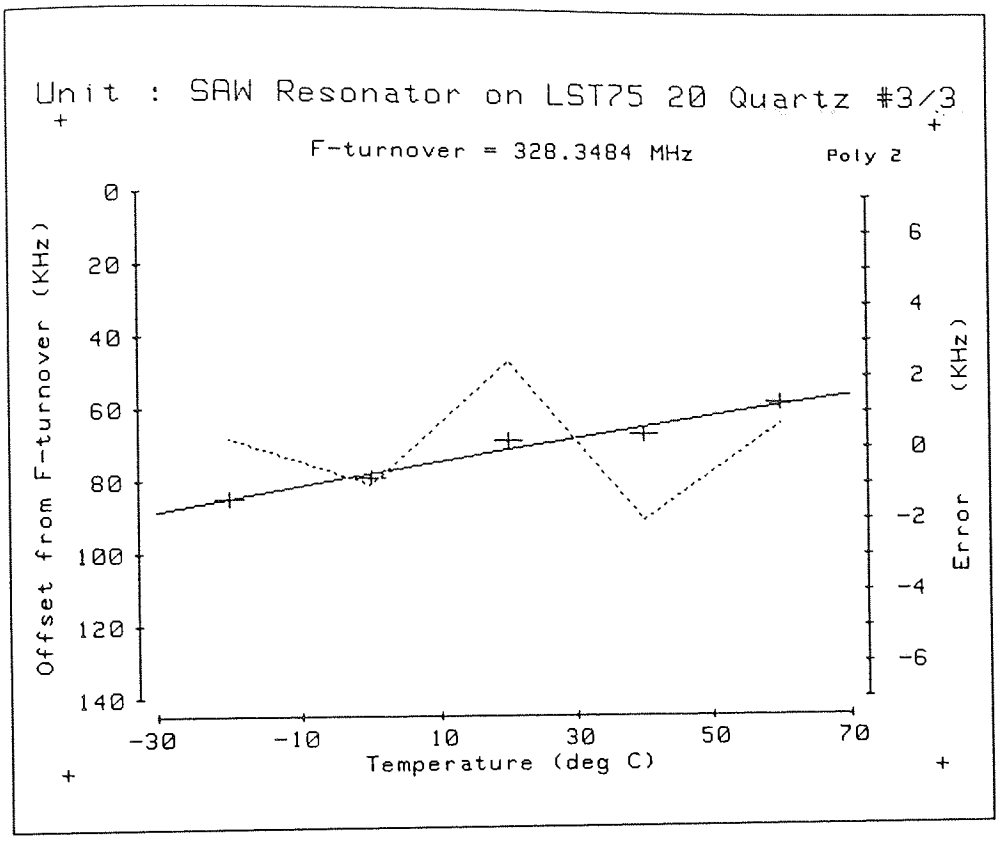

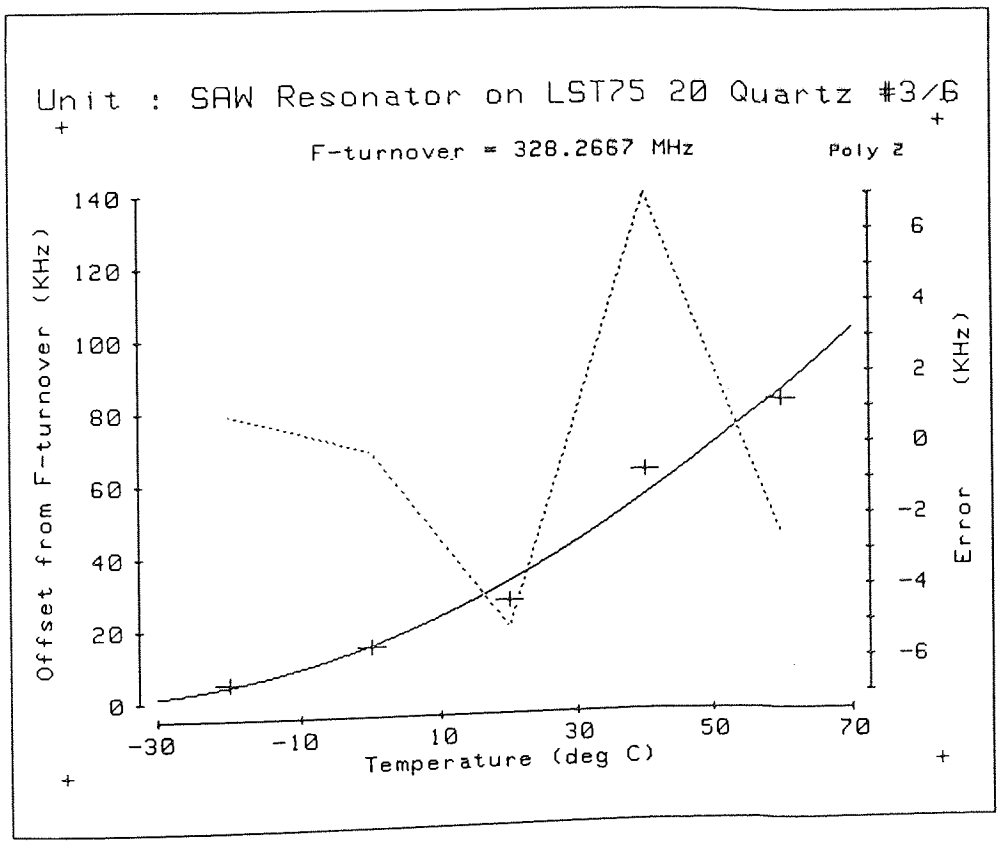

FIGURE 48 LST7520-Quartz Temperature Performance

Device No	Type	Insertion Loss (dB)	Centre Frequency (MHz)	Bandwidth (kHz)	Q
1/1	1F	13.8	262.548	25	10502
1/2	2F	13.8	262.626	25	10505
1/3	2F	14.7	262.629	26	10101
1/4	1F	13.6	262.559	25	10502
1/5	1F	19.3	262.614	36	7295
1/6	1F	14.4	262.559	26	10098
1/7	2F	20.3	262.692	34	7726
1/8	2F	14.0	262.612	26	10100
1/9	1F	18.5	262.616	34	7726

TABLE 7 Resonators on ST-cut Quartz

Device No	Type	Insertion Loss (dB)	Centre Frequency (MHz)	Bandwidth (kHz)	Q
1/1	2F	9.6	262.099	23	11396
1/2	1F	10.1	261.956	23	11389
1/3	1F	11.6	262.015	23	11392
1/4	1F	10.4	262.001	22	11909
1/5	2F	9.6	262.005	22	11909
1/6	2F	10.6	262.006	23	11392
1/7	2F	11.2	262.125	24	10922
1/8	1F	9.8	262.979	22	11908
1/9	1F	11.0	262.002	23	11392
1/10	1F	11.2	261.994	22	11908
1/11	1F	10.3	261.991	22	11909
1/12	2F	10.7	262.115	22	11914

Note: Type 1F and 2F refers to single and split finger transducers respectively

TABLE 8 Resonators on AT-cut Quartz

Device No	Type	Insertion Loss (dB)	Centre Frequency (MHz)	Bandwidth (kHz)	Q
3/1	1F	22.8	298.508	86	3448
3/2	1F	30.1	296.495	84	3530
3/3	2F	24.0	295.680	67	4413
3/4	1F	23.1	296.506	88	3369
3/5	2F	23.8	295.643	66	4479
3/6	2F	23.8	295.714	70	4224
3/7	No response				
3/8	1F	22.2	296.527	78	3802
3/9	1F	22.5	296.482	84	3529
3/10	1F	23.9	296.476	98	3025
3/11	No response				
3/12	2F	23.4	295.672	62	4769
3/13	1F	21.8	296.548	80	3707

TABLE 9 Resonators on X33-cut Quartz.

Device No	Type	Insertion Loss (dB)	Centre Frequency (MHz)	Bandwidth (kHz)	Q
1/1	2F	12.7	301.963	27	11184
1/2	No response				
1/3	2F	13.8	301.973	28	10785
1/4	2F	12.8	301.916	30	10064
1/5	2F	13.8	301.978	35	8628
1/6	1F	19.6	302.080	27	11188
1/7	No response				
1/8	1F	20.2	302.095	32	9440
1/9	1F	20.4	302.063	29	10416

TABLE 10 Resonators on SST-cut Quartz.

Device No	Type	Insertion Loss (dB)	Centre Frequency (MHz)	Bandwidth (kHz)	Q
3/1	2F	12.8	328.042	73	4495
3/2	1F	18.6	327.261	135	2424
3/3	1F	17.2	327.320	113	2896
3/4	1F	17.5	327.309	100	3237
3/5	1F	19.4	327.333	171	1914
3/6	1F	17.0	327.264	98	3339
3/7	1F	18.5	327.258	139	2355
3/8	1F	18.4	327.259	141	2322

TABLE 11 Resonators on LST7420-cut Quartz Slice 1

Device No	Type	Insertion Loss (dB)	Centre Frequency (MHz)	Bandwidth (kHz)	Q
4/1	No response				
4/2	2F	14.8	328.122	100	3280
4/3	2F	14.2	328.127	100	3280
4/4	1F	20.8	327.330	197	1661
4/5	1F	19.6	327.263	155	2111
4/6	1F	19.4	327.214	166	1972
4/7	1F	20.0	327.292	170	1925
4/8	No response				
4/9	1F	22.0	327.180	238	1375

TABLE 12 Resonators on LST7420-cut Quartz Slice 2

Device No	Type	Insertion Loss (dB)	Centre Frequency (MHz)	Bandwidth (kHz)	Q
1/1	2F	13.7	328.780	77	4270
1/2	2F	12.8	328.777	66	4981
1/3	2F	11.9	328.767	53	6203
1/4	1F	17.4	328.106	90	3646
1/5	2F	14.2	328.794	68	4835
1/6	1F	20.8	328.095	161	2038
1/7	2F	12.2	328.778	60	5479
1/8	1F	21.4	328.087	175	1875
1/9	1F	22.4	328.068	207	1585
1/10	1F	18.6	328.097	114	2804
1/11	2F	16.2	328.799	103	3192
1/12	1F	23.6	328.035	285	1147
1/13	2F	13.8	328.800	67	4907

Table 13 Resonators on LST75 Quartz

Device No	Type	Insertion Loss (dB)	Centre Frequency (MHz)	Bandwidth (kHz)	Q
3/1	1F	24.4	328.263	333	985
3/2	1F	24.8	328.224	354	927
3/3	1F	22.6	328.293	193	1700
3/4	1F	23.6	328.296	241	1362
3/5	1F	22.4	328.274	199	1649
3/6	1F	23.4	328.313	223	1471
3/7	1F	24.8	328.209	249	1318

TABLE 14 Resonators on LST7520-cut Quartz Slice 1

Device No	Type	Insertion Loss (dB)	Centre Frequency (MHz)	Bandwidth (kHz)	Q
4/1	1F	24.8	328.191	382	857
4/2	1F	24.0	328.139	277	1184
4/3	1F	23.6	328.137	273	1202
4/4	1F	23.8	328.131	263	1248
4/5	1F	24.6	328.182	364	901
4/6	2F	17.9	328.907	160	2055
4/7	2F	16.9	328.895	150	2193
4/8	2F	17.1	328.861	136	2418
4/9	2F	17.6	328.906	150	2193
4/10	2F	16.3	328.898	129	2550
4/11	2F	16.3	328.891	136	2418
4/12	2F	17.8	328.896	152	2164

TABLE 15 Resonators on LST7520-cut Quartz Slice 2

Quartz Cut	Type	No in Sample	Insertion Loss (dB)	Centre Frequency (MHz)	Q
ST	1F	5	15.9	262.579	9224
ST	2F	7	15.7	262.644	9608
AT	1F	7	10.6	261.989	11689
AT	2F	5	10.3	262.070	11505
X33	1F	7	23.8	296.506	3487
X33	2F	4	23.8	295.677	4471
SST	1F	3	20.1	302.076	10348
SST	2F	4	13.3	301.972	10165
LST7420/1	1F	7	18.1	327.286	2646
LST7420/1	2F	1	12.8	328.042	4495
LST7420/2	1F	5	20.4	327.368	1809
LST7420/2	2F	2	14.5	328.124	3280
LST75	1F	6	20.7	328.081	2183
LST75	2F	7	13.5	328.785	4838
LST7520/1	1F	7	23.7	328.267	1345
LST7520/2	2F	0	-	-	-
LST7520/1	1F	5	24.2	328.156	1078
LST7520/2	2F	7	17.1	328.893	2284

Note: /1 and /2 on LST cuts refers to slice 1 and slice 2.

TABLE 16 New Quartz Cuts - Electrical Results Summary
Average Values

Quartz Cut	Unit	Type	Frequency Turning Point (°C)	Parabola Constant (x 10^{-9})
ST	1/1	1F	4.1	-3.17
ST	1/2	2F	6.2	-3.40
AT	1/2	1F	62.3	-3.21
AT	1/1	2F	64.4	-3.09
X33	3/1	1F	33.4	-3.11
X33	3/4	1F	31.4	-3.38
SST	1/6	1F	39.3	-4.00
SST	1/1	2F	46.5	-3.99
LST7420	3/3	1F	-54.7	+0.49
LST7420	3/1	2F	1197.1	+0.07
LST75	1/4	1F	-159.4	+0.65
LST75	1/3	2F	29.8	+1.25
LST7520	3/3	1F	445.1	-0.12
LST7520	3/6	1F	-43.3	+2.42

Notes:

For each cut the single-finger transducer result is shown first.

Both X33 and LST7520 devices were single-finger as indicated.

Parabola constant, (-) indicates a maxima or turn-over point and (+) a minima or turn-under point.

Parabola constant accuracy estimated as +/- $1x10^{-9}$.

TABLE 17 New Quartz Cuts - Temperature Performance Results Summary

appears to make very little difference to recorded performance. The split-finger devices operate at a frequency approximately 75kHz higher than single-finger units. This increase may be due to SAW velocity effects and mask-making tolerences.

It is clear from Table 16 that all cuts operate at higher frequencies than ST, implying higher acoustic wave velocities. In general, all new cuts investigated have a less well defined cavity response than ST and AT-cuts. In particular, the SST-cut has three peaks with the centre peak lowest. On the LST-cuts the side peaks are always at least 5dB below the main response. On all new cuts split-finger transducers produced a less distorted response. This is most probably due to the cancellation of spurious reflections. Also, in all cases, except for the X33-cut, split-finger devices gave lower insertion losses and higher Q values. On the LST-cuts split-finger transducers also gave much higher operating frequencies.

The 263MHz resonator mask is based upon a 12um acoustic wavelength. From the average frequencies of Table 16 it is possible to calculate the actual acoustic wave velocity for each quartz cut. These are listed in Table 18, together with the percentage increase over the ST-cut.

In comparing device performances, it is assumed that differences are due mainly to the quartz orientation. There are always processing variations between slices affecting, in particular, insertion loss and Q-value. As far as possible such variations are minimised by adopting stringent quality controls. Ideally, a very large number of test devices would allow slice-to-slice differences to be averaged out. Such numbers have not been tested due to material availability constraints.

The X33-cut (Figures 33, 34 and Table 9) suffers from a relatively high insertion loss and moderate Q-level. The frequency value relates to a 13% acoustic velocity increase over the ST-cut. The acoustic velocity of 3550m/s is not in agreement with that quoted by Webster[48] of 3175m/s. Further, as is shown below, the computed TCD is also similar to ST and not an improvement as claimed by Webster. Although Webster does not demonstrate resonators on X33 quartz, the TCD and acoustic velocities should be in agreement. The most likely reason for such discrepancies is that the quartz

Quartz Cut	Type	Centre Frequency (MHz)	Acoustic Wave Velocity (m/s)	Improvement over ST-cut (%)
ST	1F	262.579	3151	-
ST	2F	262.644	3152	-
AT	1F	261.989	3144	-0.25
AT	2F	262.070	3145	-0.23
X33	1F	296.506	3558	12.92
X33	2F	295.677	3548	12.60
SST	1F	302.076	3625	15.04
SST	2F	301.972	3624	15.00
LST7420	1F	327.327	3928*	24.66
LST7420	2F	328.073	3937*	24.94
LST75	1F	328.081	3937	24.94
LST75	2F	328.785	3945	25.21
LST7520	1F	328.212	3939*	25.01
LST7520	2F	328.898	3947	25.25

Notes:

* Reading is the average of two slices (Table 16)

TABLE 18 New Quartz Cuts - Acoustic Wave Velocities.

material reported here was not of the correct cut. The inferior performance of the material tested precluded its use for real devices and, in view of the uncertainty described, no further work was done on this cut.

Only the SST-cut has a Q-value similar to ST and AT quartz. However, the triple peak nature of the response (Figures 35 and 36) would severely restrict its use in most oscillator applications. The triple peak is probably associated with the large power flow angle and suggests several cavity modes. Also significant on SST-cut is the insertion loss variation between single-finger and split-finger devices (Table 10). Lukaszek and Ballato[47] claim reduced acoustic attenuation and higher phase velocity. The split-finger insertion loss results (Table 10) show a small improvement over ST (13.3dB versus 15.7dB). Insertion loss on the single-finger device suggests non-optimal coupling in the acoustic cavity. The acoustic wave velocity shows a 15% improvement.

These results are therefore in broad agreement with published figures. However, the multi-moding effect suggests that the improvements offered by the SST-cut may be used to best advantage in filter design.

The results for the three LST-cuts show several common features (Tables 11 to 16). In all cases there is an acoustic wave velocity approximately 25% higher than ST-cut. The value of 3947m/s for LST7520 is in excellent agreement with Shimizu et al[50]. On all LST-cuts the split-finger devices consistently out-perform the single-finger units in terms of insertion loss and Q. Also, split-finger units result in a centre frequency increase of approximately 700kHz. On the split-finger devices the Q-values are much lower than those for the ST and AT-cuts even though the insertion loss levels on LST7420 and LST75 are comparable to ST.

Plots of the responses of the LST-cuts are shown in Figures 37 to 41. In comparing LST7420 units 3/3 and 3/1 (Figures 37 and 38) the split-finger device clearly has a less distorted passband and close-in stopband with improved transducer response suppression. The two responses are shown overlapped in Figure 49, clearly indicating the passband variations. As similar split-finger transducer resonators on LST-quartz have not been reported elsewhere, comparisons cannot be made. The results presented here suggest that split-fingers are

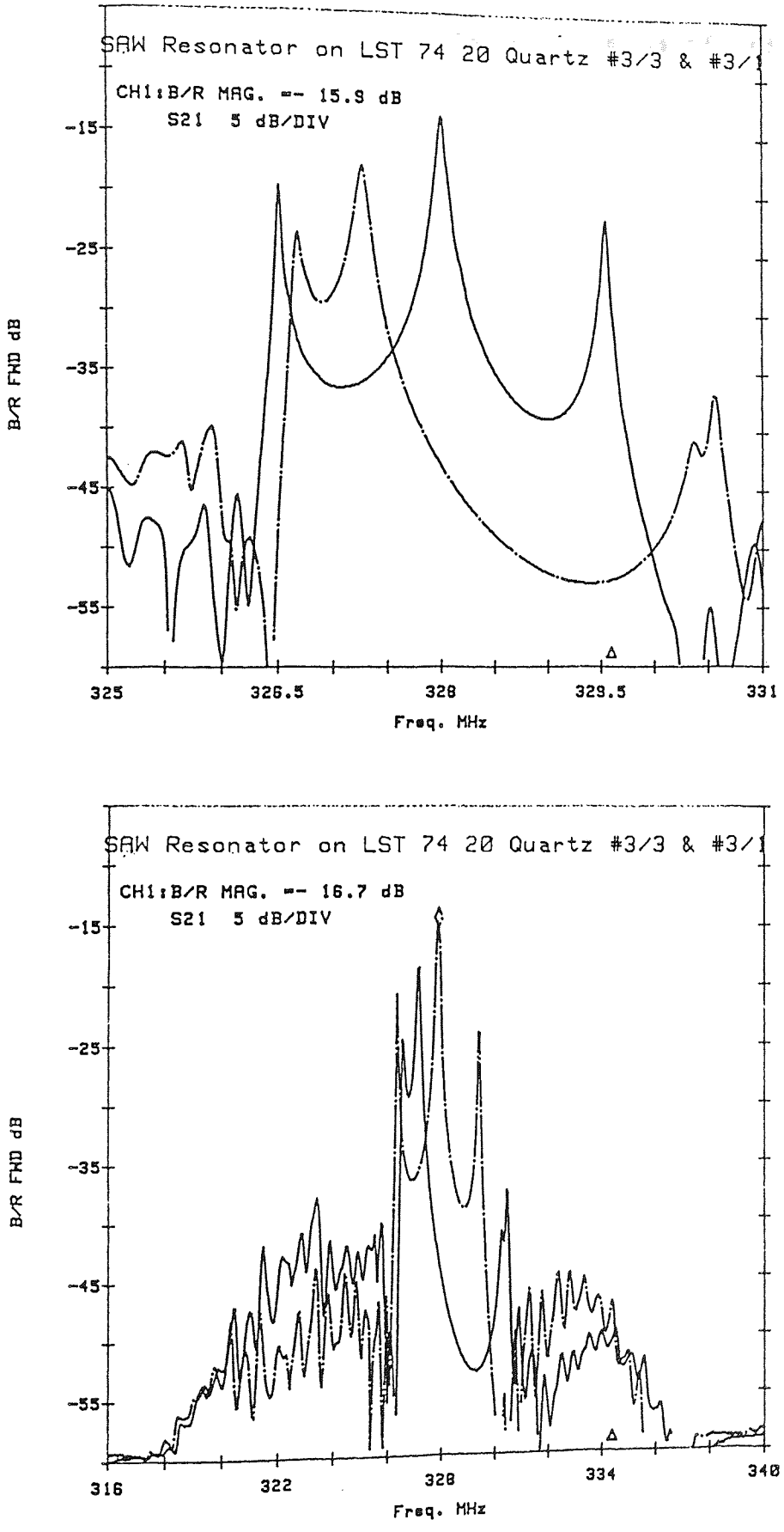

FIGURE 49 LST7420-Quartz Split-Finger v Single-Finger Frequency Performance

necessary to maximise performance in terms of insertion loss and Q.

Similar comparisons can also be made for the LST75-cut. Figure 50 shows the close-in responses for both device types on LST75. Figure 50 also illustrates the repeatability of the devices as each plot contains three devices super-imposed. The results for LST75 are marginally better than those for LST7420 and substantially superior to those for LST7520. One LST75 device, unit 1/3, had an insertion loss of only 11.9dB and a Q-value of 6203. This result suggests that LST75 has an attenuation constant close to that for ST, again in agreement with Shimizu et al[50].

The consistently poor results for LST7520 preclude its use in resonator applications. Insertion loss is 3 to 4dB higher than other LST-cuts and the Q-value is approximately 50% lower. Shimizu and Tanaka[49] suggest large variation in device performance for small changes, less than one degree, in quartz Y-axis rotation. With suitable optical alignment precision this may be an advantage. At STC the lack of a strong X-ray reflection degraded the alignment accuracy. Therefore, unless the accuracy is improved large batch variations in processing are likely. In a volume production environment such variations would be expensive and probably unacceptable.

Equally important is the temperature performance of the new cuts. The computed plots of frequency versus temperature are shown in Figures 42 to 48 and data generated is summarised in Table 17. Each plot, for example Figure 42, shows the actual data points and the curve fitted to those points. Also given is the error between the polynomial fit and the actual test data. This is an indirect measure of the quality of the data and therefore of confidence in the result. Figure 42 indicates a maximum error of 1.5kHz for ST-quartz.

In comparing different temperature performance plots, it should be noted that the computer programme included an auto-scaling facility. Vertical scales are not directly comparable as can be seen, for example, in Figure 46. Here, LST7420 unit 3/1 has an excellent curve fit. This is due to the fact that the turnover temperature is very high and therefore at room temperature the slope of the curve approaches a straight line. Table 17 shows that this unit has the best parabola constant.

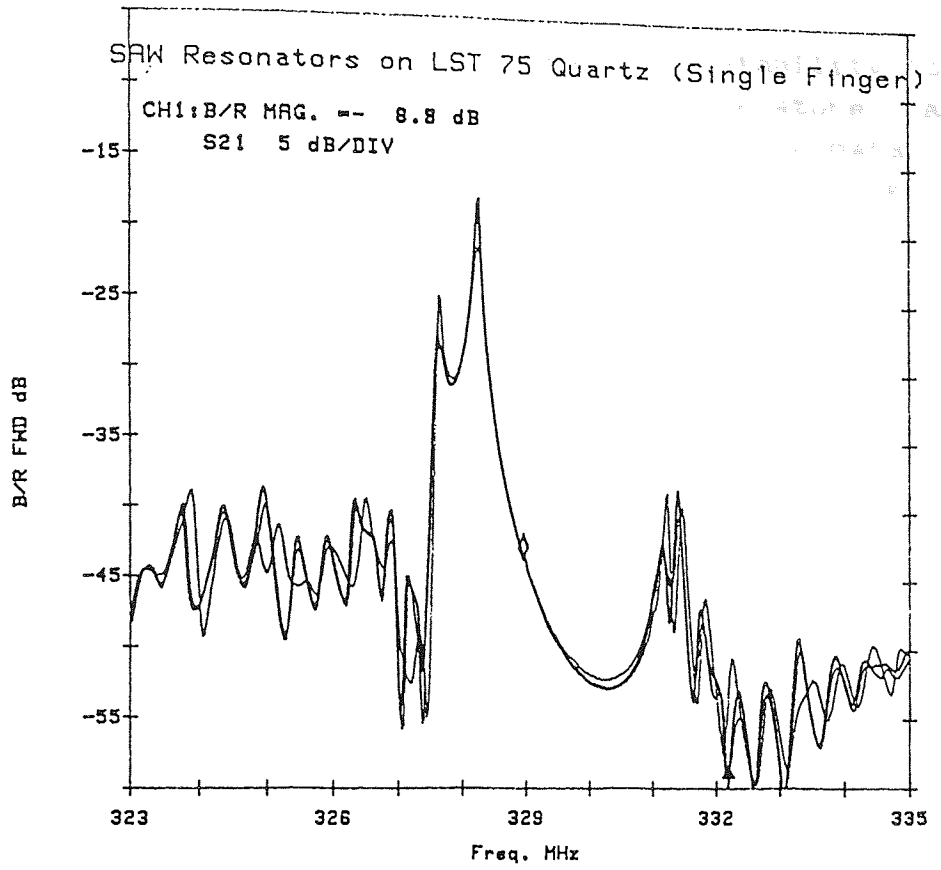

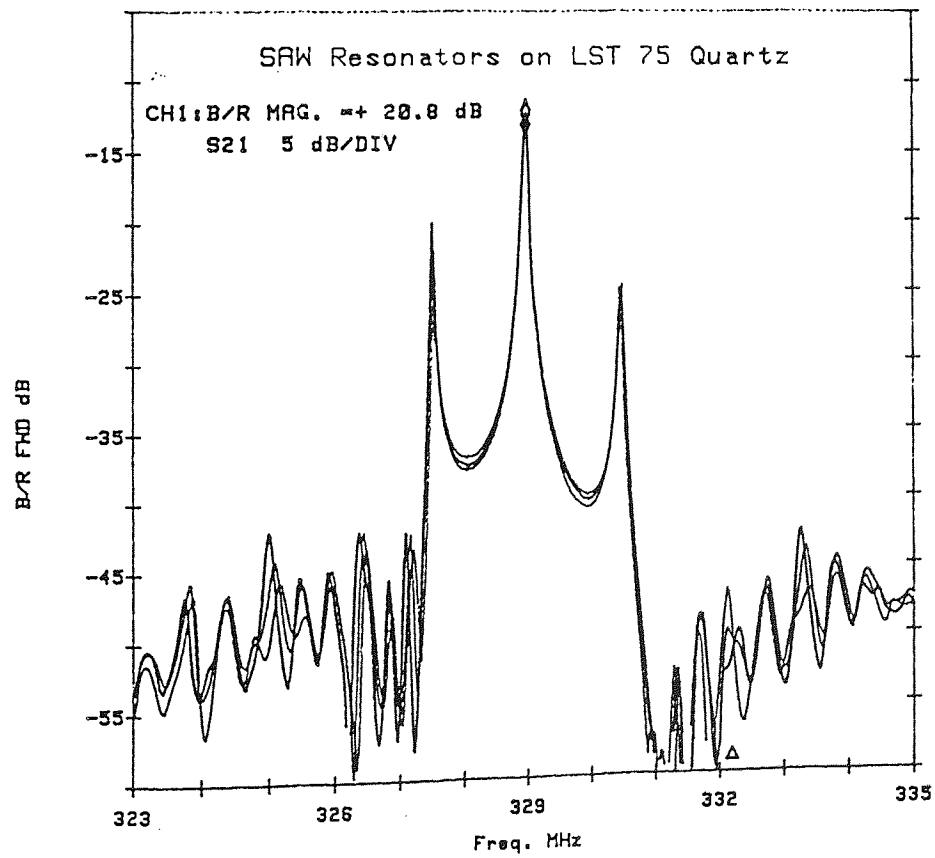

FIGURE 50 LST75-Quartz Split-Finger v Single-Finger Frequency Performance

A more useful measure of temperature stability is the total frequency shift over a typical temperature range. This takes into account both the parabola constant and turning point. Table 19 lists the resultant frequency shift for a typical military overband specification, namely -40 to +85°C. Although LST7420 unit 3/1 has the best TCD, its performance on real devices is limited by the very high turning point. Table 19 clearly indicates that the best performance is achieved with a split-finger device on LST75 quartz (unit 1/3).

The ST and AT results are again as expected and are in agreement with Table 3. As with the frequency results there is very little difference between single and split-finger devices. In practice the SAW designer would attempt to place the turnover temperature in the centre of the overband range, utilising the results of Section 4.2.

As described briefly above, the results for the X33-cut are not as expected. Parabola constants are similar to those for the ST-cut. This fact together with the electrical performance anomalies implies an incorrect angle of cut. Only the turnover temperature and sign of the parabola constant agree with Webster[48]. In view of the moderate level of improvement claimed for the true X33-cut, and the time needed to acquire new material, it was decided not to attempt a repeat trial using new quartz.

The SST-cut gives almost identical results for both single and split-finger units. Parabola constants are not as good as ST but are of a similar order. Lukaszek and Ballato[47] claim that the parabola constant can be improved by rotating the propagation direction. The results achieved here are in broad agreement with Lukaszek and Ballato for the cut as defined in Table 6.

The LST-cuts are unusual in that some have a frequency minima rather than maxima as for the other cuts tested. This is indicated by the sign of the parabola constant in Table 17. In all LST cases there is a marked difference between the single and split-finger device results. All TCD's show an improvement over that for ST whilst the high and low level of frequency turning points reduces the practical value of such TCD's. This is best illustrated with the result for the LST7420 split-finger device. At 0.07×10^{-8} the TCD shows a four-fold

Quartz Cut	Unit	Type	Frequency Shift -40 to +85°C (ppm)
ST	1/1	1F	210
ST	1/2	2F	211
AT	1/2	1F	333
AT	1/1	2F	336
X33	3/1	1F	165
X33	3/4	1F	171
SST	1/6	1F	250
SST	1/1	2F	299
LST7420	3/3	1F	95
LST7420	3/1	2F	205
LST75	1/4	1F	295
LST75	1/3	2F	61
LST7520	3/3	1F	127
LST7520	3/6	1F	393

Notes:

For each cut the single-finger transducer result is shown first.

Both X33 and LST7525 devices were single-finger as indicated.

The frequency shift is calculated, for a typical overband requirement of -40 to +85°C, from the corresponding parabola constants and turning points of Table 17.

TABLE 19 New Quartz Cuts - Frequency Shift

improvement over ST. When the turning point of 1197°C is taken into account a typical frequency shift (Table 19) is of the same order as that for ST.

The LST7420 and LST75 results indicate usable temperature performance even with the turning points outside the overband range of normal devices. The LST75 split-finger device gives excellent results in line with those of Shimizu et al[50]. Plots for these devices (Figures 46 and 47) show relatively small errors generated in the curve fitting routine.

Results for LST7520 show an anomaly. Both devices are single-finger transducer yet very different results are achieved. Reference to the plots for these devices shows that a large error was needed in curve fitting at two points on unit 3/6. This suggests another predominant mechanism influencing device performance, such as surface contamination or possible thermal strain in the cantilevered device die. For these reasons the result for this device is discounted.

Large differences in temperature performance between the three LST-cuts are expected (Shimizu et al[50]). The small sample precluded any conclusions on the transducer induced variations. Significant errors may have arisen in the curve plotting due in part to the number of temperature readings taken and also to the accuracy of those readings. Therefore it was decided to test four LST75 devices in more detail. LST75 was chosen because of its acceptable temperature and frequency performance, especially with split-finger transducers. Devices were tested over a wider temperature range at eight settings from -60 to +80°C. Results are given in Table 20 and in Figures 51 and 52. The test included a repeat measurement on LST75 unit 1/3.

From Table 20 it can be seen that all devices had a parabola constant of the same order with an average for split-finger devices of 0.60×10^{-6}. Also, the frequency turning point for these devices was consistently around 30 to 45°C with an average of 39°C. For the split-finger devices the resultant frequency shift was as low as 29ppm, averaging at 36ppm. This compares with 211ppm for the same device on ST-cut quartz.

The result for LST75 unit 1/3 can be compared with

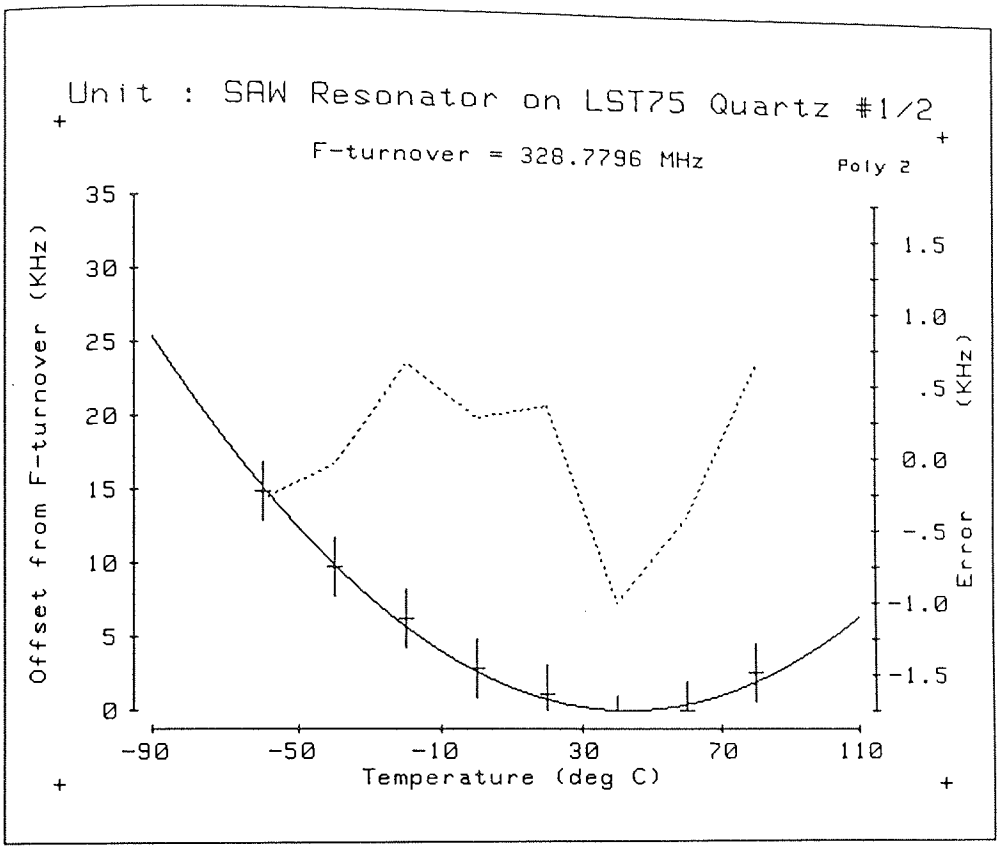

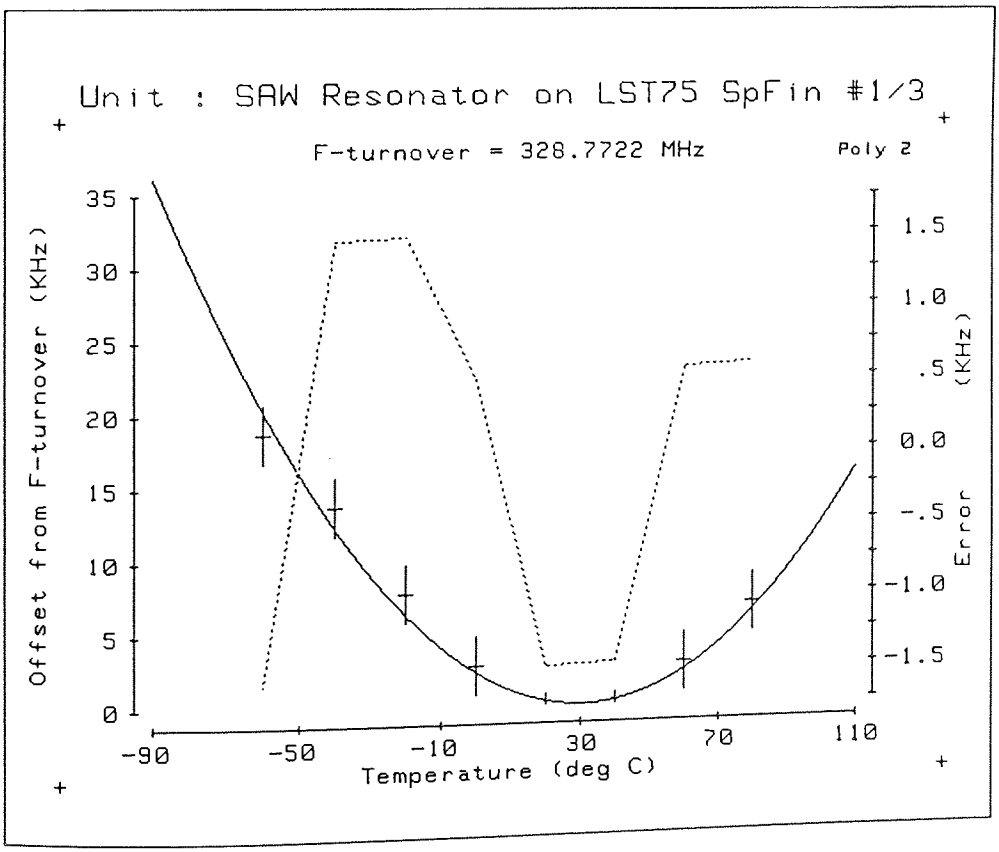

FIGURE 51 Temperature Performance LST75-Quartz units 1/2 and 1/3

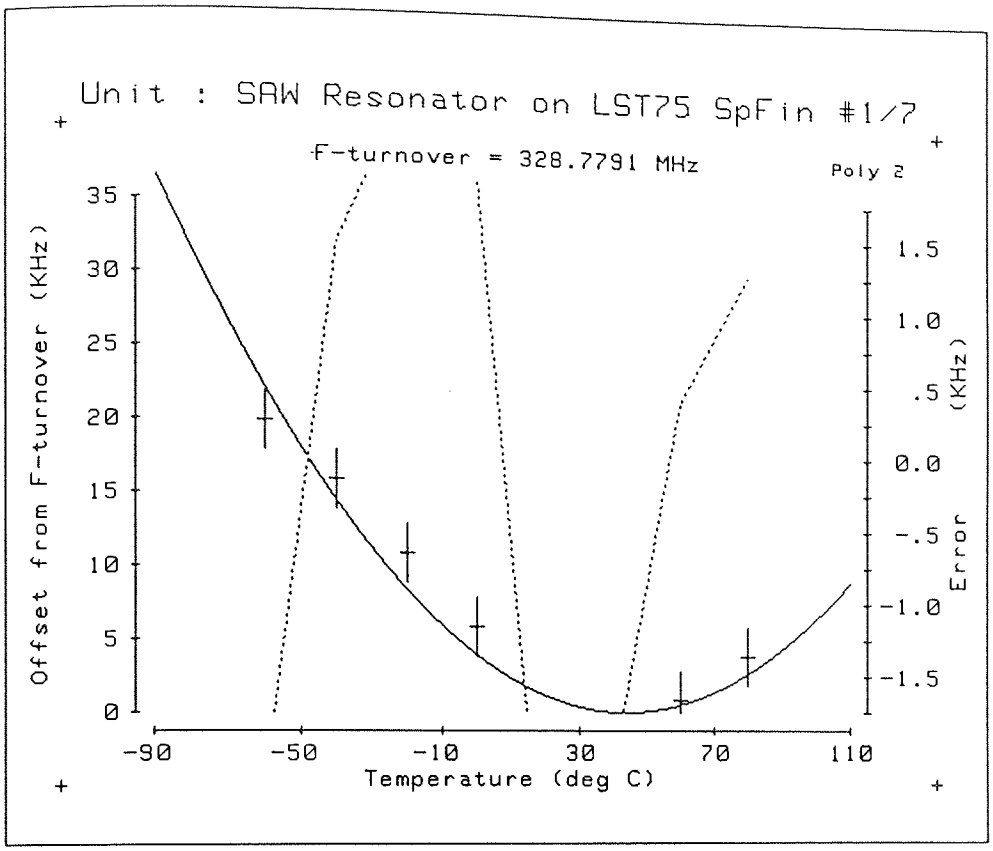

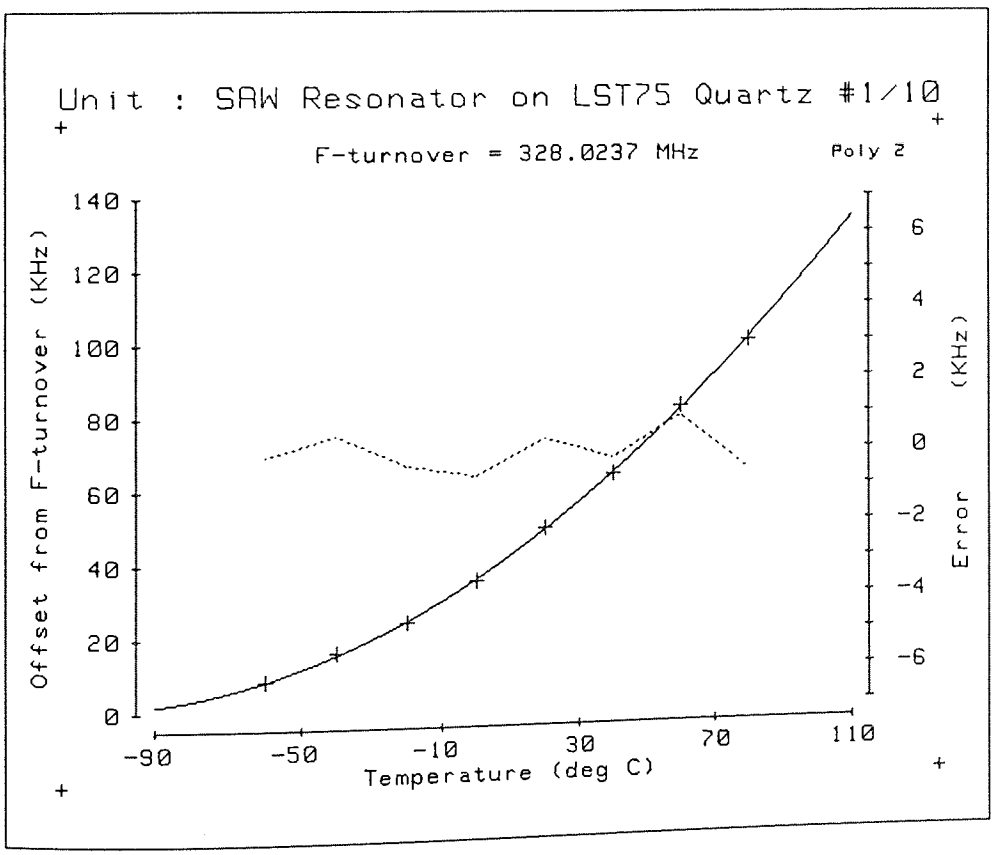

FIGURE 52 Temperature Performance LST75-Quartz units 1/7 and 1/10

Unit	Type	Frequency Turning Point (°C)	Parabola Constant (x 10^{-6})	Frequency Shift -40 to +85°C (ppm)
1/2	2F	42.9	0.43	29
1/3	2F	30.2	0.76	37
1/7	2F	43.9	0.62	43
1/10	1F	-116.8	0.79	264
ST-Cut	2F	6.2	-3.40	211

Notes:

Result for typical ST-device shown for comparison.

TABLE 20 Temperature Performance - LST75 Quartz

previous results in Tables 17 and 19. Although the turning point is approximately the same, the parabola constant is significantly improved where more data points have been used.

Single-finger LST75 unit 1/10 was tested to give comparison with unit 1/4 of Table 17. The parabola constant is in close agreement although unit 1/10 has a turning point of -117°C compared to -159°C for unit 1/4. Such differences are likely to arise where the turning point is outside the actual overband readings taken. The additional readings for unit 1/10 suggest that in most practical cases the turning point will be of the order of -120°C.

This second test has shown that the parabola constant difference between single and split-finger devices, as indicated in Table 17, may be due to factors induced by the curve-fitting programme. These include the problem of determinimg the constant where the turning point is outside the range of readings taken. However, there remains a large difference in turning point, with the low value on LST7420 and LST75 single-finger devices negating the TCD improvement. Results for split-finger devices on LST75 are excellent giving a frequency shift of less than +/- 20ppm for the temperature range -40 to +85°C.

During testing and evaluation of LST75 units a variation in insertion loss with temperature was observed. Initially this was assumed to be due to jig effects. However, the phenomenon was noted in several jigs. A brief series of experiments was conducted essentially to record the effect. The experiment consisted of plotting the passband response of the device at room temperature and two temperature extremes. A low temperature of approximately -30°C was induced with a Freon freezer spray and a high temperature of approximately 90°C with a hot air blower. The results for both single and split-finger devices are shown in Figure 53. Clearly illustrated is the superior frequency stability of the split-finger device, unit 1/3. In both cases the insertion loss increased by approximately 5dB. Measurement of device Q-value also indicated a deterioration with increasing temperature. A similar ST-device in the same jig did not show any insertion loss or Q-level variation.

This temperature effect has obvious implications for

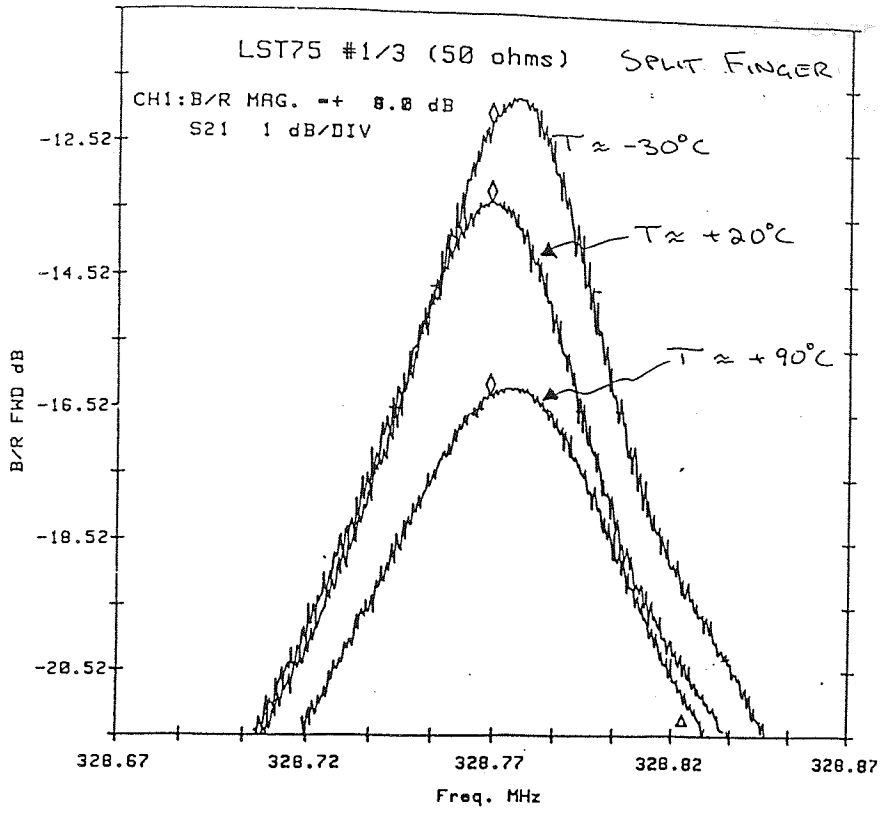

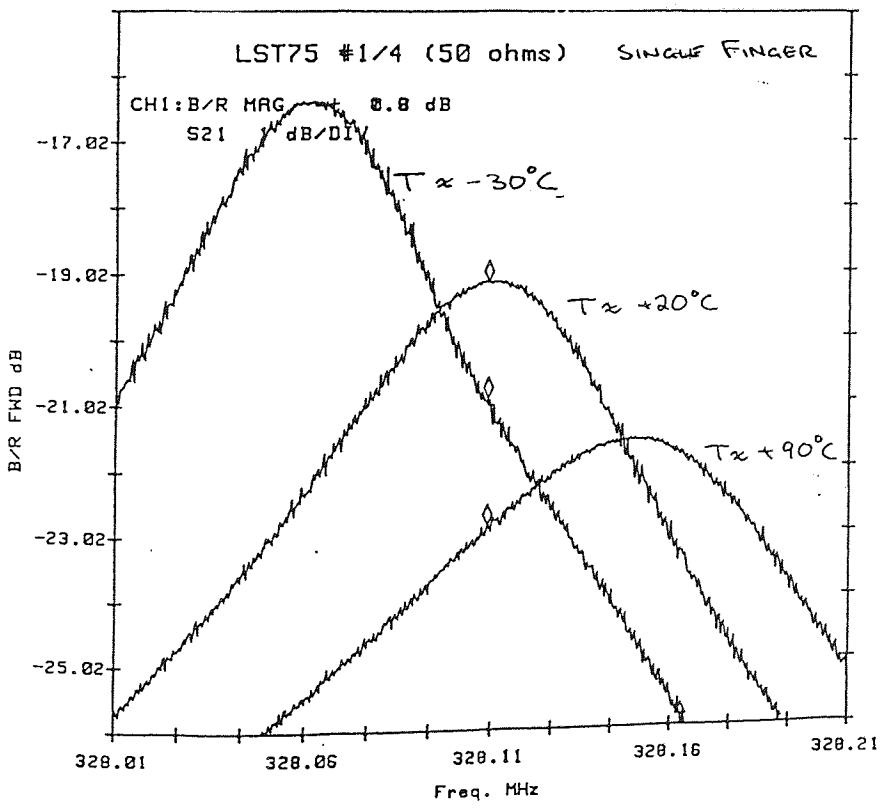

FIGURE 53 LST75-Quartz Insertion Loss Variation with Temperature

device performance. Such devices would be unsuitable for resonator oscillator applications, except over relatively small temperature bands. As this effect only appears to occur on devices with multiple peaks the phenomenon may be due to coupling of acoustic modes. No measurements were made on the temperature performance of the subsidiary peaks.

In summary, the split-finger LST75 cut gives the best TCD result together with acceptable resonator performance. Other cuts offer little or no advantage. The problem of insertion loss drift with temperature may restrict the LST75 cut to devices required to operate over small temperature bands. In practice this will reduce the potential application of this new cut.

4.3.4 Results - SAW Filters.

Filter trials made use of an existing 442MHz PCM filter design. This device had been designed with single-finger transducers in view of the high frequency involved. To suppress internal reflections the transducers were based upon three and four-finger groups as described by Minowa et al[20]. The physical layout of the filter is described in Figure 54. Typical electrical specification is as follows:

Centre frequency	-	442MHz
Insertion loss	-	<13dB
Q-value	-	800
Phase linearity	-	+/-10°
Sidelobe attenuation	-	>20dB
Temperature range	-	0 to 40°C

Devices for PCM transmission systems are generally used for timing extraction in submerged repeaters. Therefore, in addition to the outline specification given above the devices have to meet certain demanding criteria. These include maximum permitted parameter shifts over a 25 year system lifetime. Other requirements are reviewed by Rosenberg et al[19].

The aim of the work reported here was to manufacture SAW filters on SST and LST-cuts and then compare resultant frequency performance with that of standard production devices. As described above, the X33-cut was not tested further. For comparison purposes, filters were made on

Transducer 1	Transducer 2
12 fingers/block 74 blocks	16 fingers/block 58 blocks

Transducer 1 - Type 3 Block detail

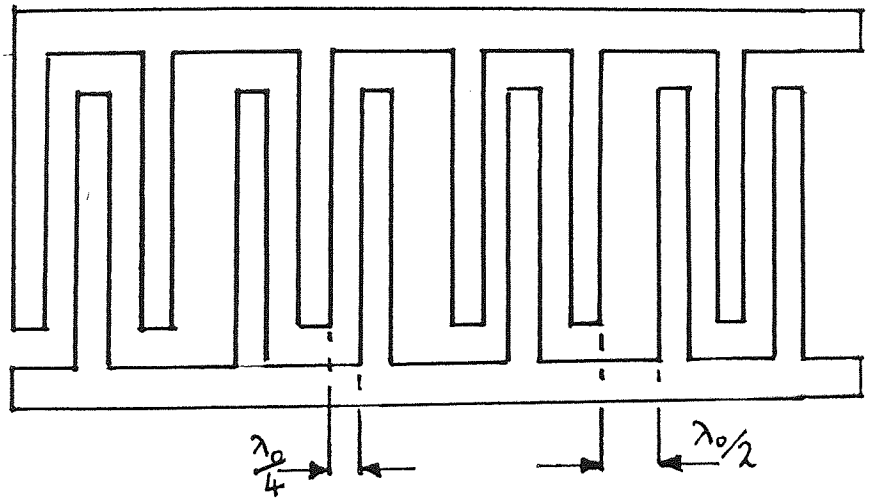

Transducer 2 - Type 4 Block detail

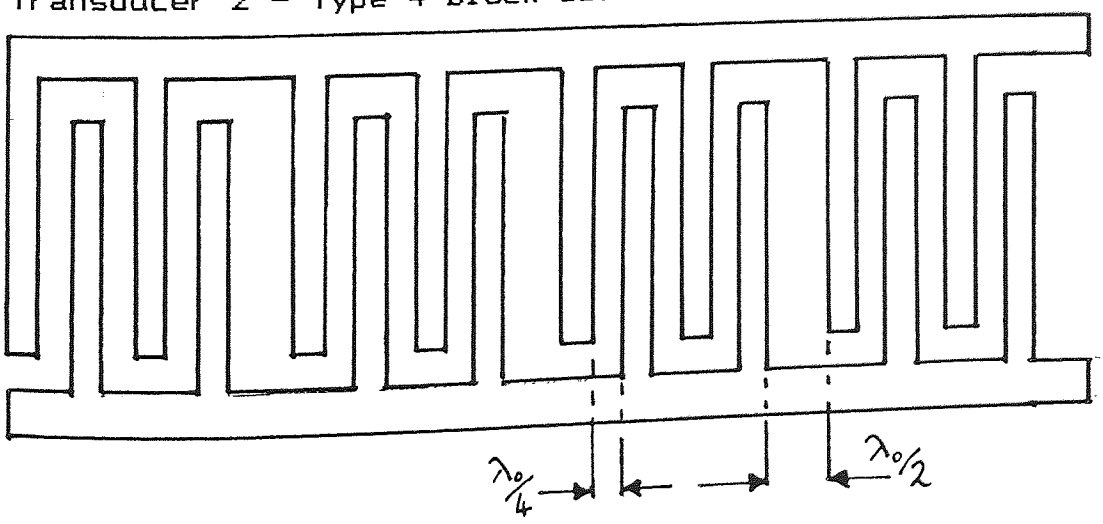

FIGURE 54 442MHz PCM Filter Layout

AT-cut. Two slices were processed for each of the following cuts:

AT, SST, LST7420, LST75 and LST7520.

All were produced in the same photolithographic process using an aluminium thickness of 810Å.

In view of the high reliabilty requirements of PCM retiming filters, calibrated precision test jigs were available for production device measurement. These jigs included clamping rings to firmly hold the device under test in place, thus eliminating spurious earthing and circulating current effects. Measurements were made using a Hewlett-Packard 8753A network analyser in a semi-automatic mode. This allowed direct read-off of centre frequency, insertion loss, 3dB bandwidth and Q-value. The centre frequency is defined here as the average of the 3dB frequencies and not as the frequency of minimum insertion loss. In the case of a symmetrical response the two frequencies would be equal. PCM filters are often deliberately designed to be asymmetrical to prevent error build-up in long, multi-repeatered transmission lines.

Results for filters on new quartz cuts are given in Tables 21 to 25 and a results summary is given in Table 26. Plots of sample devices are given in Figures 55 to 59. For each sample device both the passband and close-in stopband are shown.

4.3.5 Discussion - SAW Filters

With the exception of centre frequency, the plots of Figures 55 to 59 are remarkably similar in terms of the shape of response. This is in contrast to the differences between resonators as shown previously in Figures 29 to 41.

The main effect associated with the new quartz cuts appears to be an increase in insertion loss. The higher operating frequencies of these new cuts are in line with the resonator results, showing 15% and 25% increases for SST and LST-cuts respectively. All results give a similar passband shape with that of LST7420 showing a little more ripple than the others. For production testing the level of ripple is measured as a defined jitter function. The

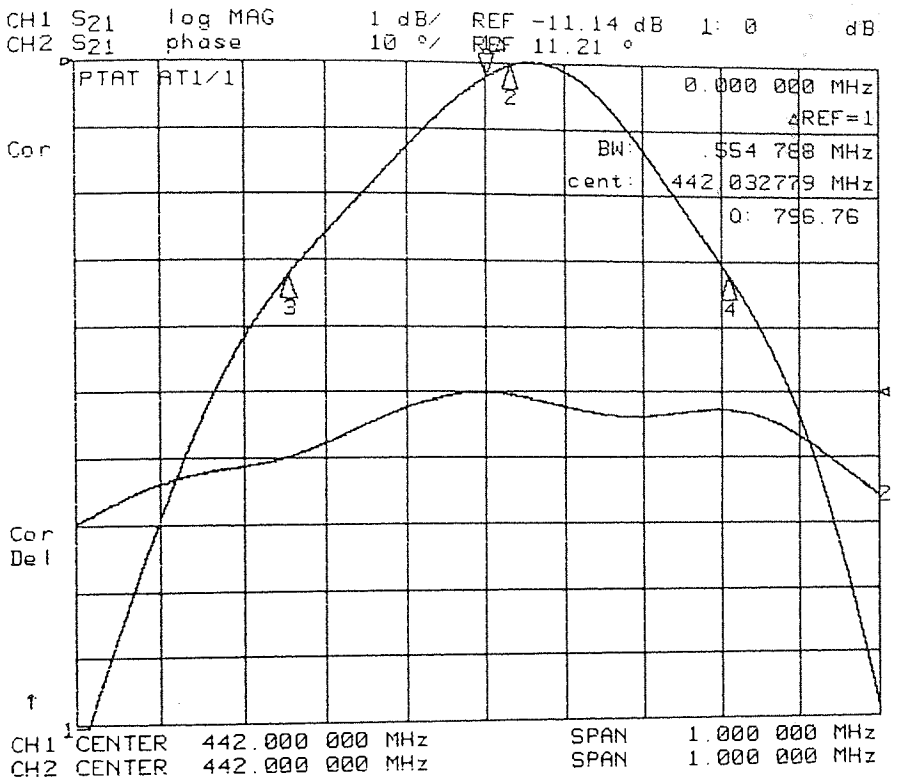

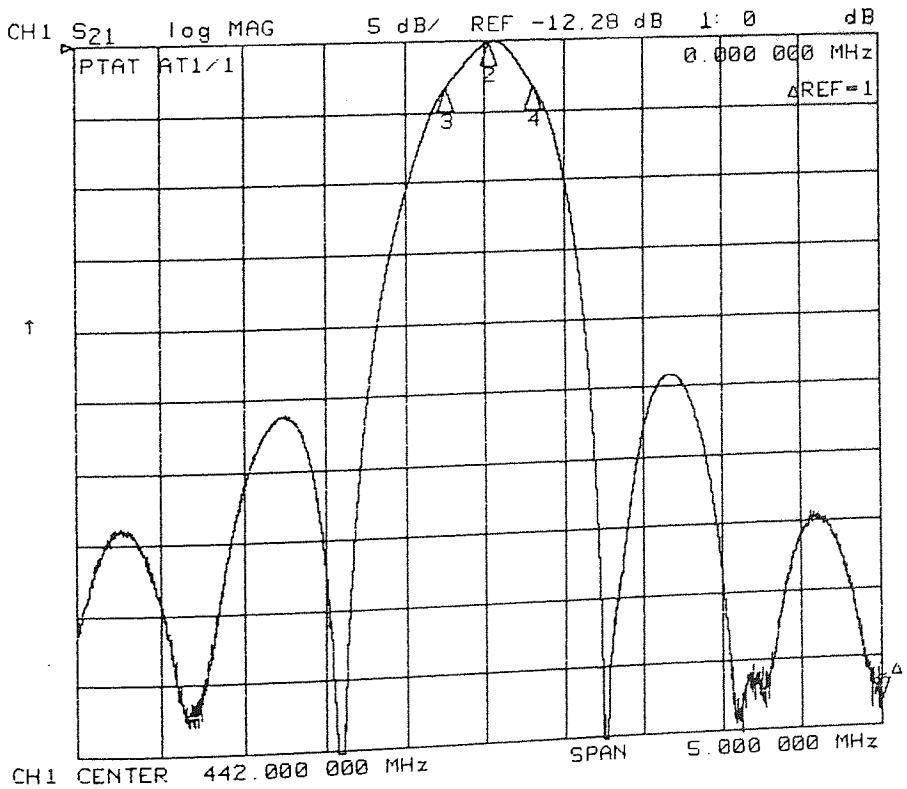

Passband plot shows linearised phase

FIGURE 55 SAW Filter on AT-Quartz

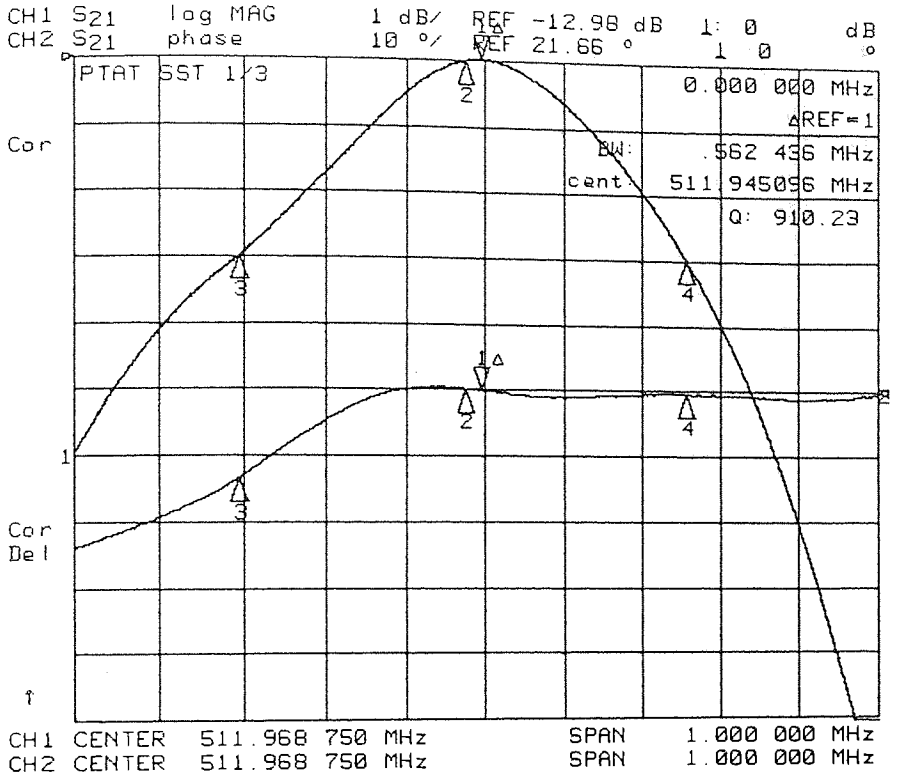

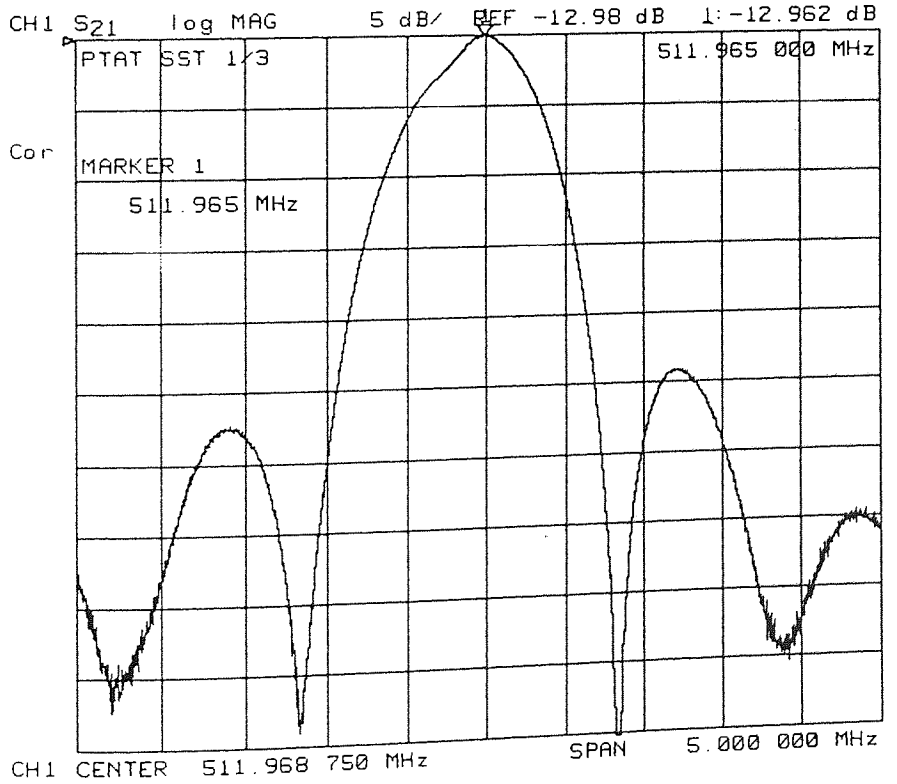

FIGURE 56 SAW Filter on SST-Quartz

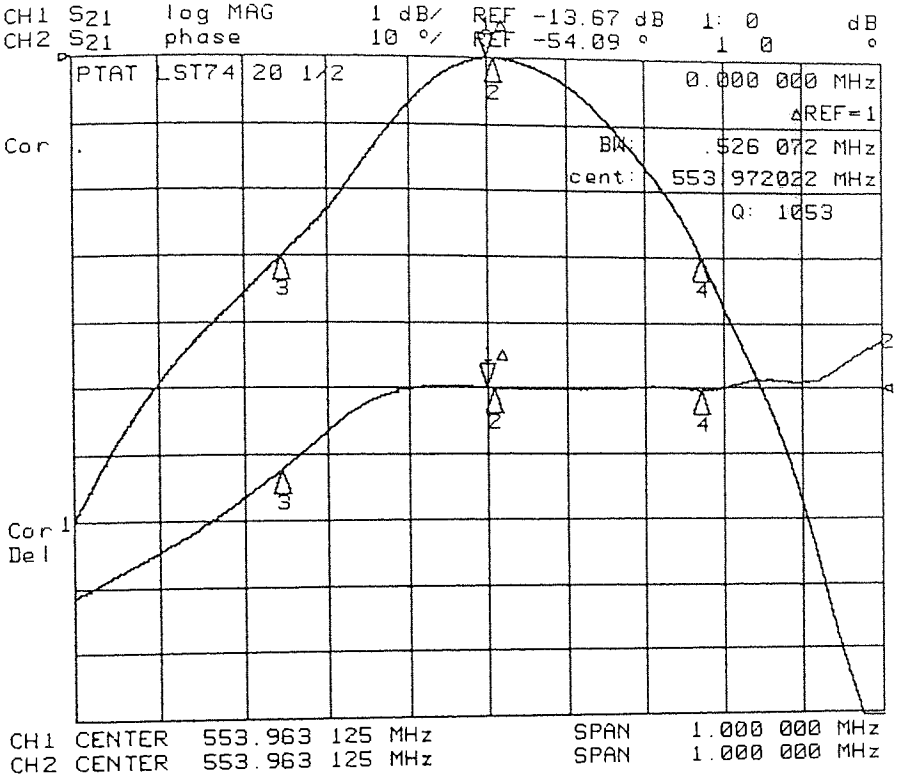

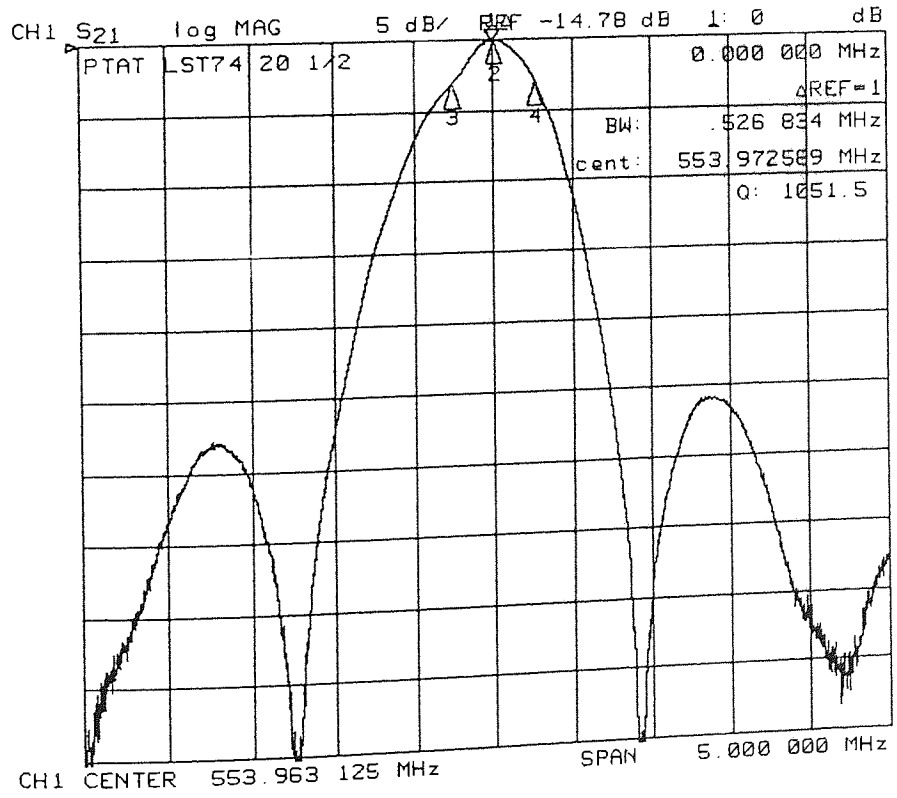

FIGURE 57 SAW Filter on LST7420-Quartz

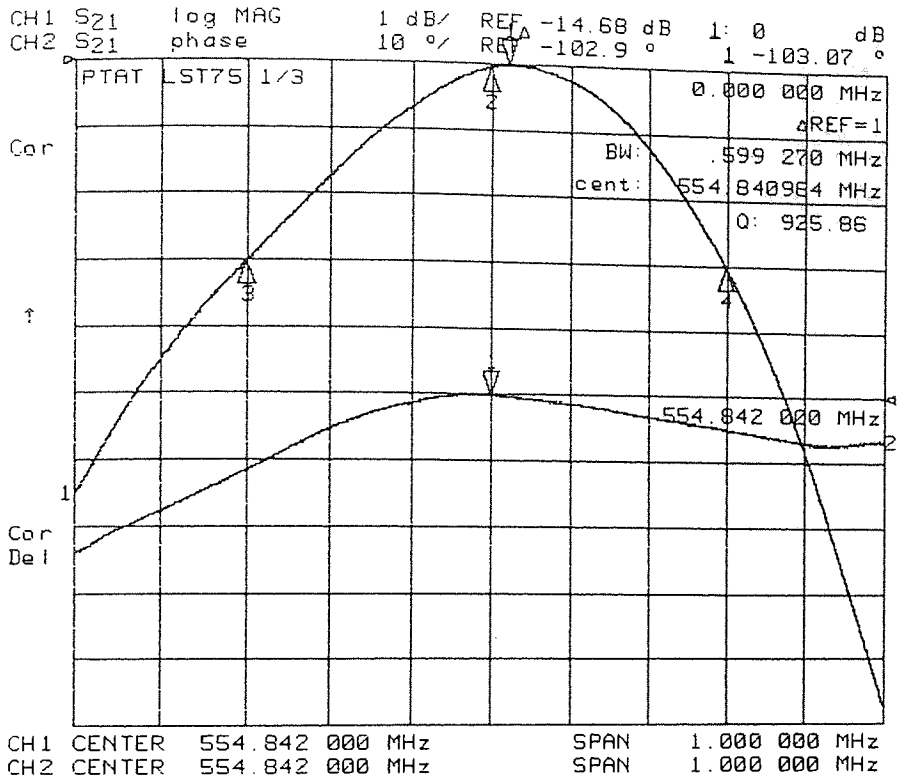

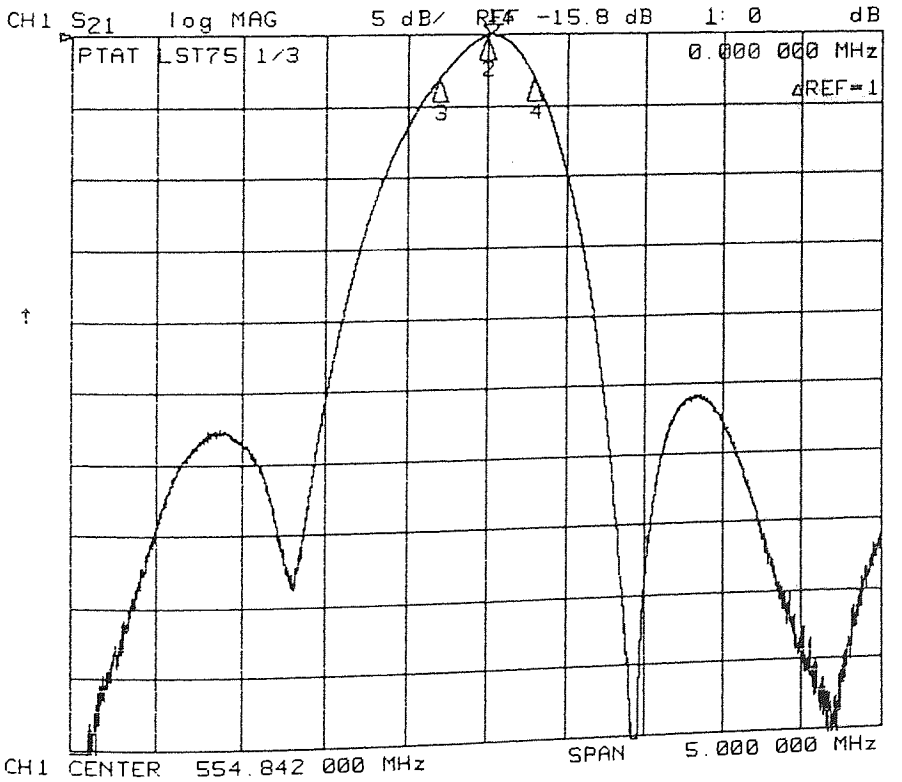

FIGURE 58 SAW Filter on LST75-Quartz

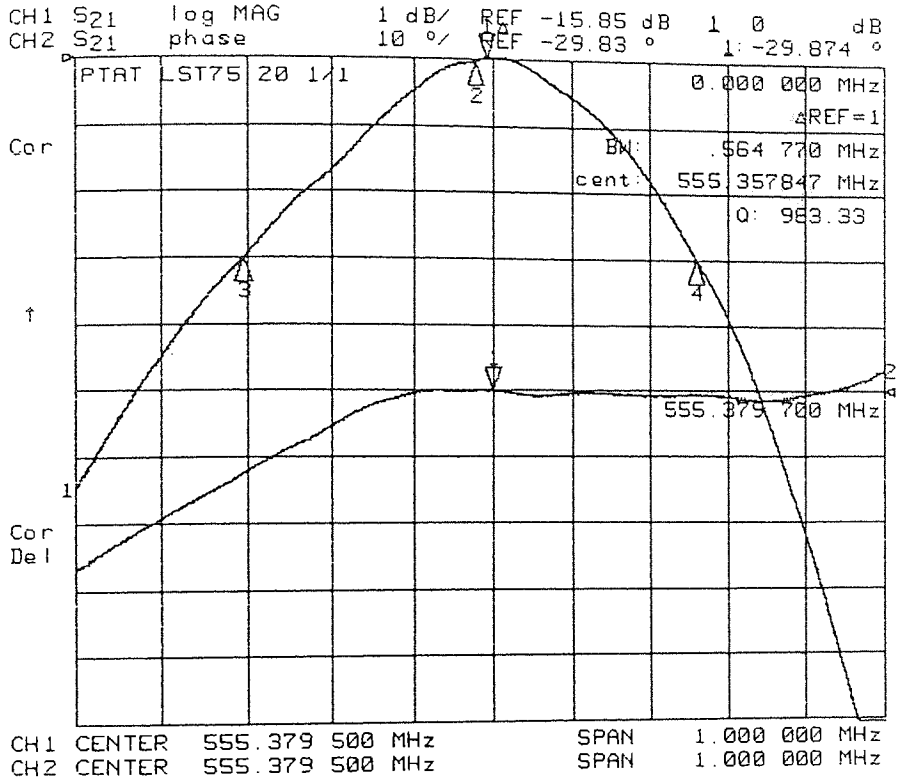

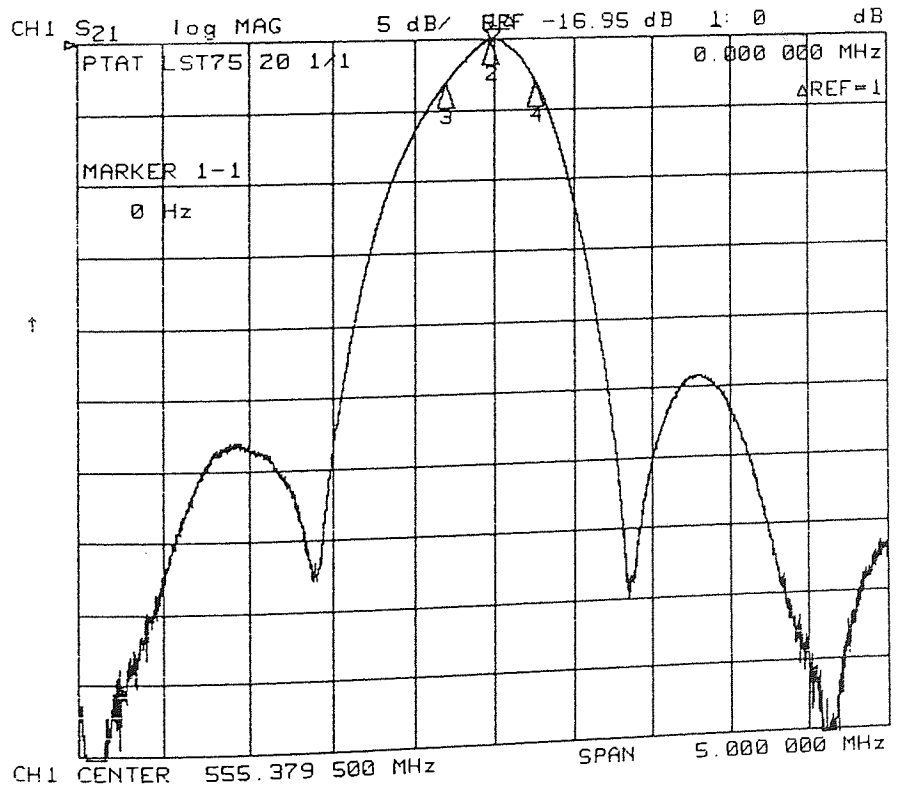

FIGURE 59 SAW Filter on LST7520-Quartz

Device No	Insertion Loss (dB)	Centre Frequency (MHz)	Bandwidth (kHz)	Q
1/1	11.12	442.034	530	835
1/2	10.69	442.097	479	924
1/3	10.79	442.063	495	892
1/4	11.31	442.047	599	737
1/5	12.12	442.086	496	891
1/6	11.70	442.079	509	864
Mean values	11.29	442.068	518	857
2/1	11.41	442.046	580	762
2/2	11.18	442.055	533	829
2/3	11.06	442.043	511	863
2/4	11.12	442.046	507	871
2/5	11.46	442.046	593	745
2/6	11.09	442.059	528	836
2/7	11.14	442.062	515	858
Mean values	11.13	442.051	538	823

Notes:

First digit of the device number indicates the slice number.

Mean values are for each slice.

TABLE 21 PCM Filters on AT-cut Quartz.

Device No	Insertion Loss (dB)	Centre Frequency (MHz)	Bandwidth (kHz)	Q
1/1	13.37	511.943	565	905
1/2	13.00	511.946	562	910
1/3	12.46	511.972	519	985
1/4	13.09	511.978	562	910
1/5	13.05	511.952	597	856
1/6	12.94	511.946	542	944
1/7	12.79	511.962	575	892
Mean values	12.96	511.957	560	915
2/1	12.79	512.073	540	948
2/2	13.21	512.019	562	909
2/3	12.86	512.028	606	844
2/4	12.52	512.019	534	960
Mean values	12.85	512.035	561	915

Notes:

First digit of the device number indicates the slice number.

Mean values are for each slice.

TABLE 22 PCM Filters on SST-cut Quartz.

Device No	Insertion Loss (dB)	Centre Frequency (MHz)	Bandwidth (kHz)	Q
1/1	No Response			
1/2	13.70	553.971	527	1049
1/3	14.22	553.963	568	973
1/4	14.03	553.923	610	908
Mean values	13.98	553.952	568	977
2/1	14.39	553.846	517	1073
2/2	15.20	553.636	603	918
2/3	15.10	553.700	588	942
2/4	14.62	553.787	548	1008
Mean values	14.83	553.742	564	985

Notes:

First digit of the device number indicates the slice number.

Mean values are for each slice.

TABLE 23 PCM Filters on LST7420-cut Quartz.

Device No	Insertion Loss (dB)	Centre Frequency (MHz)	Bandwidth (kHz)	Q
1/1	14.44	554.809	586	948
1/2	15.87	554.786	706	781
1/3	14.68	554.840	600	924
1/4	14.70	554.851	575	965
Mean values	14.92	554.822	617	905
2/1	No response			
2/2	18.04	554.733	707	791
2/3	17.01	554.570	807	686
2/4	17.24	554.580	739	752
Mean values	17.43	554.628	751	743

Notes:

First digit of the device number indicates the slice number.

Mean values are for each slice.

TABLE 24 PCM Filters on LST75-cut Quartz.

Device No	Insertion Loss (dB)	Centre Frequency (MHz)	Bandwidth (kHz)	Q
1/1	15.84	555.359	564	987
1/2	15.95	555.365	551	1005
1/3	16.45	555.349	625	885
1/4	16.51	555.286	618	897
Mean values	16.19	555.340	590	944
2/1	19.22	555.253	678	815
2/2	18.67	555.264	599	928
2/3	No response			
2/4	17.99	555.234	624	890
Mean values	18.63	555.250	634	878

Notes:

First digit of the device number indicates the slice number.

Mean values are for each slice.

TABLE 25 PCM Filters on LST7520-cut Quartz.

Quartz Cut	No in Sample	Insertion Loss (dB)	Centre Frequency (MHz)	Bandwidth (kHz)	Q
AT/1	6	11.29	442.068	518	857
AT/2	7	11.13	442.051	538	823
SST/1	7	12.96	511.957	560	915
SST/2	4	12.85	512.035	561	915
LST7420/1	3	13.98	553.952	568	977
LST7420/2	4	14.83	553.742	564	985
LST75/1	4	14.92	554.822	617	905
LST75/2	3	17.43	554.628	751	743
LST7520/1	4	16.19	555.340	590	944
LST7520/2	3	18.63	555.250	634	878

Note:

Last digit of quartz cut indicates slice number.

Number in sample does not include devices with no response.

TABLE 26 PCM Filters on New Quartz Cuts - Results Summary

LST7420 device of Figure 57, even with the ripple shown, would probably pass this test.

The two other parameters of most interest to system designers are close-in stopband (side-lobe attenuation) and phase linearity in the 3dB passband. All devices show a side-lobe attenuation of better than 20dB (25dB in most cases) and therefore easily meet the specification of better than 20dB. In all cases the phase change over the 3dB bandwidth is approximately 10°, or +/-5°, far exceeding the specification requirements of +/- 10°.

The results for LST7520 show an insertion loss consistently higher than the other cuts. LST75 slice 2 has inferior results to LST75 slice 1 suggesting a processing problem with the second slice. The lower average Q-value for this second slice tends to confirm a photolithography problem such as poor resolution or contamination resulting in line shorts or breaks. As was shown with resonators, the results for LST7520 appear inferior to those for LST75 and LST7420.

It should be remembered that these results were obtained using an existing photomask designed to give filters on AT-quartz at 442MHz. In practice designs can be optimised to take into account the marginally lower electromechanical coupling coefficient of the LST-cuts, 0.10% compared with 0.14% for the ST-cut (Shimizu et al[50]). This will allow devices to be fabricated with the correct bandwidth at minimum insertion loss.

When comparing the insertion losses of the LST-cut filters with the AT-cut results allowance must be made for the higher operating frequencies. For any given quartz cut and SAW device design, the insertion loss of devices increases as the operating frequency increases. Losses may be associated with the quartz material such as acoustic attenuation and bulk wave generation, or with the device design such as diffraction and beam steering effects. Therefore, although the LST-cuts exhibit higher insertion loss values, comparison with devices designed to operate on AT-quartz at similar frequencies would result in much narrower differences. As LST7420 and LST75-cuts have resultant insertion loss values only 3-4dB below AT-cut but at a frequency 25% higher, comparison at the same frequency should give similar values.

The greatest advantage offered by the new cuts for filter design is the higher operating frequency. A 25% increase in SAW acoustic velocity equates to a 25% increase in photolithographic linewidth. In view of the limits of standard processing at which SAW technology operates, this increase in linewidth can offer a several-fold increase in yield, without the need for expensive equipment replacement. As was stated in Chapter 1, the current practical limit for SAW devices, based upon single-finger transducers and an acceptable yield, is a linewidth resolution equating to a frequency of approximately 1GHz. A 25% increase will allow devices at 1.25GHz which happens to be one of the predicted transmission rates for optical fibre PCM systems.

No attempt was made to measure the temperature performance of the SAW filters. It was assumed that the quartz would behave in the same way as for SAW resonators. In view of the observed temperature performance of resonators on the LST-cuts, in particular the variation of insertion loss with temperature and the difference between single and split-finger transducers, this assumption cannot be made.

The inferior performance of the LST7520-cut again highlights the variation between the three LST-cuts. As with resonators, difficulty of alignment may preclude the use of these cuts in large scale production.

4.3.6 Recommendations for Further Work.

The availability of quartz material limited the number of devices that could be produced for the trials reported here. In some instances additional testing is necessary to substantiate the results.

None of the new cuts reported appear to be ideally suited to resonator applications. LST75 needs further investigation as its temperature performance is excellent. To ensure that this cut can be accurately produced on a repetitive production basis, the problem of batch to batch accuracy alignment needs investigation.

Other aspects requiring further work are the nature of the difference between single and split-finger transducers and the problem of insertion loss drift with temperature. These factors will seriously limit the range

of application of these new cuts.

The work on SAW filters is not complete and requires measurement of temperature performance. Simple measurement of the 3dB bandwidth as in the case of high-Q resonators does not give sufficient accuracy. STC, in collaboration with British Telecom, have developed a "notch" system for determining the temperature drift of filters (Bickers and Leveridge[51]). A deep notch is produced in the passband and the drift of the notch minima with temperature is measured. This work would allow direct comparison with the resonator results and indicate the presence of insertion loss variation with temperature.

5. INSERTION LOSS.

5.1 Scope

The main insertion loss objectives of this project are:

To develop the concept of transducer coupled resonator filters for a production environment and, at the same time, to meet a target bandwidth and insertion loss specification. These devices will be used as narrow-band front-end filters and therefore require the lowest possible insertion loss.

To demonstrate low-loss SAW devices suitable for use as PCM retiming filters based upon the single-phase unidirectional transducer. The design incorporates quarter wavelength fingers in the transducers. The target frequency of 565MHz is based upon proposed transmission rates for the next generation of long-haul telecommunications systems.

5.2 Coupled Resonator Filters

5.2.1 Methodology

Much has been written on the use of coupled resonators as low-loss, narrow-band filters. This has been summarised in Chapter 3. Losses as low as 1dB have been reported but at relatively narrow bandwidth, 70kHz, or at frequencies between 75 and 150MHz. STC has identified a major market requirement for devices with the following specification:

Centre frequency	- 400 to 500MHz
Bandwidth	- 200kHz
Insertion loss	- <3.5dB
Passband ripple	- <1.0dB
Out of band rejection	- >40dB
Temperature range	- -40 to +85°C

All parameters must be met over the entire temperature band. To allow for the temperature drift associated with ST-cut quartz it is necessary to design for a much wider bandwidth. This effect and the general specification is

shown in Figure 60. Assuming the device frequency turning point is at the centre of the temperature band, it will be necessary to increase the bandwidth by approximately 50kHz at 400MHz. In addition, it is necessary to allow for processing variations and, therefore, a larger bandwidth is required. A realistic target bandwidth of 300kHz represents a much larger value than has been reported elsewhere.

The first task was to investigate the feasibility of connecting two similar resonators in parallel. As large numbers of resonators were available, the first trial involved measuring the response of a pair of 250MHz resonators in a matched configuration. The resonators were housed in separate casings and therefore interconnection was made on a small printed circuit board. Resonators were selected with an offset similar to the required bandwidth.

One of the application requirements of narrow-band filters is a large out-of-band rejection. For this reason it was decided to connect the outputs from the resonators in anti-phase (Figure 61). At, or near, the synchronous frequencies of the two devices the outputs are in phase. Further out in the response there is anti-phase addition which further decreases the stopband level.

The need for good stopband suppression impacts on packaging and test jig design. The 250MHz devices, which were used to test the principles of tranducer coupling, were housed in TO8 packages. At higher frequencies smaller packages are required for both electrical and board area reasons. It was decided to attempt to mount both devices in the same package and undertake the interconnection as part of the normal die wire bonding exercise. It was anticipated that factors such as bond-wire configuration, die paste location and earth screening would influence the stopband level.

Taking the interconnection problem a stage further, it was considered worthwhile to investigate the possibility of connecting the devices as part of the mask-making exercise, that is, on-chip connection. This would place considerable difficulties on the mask-maker as the mask has to include two identical resonator designs at almost the same frequency. The required offset between devices of approximately 300kHz at 400MHz equates to a very small address unit change by the mask-maker at the writing

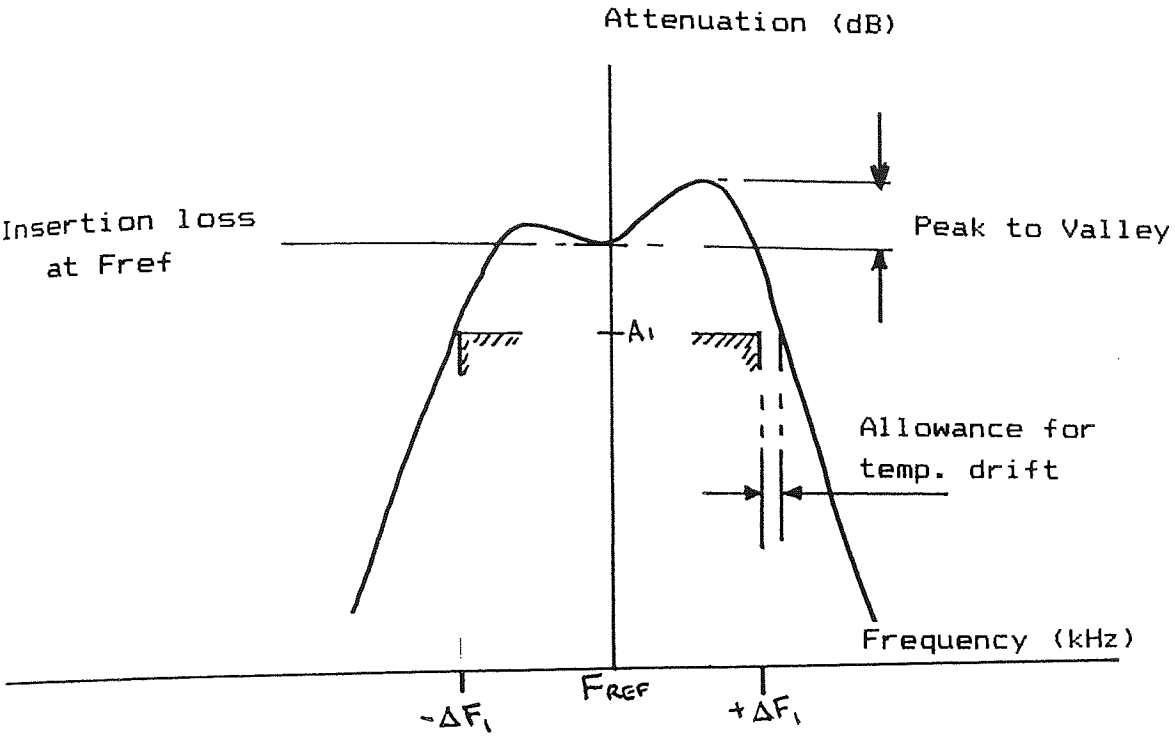

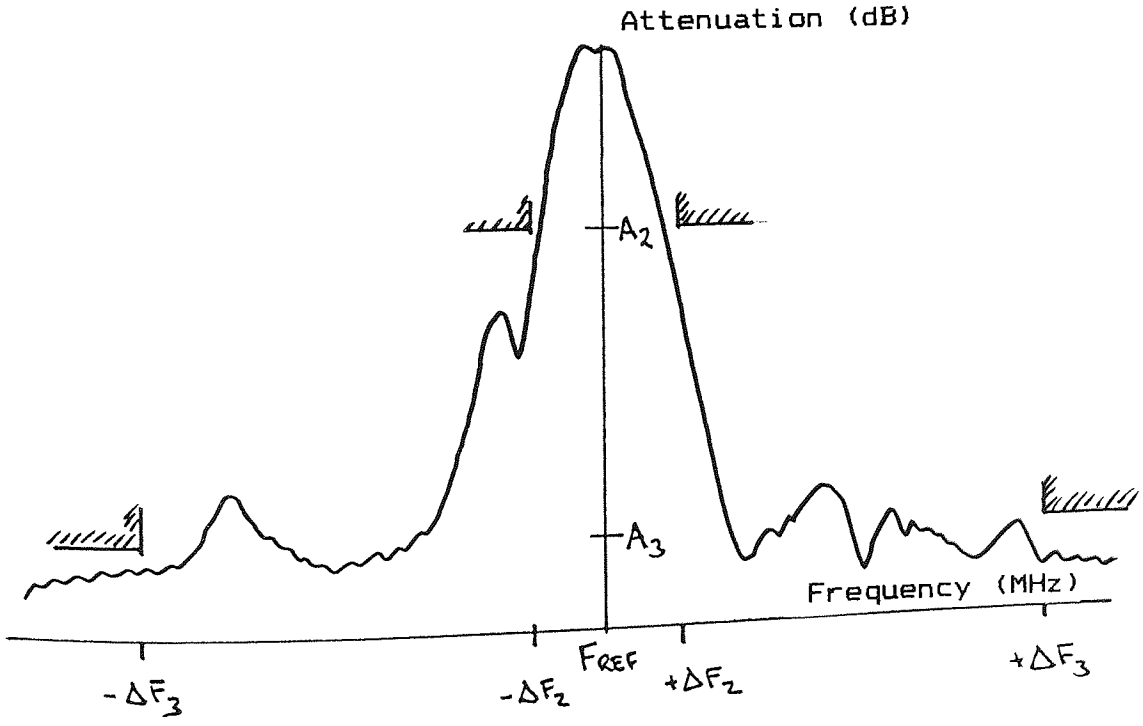

Discrimination:

Attenuation A1 @ -/+Δ F1
A2 @ -/+Δ F2
A3 @ -/+Δ F3

FIGURE 60 Specification Format - Coupled Resonator Filters

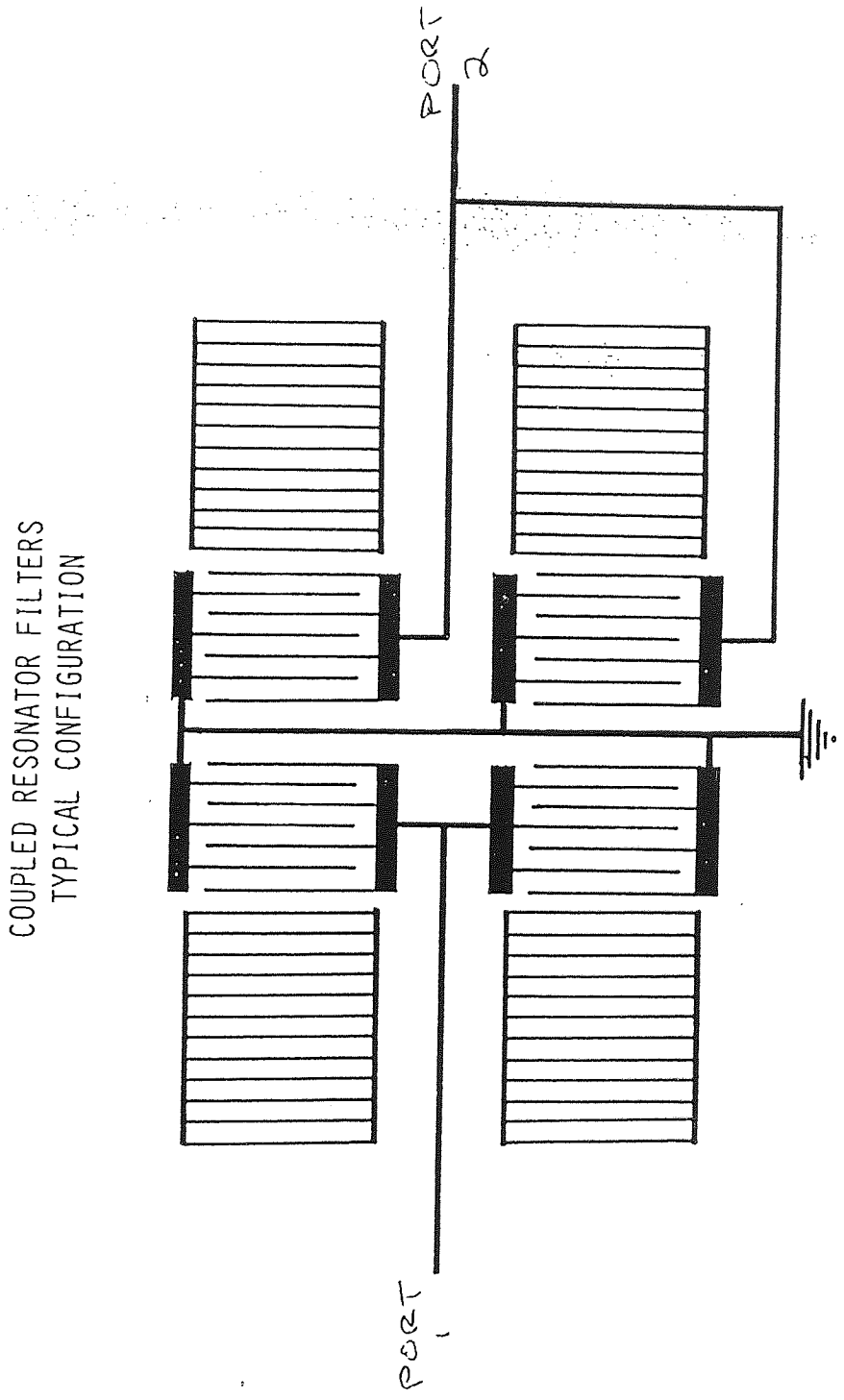

FIGURE 61 Coupled Resonators - Interconnection

stage.

At an early stage the problem of passband ripple was identified. To achieve a wide bandwidth required devices with a wide offset. The larger the offset the greater the passband ripple when interconnected. This ripple was found to reduce as the device pair was matched into the 50ohm test system. It was decided to reduce the ripple by adjusting the reflectivity of one of the resonator mirrors. At the development stage it would be necessary to undertake this mirror modification as part of device assembly. Any technique would need to be repeatable, controllable and suitable for a "clean room" environment.

Standard resonator designs were used for this work, based upon the design routines described in Chapter 2. The objective was to produce a high-Q device with minimum insertion loss. From the work reported in Section 4.2, it was possible to select the most suitable cut of quartz for this application. The selection of cut angle could then be modified to take account of any minor mask errors. For these reasons the cut used for this work was YX1(38°).

To facilitate ease of manufacture, and in light of the mask-making difficulty of resolving very small linewidth variations, one-quarter wavelength fingers were used in transducers and reflectors. The frequency offset was obtained through a change in reflector dimension only. This was achieved by specifying two address units to the mask-maker. In practice the address units differed by as little as 0.0003um.

It was anticipated that this design would have a relatively low manufacturing yield. The major problem, sufficiently wide bandwidth, would be eased if the temperature effects could be reduced. An attempt was made to manufacture similar devices on LST75-quartz. LST75-quartz has a turning point in the centre of the specified temperature band resulting in a frequency shift of approximately 60ppm, or 24kHz at 400MHz. The results of Chapter 4 suggest that its use may be limited by the variation of insertion loss with temperature.

5.2.2 Results

All frequency response results presented were made using

either a Hewlett-Packard 8505A or 8753A Network Analyser. The 8753A is a more recent instrument allowing fully automatic testing over a wider range of parameters. Unless stated otherwise, all readings were taken in an environmentally controlled area at a temperature of 22+/-1°C.

Sample 250MHz resonators were selected from an existing batch of devices. These were then connected in parallel as shown in Figure 61. Figures 62 and 63 show the response of a device pair with a resultant 1.0dB bandwidth of 120kHz. Figure 62 shows the passband and close-in responses and Figure 63 shows the stopband levels. The device pair has been matched into a 50ohm system using a simple shunt and series inductors configuration. With a wide offset between devices it was noted that a considerable dip resulted in the passband.

The next stage involved designing a photomask to yield devices at the correct frequency, nominally 400MHz. The resonator structure is exactly as shown in Figure 28, but with dimensions scaled down to give the higher operating frequency. The first approach was to produce a mask with the two device types in alternate rows. This would allow several manufacturing options including individual die packaging, use of separate photolithographic runs to generate greater frequency offsets and twin die packaging. Devices were mounted in a 4-pin TO39 package as shown in Figure 64.

When measured, unmatched, in a 50ohm test circuit the resultant response gave two distinct resonator peaks. A typical set of data is given in Table 27. The measurement in an unmatched test jig gave an indication of the "quality" of the devices, together with centre frequency and offset data. When placed into a matching circuit (Figure 65), and tuned for minimum insertion loss, the dip in the passband between the device peaks reduced, but was not eliminated. A simple technique was developed to modify the reflectivity of one device mirror, hence lowering its Q-value. The technique involved the application of a small spot of epoxy paste to the edge of one mirror, as shown in Figure 66. The paste was the same as that used for die mounting and end absorber. The effects of successive paste-spot increments on the passband shape are shown in Figures 67 and 68.

Using the bond wire configuration and die mounting

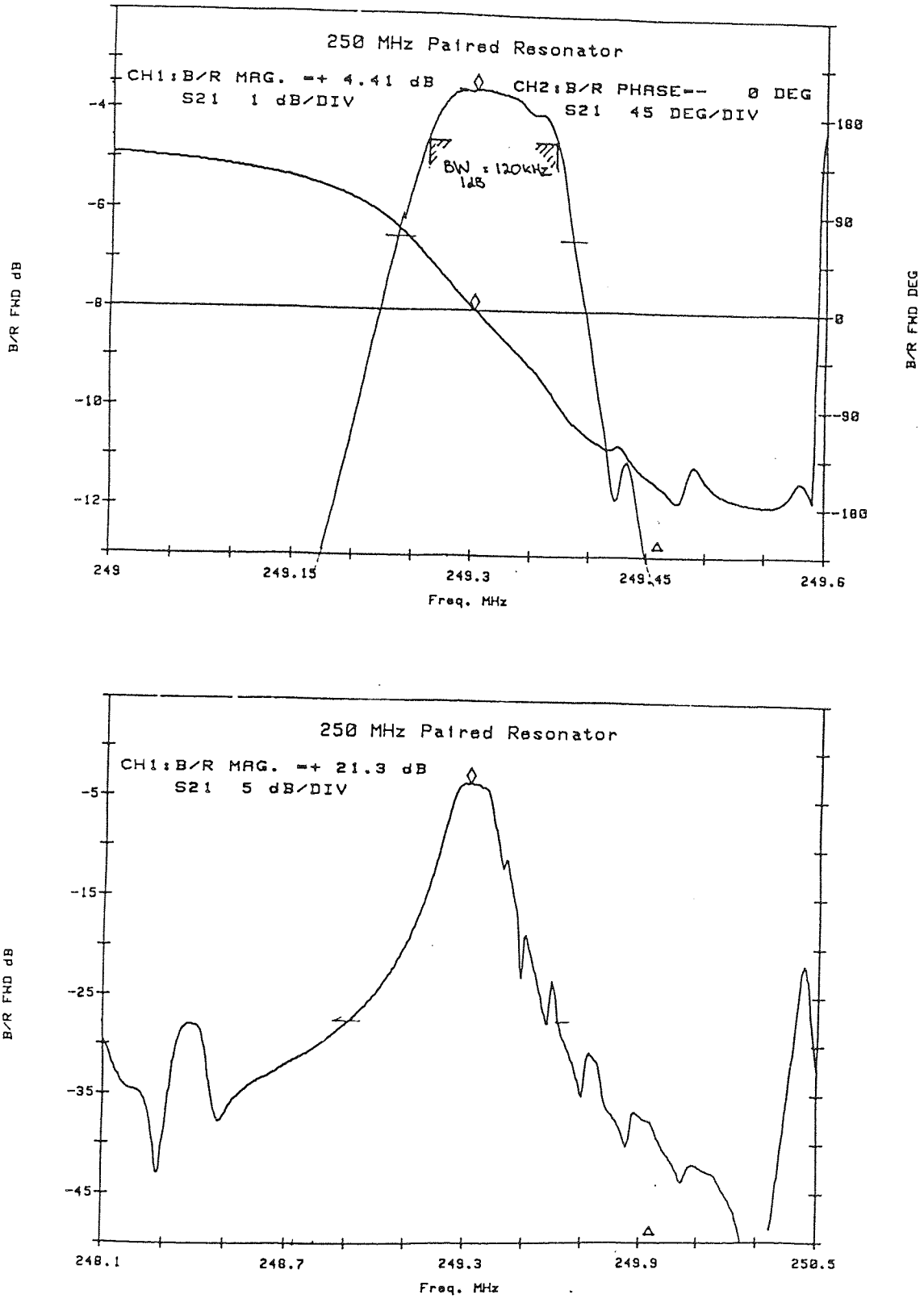

FIGURE 62 Frequency Response - 250MHz Filter

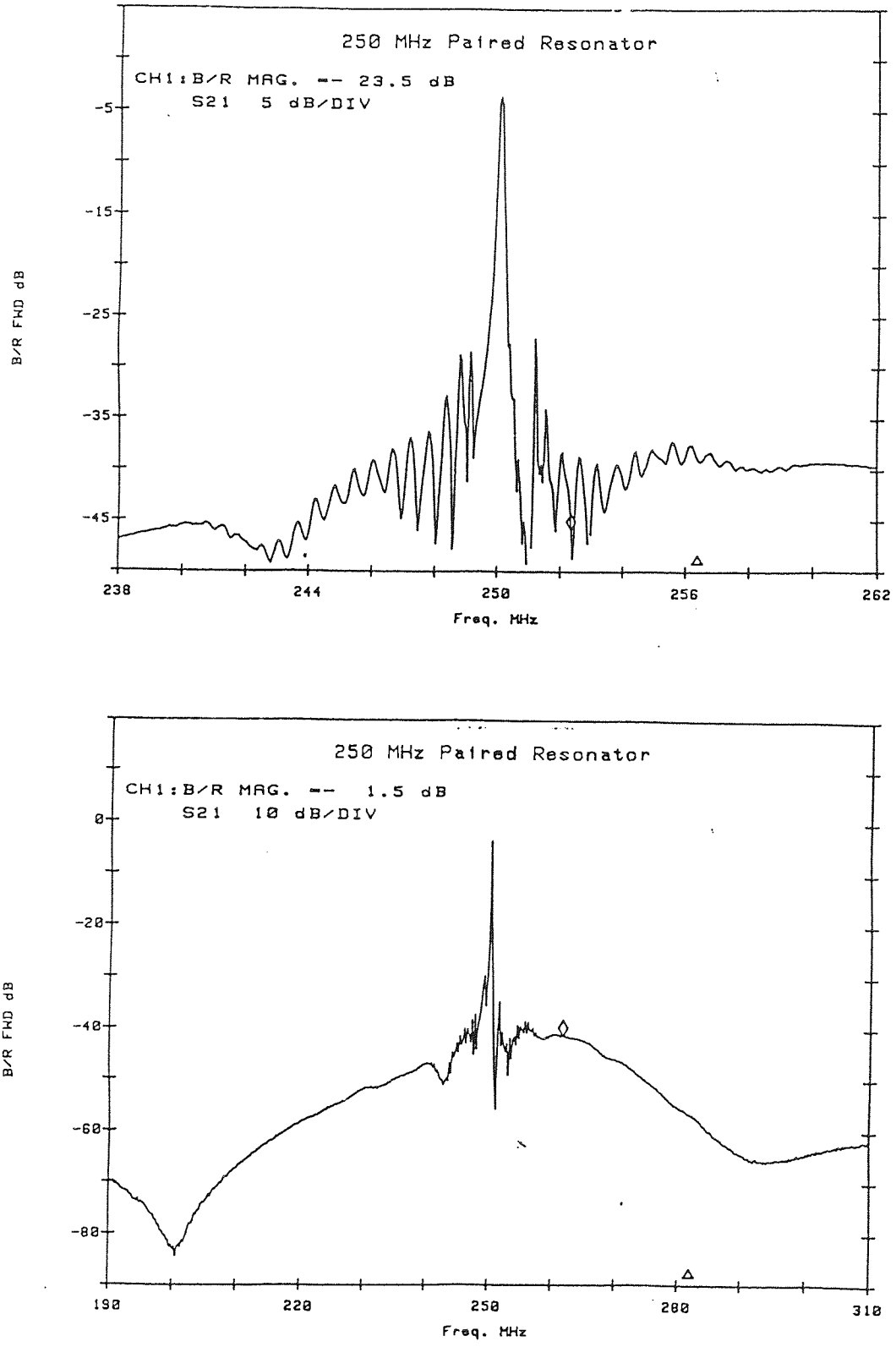

FIGURE 63 Frequency Response - 250MHz Filter

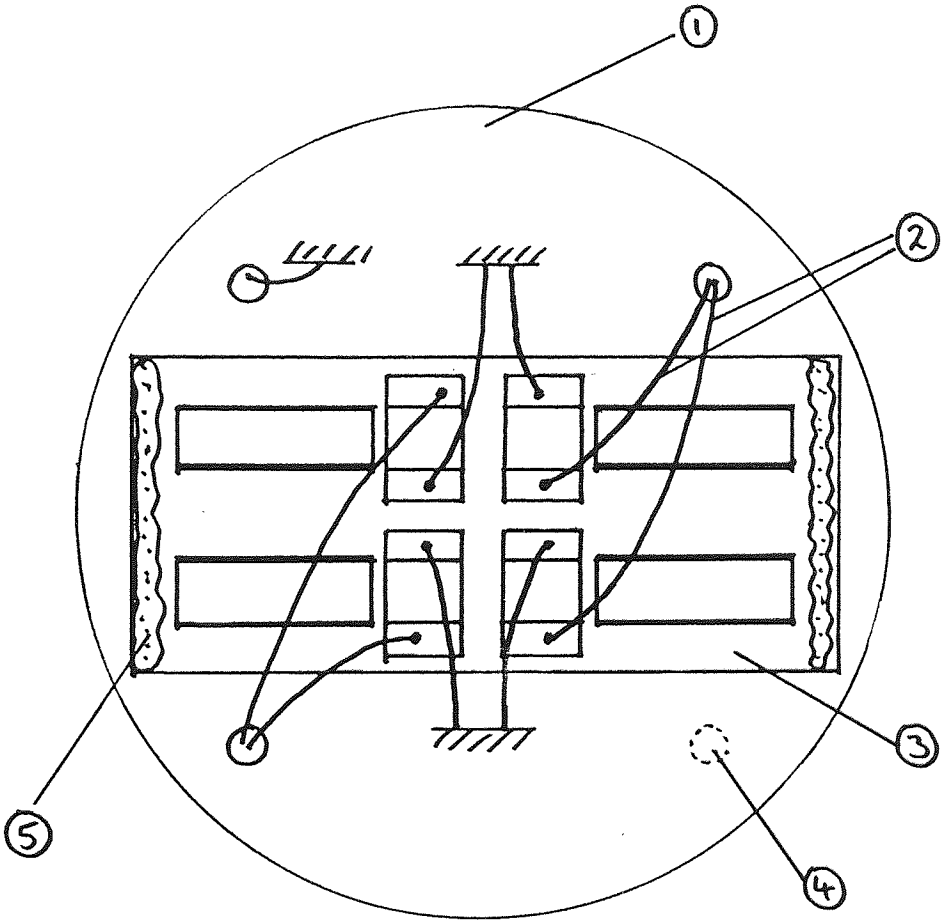

1 TO39 "Header"
2 Bond wires
3 SAW die
4 Base earth pin
5 End absorber

FIGURE 64 Mounting Configuration - Coupled Resonator Filters

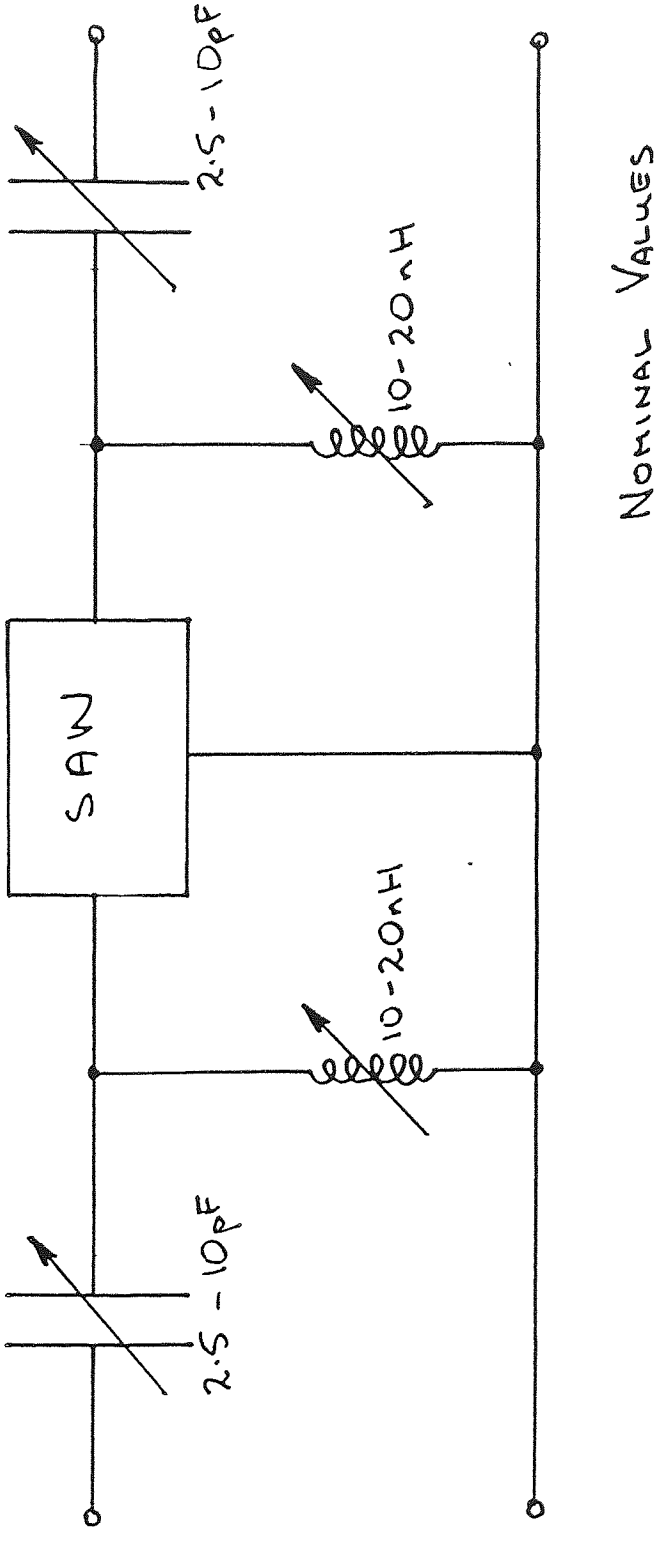

FIGURE 65 Matching Network - Coupled Resonator Filters

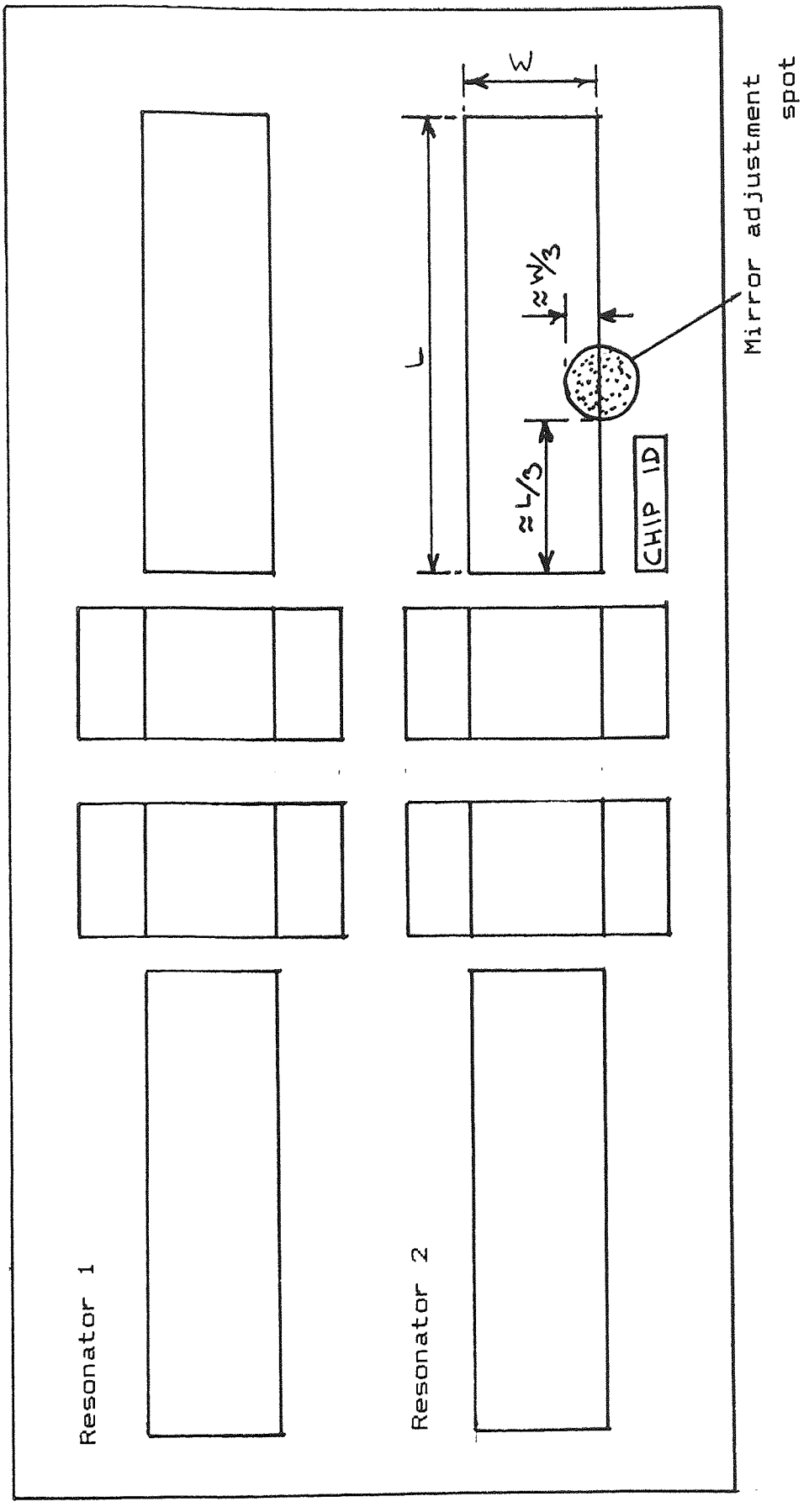

FIGURE 66 SAW Die Showing Mirror Adjustment Spot

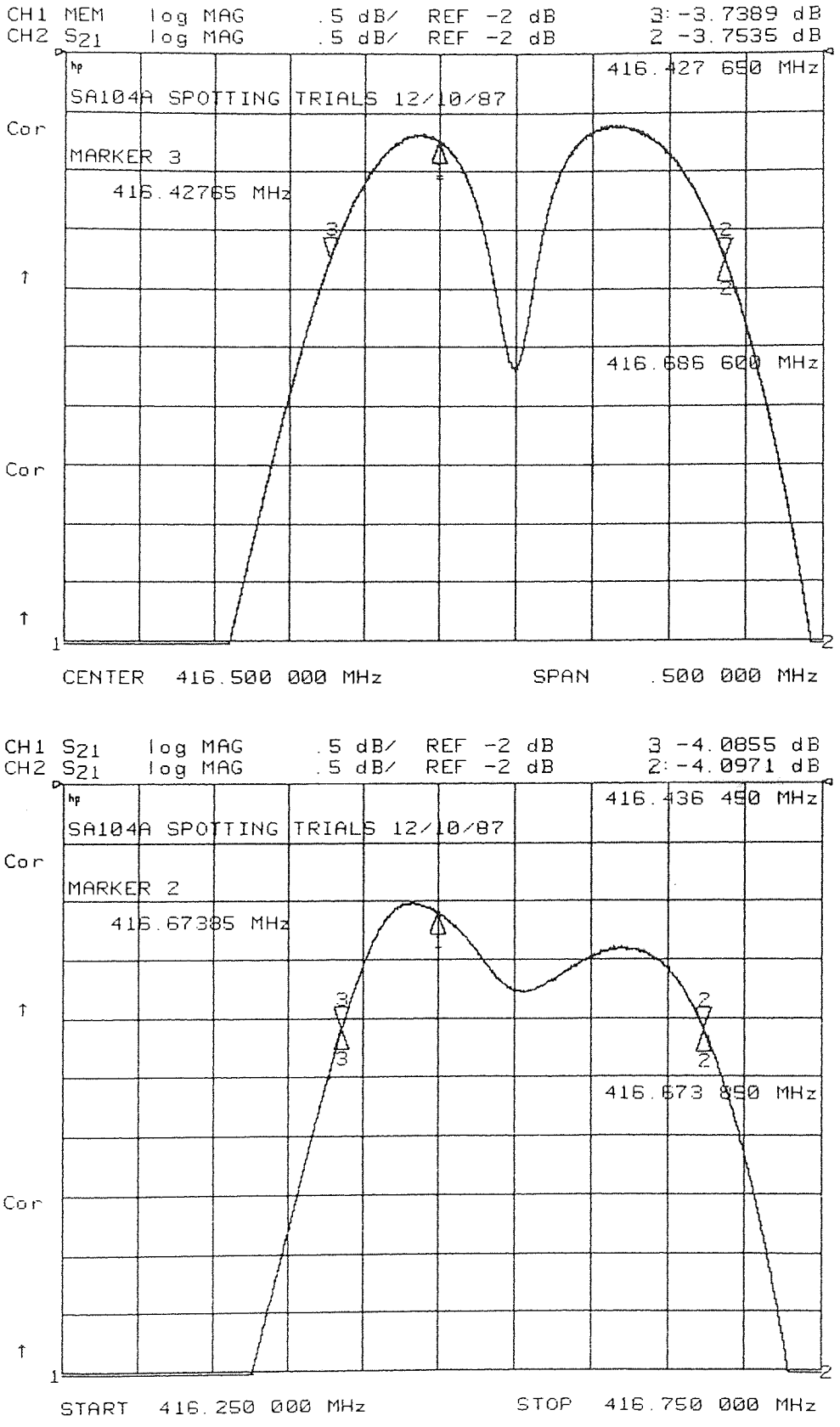

FIGURE 67 Passband Change During Mirror Adjustment

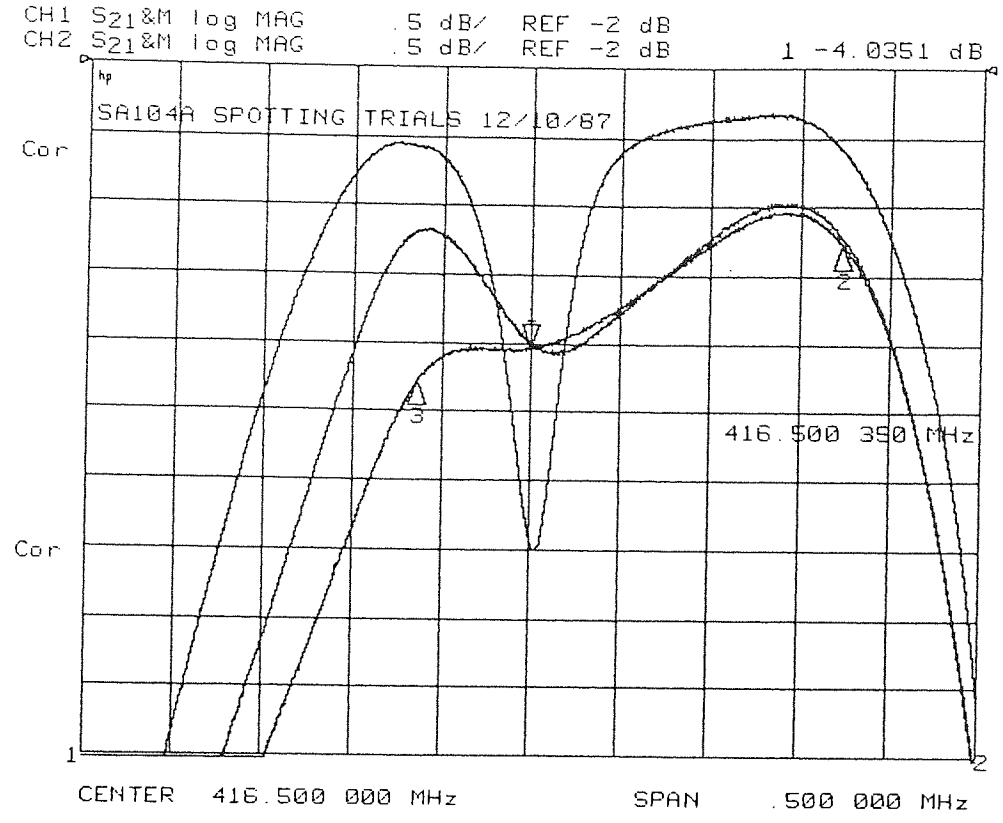

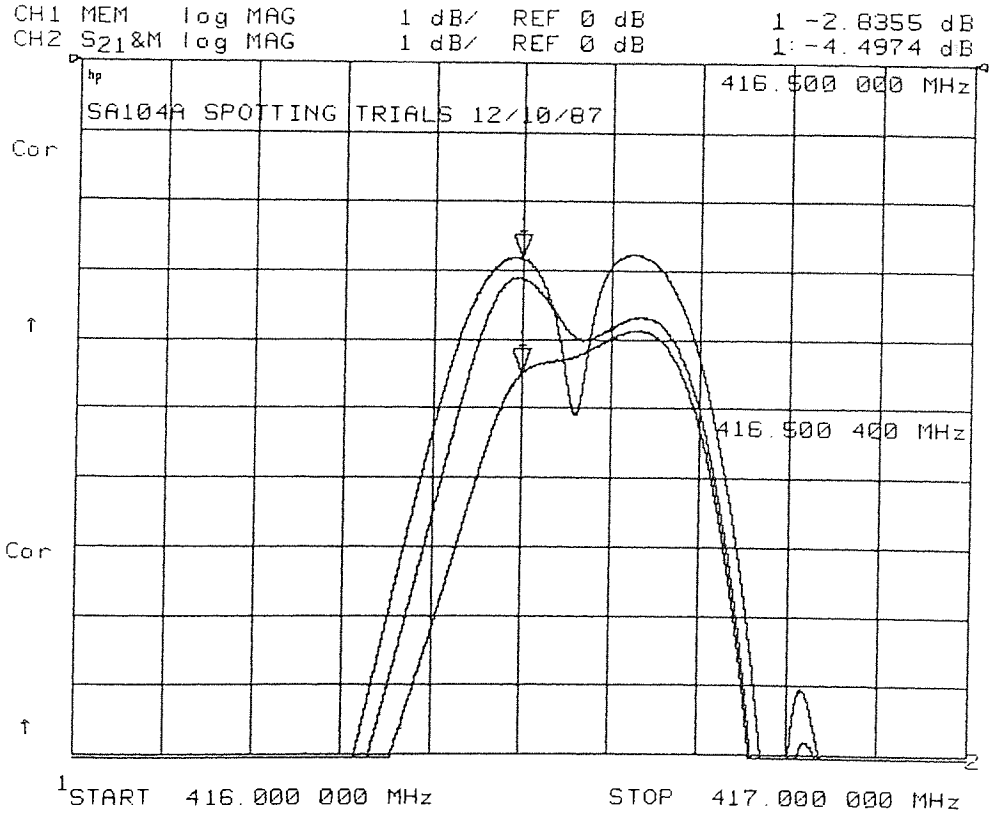

FIGURE 68 Passband Change During Mirror Adjustment

Unit	Insertion Loss (dB)	Frequency Peak 1 (MHz)	Frequency Peak 2 (MHz)	Centre Frequency (MHz)	Offset (kHz)
1	11.4	416.350	416.538	416.444	188
2	10.8	416.354	416.552	416.453	198
3	12.0	416.363	416.575	416.469	212
4	11.8	416.363	416.566	416.465	203
5	11.8	416.374	416.572	416.473	198
6	11.2	416.340	416.558	416.449	218
7	9.7	416.328	416.522	416.425	194
8	10.5	416.362	416.535	416.449	173

Notes:

All measurements were made unmatched in a 50ohm system.

The insertion loss value is the minimum of the two peaks.

Centre frequency is the average of the frequencies of the two peaks and was used for device selection purposes.

TABLE 27 Coupled Resonator Filters- Unmatched - Typical Results.

techniques described above, a series of production tests were undertaken. A typical set of results is given in Table 28. These results show the frequency offsets at 1.5dB below the reference frequency. The responses of two of these devices are shown in Figures 69 and 70.

At this stage it was deemed necessary to seek further improvement of the stopband rejection. The relatively poor stopband of Figures 69 and 70 was thought to be associated with electrical breakthrough between bond wires and poor earthing within the test jig. The test jig was improved with the addition of an earthing screen between input and output ports. To reduce the complexity of bond wire layout and attachment, the device design was modified to include interconnection through the metal film. At the same time one of the SAW resonator transducers was also modified by transposing it through one half wavelength. This had the effect of providing the necessary anti-phase output from one device but with much simplified electrical connection. The resultant device layout is shown in Figure 71.

Coupled resonator devices, based upon this modified layout, were fabricated using standard production processes. During die mounting and bonding all devices were "mirror spotted" using a specially designed applicator to assist in achieving repeatability in production. A set of results for a typical batch are given in Tables 29, 30 and 31. Performance plots for one of these devices are shown in Figures 72 and 73.

Table 31 clearly demonstrates how the bandwidth drifts with temperature. In an attempt to reduce this effect, devices were fabricated on LST75-cut quartz. This required a new photomask to be produced. In this case the transducers comprised of split-fingers as these had been shown to improve the device response (Chapter 4). The results on LST75 coupled resonator filters are given in Table 32. Typical performance plots are shown in Figure 74. Figures 75 and 76 show the changes in the passband level and also in the passband shape at temperatures between -40 and +85°C.

5.2.3 Discussion.

In this work on coupled resonator filters the bandwidth is specified between the - 1.0 or -1.5dB points. These

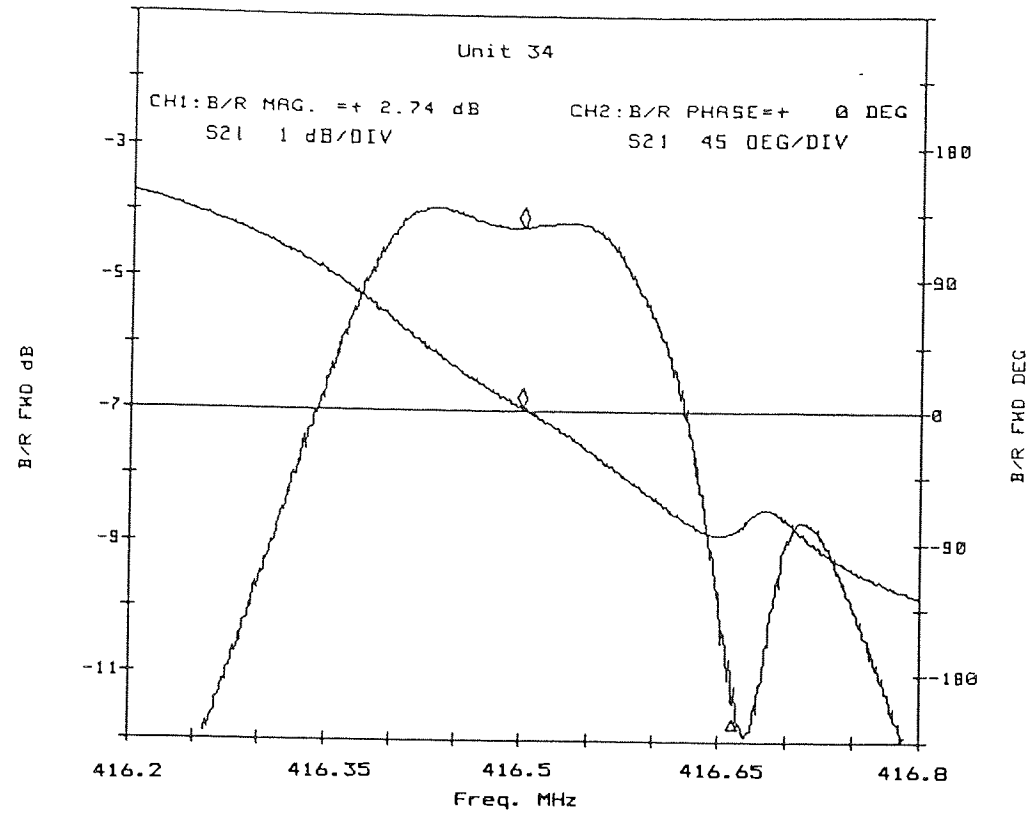

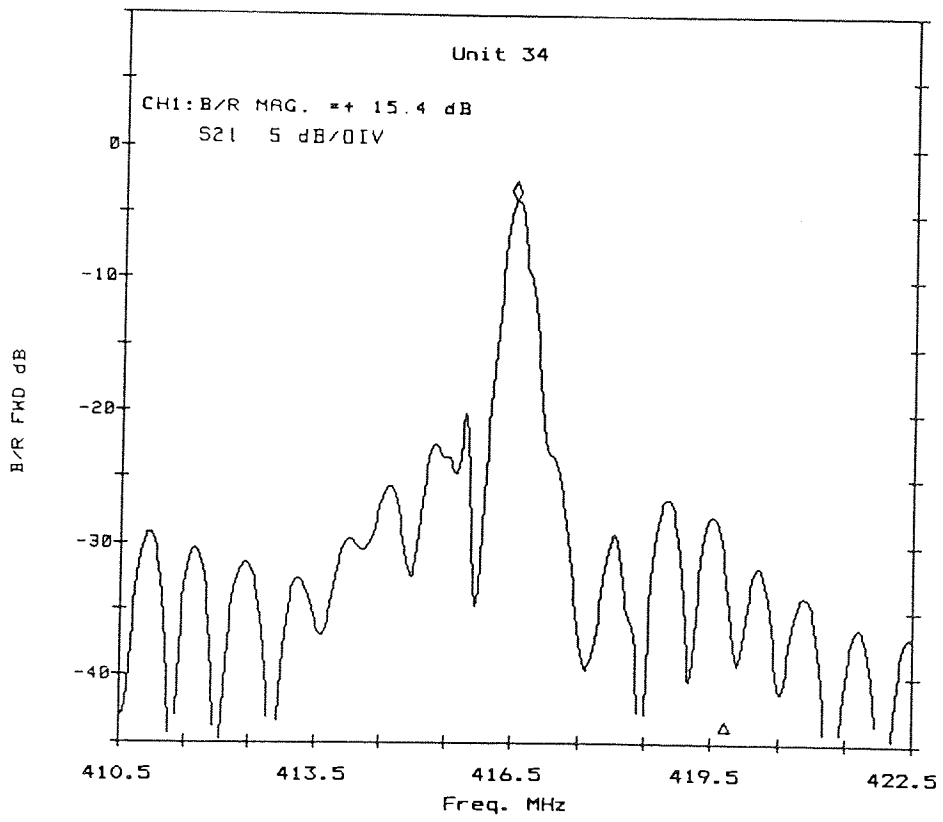

FIGURE 69 416MHz Filter - Unit 34

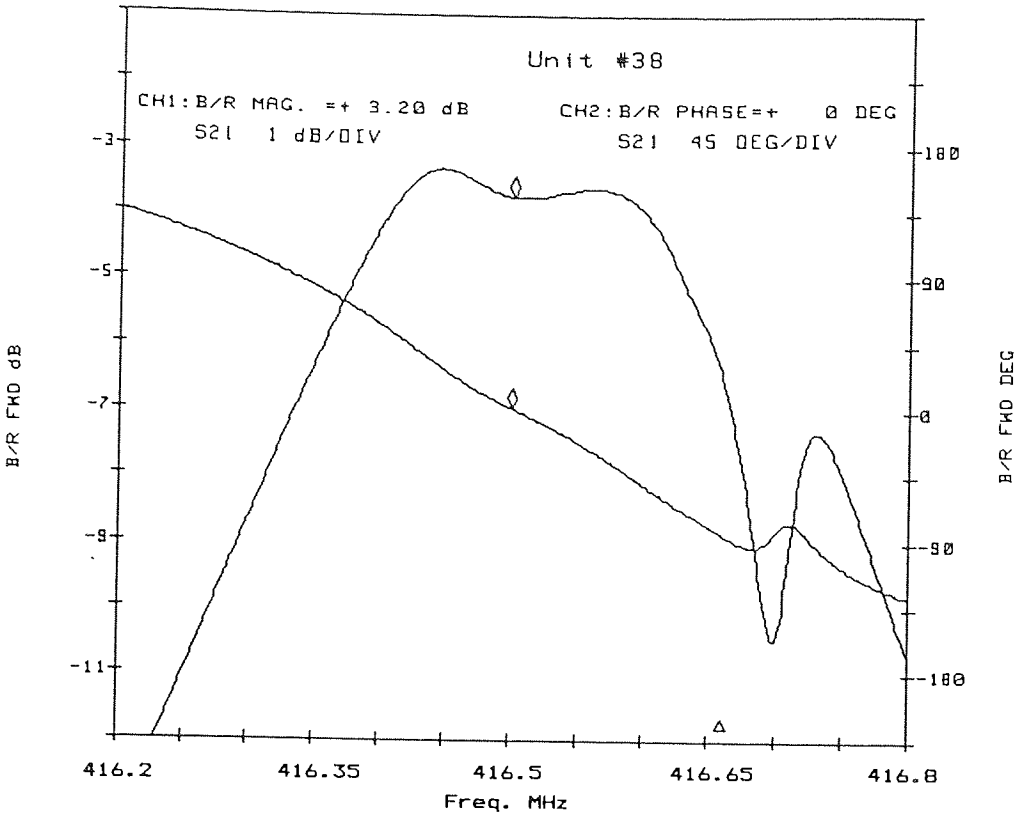

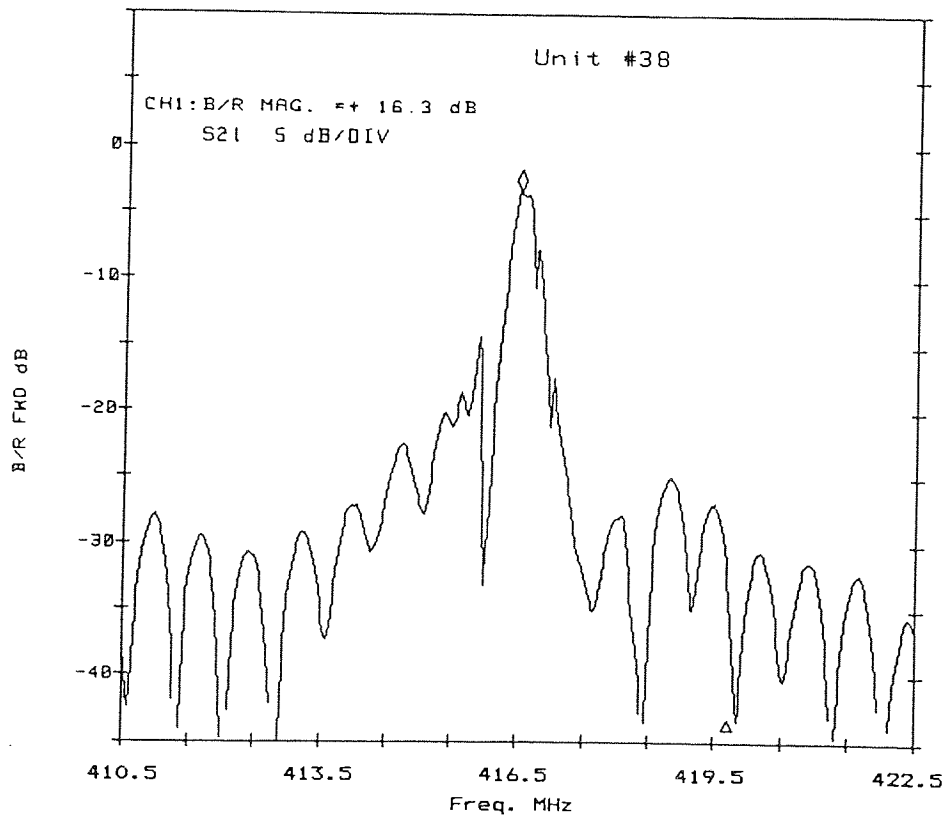

FIGURE 70 416MHz Filter - Unit 38

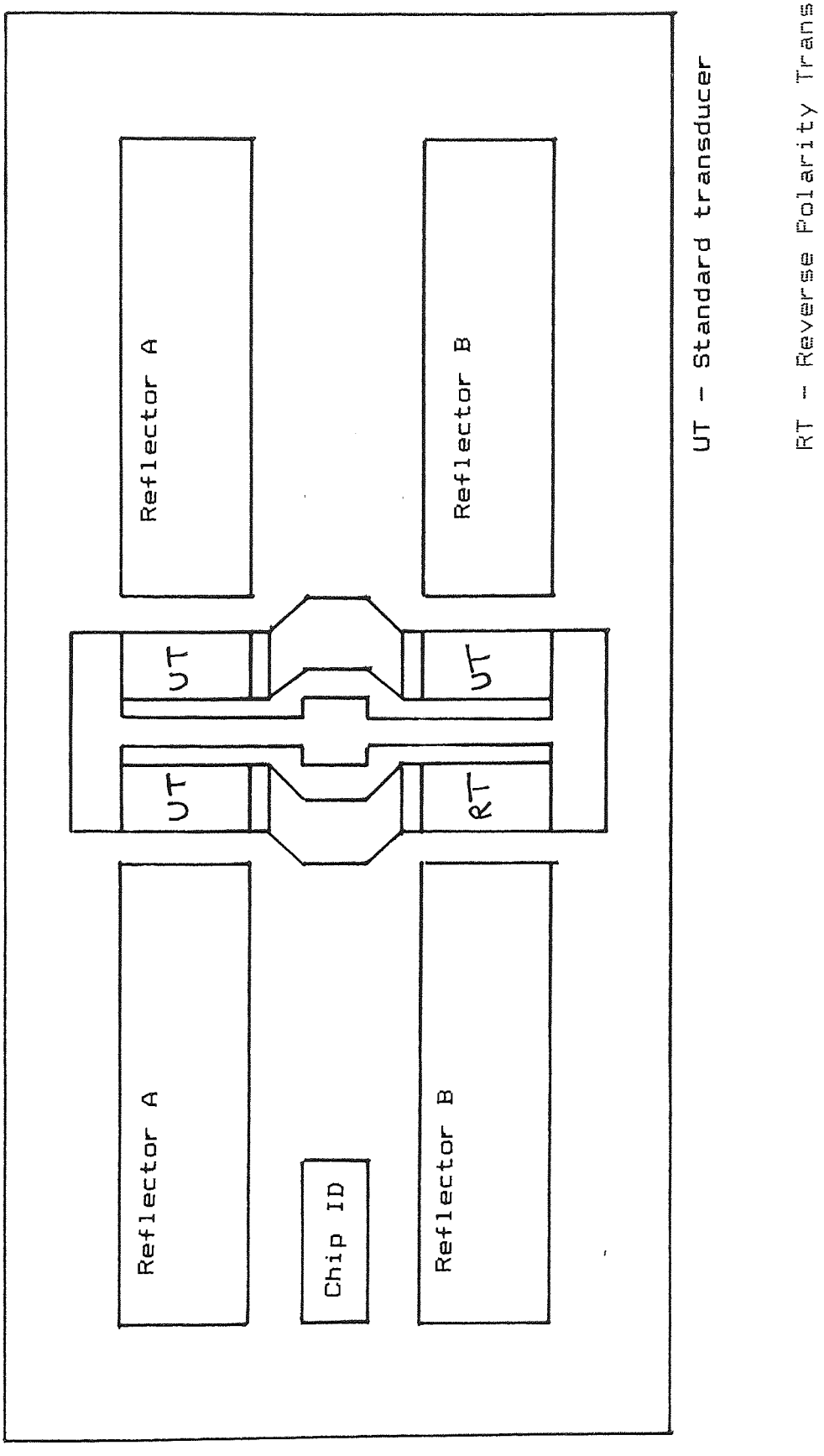

FIGURE 71 Coupled Resonator Filter - Revised Layout

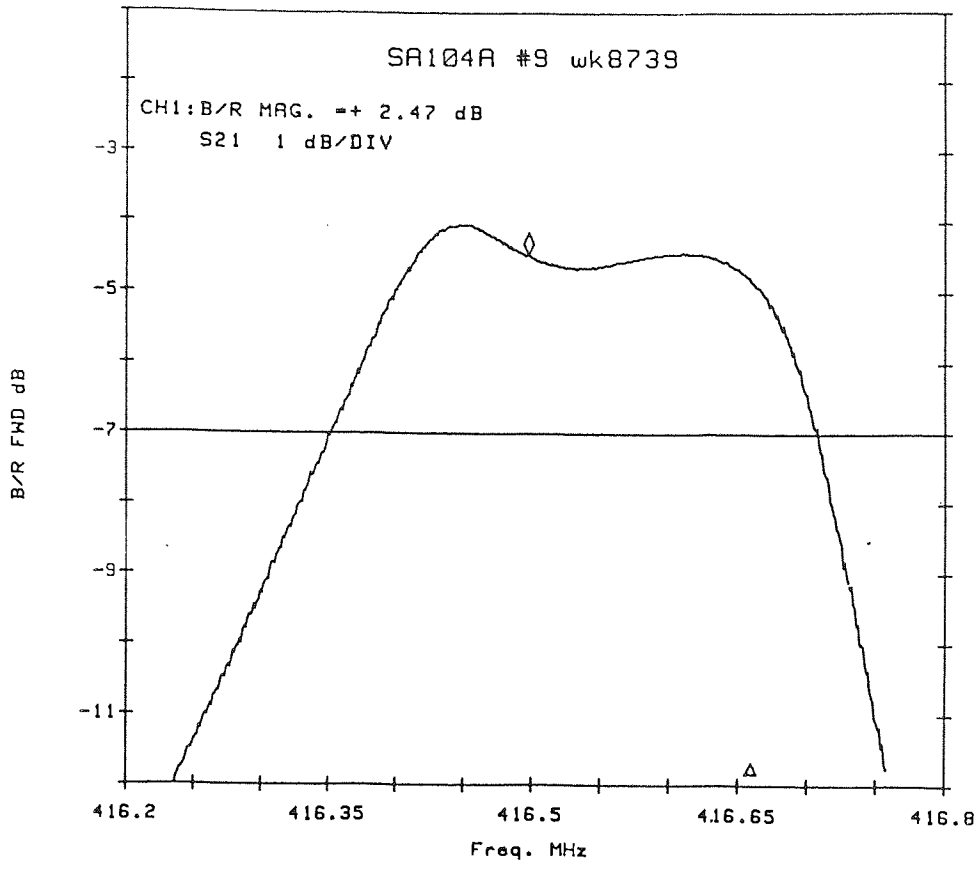

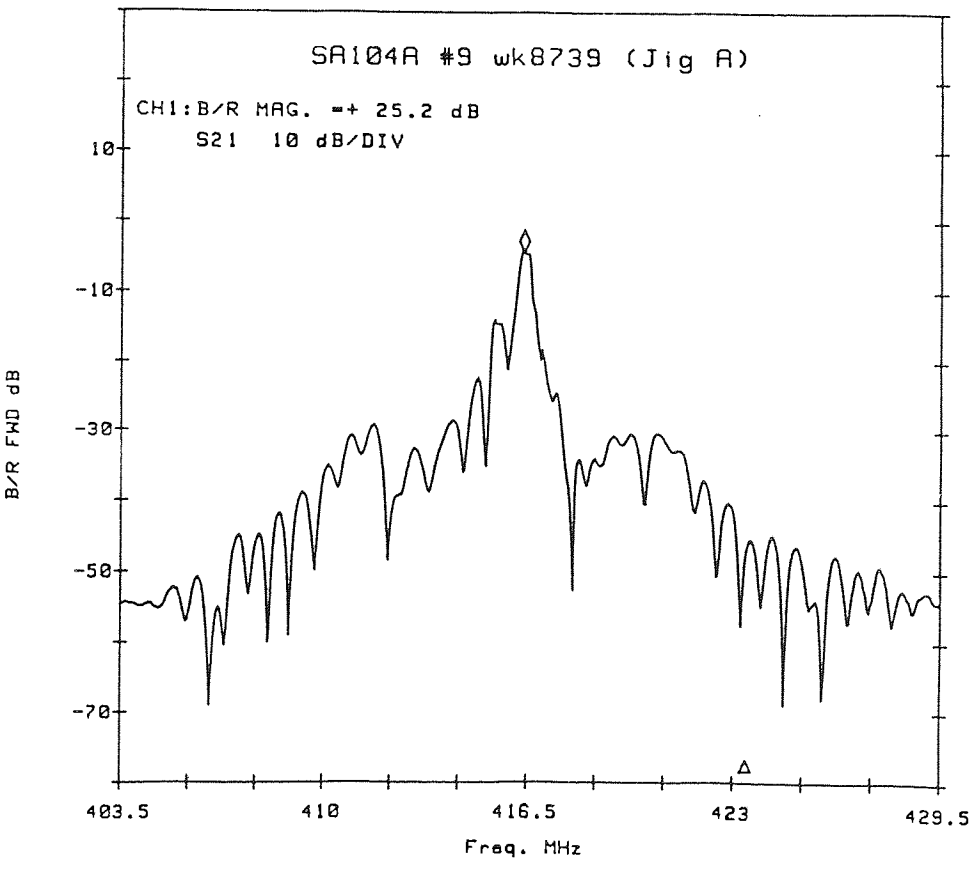

FIGURE 72 416MHz Filter - Close-in Performance

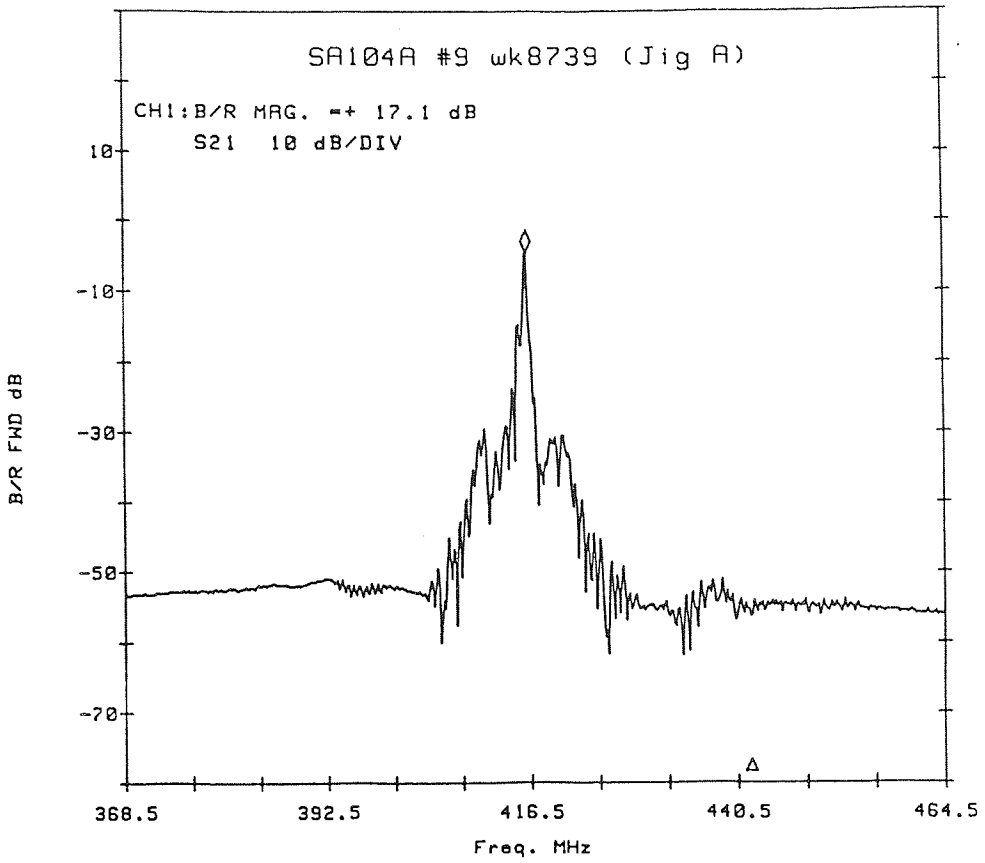

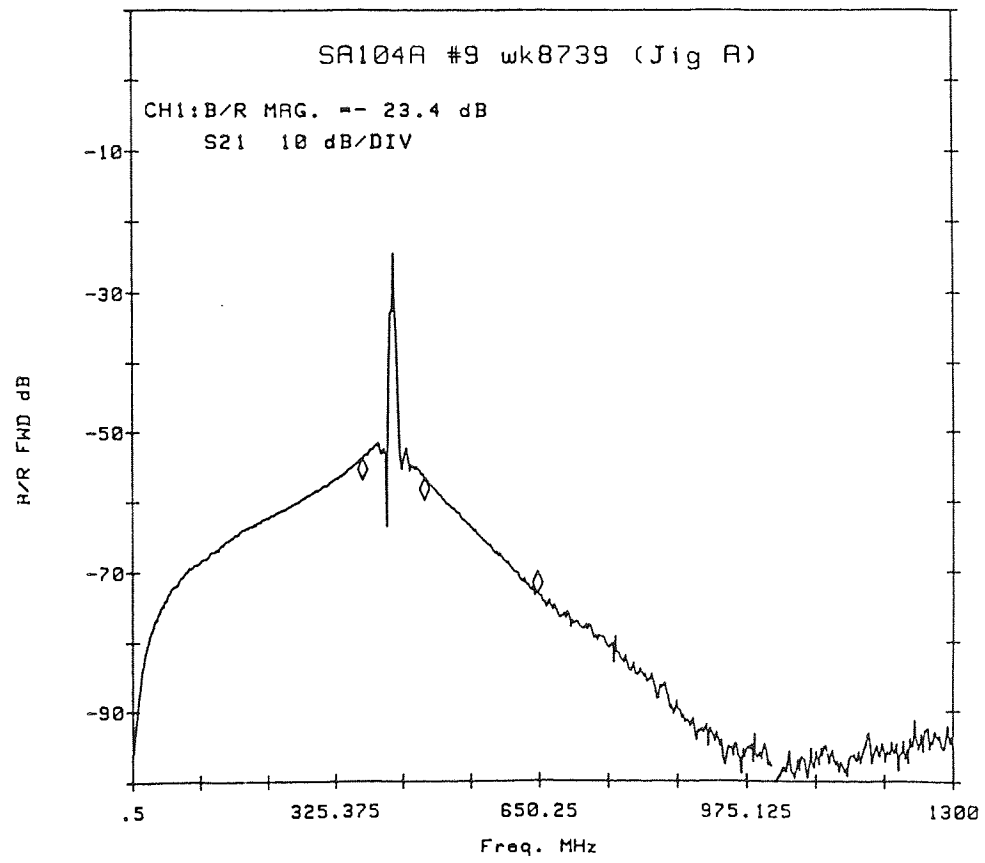

FIGURE 73 416MHz Filter - Stopband Performance

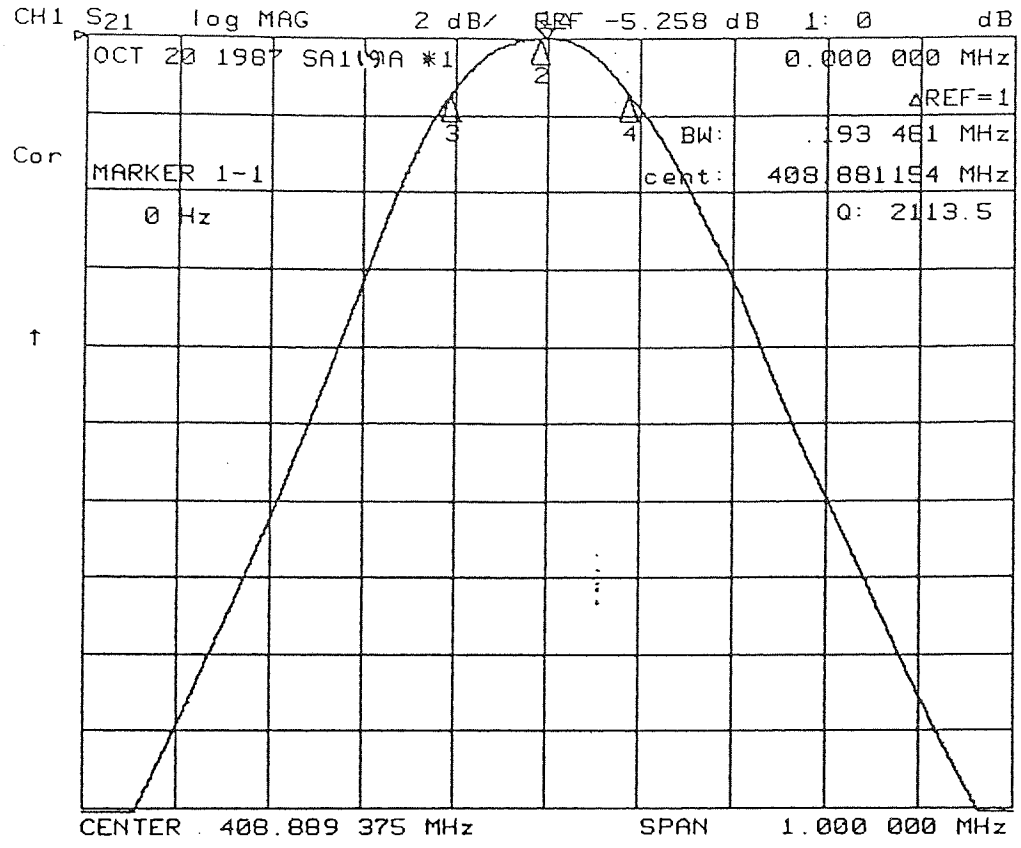

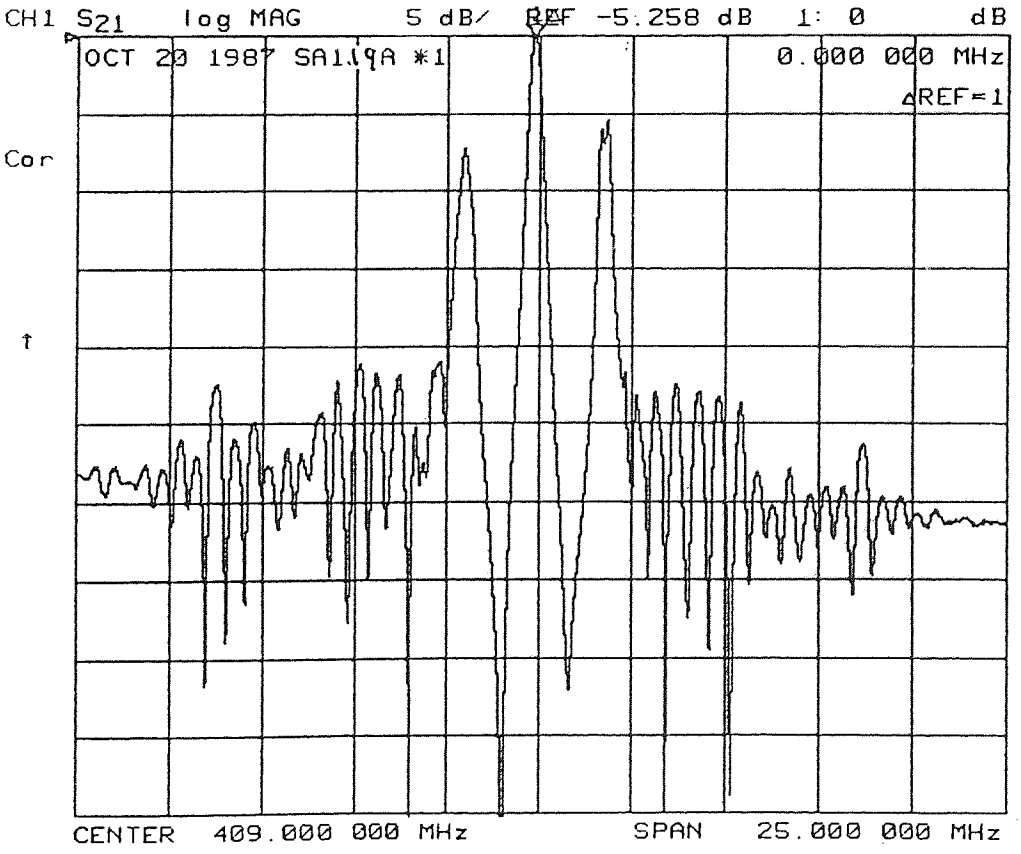

FIGURE 74 Coupled Resonator on LST75-Quartz

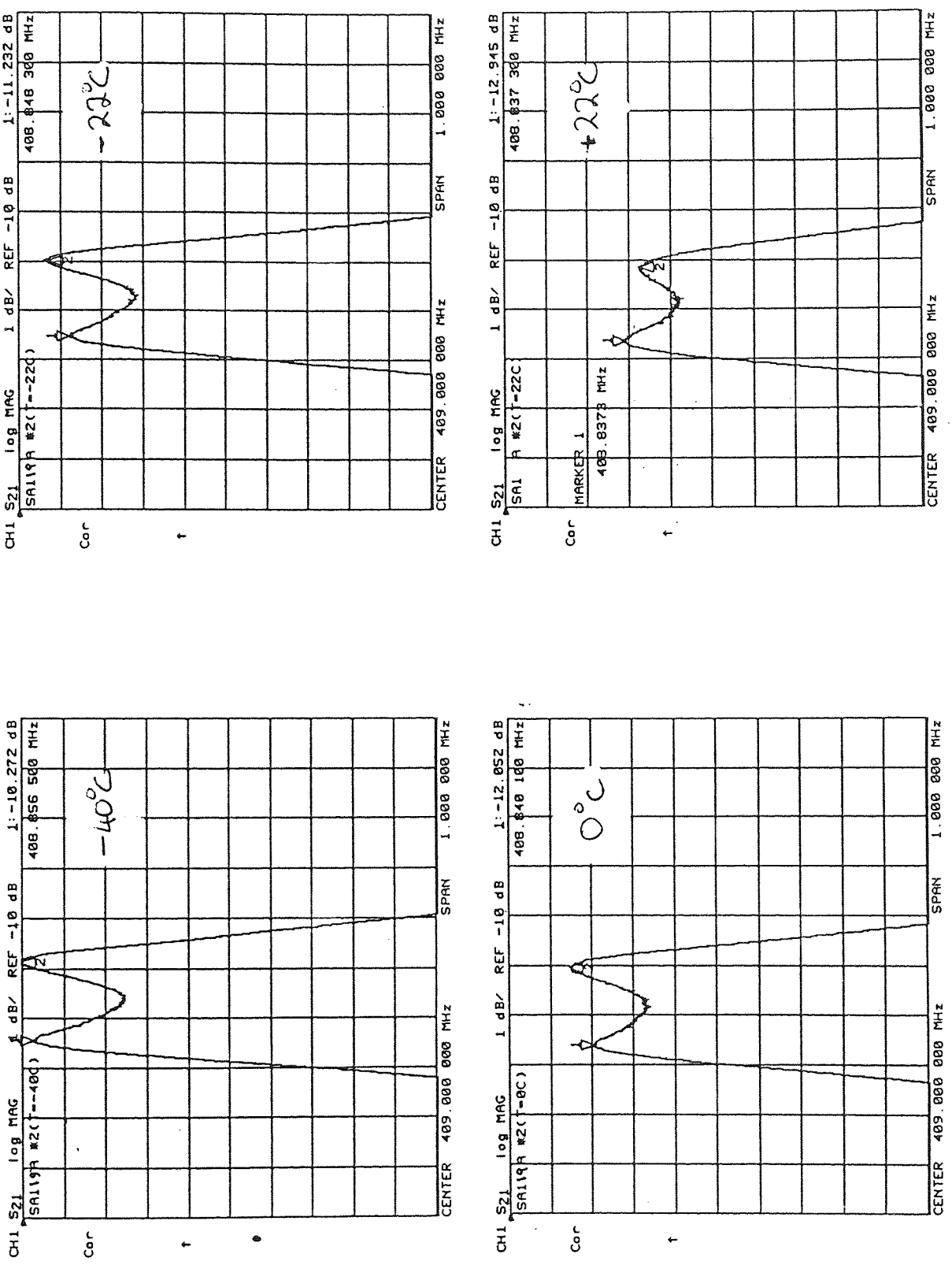

FIGURE 75 LST75 Filter Passband Change with Temperature (-40 to +22°C)

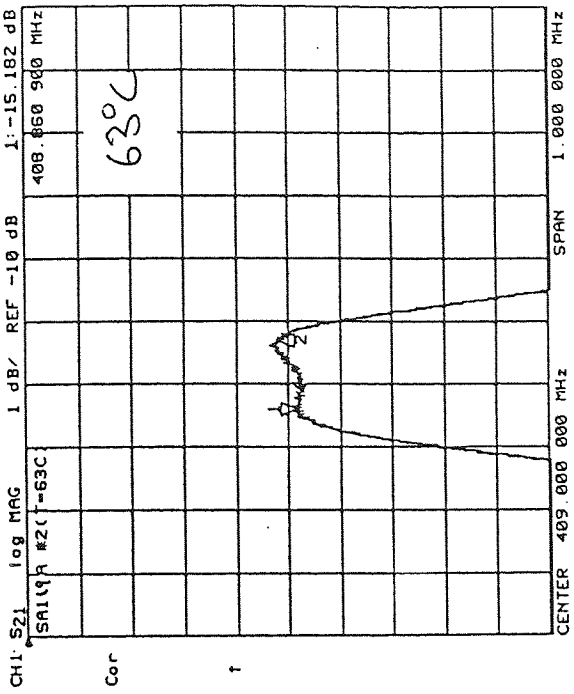

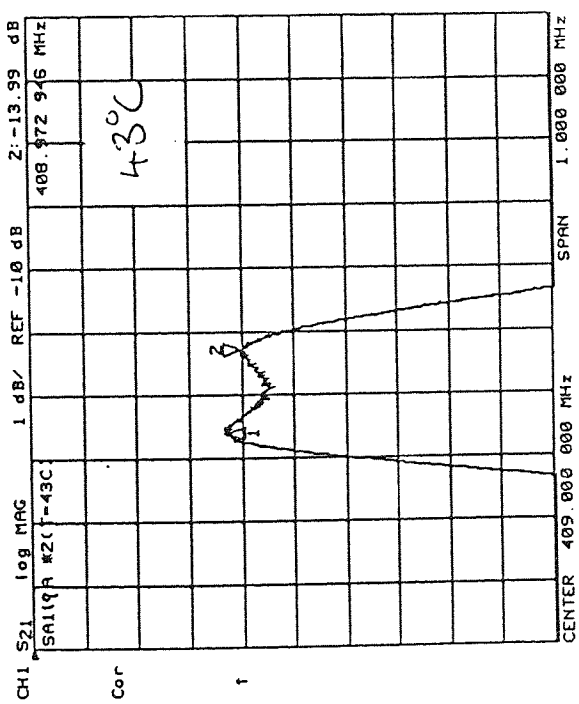

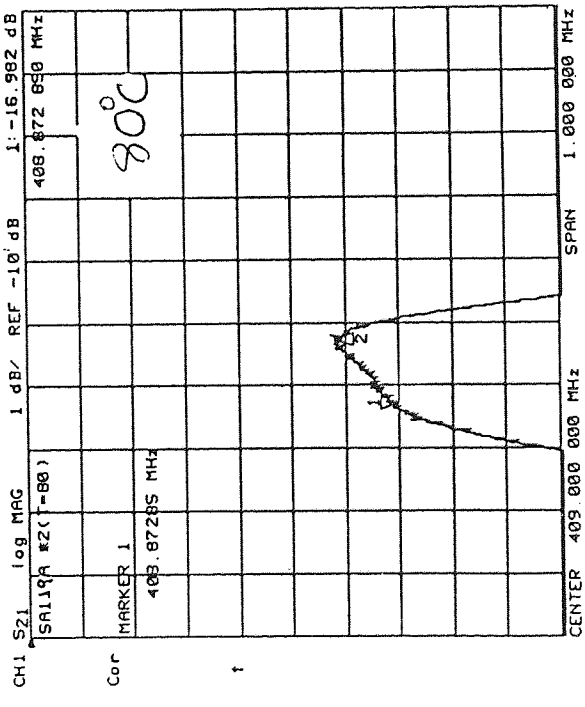

FIGURE 76 LST75 Filter Passband Change with Temperature (+43 to +80°C)

Unit	Insertion Loss @ F(ref) (dB)	Frequency Offset from F(ref) @ 1.0dB Below F(ref) Lower (kHz)	Upper (kHz)	Passband Ripple Pk-Pk (dB)
30	3.7	60	110	0.5
31	4.0	110	60	0.5
32	4.4	230	30	0.8
33	3.9	110	110	0.6
34	4.3	100	130	0.3
35	3.9	80	80	0.2
37	3.7	110	110	0.1
38	3.6	100	150	0.6
39	4.0	70	150	0.5
41	3.5	80	130	0.3
42	3.7	120	80	0.2
43	3.6	95	110	0.3
44	3.9	90	120	0.3
47	3.8	90	150	0.2
49	3.7	80	110	0.2
50	4.1	120	110	0.4
51	3.8	100	150	0.4
52	3.7	70	130	0.1
54	3.9	70	130	0.3

Notes:

F(ref) = 416.5MHz.

Unit numbers refer to actual process data. Failed devices are not included. (STC in-house ref. BR146)

All measurements were made in a test jig incorporating a matching network.

TABLE 28 Coupled Resonator Filters - Matched - Typical Results

Unit	Resonator 1		Resonator 2		Offset
	Insertion Loss (dB)	Frequency (MHz)	Insertion Loss (dB)	Frequency (MHz)	(kHz)
1	14.0	416.441	13.8	416.681	240
2	13.7	416.385	13.8	416.644	259
3	13.4	416.360	13.4	416.602	242
7	13.4	416.354	13.9	416.589	225
8	13.6	416.409	13.2	416.604	195
9	13.6	416.404	13.8	416.671	267
10	13.6	416.431	13.6	416.676	245
13	13.4	416.427	13.4	416.669	242
14	15.4	416.402	14.6	416.668	266
15	14.4	416.440	13.8	416.676	236
18	14.8	416.435	14.4	416.697	262
20	13.4	416.343	13.6	416.632	289
31	14.2	416.355	13.8	416.605	250
34	14.6	416.388	14.8	416.688	300
35	14.8	416.423	15.6	416.748	325

Notes:

Device target frequency 416.5MHz.

All measurements were made in a 50ohm system, unmatched.

Unit numbers refer to actual process data. Failed devices are not included. (STC in-house ref. BR460)

TABLE 29 Coupled Resonator Filters - Modified Design Unmatched

Unit	Insertion Loss @ F(ref) (dB)	Frequency Offset from F(ref) @ 1.0dB Below F(ref) Lower (kHz)	Upper (kHz)	Passband Ripple Pk-Pk (dB)
1	3.9	74	174	0.3
2	3.9	162	149	1.0
3	3.0	155	84	0.4
7	2.9	158	71	0.4
8	2.5	90	74	0
9	4.0	125	180	0.6
10	4.2	86	175	0.8
13	3.2	95	170	0.7
14	3.8	80	190	0.8
15	3.3	105	178	0.9
18	4.5	113	200	1.4
20	3.5	154	130	0.3
31	3.5	144	110	0.4
34	4.6	134	206	1.0
35	5.4	80	258	0.6

Notes:

F(ref) = 416.5MHz

All devices measured in test jig incorporating a matching network at room temperature (22°C).

Unit numbers refer to actual process data. Failed devices are not included. (STC in-house ref. BR460)

TABLE 30 Coupled Resonator Filters - Modified Design Matched

Unit number 14

Measured value			Temperature (°C)		
			-40	+23	+85
Insertion loss at F(ref) (dB)			3.2	4.0	4.1
Passband peak to valley (dB)			0.9	0.9	0.9
Discrimination	1dB	-F(kHz)	-184	-127	-163
	1dB	+F(kHz)	128	190	135
	12dB	-F(kHz)	-1038	-994	-1043
	12dB	+F(kHz)	358	435	384
	45dB	-F(MHz)	-9.9	-9.9	-11.0
	45dB	+F(MHz)	45	45	46
Stopband @ F(ref)-13MHz (dB)			47	47	46
F(ref)+13MHz (dB)			42	42	42

Unit number 17

Measured value			Temperature (°C)		
			-40	+23	+85
Insertion loss at F(ref) (dB)			3.1	3.6	4.1
Passband peak to valley (dB)			0.9	0.9	0.8
Discrimination	1dB	-F(kHz)	-162	-101	-136
	1dB	+F(kHz)	115	179	124
	12dB	-F(kHz)	-1052	-997	-1050
	12dB	+F(kHz)	350	420	384
	45dB	-F(MHz)	-9.9	-10.3	-9.9
	45dB	+F(MHz)	9.8	9.9	11.6
Stopband @ F(ref)-13MHz (dB)			47	46	45
F(ref)+13MHz (dB)			47	46	46

Notes:

F(ref) = 416.5MHz

Devices measured in a matching network.

Discrimination is the frequency offset from F(ref) at which the stated attenuation is achieved.

TABLE 31 Coupled Resonator Filters - Production Test at Temperature Extremes

Unit	Insertion Loss (dB)	Centre Frequency (MHz)	Bandwidth at 1.5dB (kHz)
1	5.3	408.881	193
2	5.5	408.943	197
3	5.8	408.945	184
4	6.3	408.921	220
5	5.6	408.954	184

(a) Frequency Performance

Temperature (°C)	Centre Frequency (MHz)	Insertion Loss (dB)
-40	408.9113	3.8
-22	408.9031	4.3
0	408.8931	4.6
22	408.8858	5.2
43	408.8838	5.7
63	408.8848	6.6
80	408.8856	7.6

Frequency Temp. Coeff = 0.008ppm/°C²
Inversion Temp = 53°C

(b) Temperature Performance

Notes:

All measurements made in a matching network

TABLE 32 Coupled Resonator Filters on LST75-quartz

are the levels at which most application specifications set the bandwidth targets.

Figures 62 and 63 show the resultant plots for two 250MHz resonators connected in parallel as described above and matched for minimum insertion loss into a 50ohm line. The salient features are:

Low insertion loss - 3.5dB
Bandwidth - 120kHz
Low passband ripple - < +/-0.25dB
Good stopband - > 40dB at F(ref) +/-6MHz
Linear phase in passband

These devices were not designed specifically for this application but were used to illustrate the potential of realising narrow-band low-loss filters. The use of twin packages may have influenced the result through electrical jig effects. The result suggested that at frequencies in the range 400 to 500MHz similar structures and combinations would yield devices with bandwidths of 250kHz. This order of bandwidth is required for useful devices. The result also indicated that there would be a small level of passband ripple.

The next stage was to produce devices at a higher frequency and with both resonators mounted in a single package, as shown above in Figure 64. The target frequency was in the range 400 to 450MHz with a nominal bandwidth of 200kHz at 1.0dB. Table 27 gives the results for a batch of devices measured in a 50ohm test jig. Clearly shown is the offset frequency between the two resonator peaks and the typical insertion loss associated with unmatched resonators.

Section 5.2.2 above described the "mirror spotting" technique developed to remove the passband dip in matched devices. Table 28 illustrates a batch of "mirror spotted" devices similar to those of Table 27, but matched into a 50ohm line. All devices were measured in the same test jig with the same matching configuration (Figure 65). The results are presented in the form required by end-users. The insertion loss is measured at the reference frequency (F(ref)) and is not necessarily the minimum loss in the passband. The frequency offset is defined as the difference between F(ref) and the frequency at which the attenuation falls to 1.0dB below that at F(ref). Consequently, there is a lower and upper offset value

which, when added together, give the bandwidth. Passband ripple is the maximum ripple between the offset frequencies.

This set of results highlights several important features. There is a high level of consistency in the insertion loss values, varying from 3.5dB to 4.4dB. However there are large differences in the offset values and passband ripple levels between devices. The variation in offset values is an indication of the frequency spread associated with photomask and processing repeatability. This impacts on passband ripple as this is generally high where the offset values are large. Variations in ripple are also likely because of the mirror spotting technique descibed above.

Figures 67 and 68 clearly demonstrate the dependence of ripple on the mirror adjustment. Figure 67 shows the same device before and after adjustment. Figure 68 illustrates the problem of over-adjustment. This shows that as the mirror is spotted the ripple reduces and the passband shape changes. Over-adjustment eliminates ripple but increases attenuation. Adjusting only one mirror also increases preferentially the attenuation of one device such that the centre frequency of the coupled device tends to increase. These factors need to be evaluated as they will seriously reduce device yield in production.

Plots of two of the devices listed in Table 28 are shown in Figures 69 and 70. Again they illustrate good passband shape and low insertion loss. Noticeable is the close-in sidelobe on the high frequency side of the main response. At 5dB below the loss at F(ref) this sidelobe does not affect the passband response. However it does influence the roll-off on the high frequency side and therefore the discrimination at close-in frequencies. This side-lobe is thought to be associated with cavity modes, possible because the quartz cut ,YXl(38°), does not have a non-zero power flow angle. The 250MHz devices described above were fabricated on ST-cut quartz and did not exhibit this problematic side-lobe. The 38°-cut was needed to locate the inversion temperature at the centre of the temperature band.

The basic matching circuit for the coupled resonator filters was a simple two component, wide bandwidth, LC-filter on each port. This was chosen for its simplicity and repeatability. A more complex

configuration of narrower bandwidth would have reduced the sidelobe level and increased close-in stopband rejection. Generally, as was shown in the technical review of Chapter 3, the simplest circuit is desirable.

The devices illustrated in Figures 69 and 70 were coupled within a single package by appropriate bond-wire configuration. Each device required a total of nine bond-wires and, therefore, 18 mechanical bonds. Not only was this time consuming, but also relatively difficult as wires had to cross and be carefully routed. The chance of one failed bond was high, resulting in possible device rejection by Quality Control inspection. It was also thought that this arrangement of bond-wires was reducing the stopband level because of direct electrical breakthrough. Figures 69 and 70 show rejection levels of approximately 25dB at 6MHz from the reference frequency.

To reduce electrical breakthrough and also to reduce the number of bonds required, a design was generated with interconnection on the device chip. The need to reverse the output of one transducer was achieved by reversing the finger polarity sequence. This simplified the on-chip pattern and hence the mask-making procedure. The layout is shown in Figure 71.

Results for devices based upon this revised layout are given in Table 29. This gives results in an 50ohm test jig. The design deliberately aimed to give a higher frequency offset than the results of Table 27. Table 30 lists the same devices when measured in a matched system. Again there are considerable device to device variations in offset frequency and ripple values. Detailed results for two of the devices are given in Table 31. These show the values of the key parameters at the temperature extremes. A set of plots for a typical device are given in Figures 72 and 73. Table 31 suggests that the insertion loss value increases by 1.0dB with temperature. Much of this change is due to the drift of the passband response such that the reference frequency moves into the passband valley.

The 1dB discrimination level clearly illustrates the temperature induced frequency shift of approximately +/-30kHz overband. The 12dB discrimination values show the effect of the sidelobes, in this case on the lower frequency side. The results indicate that on the high frequency side the 12dB level is reached at approximately

400kHz from F(ref). On the low frequency side the corresponding value is approximately 1000kHz. These results and plots also show an improvement in the rejection levels. At 6MHz from F(ref) the rejection is 30-35dB compared with 25dB for the previous design. Figure 73 indicates a general stopband level of better than 50dB.

In practice, several other factors were found to influence the stopband level. It was found necessary to clamp the device under test into the test jig to reduce spurious effects. Also, the position of the die mounting spot was found to be important. There are three basic methods for paste fixing a SAW die to its header, all-over paste, centre spot and cantilever. In a resonator it is usual to cantilever mount the die to avoid stresses that may occur below the active transducers during encapsulation. It was found that a centre spot mount improved the stopband level by several dB. However, the change in device centre frequency during the sealing process was unpredictable. Further, the characteristics of any stress relief over time were unknown. For this reason the standard cantilever mount was retained.

These results have demonstrated narrowband coupled resonator filters at relatively high freqencies, at sufficiently high bandwidths to allow for a large frequency drift with temperature and with insertion loss levels suitable for front-end filtering applications. Other advantages of this approach are the small package size and simple matching network that does not require optimising for each individual device.

However, device yields in production are low. This is due, in part, to the close tolerences required by the professional users of such devices. One of the main factors affecting yield is the temperature drift. This requires a much larger bandwidth than is necessary at any one temperature. The larger bandwidth requires a greater offset between the devices that form the resonator pair. In turn the wider offset creates a greater passband ripple. The need to adjust the mirror by application of a paste spot is not satisfactory as it is difficult to control. Finally, at high frequencies the offset accuracy requires very high mask-making precision which can only be tested through device manufacture.

It should be remembered that devices of this type are almost always intended for professional application and are generally produced in relatively small numbers. Although the highest possible device yield in manufacture is always desirable, the low yield with this type of structure will, in most cases, be acceptable.

Chapter 4 illustrated the much improved temperature performance of LST75 quartz. A brief experiment was conducted in the use of this quartz for coupled resonator filters. The resonator design incorporated split-finger transducers and therefore the advantage of wider linewidths associated with the LST-cuts was negated. Results are shown in Table 32. The temperature coefficient is approximately four times better than 38°-quartz, as expected. Typical performance plots are shown in Figure 74. The smooth passband is due to the relatively narrow offset between the two devices. Clearly shown are the two side peaks as in previous LST devices. Figures 75 and 76 demonstrate the change in passband shape and level with temperature. In Chapter 4 this was cited as the major problem with LST-quartz. Again, such large variations are unacceptable and preclude the use of LST-quartz over wide temperature bands.

5.2.4 Recomendations for further work.

This work has demonstrated devices that fully meet real technical specifications. The wide bandwidths coupled with low insertion loss at high frequencies had not previously been realised at STC or reported elsewhere. Much work is necessary to "value engineer" this technique, thus improving device yield. There is scope to modify the design of the device such as to remove the need for mirror adjustment in manufacture.

The dependence of the stopband level and close-in sidelobes on packaging methods requires further investigation. A standard TO39 four-pin package was used for this work. Other packages are available which are claimed to have an improved RF performance and therefore may be more suitable.

No attempt has been made in this work to optimise the matching circuit or to test devices in specific applications. Such work may give improved stopband levels.

5.3 Single-Phase Unidirectional Transducers.

5.3.1 Methodology.

In Section 3.1.4 the target specification for a low insertion loss filter suitable for a PCM retiming application was given as follows:

Centre frequency	500 - 700MHz
Q value	400 - 800
3dB bandwidth	1.0MHz nominal
Insertion loss	5 - 10dB
Side-lobe rejection	>20dB

In an attempt to achieve this result, the SPUDT as proposed by Lewis[36] was the basis for the work reported here. Lewis demonstrates a device on ST-quartz at 400MHz with an insertion loss of approximately 6dB and a 3dB bandwidth of 0.6MHz. The basic structure of this device has been described in Section 3.1.2 and shown in Figure 17. Each transducer is based upon a ladder structure with each active rung surrounded by "blooming reflectors" which act to cancel out the internal reflections of the single-finger transducer rungs. A second set of reflectors are placed in the rung-to-rung gaps. These are offset one-eighth wavelength away from the other transducer and generate unidirectional operation.

The Lewis device was investigated in more detail to determine the number of low-loss reflectors, blooming reflectors and active fingers in each rung. An existing computer program, based upon a modified impulse response model, had previously been altered to allow the analysis of ladder transducers. This model did not attempt to analyse the effect of reflectors placed in the gaps between rungs. It was used primarily to search for the most suitable transducer structures to meet bandwidth and sidelobe specifications.

The detailed structure of the Lewis[36] device is shown in Figure 77. Details are:

	Transducer 1	Transducer 2
Rungs/transducer	12	9
Fingers/rung	19	25
Blooming reflectors/rung	19	25
Low loss reflectors/rung	30	40
Total no. of fingers	816	810

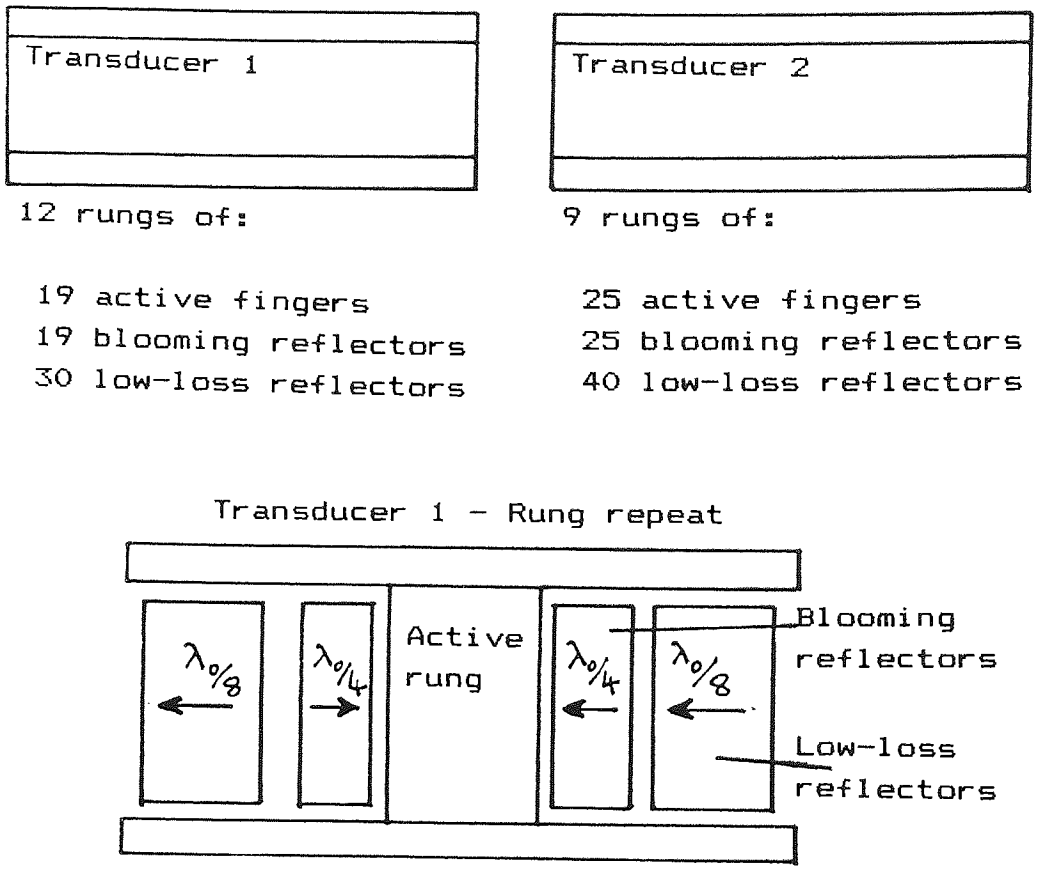

FIGURE 77 Structure of SPUDT (Lewis[36])

This data was used to "check" the computer model by comparing predicted results with the known device response. The results are shown in Figure 78. It should be noted that the computer prediction was targeted at the required frequency of 565MHz. The resultant bandwidth of 0.84MHz is equivalent to a Q-value of 673, almost identical to that for the Lewis device. The sidelobe levels also show agreement between predicted and actual.

For the PCM filter described above, a wider bandwidth was required. Using the computer model several possible structures were investigated. It was expected that the results would also indicate the effects of varying the number of rungs per transducer, the number of fingers per rung and the rung-to-rung gap. Once a suitable structure was found a photomask could be generated and devices manufactured. It was decided to include a conventional PCM filter structure on the photomask. Unlike the low-loss structure, this required the resolution of split-finger transducers at sub-micron line-space geometries.

A simple matching network is required to minimise insertion loss. In practice the end-user of these devices would prefer to use fixed-value matching components rather than individually tune each device for minimum loss. Therefore, a production test of the proposed PCM design was undertaken and a number of devices measured with the same matching component values. These would be supplied to a telecommunications authority for test and comment.

At an early stage it was thought that this design would be more suited to narrow bandwidths. The unidirectional power flow depends upon low-loss reflectors in the rung gaps. Increasing the number of rungs or the rung-to-rung spacing reduces the bandwidth. It was decided to undertake an exercise to determine the level of insertion loss that could be achieved with a relatively large bandwidth device. In this case the number of fingers per transducer rung and the number of reflectors per rung would be reduced to a minimum. This device was termed a "maximally distributed SPUDT". The target values for this device, which were selected to meet an actual requirement for a 450MHz delay line, were as follows:

Centre frequency 450MHz

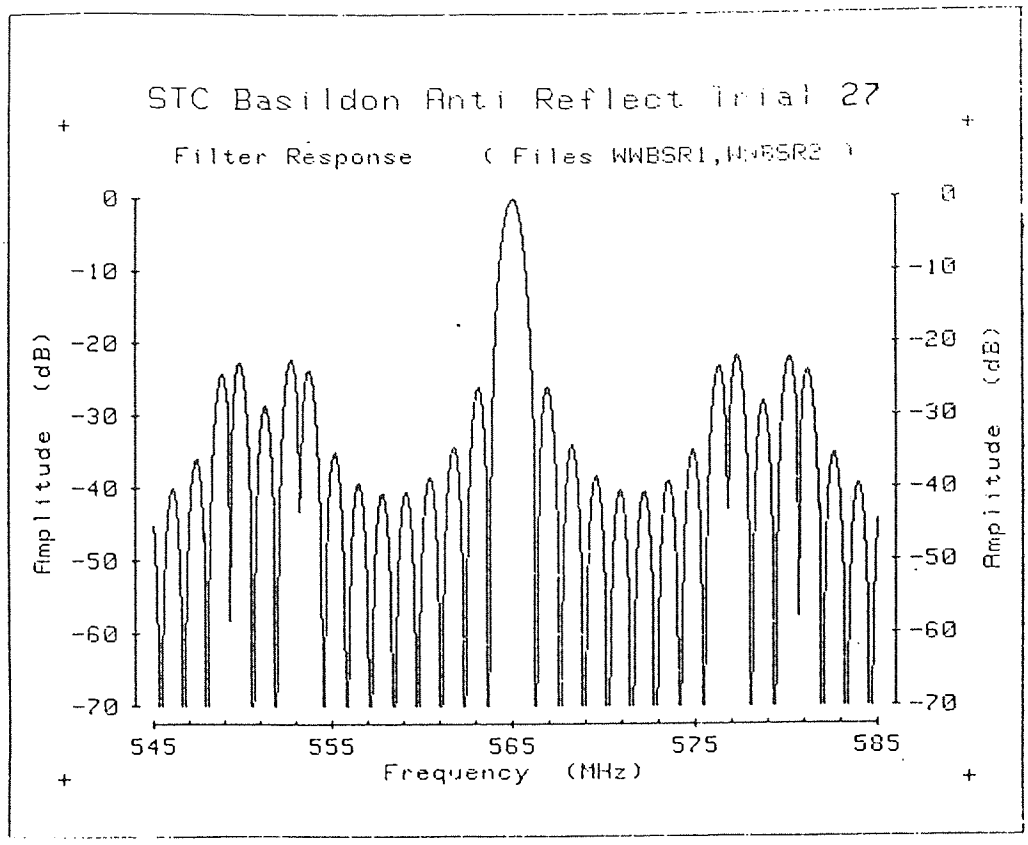

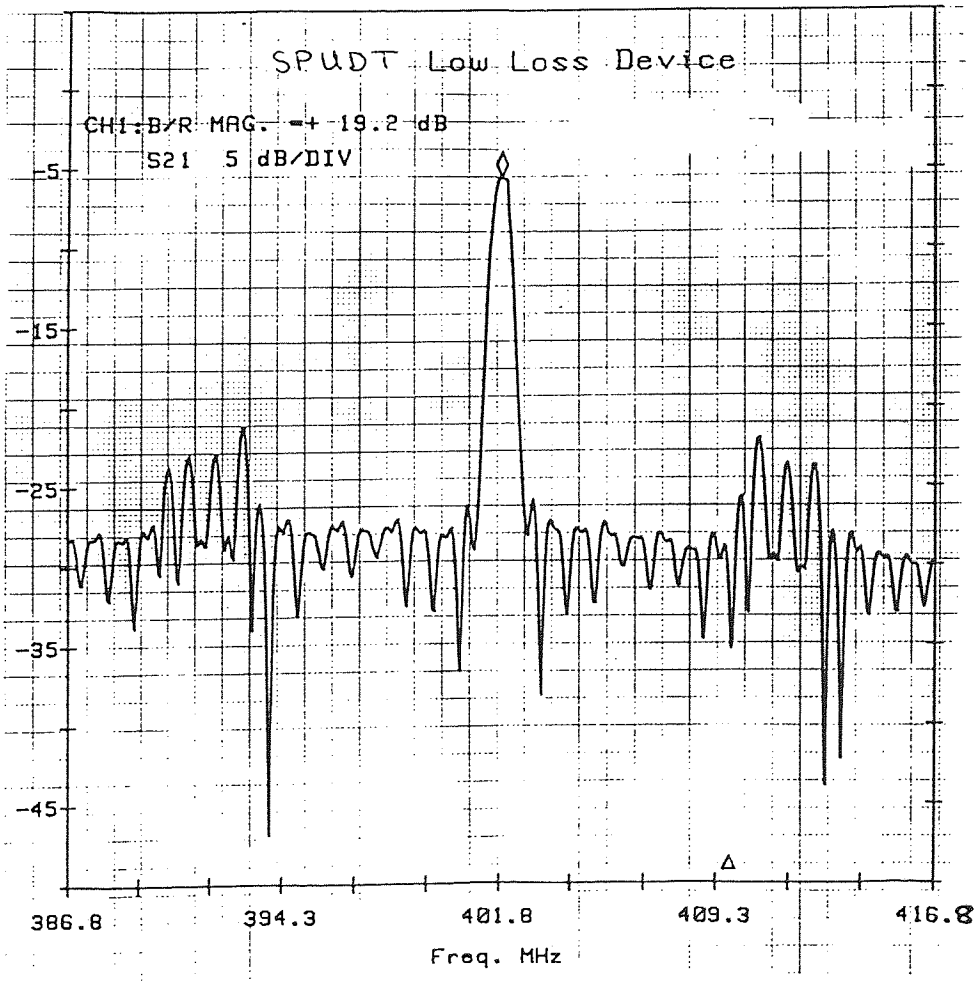

FIGURE 78 Lewis Device Response - Computed v Actual

Bandwidth (3dB)	1.5MHz
Sidelobe suppression	>25dB
Phase linearity in passband	<5° pk-pk

5.3.2 Results.

The computer analysis to find a suitable low-loss structure was based upon the input of three parameters for each transducer. The parameters were:

Number of fingers per rung
Number of rungs per transducer
Rung-to-rung spacing (number of fingers between rung centres)

The frequency response of each transducer was evaluated and then the two responses interlaced to give the total filter response. The starting point was the Lewis[36] layout with 3.2 low-loss reflectors for every two blooming reflectors and active fingers. Data from a series of trials is given in Table 33. The resultant frequency responses predicted by the computer model for these filters are shown in Figures 79 and 80. The final plot of Figure 80 shows the computed response for the structure selected to meet the target specification. The device structure was as follows:

	Transducer 1	Transducer 2
Rungs/transducer	12	10
Fingers/rung	20	30
Blooming reflectors/rung	20	30
Low loss reflectors/rung	24	36
Total no. of fingers	768	960

The detailed layout of one rung of transducer 1 is shown in Figure 81. Figure 82 demonstrates the interlacing of the two transducers and the resultant total response.

A photomask was fabricated to include this low-loss structure and a standard uniform transducer device to operate at the same frequency. The conventional device included a split-finger transducer requiring a fine-line resolution of 0.7um. On the low-loss device the smallest dimension was 1.4um. Devices were fabricated on

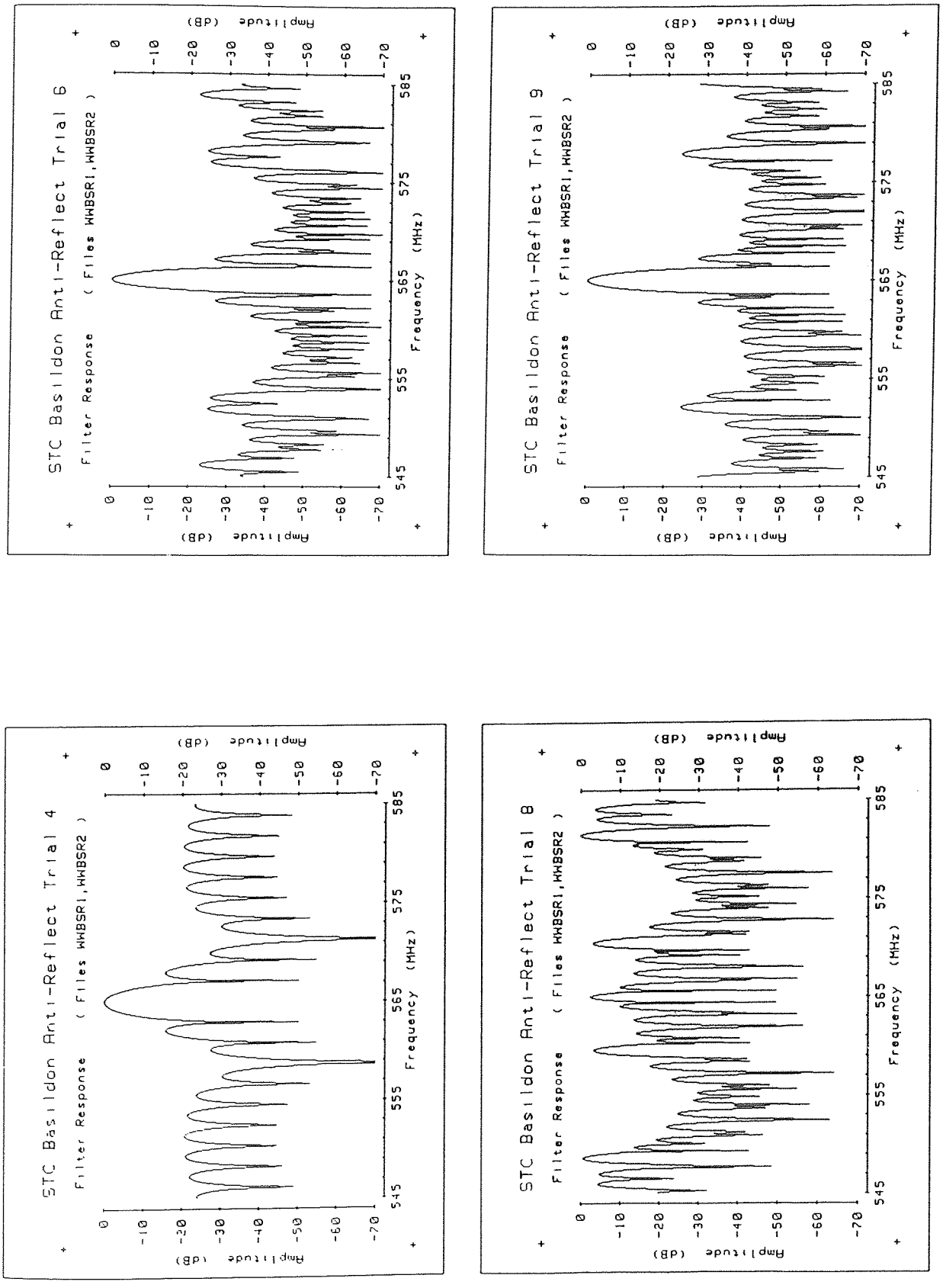

FIGURE 79 SPUDT Devices - Computed Responses

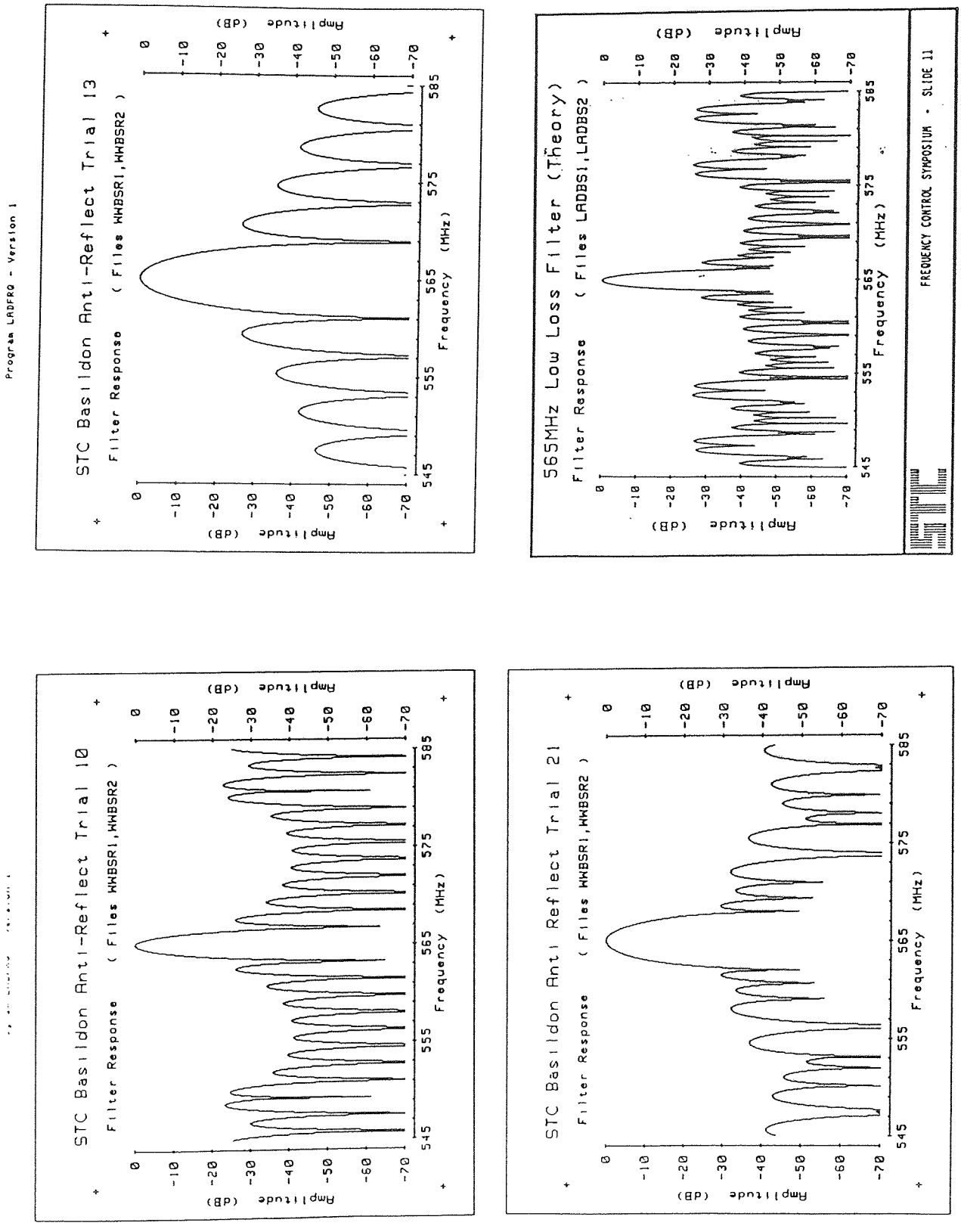

FIGURE 80 SPUDT Devices - Computed Responses

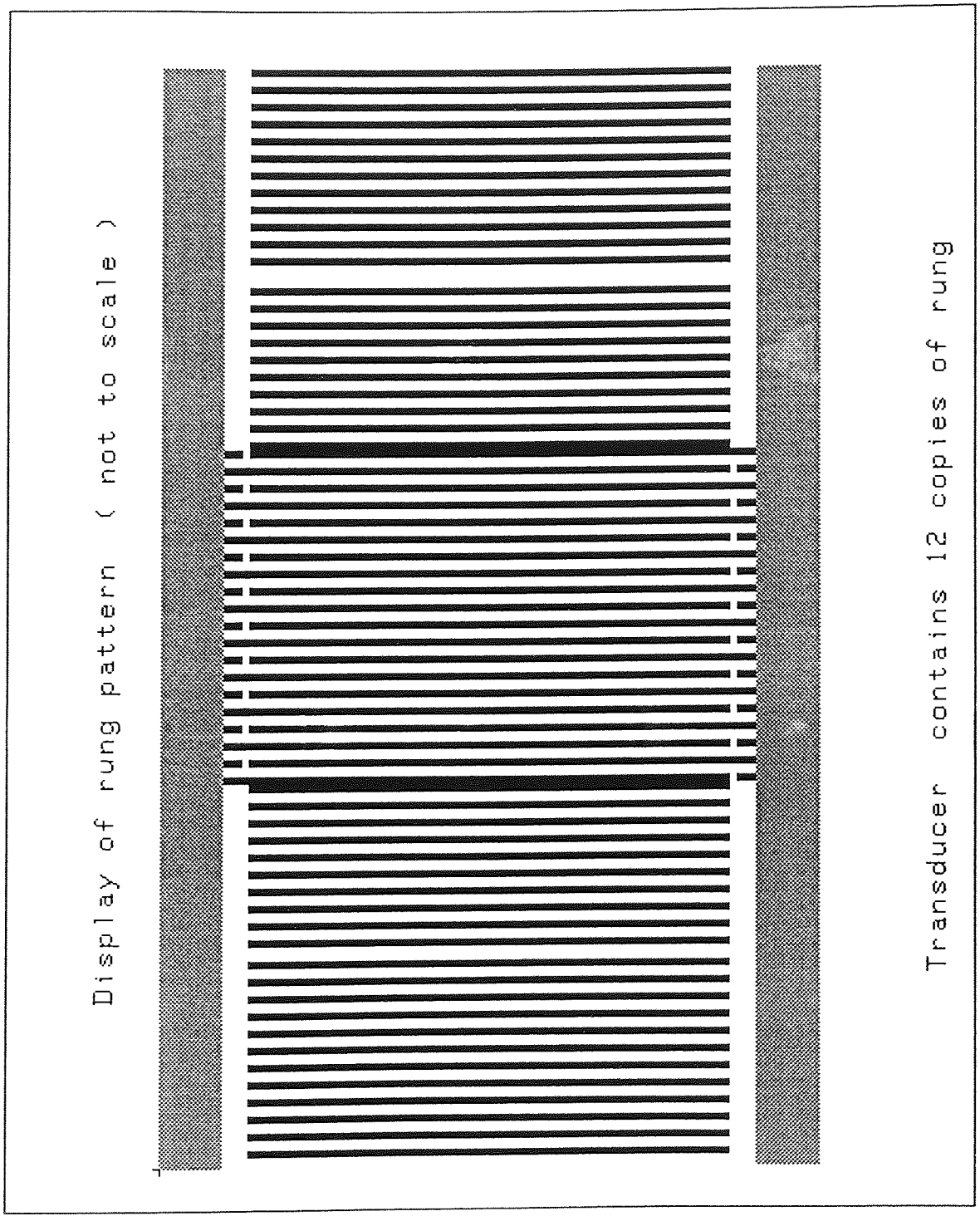

FIGURE 81 Transducer Detail for 565MHz PCM Filter

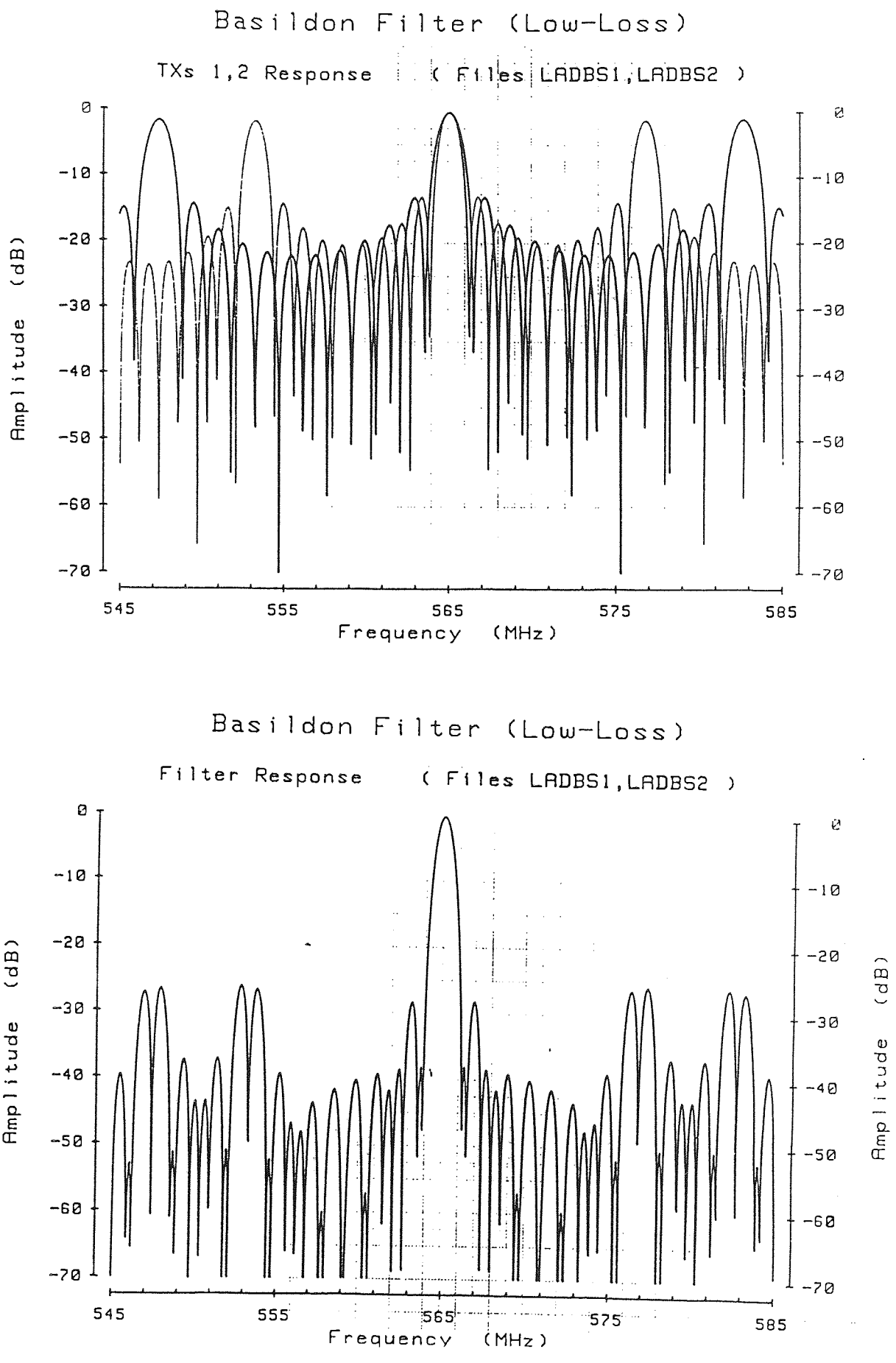

FIGURE 82 Interlacing of Individual Transducers

Trial No	Transducer 1 Rungs	F/Rung	RSep	Transducer 2 Rungs	F/Rung	RSep	BW (MHz)	SL (dB)
4	6	18	90	3	36	60	2.0	15
6	12	18	60	9	24	90	1.5	27
8	12	18	60	9	24	96	<1.0	<5
9	12	18	54	9	24	90	1.0	28
10	12	18	54	9	24	72	1.0	26
13	8	36	36	6	48	48	3.5	27
21	10	18	38	10	12	26	2.2	30
Layout for Test	12	20	52	10	30	78	1.1	25

Notes:

F/Rung - Fingers per rung
RSep - Rung-to-rung seperation
BW - 3dB bandwidth
SL - Level of first major sidelobe

TABLE 33 Computer Predictions - Low-loss SPUDT Filters.

39°-quartz with a metal film thickness of 850A.

Tables 34 and 35 give typical sets of results from this mask for both low-loss and conventional devices in a 50ohm test jig. Whilst this is the normal operating mode for the conventional device, the low-loss devices require matching into a 50ohm line for minimum loss. Figure 83 gives the response of the conventional device and Figure 84 the low-loss device in a matched configuration. The matching network comprised a series capacitor and shunt inductor on each port.

The main features of the low-loss device of Figure 84 are:

Centre frequency	565MHz
Insertion loss	5.5dB
Bandwidth	1.1MHz
Q-value	514
Sidelobe rejection	>20dB
Phase linearity	<10° pk-pk

A small-scale production test was undertaken to produce ten low-loss filters. All were measured with the same matching component values. The resultant passband responses are shown in Figures 85 to 87. For the first device the close-in stopband is also shown.

A second low-loss design, the Maximally Distributed SPUDT, was fabricated. In this filter the structure was as follows:

	Transducer 1	Transducer 2
Rungs/transducer	25	23
Fingers/rung	4	4
Blooming reflectors/rung	4	4
Low loss reflectors/rung	4	4
Total no. of fingers	300	276

The resultant responses for this device in a matched configuration, manufactured on 39°-quartz with a metal film thickness of 1000Å, are shown in Figure 88. The main features are:

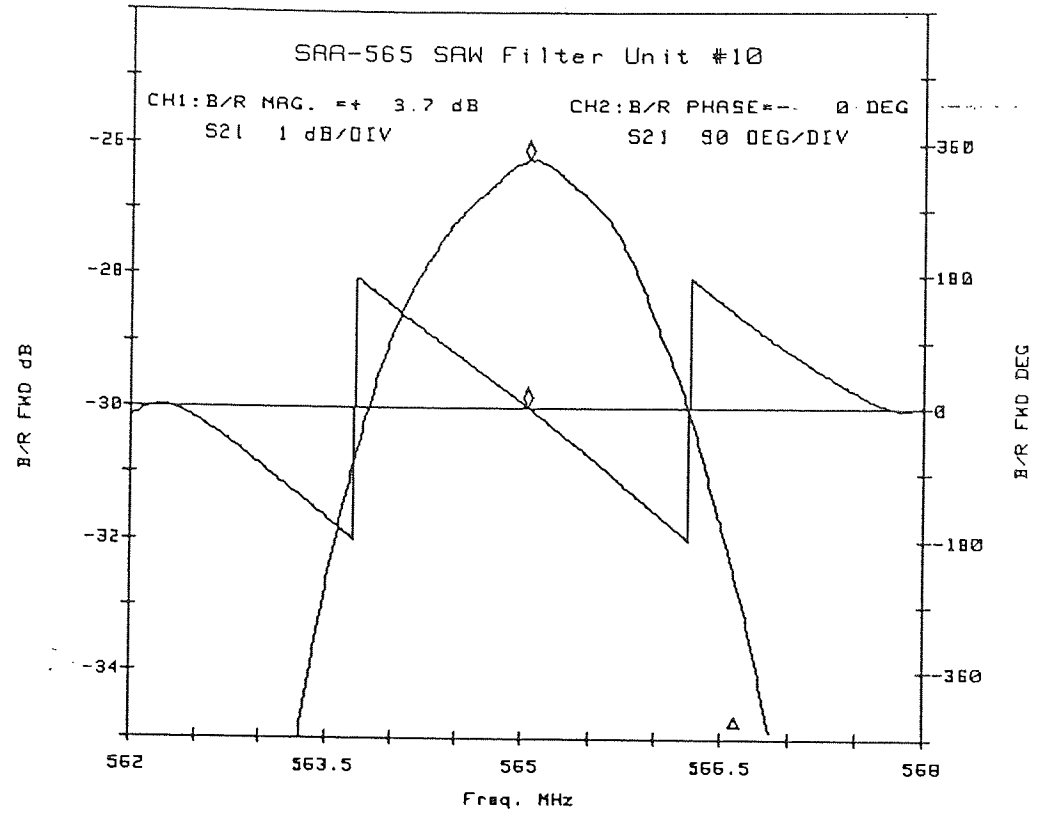

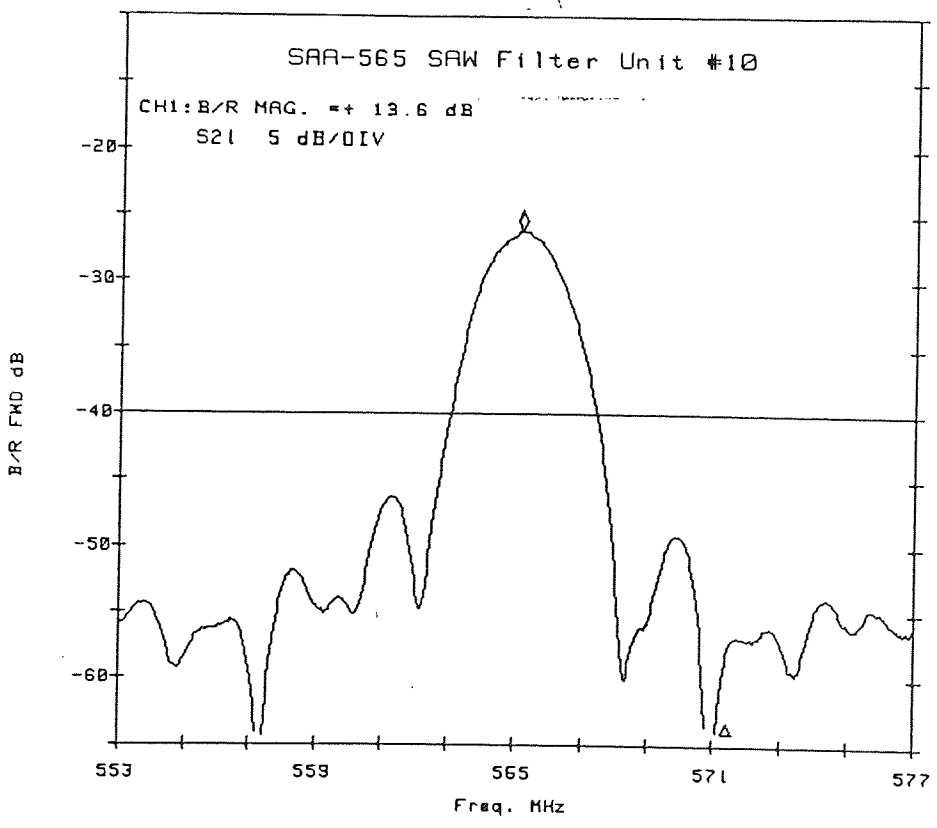

FIGURE 83 Frequency Response - 565MHz Filter with Uniform Transducers

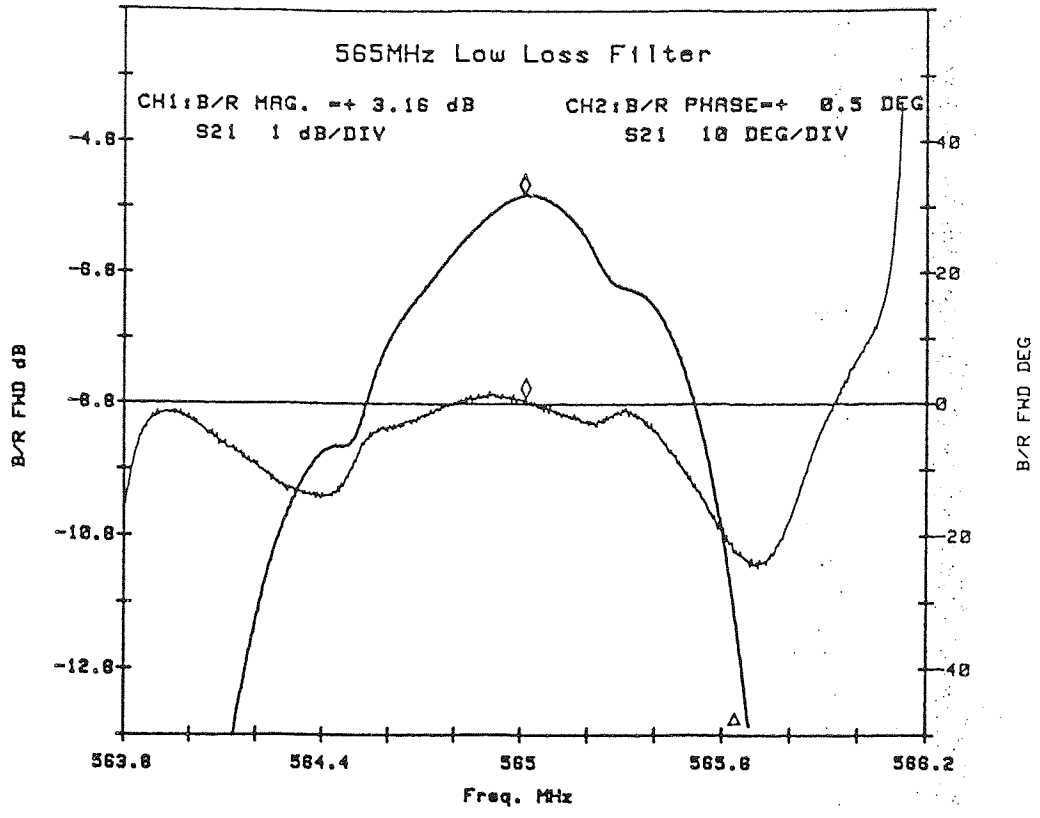

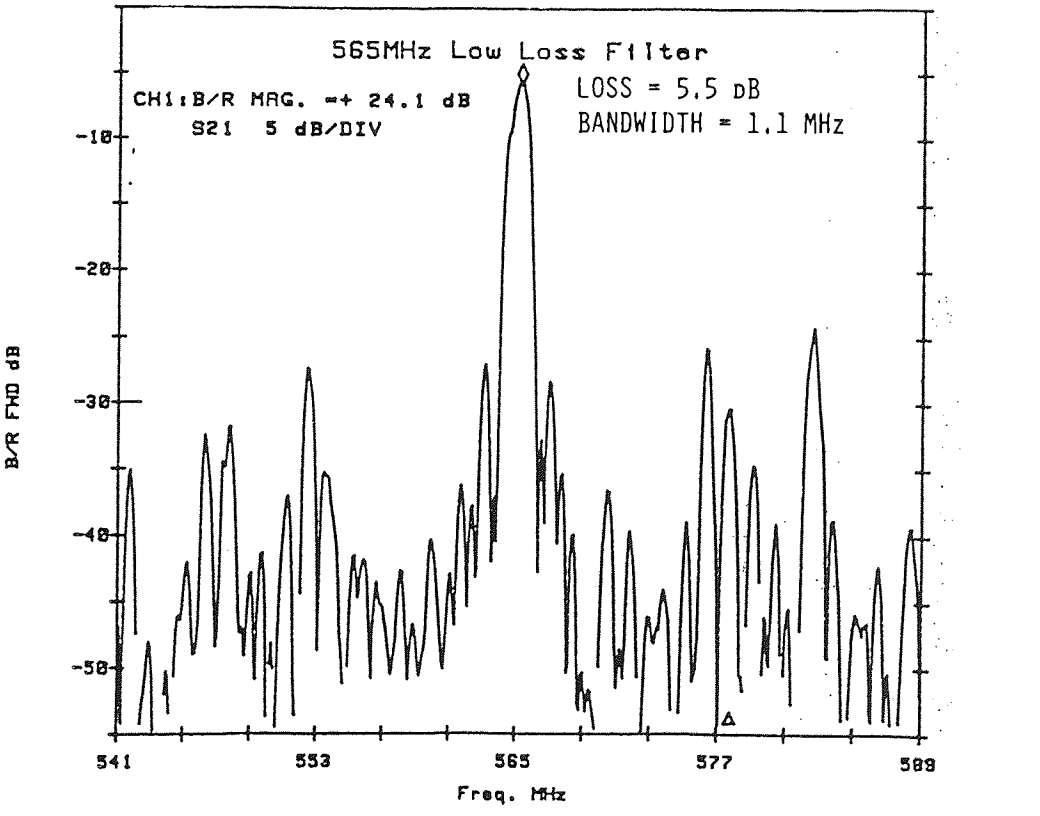

FIGURE 84 Frequency Response - Low-Loss 565MHz Filter

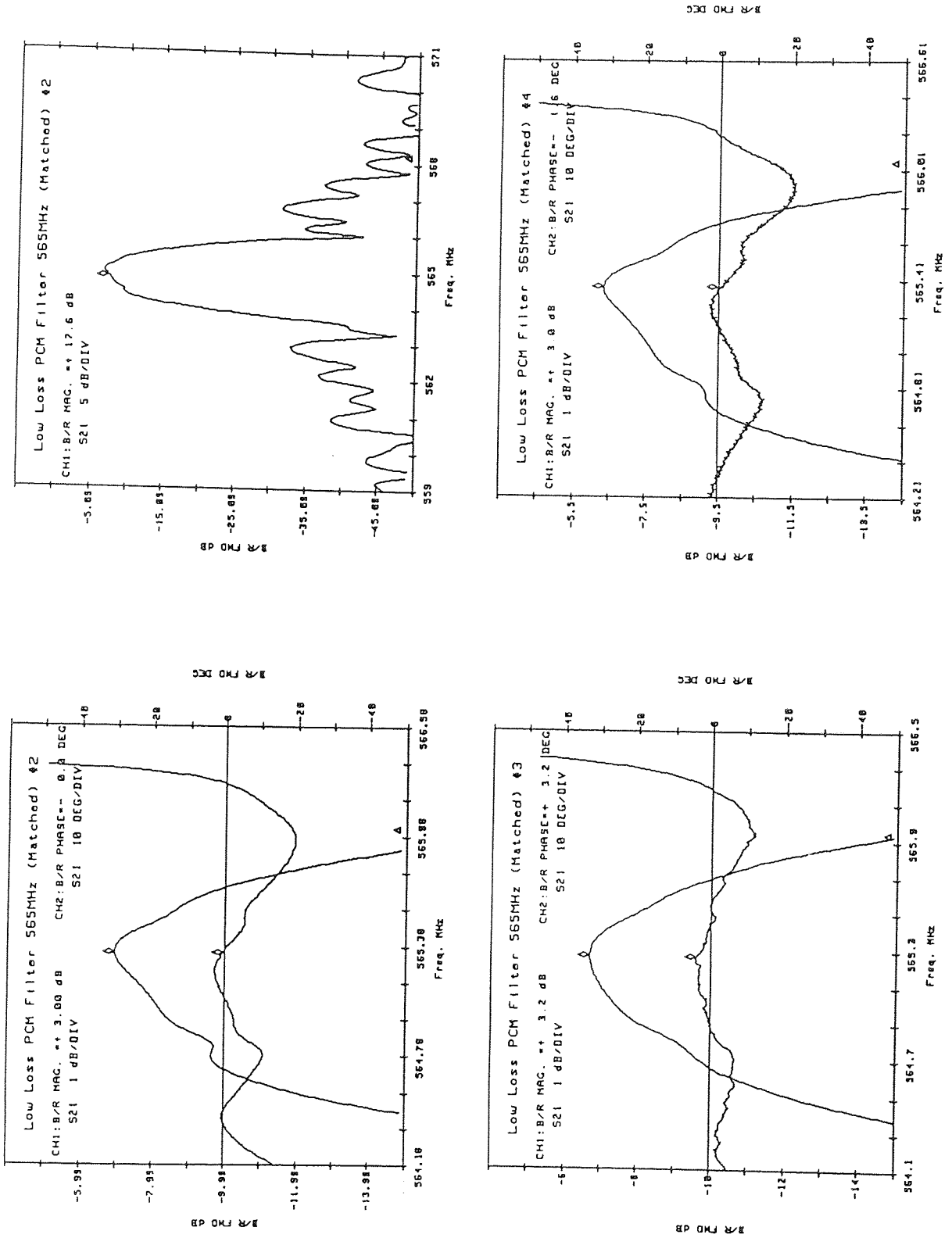

FIGURE 85 Frequency Responses - Production Units

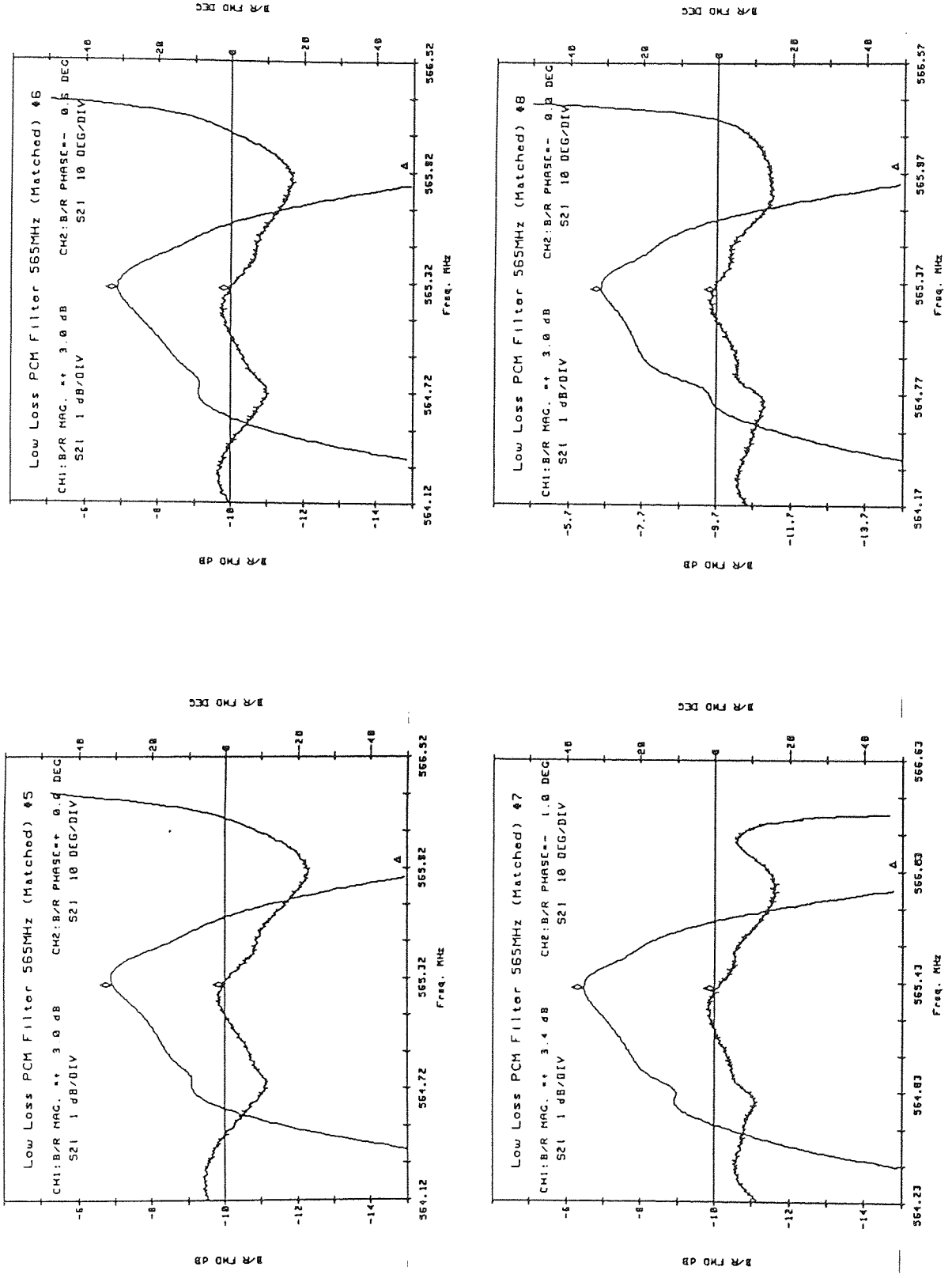

FIGURE 86 Frequency Responses - Production Units

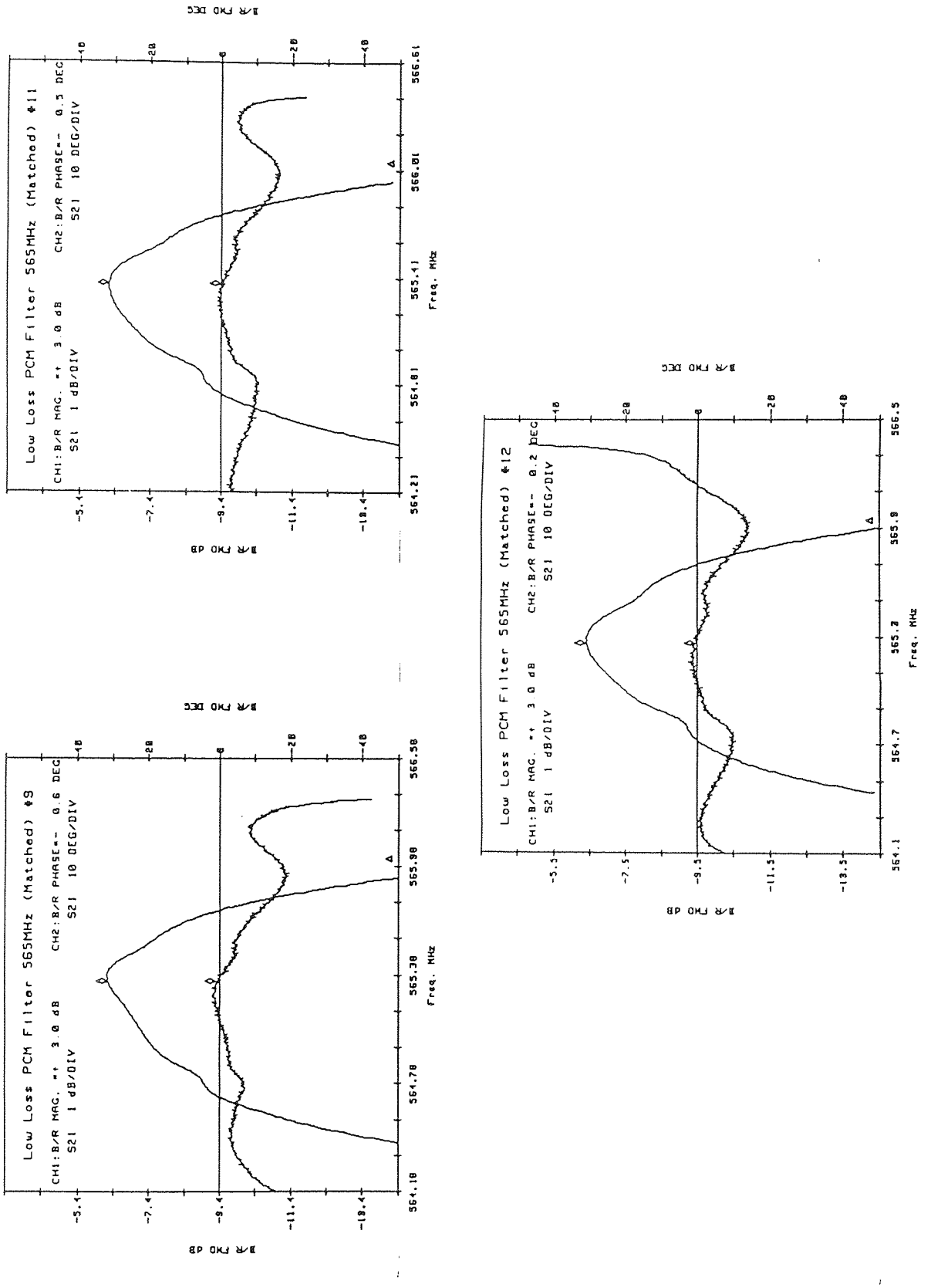

FIGURE 87 Frequency Responses - Production Units

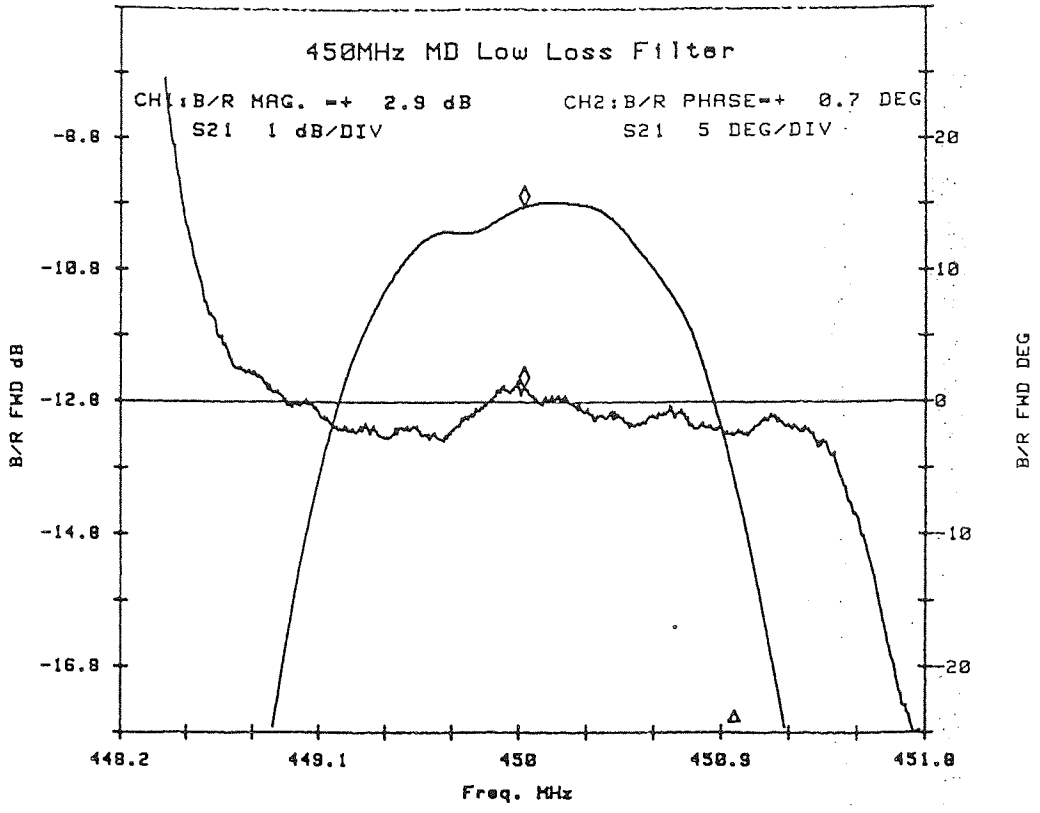

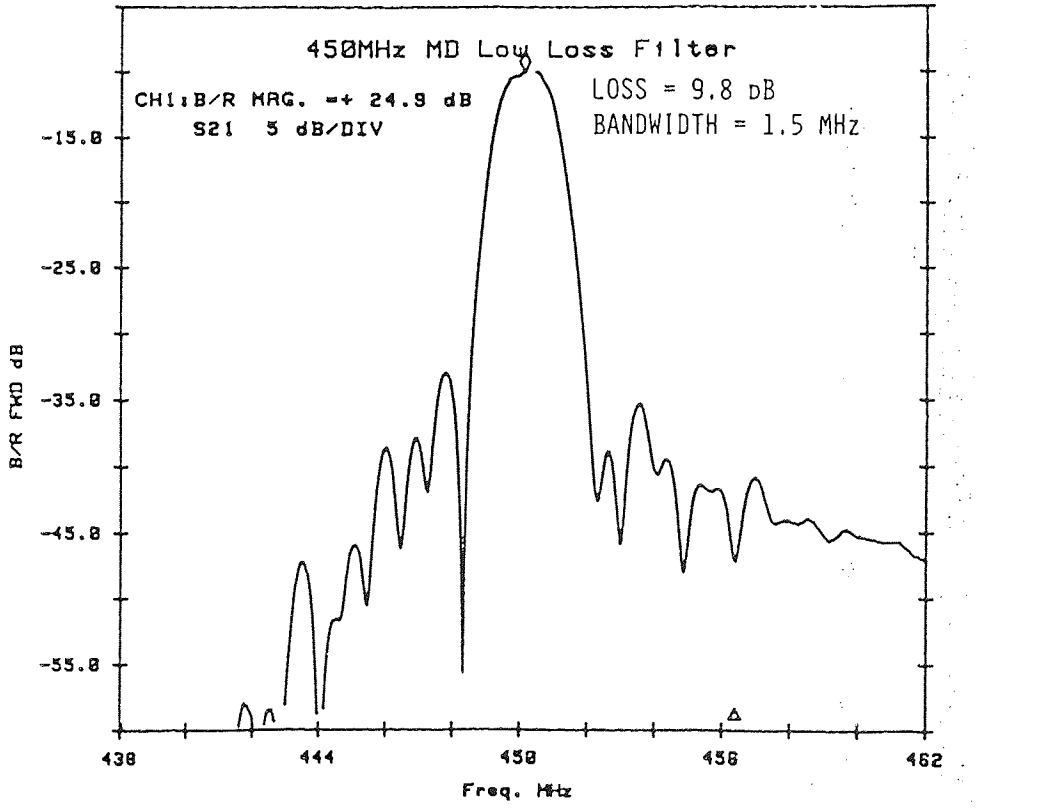

FIGURE 88 Maximally Distributed SPUDT - 426MHz Filter

Unit	Insertion Loss (dB)	Centre Frequency (MHz)	Sidelobe (dB)
1	16.0	565.10	35
2	17.2	565.25	32
3	17.0	565.25	32
4	15.6	565.24	33
5	17.5	565.13	33
6	18.8	565.14	30
7	16.3	565.22	33
8	17.3	565.22	32
9	16.6	565.21	32
10	20.0	565.21	31
11	16.6	565.26	33
12	16.6	565.22	33

Notes:

All measurements were made with an Anritsu Spectrum Analyser with Tracking Generator.

Measurements were made in a standard test fixture, in a 50ohm system.

Individual bandwidth readings were not taken. All devices had a 3dB bandwidth of approximately 1.1MHz.

Device numbers refer to STC in-house batch ref. BR117.

TABLE 34 Low-loss SPUDT 565MHz Filters - Un-matched.

Unit	Insertion Loss (dB)	Centre Frequency (MHz)	Sidelobe (dB)
1	25.3	564.97	21
2	25.4	565.05	20
3	25.5	564.94	20
4	25.8	564.99	21
6	25.7	565.14	19
7	25.7	565.07	19
8	25.7	564.97	21
9	25.5	565.02	19
10	25.6	565.00	20
11	25.6	565.02	20
12	26.0	564.87	20
13	26.2	565.03	20

Notes:

All measurements were made with an H-P 8505A Network Analyser with Tracking Generator.

Measurements were made in a standard test fixture, in a 50ohm system.

Individual bandwidth readings are not recorded here. All devices had a 3dB bandwidth of approximately 2.0MHz.

Device numbers refer to STC in-house batch ref. BR79.

TABLE 35 Conventional 565MHz Filters - Un-matched.

Centre frequency	450MHz
Insertion loss	9.8dB
Bandwidth	1.5MHz
Q-value	300
Sidelobe rejection	>25dB
Phase linearity	<5° pk-pk

5.3.3 Discussion.

Table 33 and the plots of Figures 79 and 80 show the manner in which the structure of the two low-loss transducers influences the device response. With relatively few rungs per transducer, as in Trials 4 and 13, the bandwidth of the main response increases. There are also fewer sidelobes, although in Trial 4 the close-in sidelobe is only 15dB below the main response. In Trial 13 the number of fingers per rung and rung-to-rung spacing are equal. This structure is a basic uniform transducer, as indicated by the expected sinx/x response of the corresponding plot.

Trials 6 and 8 clearly illustrate the problem of interlacing the individual transducer responses to maximum effect. The device structures are almost identical except for a slightly larger rung separation in the second transducer of Trial 8. However, the resulting responses show vastly different sidelobe attenuations. This is due entirely to more effective interlacing of the transducer responses in Trial 6. These two trials also show that the bandwidth increases as the rung separation decreases.

The plots of Figures 79 and 80 give the frequency response over a 40MHz band centred at the reference frequency. Where similar responses resulted, as in the case of Trials 9 and 10, it was necessary to look at the degree of interlacing further out from the main response. The result for trial 21 gave an excellent sidelobe rejection together with a wide bandwidth. However, the rung separation was relatively small and there was insufficient space for a substantial number of low-loss reflectors.

These trials indicated that it was not possible to maintain the Lewis[36] proportions of active fingers to reflectors and at the same time generate the desired bandwidth. It was on this basis that the final layout for

the 565MHz test device as described in Section 5.3.2 was chosen.

In both transducers the number of low-loss reflectors to blooming reflectors to active fingers was 2.4:2:2 compared with 3.2:2:2 for the Lewis device. This compromise was necessary to achieve the 1.1MHz bandwidth. A secondary issue was the need to keep the device relatively short such that it could be mounted in a standard TO8 package. The predicted response for this structure, shown in the final plot of Figure 80, has a close-in sidelobe 30dB below the main response and other sidelobes better than 25dB down. The responses of the individual transducers, illustrating the interlacing, are shown in Figure 82.

The photomask produced for this low-loss filter also included a conventional device as decribed in Section 5.3.2. It is worth noting that several photomasks were supplied from the mask-maker, on which only the low-loss structure was correctly defined. This was due to difficulties experienced in writing the fine-lines of the conventional structure. As the layout of Figure 81 shows, even though the low-loss structure requires the low-loss reflectors to be moved by one-eighth wavelength relative to the other fingers, the minimum line or space dimension is one-quarter wavelength. This is a significant manufacturing and processing advantage.

Table 34 gives typical results for a batch of low-loss devices. These were measured in a 50ohm jig. For direct comparison, Table 35 gives results for conventional devices. In terms of frequency and sidelobe levels both sets of results indicate consistency of manufacture. The low-loss devices have a greater spread of insertion loss. However, these results are for unmatched devices. The low-loss filters require matching for minimum loss which tends to reduce the range of insertion loss values.

The passband and close-in stopband responses for the conventional device are shown in Figure 83. These clearly show the ripple-free passband and linear phase. The first sidelobe is approximately 20dB below the main response. The insertion loss level of 25dB is typical for this type of uniform transducer device.

Figure 84 shows similar responses for a low-loss filter matched for minimum loss. The level of ripple in the

passband was typical for devices tested. The plot also indicates a phase ripple of +/-5° which is similar to that for conventional filters. The insertion loss, at 5.5dB, and the sidelobe levels, at 25dB down, represent substantial improvements over the conventional device.

The need to match low-loss filters to achieve a low insertion loss represents a considerable disadvantage. In testing of devices, the passband shape was found to be critically influenced by the matching network. Also, when matched, other factors, such as precise location in the test jig were found to influence device performance. Whilst it was possible to match a single device to virtually eliminate the passband ripple (Figure 89), the matching needed individual adjustment for other devices.

A small-scale production test was performed to provide devices for testing in real systems. This also gave the opportunity to measure the passband ripple for a batch of devices in the same matched test jig. Ten devices were fabricated and the passband plots are shown in Figures 85, 86 and 87. The plots show a significant variation in the level of passband ripple with insertion loss levels ranging from 6.0 to 7.0dB. As expected, there is also variation in the levels of phase ripple. In this test, the objective was to find a matching network that would provide optimum results for all devices. As a result, the devices have a higher loss than the minimum value of Figure 89.

Following the supply of these devices to a telecommunication system supplier, several comments were received. It was found that all devices met the basic requirements of PCM retiming filters. The level of passband ripple could be reduced to acceptable levels by individual matching. However, considerable reservations were expressed regarding the close tolerances required in matching and, consequently, possible changes in passband shape due to ageing of both the SAW device and matching components. The devices have been retained for further investigation.

The maximally distributed SPUDT (MD-SPUDT) described in Section 5.3.2 has a large number of small rungs in each transducer with a much reduced rung separation. The objective in the design of this structure was to produce a wider bandwidth device at the expense of very low insertion loss. Figure 88 contains the passband and

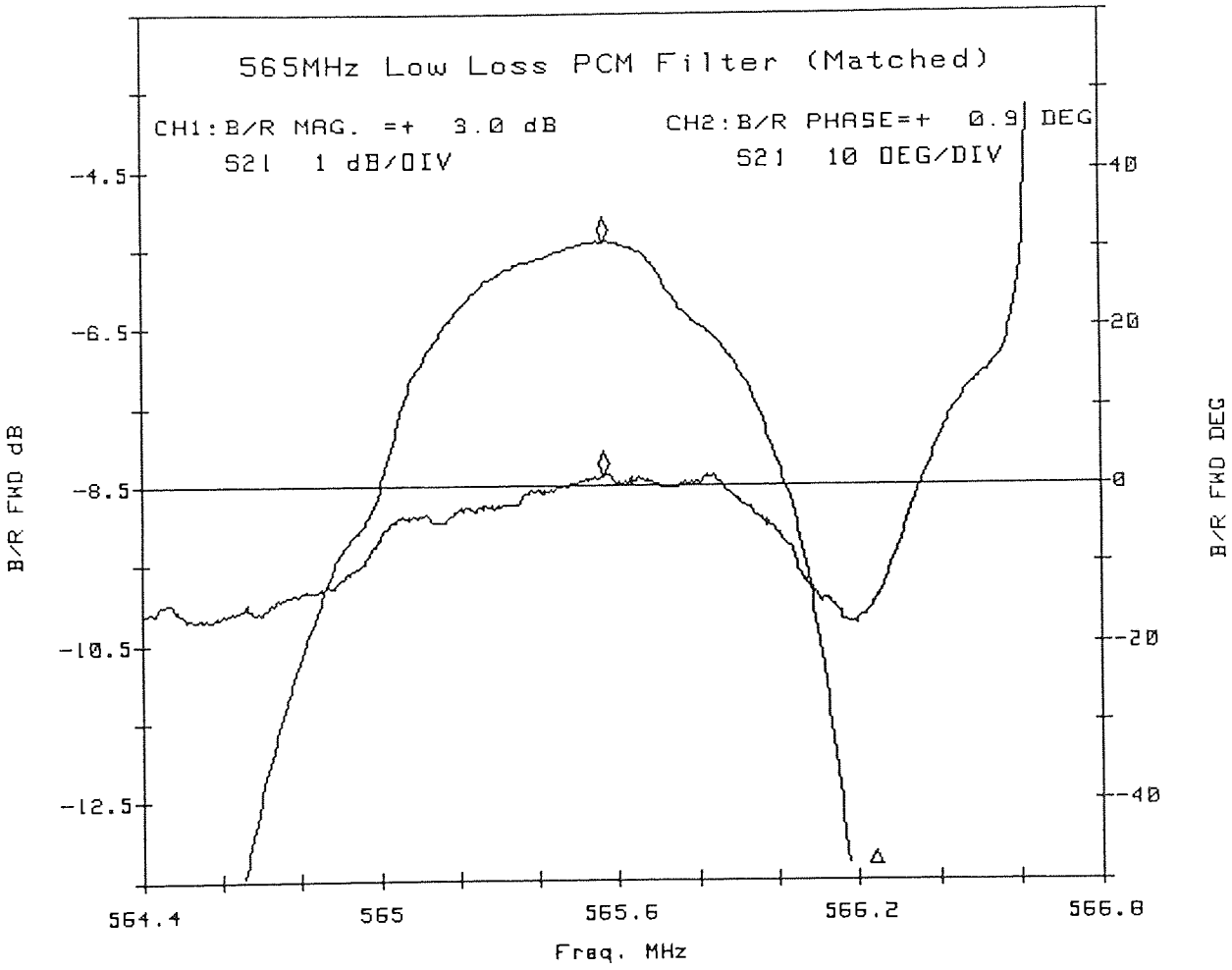

FIGURE 89 Low-Loss 565MHz Filter with Minimum Ripple

close-in stopband plots for the MD-SPUDT. In this matched configuration the insertion loss is 9.8dB with a 3dB bandwidth of 1.5MHz. The Q-value of 300 is much lower than the 514 figure for the PCM low-loss filter. The passband ripple and phase ripple also show a substantial improvement over the PCM filter. The level of ripple was found to be more tolerant of the matching network values. Although the insertion loss value is inferior to the 5.5dB of the PCM filter, it compares favourably with typical values of 15dB for conventional delay lines at 450MHz.

The MD-SPUDT design exhibits good sidelobe rejection. Figure 88 shows the close-in sidelobes at approximately 25dB below the main response. An advantage of this design is that the rung repeat sections of both transducers are the same except for the offset of the low-loss reflectors. The level of interlacing to achieve maximum sidelobe rejection is simply a function of the number of rungs in each transducer.

The MD-SPUDT indicates that a compromise or trade-off situation exists with the Lewis[36] low-loss filter. Very low losses can be achieved, but with a problem of repeatability in the production environment. Reducing the rung spacing of the transducer, as in the MD-SPUDT, eases the matching requirements but degrades the insertion loss level as there are also fewer low-loss reflectors. A version of the MD-SPUDT, with its low passband ripple, excellent phase linearity and good sidelobe rejection, designed to operate at 565MHz, would offer substantial advantages over conventional PCM filters. In addition to these electrical performance advantages, the SPUDT is relatively simple to design and is suitable for manufacture up to frequencies as high as 1.2GHz using existing processing equipment.

5.3.4 Recommendations for further work.

The modelling of the two SPUDT devices presented here was limited to prediction of the shape of the frequency response and evaluation of the bandwidth. No attempt was made to model the insertion loss. It is likely that commercial devices will be designed to meet a specified matched insertion loss. Modelling will need to predict insertion loss together with estimates of passband ripple. Recently, Campbell and Saw[52] have reported a

design and analysis routine for this type of SPUDT device based upon a coupling-of-modes theory. Campbell and Saw support the claim made in Chapter 3 of this report, namely that the Lewis device is the most versatile of the published SPUDT structures. The analysis methods of Campbell and Saw require investigation and, if appropriate, implementation.

Further discussions are necessary between SAW device designers and PCM systems designers to establish the trade-offs between insertion loss, bandwidth and passband ripple. The MD-SPUDT version requires further development and re-scaling to offer improvements over conventional filters at PCM transmission frequencies.

6. CONCLUSIONS.

6.1 Review of Objectives.

This project has taken place in a commercial manufacturing environment. The overall objectives were set out at the end of Chapter 1, namely

> To develop a design and manufacturing capability to produce high frequency SAW devices with improved insertion loss levels and improved temperature performance.

These objectives were influenced by the nature of STC's business environment, that is, professional communications and telecommunications, and by the available production facilities. The market review of Section 1.3.4 identified future trends in SAW devices and highlighted those areas that met STC's business requirements. The specific targets for this project were the production of a low-loss high frequency filter for PCM retiming applications and improved front-end narrowband filters for professional communications systems.

The processing review of Chapter 2 and the technical review of Chapter 3 identified several inter-related areas in need of development:

> Greater advantage could be taken of the in-house quartz growing and finishing facility. Almost all devices used the same substrate orientation, ST-X. By categorizing a range of cuts close to this common cut an extra dimension could be added to the design routine. Although quartz cuts in the AT to ST range have similar temperature coefficients, they have different inversion points and, therefore, offer advantages of flexibility to the system designer.
>
> Several new quartz cuts had recently been identified. The published reports suggested that these cuts offered much improved temperature coefficients and higher acoustic wave velocities. No previous attempt, at STC, had been made to manufacture devices on these

new cuts or to investigate the performance claims and identify potential disadvantages.

STC manufactured conventional SAW filters with the associated high insertion loss levels. The market was demanding high frequency devices with reduced insertion loss. STC's involvement with quartz precluded serious work on wide bandwidth devices which require other substrate material. Therefore, a need existed to develop low-loss narrow bandwidth filters for both telecommunications and professional radio applications.

6.2 Achievements.

All these achievements share the aim of improving the maunfacturing capability of the company.

6.2.1 Quartz Material.

The temperature performance of a range of quartz orientations between the AT and ST-cut has been measured using a 295.6MHz PCM filter as the test vehicle. The results have shown that the choice of orientation does not significantly alter the device frequency response. An inversion temperature range of 60°C has been demonstrated.

With the three relationships generated (Section 4.2.2, pages 97-99) it is possible to design a device to a pre-determined inversion temperature. In some cases this is not necessarily at the centre of the temperature band. The technical review has described the use of the SAW device temperature characteristic to offset external circuit effects.

The three relationships also allow minor photomask errors to be corrected without the need for a new photomask. In the same way, it is possible to produce devices from an existing photomask, but at a different inversion temperature. The resulting frequency change can then be corrected by rotation of the SAW pattern during photolithography. In this way, a change in customer specification can be met in a short time and at minimal cost.
The results reported on AT-ST quartz have been adopted by

the company and are now used as part of a computer-based design routine to optimise cut angle, turnover temperature and metal film thickness.

Three recently identified, quartz orientations have been investigated, SST, X33 and LST. In view of the claimed performance of a range of cuts very close to LST, three LST orientations have been investigated, making five new cuts in total. These cuts were used as the basis for both filters and resonators. At an early stage the X33-cut was discounted as its performance offered no improvement over the ST-cut, in contradiction to published results. It is believed that the wrong cut of material had been supplied.

The SST and LST-cuts offer a higher acoustic wave velocity than ST-quartz (Section 4.3.3) and would be useful for high frequency devices. The increases are 15% and 25% for SST and LST respectively. The frequency responses of resonators on these cuts were found to suffer from high secondary peaks and Q-values lower than the ST-cut.

The LST-cuts have excellent temperature performance with a temperature coefficient approximately five times better than the ST-cut. The LST75-cut was found to offer reasonable resonator performance.

All resonator trials of these new quartz cuts included two transducer options, single and split-finger. On ST and AT-quartz the transducer format had very little effect on the frequency response. On both SST and LST-cuts the split-finger devices had a superior insertion loss. Split-finger LST devices also had a higher centre frequency and lower Q-value. These effects have been documented and, it is believed, they have not been reported elsewhere.

Another phenomenon noted on LST-quartz resonators was the variation of insertion loss level with temperature (Section 4.3.3). This has not been reported elsewhere and represents a serious disadvantage associated with these new cuts. This phenomenon has since been reported by the author (Bower and Oliver[53]), see Appendix 1.

SAW filters have been manufactured on SST and LST-cuts with good results. The results clearly demonstrated the advantage of higher acoustic velocities. For example, a

standard 442MHz photomask, designed for AT-quartz, yielded LST devices at 554MHz.

The three LST-cuts investigated were at orientations differing in total by one degree. During the quartz processing stage some difficulty was experienced in alignment of the crystallographic axis due to weak x-ray reflections. This alignment problem, together with large performance variations for only small rotational changes, may preclude the use of LST-quartz in a production evnvironment. Conversely, with suitable control of alignment, the performance dependence on cut angle could add an extra dimension to device design.

Of all the cuts investigated, the LST75-cut requires further investigation.

6.2.2 Low-loss Devices.

Coupled resonator filters using transducer coupling have been demonstrated atfrequencies from 400 to 500MHz (Section 5.2.2). Insertion loss levels as low as 3.0dB have been consistently achieved in a production environment. Devices have exhibited a 1.0dB bandwidth of 200kHz over a wide temperature band of -40 to +85°C.

The necessity of reducing passband ripple has been demonstrated and a simple mirror adjustment technique developed. This technique, which involves a manual adjustment, requires further refinement for large-scale processing.

The need to achieve a wide bandwidth to allow for temperature induced frequency shift has been described. This adds to the difficulty of eliminating the passband ripple. The problem of maintaining bandwidth in terms of offset has been discussed (Section 5.2.3). The limitations imposed by the mask-maker may influence production yield at high frequencies.

Devices have been made on LST75-quartz in an attempt to reduce the temperature effects. However, the use of this quartz was again precluded by the variation of insertion loss with temperature.

A simple solution to the problem of reversing the phase of one output port has been demonstrated (Section 5.2.3).

This simplified the manufacturing complexity and improved the stopband level.

Coupled resonator filters have been demonstrated as a solution to the requirement for narrow-band filters suitable for front-end RF applications. At high frequencies and wide bandwidths the problem of manufacturing yield must be addressed.

The single-phase unidirectional transducer has been developed further and a device demonstrated at 565MHz (Section 5.3.3). An insertion loss level as low as 5.5dB has been recorded with a 3dB bandwidth of 1.1MHz. This device is suitable for use in PCM transmission systems and offers a 20dB insertion loss improvement over conventional devices. These results have been published by the author (Oliver et al[54]) as shown in Appendix 2. It is believed that this is the first low-loss filter reported specifically for PCM retiming applications. The device has the advantage of using quarter-wavelength fingers and is relatively easy to manufacture at frequencies up to 1GHz.

The analysis for this structure was based upon a modified impulse response model designed for ladder structures. Good agreement has been shown between the predicted and actual responses in terms of the shape of the response and the resulting bandwidth. The need to interlace the two transducer responses to maximise the level of sidelobe rejection has been described.

The dependence of the level of passband ripple on the matching configuration has been discussed. Although any one device can be matched to eliminate almost all ripple, the matching requires individual adjustment for each device. This need for critical matching may be a disadvantage in high-reliabilty long-life systems where component ageing may adversely change the device performance.

A maximally distributed (MD) SPUDT filter has been demonstrated (Section 5.3.3) at 450MHz with a matched insertion loss of 9.8dB and bandwidth of 1.5MHz. This structure contains the minimum number of reflectors and active fingers per transducer rung. As the rung repeat sections of both transducers are identical, interlacing is simply a function of the number of rungs.

The MD-SPUDT, although incurring an insertion loss penalty, offers very low passband ripple and good sidelobe rejection. The insertion loss is considerably better than conventional filters at the same frequency. In view of its low ripple, relatively low insertion loss, good sidelobe rejection and ease of design and manufacture, the MD-SPUDT has considerable potential as a low-loss filter.

6.3 Summary.

A search for new techniques to give SAW devices with improved temperature performance and lower insertion loss at high frequencies has been reported. No one technique answers all requirements and therefore this work has addressed several related issues. The issues are related through the need for ease of design and manufacture.

From the viewpoint of STC, the major results are the capability to design and manufacture low-loss filters by two distinct methods and a greater flexibilty in the application of in-house quartz.

7. REFERENCES.

[1] Cochrane, A.J. "Vocational PhD's : Aston's IHD Scheme." Aston University, Birmingham, 1981.

[2] van Rest, D. J. "The Principles and Practice of IHD Research." Aston University, Birmingham, 1981. (also appendix in [1]).

[3] STC plc. "Annual Report 1985." STC plc, London, April 1986.

[4] Young, P. "Power of Speech : A History of Standard Telephones and Cables Ltd 1883-1983". George Allen and Unwin, London, 1983.

[5] STC plc. "Quartz Crystal - A Total Capability." STC Components Ltd., Harlow, UK, February 1985.

[6] Brice, J C. "Crystals for Quartz Resonators." Reviews of Modern Physics, Vol. 57, No. 1, New York, January 1985, pp105-146.

[7] Holmyard, E. J. "A Higher School Inorganic Chemistry." J. M. Dent and Sons Ltd., London, 1952.

[8] ITT Corporation. "ITT Synthetic Quartz." ITT Components Group Europe, Harlow, UK, 1976.

[9] Croven Crystals. "Croven Crystals." Kidde Canada Ltd., Ontario, 1983.

[10] Morgan, D. P. "Surface Wave Devices for Signal Processing." Elsevier Science Publishers B.V., Amsterdam, 1985.

[11] Lord Rayleigh. "On Waves Propagated Along the Plane Surface of an Elastic Solid." Proc. London Mathematical Society, Vol. 17, No. 4, London, 1885.

[12] Matthews, H. (ed.) "Surface Wave Filters : Design, Construction and Use." John Wiley and Son, New York, 1977.

[13] White, R. M., Voltmer, F. W. "Direct Piezoelectric Coupling to Surface Elastic Waves." Applied

Physics Letters, Vol. 7, New York, December 1965.

[14] Lewis, M. F., West, C. L., Deacon, J. M., Humphryes, R. F. "Recent Developments in SAW Devices." Proc. IEE, Vol. 131, Part A, No. 4, London, June 1984, pp186-215.

[15] Hartmann, C. S. "Future High Volume Applications of SAW Devices." Proc. 1985 Ultrasonics Symposium, IEEE, New York, pp64-73.

[16] Murray, R. J., White, P. D. "SAW Components Answer Today's Signal Processing Needs." Electronics, Vol. 54, No. 18, London, September 1981, pp120-124.

[17] White, R. M. "Surface Acoustic Wave Sensors." Proc. 1985 Ultrasonics Symposium, IEEE, New York, pp490-494

[18] Coldren, L. A., Rosenberg, R. L. "Surface Acoustic Wave Resonator Filters." Proc. IEEE, Vol. 67, No. 1, New York, January 1979, pp147-158.

[19] Rosenberg, R.L., Ross, D. G., Trischitta, P. R., Fishman, D. A., Armitage, C. D. "Optical Fibre Repeatered Transmission Systems Utilising SAW Filters." Proc. 1982 Ultrasonics Symposium, IEEE, New York, pp238-246.

[20] Minowa, J., Nakagawa, K., Okuno, K., Kobayashi, Y., Morimoto, M. "400MHz SAW Timing Filter for Optical Fibre Transmission Systems." Proc. 1978 Ultrasonics Symposium, IEEE, New York, pp490-493.

[21] Walton, J. P. "Perspective on Clean Room Design." European Semiconductor Design and Production, Vol 8, No 2, March/April 1987, London, pp21-29.

[22] Tanski, W. J. "The Influence of a Chrome Film Bonding Layer on SAW Resonator Performance." Proc. 1985 Ultrasonics Symposium, IEEE, New York, pp253-257.

[23] Dawson, P. A. "Measurement of the Ageing of Surface Acoustic Wave Filters for Submerged Cable Systems." British Telecom Technology Journal, Vol 5, No 3, July 1987, London. pp49-53.

[24] Rosenberg, R. L. and Coldren, L. A. "Scattering Analysis and Design of SAW Resonator Filters." IEEE Trans. Sonics and Ultrasonics, Vol SU-26, No 3, May 1979, New York. pp205-230.

[25] Datta, S. "Surface Acoustic Wave Devices", Prentice-Hall, New Jersey, 1986.

[26] Marshall. F. G., Paige, E. G. S., Young, A. S. "New Unidirectional Transducer and Broadband Reflector of Acoustic Surface Waves." IEE Electronics Letters, Vol 7, No 21, 21st October 1971, London, pp638-640.

[27] Rosenfield, R. C., Brown, R. B., Hartmann, C. S. "Unidirectional Acoustic Wave Filters with 2dB Insertion Loss." Proc. 1974 Ultrasonics Symposium, IEEE, New York, pp425-428.

[28] Yamanouchi, K., Nyffeler, F. M., Shibayama, K. "Low Insertion Loss Acoustic Surface Wave Filter using Group-Type Unidirectional Interdigital Transducer." Proc. 1975 Ultrasonics Symposium, IEEE, New York, pp317-321.

[29] Hartmann, C. S., Wright, P. V., Kansy, R. J., Garber, E. M. "An Analysis of SAW IDT's with Internal Reflections and the Application to the Design of Single-Phase Unidirectional Transducers." Proc. 1982 Ultrasonics Symposium, IEEE, New York, pp40-45.

[30] Lewis, M. F. "SAW Filters Employing Interdigitated Interdigital Transducers." Proc. 1982 Ultrasonics Symposium, IEEE, New York, pp12-17.

[31] Yamanouchi, K., Furoyashiki, H. "New Low-loss Filter Using Internal Floating Electrode Type of Single-Phase Unidirectional Transducer." IEE Electronics Letters, Vol 20, No 24, 22 Nov 1984, London, pp989-990.

[32] Wright, P. V. "The Natural Single-Phase Unidirectional Transducer: A New Low-loss SAW

Transducer." Proc. 1985 Ultrasonics Symposium, IEEE, New York, pp58-63.

[33] Malocha, D. C., Hunsinger, B. J. "Tuning of Group-Type Unidirectional Transducers." IEEE Trans. Sonics and Ultrasonics, Vol SU-26, No 3, May 1979, New York, pp243-245.

[34] Gautam, J. K., Meguro, T., Yamanouchi, K. "Low-loss Unidirectional SAW Filters Using Integrated Microinductors." IEE Electronics Letters, Vol 19, No 20, 29 September 1983, IEE, London.

[35] Lewis, M. F. "Low-loss SAW Devices Employing Single Stage Fabrication." Proc. 1983 Ultrasonics Symposium, IEEE, New York, pp104-108.

[36] Lewis, M. F. "A Study of Group-Type Single Phase Unidirectional Transducers on $LiNbO_3$ and Quartz." RSRE Memorandum 3833, Royal Signals and Radar Establishment, Malvern, UK, 1985.

[37] Staples, E. J., Smythe, R. C. "SAW Resonators and Coupled Resonator Filters." Proc. 1976 Frequency Control Symposium, IEEE, New York, pp322-327.

[38] Shreve, W. R. "Surface Wave Resonators and Their Use in Narrowband Filters." Proc. 1976 Ultrasonics Symposium, IEEE, New York, pp706-713.

[39] Coldren, L. A., Rosenberg, R. L., Rentschler, J. A. "Monolithic Transversely Coupled SAW Resonator Filters." Proc. 1977 Ultrasonics Symposium, IEEE, New York, pp888-899.

[40] Cross, P. S., Schmidt, R. V. "Coupled Surface Acoustic Wave Resonators." The Bell System Technical Journal, Vol 56, No 8, October 1977, AT&T Co., New Jersey, pp1446-1482.

[41] Coldren, L. A., Rosenberg, R. L. "Multipole SAW Resonator Filters." Proc. Int. Symposium on Circuits and Systems, 1978, IEEE, New York, pp548-552.

[42] Bebois, J. "The Problem of the Accuracy of Fabrication of Multipole SAW Resonator Filters."

Proc. 1979 Ultrasonics Symposium, IEEE, New York, pp841-844.

[43] Meyer, P. C., Gunes, D. "Design and Fabrication of SAW Multipole Filters." Proc 1983 Ultrasonics Symposium, IEEE, New York, pp66-71.

[44] Lewis, M. F. "Temperature Compensation Techniques for SAW Devices." Proc. 1979 Ultrasonics Symposium, IEEE, New York, pp612-622.

[45] Newton, C. O. "A Study of the Propagation Characteristics of the Complete Set of SAW Paths on Quartz with Zero Temperature Coefficient of Delay." Proc. 1979 Ultrasonics Symposium, IEEE, New York, pp632-636.

[46] Williams, D. F., Cho, F. Y., Sanchez, J. J. "Temperature Stable SAW Devices Using Doubly Rotated Cuts of Quartz." Proc. 1980 Ultrasonics Symposium, IEEE, New York, pp429-433.

[47] Lukaszek, T., Ballato, A. "What SAW Can Learn From BAW: Implications for Future Frequency Control, Selection and Signal Processing." Proc. 1980 Ultrasonics Symposium, IEEE, New York, pp173-183.

[48] Webster, R. T. "X-Cut Quartz for Improved Surface Acoustic Wave Temperature Stability." J. Applied Physics, Vol 56, No 5, 1 Sept 1984, pp1540-1542.

[49] Shimizu, Y., Tanaka, M. "New Cut of Quartz for SAW Devices with Extremely Small Temperature Coefficient." IEE Electronic Letters, Vol 21, No 6, 14 March 1985, IEE, London, pp225-226.

[50] Shimizu, Y., Tanaka, M., Watanabe, T. "A New Cut of Quartz with Extremely Small Temperature Coefficient by Leaky Surface Wave." Proc. 1985 Ultrasonics Symposium, IEEE, New York, pp233-236.

[51] Bickers, L., Leveridge, P. "Test Equipment for the Time and Frequency Domain Measurement of SAW Filters." Proc. Ultrasonics International Symposium 1985, Butterworths, London, pp528-531.

[52] Campbell, C. K., Saw, C. B. "Analysis and Design of Low-Loss SAW Filters Using Single-Phase

Unidirectional Transducers." IEEE Trans. Ultrasonics, Ferroelectrics and Frequency Control, Vol UFFC-34, No 3, May 1987, New York, pp357-367.

[53] Bower, D. E., Oliver, T. N. "Novel Quartz Cuts for SAW Devices." Proc. 2nd European Frequency and Time Forum, Neuchatel, 16-18 March 1988, Swiss Foundation for Research in Microtechnology, pp731-738

[54] Oliver, T. N., Bower, D. E., Dowsett, J. "Low Loss, Highly Stable SAW Devices on Quartz." Proc. 1986 Frequency Control Symposium, IEEE, New York, pp269-274.

8. APPENDICES

Appendix 1 "Novel Quartz Cuts for SAw Devices."

Paper Presented at 2nd European Frequency and Time Forum, 1988

Appendix 2 "Low Loss, Highly Stable SAW Devices on Quartz."

Paper Presented at IEEE Frequency Control Symposium, 1986.